SEISMIC FRAGILITY OF REINFORCED CONCRETE BUILDINGS WITH MASONRY INFILLS

by

Trishna Choudhury

DEPARTMENT OF CIVIL ENGINEERING
INDIAN INSTITUTE OF TECHNOLOGY GUWAHATI
GUWAHATI – 781039 (INDIA)

April 2018

SEISMIC FRAGILITY OF REINFORCED CONCRETE BUILDINGS WITH MASONRY INFILLS

A Thesis Submitted in
Partial Fulfillment of the Requirement
for the Degree of

Doctor of Philosophy

by

Trishna Choudhury

DEPARTMENT OF CIVIL ENGINEERING
INDIAN INSTITUTE OF TECHNOLOGY GUWAHATI
GUWAHATI – 781039 (INDIA)

April 2018

Dedicated to

My Parents and Brother

CERTIFICATE

It is certified that the work contained in the thesis titled *Seismic Fragility of Reinforced Concrete Buildings with Masonry Infills*, by Ms. Trishna Choudhury (Roll No. 126104019), has been carried out under my supervision, and that this work has not been submitted elsewhere for a degree.

Date: 19 April 2018

Place: IIT Guwahati

Dr. Hemant B. Kaushik
Associate Professor
Department of Civil Engineering
Indian Institute of Technology Guwahati
Guwahati – 781039, Assam, India

ABSTRACT

Masonry infilled (MI) reinforced concrete (RC) buildings are commonly constructed in many places across the world. Infills contribute large lateral strength and stiffness to the building, but their influence on the lateral load behavior during a seismic event depends greatly on their distribution in the building. MI-RC frames with an open ground storey (OGS) is a typical case of irregular distribution of infills along the height of a building frame. In such buildings, infills are provided only in the upper stories that renders the ground storey relatively flexible and weaker compared to the stiffer upper stories. The columns of the open ground storey lack adequate ductility capacity, stiffness, and strength needed to resist the high demand for storey shear. This leads to an undesirable column-sway failure mechanism in OGS buildings subjected to earthquake excitations. In contrast, the infills restrain most of the relative lateral deformation in the upper stories, and thus, little or no damage is incurred in the upper stories.

Formal guidelines are not available either for design of OGS buildings or even for assessment of seismic vulnerability associated with such buildings. The issue becomes more complex socially as there appears to be a belief among various stakeholders that openings present in the infill walls on upper stories of OGS buildings offset the soft storey effect, and thus, reduces the seismic vulnerability. Clearly, there is an urgent need to carry out seismic performance and fragility assessment of these buildings and distinguish the key features influencing their vulnerability. Failure of the OGS buildings during past earthquakes reveals that the global failure of such buildings is entirely defined by the ground storey column failure. This necessitates consideration of an engineering demand parameter (EDP) that defines the component level failure of the OGS buildings. Large uncertainties are usually associated with the estimation of these EDPs needing proper consideration. It is equally important to identify the parameters on which the sensitivity of EDPs mostly depends, so that proper care can be taken in estimating the uncertainty in these parameters. Further, a large-scale fragility assessment of building stocks in an area requires a simple and rapidly applicable method. Thus, the primary objective of the present study is to quantify the seismic performance and fragility of low- to mid-rise OGS frames with due consideration of various sources of uncertainties associated with EDPs, and to assess their vulnerability in comparison with corresponding fully infilled and bare frames.

The objectives are accomplished by considering representative RC frames of three building typologies (bare frame, open ground storey frames, and fully infilled frames) and carrying out: (a) nonlinear static analyses (pushover analysis) followed by the capacity spectrum method for capacity assessment, and (b) nonlinear dynamic analyses using seven ground motions and their frequency envelop dependent samples scaled for several PGAs. A parametric study is carried out considering variations in several parameters (e.g., opening size in infill walls, number of bays, number of stories, analysis type, PGA) in order to understand their influence on seismic performance and fragility of the frames. Influence of several global and local EDPs on seismic fragility of these frames is evaluated and the importance of using component level EDPs in fragility assessment of OGS frames is demonstrated. Sensitivity of EDPs owing to the uncertainty in several input parameters is studied and the most influencing parameters for fragility assessment of all the frames are highlighted. Both the epistemic and aleatoric uncertainties are predicted for the three frame configurations through extensive dynamic analyses. This is followed by seismic fragility estimation using frame responses and uncertainty obtained by means of simplistic nonlinear static and dynamic analysis procedure.

Based on the comparative assessment, results of nonlinear static and dynamic analyses are related with amplification factors. The assumption that seismic vulnerability of OGS frames reduces due to increase in opening size in infill walls is found to be flawed. By multiple linear regression of several parameters, a two-level seismic demand model is developed that gives good estimate of building frame responses, and that can be conveniently used for rapid assessment of seismic displacement demand on the frames. Finally, fragility flow plots (FFP) are developed where the damage is represented in a continuous form without any discretization of damage states. FFPs can relate several building parameters required for rapid quantification of the fragility of buildings for a given level of uncertainty and seismic demand. FFPs can be further used in fragility-based seismic design of the frames.

❄ ❄ ❄

ACKNOWLEDGEMENT

I express my sincere gratitude to my thesis supervisor, Dr. Hemant B. Kaushik, for his guidance, motivation and continuous moral support throughout my PhD research work. His enthusiastic nature, *always-positive* attitude and *deadlines* helped me to develop myself in all aspects and bring out the best of me. The numerous technical sessions I had with him and personal lessons I learned from him helped me in overcoming several technical and personal challenges. I could not have imagined having a better advisor and mentor for my PhD study.

Besides my supervisor, I would like to thank the rest of my thesis committee: Prof. Sajal K. Deb, Dr. Kaustubh Dasgupta, and Dr. K. S. R. Krishna Murthy for their insightful comments, timely suggestions and guidance that helped in continuous improvement of this thesis. I also extend my thanks to all other faculty members of the Department of Civil Engineering for imparting me knowledge on various subjects and helping me at the time of difficulty in solving any problem.

I would like to acknowledge the *Ministry of Human Resource Department* for their funding for carrying out the research activities. I am very thankful to the Department of Civil Engineering for providing me support and infrastructure throughout my research work. I am thankful to all the entire IIT Guwahati fraternity for their relentless effort in making the campus, a wonderful environment.

I am thankful to my parents, Sri Sarat Chandra Choudhury, Smt. Kusum Choudhury, and my brother Dr. Pankaj Choudhury for supporting me spiritually at every step of my life. Their accumulated love, care, and understanding helped me in completion of this work. Without their precious support, it would not be possible to conduct this research.

Special thanks to my fellow lab mate and friends Maharshi Kintada and Atanu Purkayastha for their helping hands. I would also like to thank all my juniors and friends at IIT Guwahati who made my stay memorable. Last but not the least, I would like to express my thanks to all those who have helped me directly or indirectly for successful completion of this work.

Ms. Trishna Choudhury
(126104019)

❋ ❋ ❋

TABLE OF CONTENTS

❄ ❄ ❄

LIST OF TABLES

❋ ❋ ❋

LIST OF FIGURES

❋ ❋ ❋

LIST OF SYMBOLS

μ_D	: Ductility demand
3B-4S	: Three bay- four storey
A-D	: Acceleration – Displacement
ADRS	: Acceleration Displacement Response Spectrum
B_c	: Width of column
C	: Complete damage state
COV	: Coefficient of Variation
CP	: Collapse Prevention
C_R	: Rayleigh damping
CSM	: Capacity Spectrum Method
DAF	: Dynamic Amplification Factor
D_b	: Depth of beam
d_b	: Diameter of longitudinal steel bar in m
DI	: Damage Index
DPM	: Damage Probability Matrix
ds	: damage state
d_u	: Ultimate displacement
d_y	: Yield displacement
E	: Extreme damage state
E[.]	: Expectance
E_c	: Modulus of elasticity of concrete
E_D	: Energy dissipated by damping
EDP	: Engineering Demand Parameter
E_m	: Elastic modulus of masonry
E_m	: Modulus of elasticity of masonry
E_{S0}	: Maximum strain energy
f_{ck}	: Characteristic compressive cube strength of concrete
FFP	: Fragility Flow Plot
FI	: Fully Infilled
f_m'	: Compressive prism strength of masonry
FOSM	: First Order Second Moment
f_y	: Yield stress of longitudinal reinforcement
f_y	: Yield stress of reinforcing steel

GL : Ground storey Level

GL-ISD : Ground storey Level Interstorey Drift

HRC : Homogenized Reinforced Concrete

I : Macro-seismic Intensity

IDA : Incremental Dynamic Analysis

IL : Infill Load

IM : Intensity Measure

IO : Immediate Occupancy

ISD : Interstorey Drift

ISD_{max} : Maximum Interstorey Drift

L : Half-length of member in meter

LHS : Latin Hypercube Sampling

LN : Log-Normal distribution

l_p : Average plastic hinge length

LS : Life Safety

M : Moderate damage state

MDOF : Multi Degree of Freedom

MLR : Multiple Linear Regression

MPA : Modal Pushover Analysis

MRF : Moment Resisting Frame

MSA : Multiple Stripe Analysis

N : Normal distribution

N_B : Number of bays

N_F : Number of analysis cases where EDP exceeds the limit at an IM level

NLTHA : Nonlinear Time History Analysis

N_S : Number of stories

N_{sim} : Number of simulations

NSP : Nonlinear Static Procedures

N_T : Total number of analysis cases at an IM level

N_{var} : Number of random variables

OGS : Open Ground Storey

Op : Central opening size in infill walls

PF : Participation Factor

PGA : Peak Ground Acceleration

PL : Performance Level

PO : Pushover

PP : Performance Point

PSDM : Probabilistic Seismic Demand Model

PSHA : Probabilistic Seismic Hazard Analysis

RC : Reinforced Concrete

RVS : Rapid Visual Screening

S : Slight damage state

S_a : Spectral acceleration

$Sa(T_1)$: Spectral acceleration at first natural period

S_d : Spectral displacement demand

$\bar{S}_d$: Spectral displacement threshold

SDOF : Single Degree of Freedom

S_{du} : Ultimate spectral displacement demand

S_{dy} : Yield spectral displacement demand

S_i : Sobol' index

TDA : Tornado Diagram Analysis

TL : Top Level

TL-ISD : Top level Interstorey drift

T_N : Natural time period of vibration

Var : Variance

V_b : Base shear

Ws : Width of equivalent diagonal strut for modelling masonry infill walls

$W_{s\text{-}gr}$: Width of the strut for ground storey

$W_{s\text{-}up}$: Width of the strut for upper storey

α_1 : Modal mass coefficient

β : Predictor coefficient

β_0 : Hysteretic damping

β_C : Uncertainty in capacity

$\beta_{D|IM}$: Uncertainty in seismic demand given IM (Aleatoric Uncertainty)

β_{eff} : Effective viscous damping

β_T : Normalized standard deviation (Total uncertainty)

γ_c : Weight density of concrete

γ_m : Unit weight of infill

ε_m : Ultimate strain at failure in masonry

κ : Damping modification factor as in ATC 40 (1996)

λ	: Tuning parameter for Lasso regression
μ_d	: Ductility demand
ξ	: Equivalent viscous damping
$\phi_{1,roof}$	: Roof level amplitude of the first mode

❋ ❋ ❋

Chapter 1

INTRODUCTION

1.0 Overview

Masonry infilled reinforced concrete (RC) buildings are commonly constructed in many countries. Although infills contribute large lateral strength and stiffness to the building, their influence on lateral load behavior depends greatly on their distribution in the building. For example, an open ground storey (OGS) frame, where the masonry infill walls are present in all the stories except the ground storey. The ground storey is left open for various aesthetical and functional purposes, such as, parking or for shops and services. These configurations, which are essentially originated due to architectural decisions, have long been recognized by earthquake engineering community as seismically vulnerable. Providing infills only in the upper stories of a building renders the ground storey relatively flexible and weaker compared to the stiff upper stories and onsets the soft storey effect. Generally, the OGS columns lack adequate ductility capacity, stiffness, and strength needed to resist the high demand for storey shear. This leads to an undesirable column-sway failure mechanism in OGS buildings subjected to earthquake excitations, and the building often suffer severe damage or even collapse. In contrast, the infills restrain most of the relative lateral deformation in the upper stories, and thus, little or no damage is incurred in the upper stories.

The peculiar behavior of masonry infilled RC frames with open ground storey is that most of the lateral deformation is concentrated at the ground storey and the upper stories remain almost vertical and mostly undamaged. It is a common perception among various stakeholders that the soft storey effect in OGS buildings is reduced due to the presence of openings in the upper storey infills. However, in several past earthquakes

damage as well as collapse was also observed in OGS buildings with large openings in infill walls. Fig. 1.1 shows two such open ground storey RC buildings where the ground storey totally collapsed during 2001 Bhuj earthquake. Both the buildings had big openings in the infill walls of the upper stories. Thus, these vertically irregular buildings are highly vulnerable to earthquakes.

Figure 1.1 Collapse of open ground storey RC frame residential buildings with small to large openings at Bhuj during 2001 Bhuj earthquake [Source: *www.nicee.org* accessed on 05 February 2018].

Several documents, such as, HAZUS (2013) and GEM (D' Ayala et al. 2015) provide guidelines for seismic vulnerability assessment of some common building typologies using analytical methods. The typologies are mostly categorized based on the material used in the construction. Though the reinforced concrete buildings are categorized as either with or without masonry infill, the irregular distribution of masonry infills in these buildings that affects their structural behavior is not taken into consideration. Another important aspect in seismic vulnerability assessment is the choice of an efficient engineering demand parameter (EDP) that correctly interprets the damage associated with the building during earthquakes. Previous studies suggested various EDPs for fragility assessment of multi-storey frames; however, such categorized EDPs are not available in the literature for irregular buildings. In addition, large uncertainty is generally associated in the estimation of these EDPs that needs proper consideration.

1.1 Major Concerns and Need of the Study

It is learned from the consequences of past earthquakes that presence of open ground storey in a building really makes it seismically vulnerable. In contrast, the infills present in the ground storey imparts large lateral strength and stiffness to the building. Several past researchers (e.g., Moghaddam and Dowling 1987, Dolšek and Fajfar 2001,

Kaushik et al. 2009, Al-Nimry et al. 2015) have also reported the significant negative influence of OGS on the overall seismic performance of the buildings. However, the seismic design codes of different countries are silent on specific design methodology or fragility assessment procedure to be followed for OGS buildings. This is surprising because a large number of such buildings have collapsed during the past earthquakes with huge loss of life and property. Some previous studies (Al-Nimry et al. 2015, D'Ayala et al. 2015, Ozhendekci and Ozhendekci 2012) have attempted to assess the seismic vulnerability of RC buildings including those with masonry infills. However, there is a lack of specific literature that can assist in the seismic vulnerability assessment of OGS buildings especially those with openings in infill walls. Influence of openings in infill walls on the overall seismic vulnerability of OGS frames has not been investigated yet.

Clearly, there is an urgent need to carry out seismic performance assessment and fragility assessment of these buildings in order to classify the most vulnerable RC buildings and distinguish the key features influencing their vulnerability. Moreover, the failure of the OGS buildings during past earthquakes reveals that the global failure of such buildings is entirely defined by the ground storey failure. This necessitates consideration of an EDP that defines the local failure of the OGS buildings. Further, a large-scale assessment of fragility of buildings in an area requires a simple and rapidly applicable method that can quickly assess the vulnerability of the buildings. Thus, the primary objective of the present study is to quantify the seismic performance and fragility of low-rise to mid-rise OGS frames and assess their vulnerability in comparison with corresponding fully infilled and bare frames.

1.2 Scope and Objectives of the Study

The present study examines various aspects of seismic performance and vulnerability assessment of masonry infilled reinforced concrete (RC) frames. In order to achieve the goal of the study, rigorous nonlinear static and dynamic analyses are carried out for seismic performance assessment of the considered building typologies. Given that, this work intends to estimate the seismic fragility of masonry infilled RC frames and to examine if a simplified and rapid method can be developed for fragility estimation without compromising the accuracy. Stepwise objectives of the present study are as stated below:

i. **Seismic performance assessment of masonry infilled RC frames**

It is a general perception that openings present in the infill walls of OGS frames reduce the stiffness of upper stories, and thus, offsets the soft storey effect. This issue is investigated by assessing the seismic performance of low- and mid-rise masonry infilled RC frames with different infill configurations using nonlinear static and dynamic analyses. Based on the results of the analytical study, regression analysis is carried out in order to obtain a simple demand model relating seismic intensity to engineering demand parameter and several other structural parameters. Dynamic amplification factors are determined for displacement demand of different frame configurations.

ii. **Evaluation of effective engineering demand parameter**

Previous studies suggested various engineering demand parameters for fragility assessment of multistory frames, but irregular OGS frames were excluded from the study. Hence, several EDPs (both global and local) are considered in seismic performance assessment using nonlinear dynamic analyses and fragility analysis to ascertain an effective EDP for realistic assessment of performance and fragility.

iii. **Estimation of uncertainty in EDPs**

Fragility assessment requires consideration of all types of uncertainties – epistemic and aleatoric. Analytical estimation of EDPs often involves large uncertainty owing to the random nature of input parameters and ground motion. Judicious consideration of these uncertainties is essential in fragility assessment. Therefore, the sensitivity of EDPs to random input parameters are evaluated for masonry infilled RC frames. This is followed by estimation of various uncertainties associated with such buildings. The results are based on multiple stripe analysis (nonlinear dynamic analyses) of the building frames for several ground motions.

iv. **Seismic fragility assessment**

Structural damage probabilities for the considered frame configurations are estimated followed by the development of fragility curves and contour plots for different damage states and seismic hazard scenarios using nonlinear static and dynamic procedures. Finally, a simplified method is developed for seismic

performance and fragility assessment to evaluate seismic safety of such buildings frames.

1.3 Organization and Outline of the Thesis

The present study broadly addresses four aspects, namely, (a) performance assessment of masonry infilled reinforced concrete buildings using nonlinear static and dynamic analysis procedures, (b) evaluation of effective engineering demand parameter (EDP) for predicting component level failure of vertically irregular frames, (c) sensitivity of EDPs to random input modelling variables and ground motion variability to address the epistemic and aleatoric uncertainty associated with the EDPs, and (d) seismic fragility assessment of the frames considering both nonlinear static and dynamic analysis.

The work carried out in this study is presented in eight chapters. Chapter 1 introduces the basic subject matter of this research and stresses the need to carry out the research. A detailed review of the previous investigations on various aspects of seismic vulnerability assessment is presented in Chapter 2. Results of seismic performance assessment of multi-storey RC building frames with and without masonry infill walls are discussed in Chapter 3. A rigorous parametric study is carried out in order to evaluate the influence of several important parameters, such as, central opening size in infill walls, number of bay and storey, and PGA, on the lateral load response of these frame configurations. Based on these results, a simplified seismic displacement demand model is developed using multiple linear regression analysis, which is later used for seismic fragility assessment.

Chapter 4 presents an identification procedure for an effective engineering demand parameter for the RC frames with and without vertical irregularity by carrying out numbers of nonlinear time-history analyses with incremental seismic intensity. Analytical estimation of engineering demand parameters involves consideration of uncertain material and geometric parameters and input ground motions. Sensitivity of the output response (or EDP) to these uncertain input parameters are recognized in Chapter 5. Further, the uncertainties associated with capacity (epistemic) and demand (aleatoric) are quantified in Chapter 6 for the RC frames considered.

Chapter 7 is dedicated to the assessment of seismic fragility of the masonry infilled RC frames considered using the results obtained from both nonlinear static and nonlinear dynamic analyses. Seismic fragility flow plots are developed and suggested for use in

fragility based seismic design of building structures. A brief summary is discussed at the end of each Chapter. Additionally, the major outcomes of this research are summarized in Chapter 8, along with a discussion on salient conclusions drawn from the study. In the end, limitations of the study and scope of possible future research work are touched upon in brief.

❋ ❋ ❋

Chapter 2

A STATE-OF-THE-ART REVIEW

2.0 Overview

For assessing the seismic vulnerability of buildings, a systematic understanding of the assessment methodologies is necessary. Seismic vulnerability is defined as the degree of loss to a given element at risk, or set of such elements, resulting from an earthquake of a given magnitude or intensity (Shah 1984). This degree of loss or damage to a set of exposure (buildings) in an area depends on its seismic performance. It is thus essential to determine the seismic performance of buildings (or building stocks) under a given hazard (seismic demand) to assess their seismic vulnerability. The primary requirements for carrying out vulnerability assessment are characterization of seismic hazards, selection of building typologies for performance assessment, selection of criteria for damage levels, choosing relevant engineering demand parameters, estimation of uncertainties associated with various demand parameters, and assessing the building performance for the given hazard. The key elements in seismic vulnerability assessment, and hence seismic risk estimation procedure, are shown in Fig.2.1.

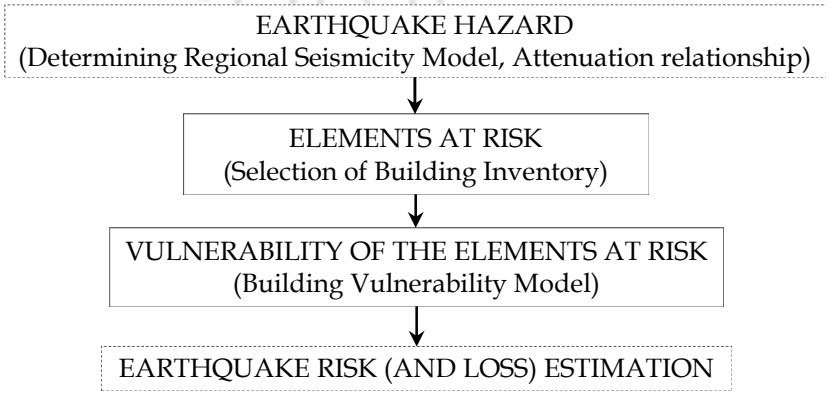

Figure 2.1 Flowchart describing the key elements in seismic risk assessment.

This chapter reviews the past work carried out on seismic vulnerability assessment of structures, primarily the RC buildings. First, the existing building classes and typologies developed by several researchers and codes of practice are reviewed, and the relevant building typology is shortlisted for vulnerability assessment in the present study. Structural damage states are required to be defined for seismic performance and vulnerability assessment of any structure. Therefore, the damage states developed by various past studies are discussed and summarized in the second section. This is followed by the review of methods available for seismic performance assessment of the select building typologies. Finally, the fourth section presents a brief discussion and review of seismic fragility and vulnerability assessment procedures adopted by researchers in the past. The pros and cons associated with the commonly used vulnerability assessment procedures are highlighted. Based on the review of the past literature, gap areas in the state-of-the-art are identified for detailing the primary objectives of the present study.

In addition to the review of the literature in the research areas mentioned above, some more specific literature is reviewed and discussed in the subsequent chapters. The commonly used engineering demand parameters (EDPs) for response assessment and their importance in vulnerability assessment of structures is discussed in Chapter 4. Methods adopted by the past researchers in assessment of the seismic response sensitivity to uncertain input variables are reviewed in Chapter 5. Various uncertainties associated with input parameters in structural capacity evaluation and assessment of record-to-record variability are reviewed in Chapter 6 along with commonly used methods for estimation of these uncertainties.

2.1 Structural Inventory for Seismic Vulnerability Assessment

Vulnerability models cannot be applied to every building in a region as the structural and other details for each of them can vary significantly and may not be easily available. The vulnerability assessment thus should be done for a building representative of a building stock that has been classified and characterized according to some homogenous behavior. A common terminology or taxonomy is critical to document variations in building design and construction practices around the world. However, extrapolation of the results obtained on a single building to an entire building stock has the drawback of not being able to exactly quantify the variability associated with the response of each building in a stock due to uncertainty of building parameters.

Exposed building stock classification and its damage description is essential for risk analysis. In seismic risk assessment, estimation of earthquake hazard, structural vulnerability and exposure of building stock are the three equally important components, out of which, the development of inventory databases is the most difficult aspect of damage prediction. Vulnerability of a building mainly depends on the form and quality of construction of the main vertical load-bearing elements. For instance, a building with unreinforced masonry walls can be expected to be much more vulnerable than a timber frame building. Therefore, preparation of a building typology is necessary for seismic vulnerability assessment. Usually the following parameters are considered for classifying the buildings-structural material, structural system, number of stories, age, function, etc. However, since in most cases the entire set of necessary data may not be available, reference is made to both the surveyed data by rapid visual screening (RVS) and to the data available from literature about the building stocks. Hundreds of building typologies from different countries are documented in the literature. Comprehensive classification of buildings is available in: MSK-64 Scale (Medvedev and Sponheuer 1969), ATC 13 (1985), European Macroseismic Scale (Grünthal 1998), FEMA 154 (2002), HAZUS (2013), Spence et al. (1992), Cardona and Yamin (1997), Eleftheriadou and Karabinis (2011), PAGER global inventory (Jaiswal et al. 2010), and Global Earthquake Model (Brzev et al. 2013), FEMA P-58 (2012).

The existing building stock of Indian cities is a rich mix of several different building types and construction technologies. In India, there exists a considerable unreinforced masonry building stock that has to be evaluated in terms of seismic safety considerations. In addition, there are also a vast number of masonry infilled RC buildings in seismically active urban and semi-urban areas. Consideration of masonry infill walls in RC buildings as non-structural elements has led to informal use and treatment of masonry walls in such buildings. This, in addition to several functional reasons, has resulted in uneven placement of masonry infill walls in RC buildings leading to creation of irregular buildings. For example, open ground storey (OGS) buildings in which masonry walls are provided in all the stories except the ground storey. Such buildings perform poorly during earthquakes, and therefore, it is essential to assess the seismic vulnerability of irregular reinforced concrete buildings with masonry infill walls. Seismic behavior and performance of such buildings in the past earthquakes is reviewed in this section. Building inventory data for other types of buildings is not reviewed in the thesis.

Masonry infill reinforced concrete buildings are commonly constructed in many other countries also. Although infills contribute large lateral strength and stiffness to the building, their influence depends greatly on their distribution in the building frame. Providing infills only in the upper stories of a building (commonly known as *open ground storey* building), renders the ground storey relatively more flexible and weaker compared to the upper stories. Generally, open ground storey columns lack adequate ductility capacity, stiffness, and strength needed to resist the high demand of storey shear. This generally leads to an undesirable column-sway failure mechanism in OGS buildings subjected to strong earthquake excitations in which plastic hinges are mainly formed in the columns of the open ground storey. In contrast, the infills restrain the deformation of the upper storey, and thus, little damage is incurred in the upper stories (Murty et al. 2006, Kaushik and Jain 2007, Kaushik and Dasgupta 2013, Yuen and Kuang 2015).

Considering this fact, past researchers (Moghaddam and Dowling 1987; Dolšek and Fajfar 2001; Chintanapakdee and Chopra 2004; Kaushik et al. 2006, Kaushik et al. 2009; Özhendekci and Özhendekci 2012; Al-Nimry et al. 2015; Rai et al. 2017) have reported the significant 'negative' influence of OGS on the overall seismic performance of such buildings. Previous experiences from earthquakes all over the world also reveal the fact that such buildings performed quite poorly even during moderate shaking, and in some cases, complete collapse of the ground storey columns was observed (Kaushik and Jain 2007; Dutta et al. 2015). Fig. 2.2 shows two such OGS buildings collapsed during 2004 Sumatra and 2011 Sikkim earthquake, respectively; both buildings had big openings in infill walls of upper stories but still both collapsed. Davis et al (2010) studied the seismic behavior of OGS frames and found them to be more vulnerable in comparison to fully infilled (FI) frames; in general, fragility increases with increase in number of stories and decrease with increasing number of bays. Chintanapakdee and Chopra (2004) and Mondal and Tesfamariam (2014) observed that stiffness irregularities in ground storey has significant effect on the seismic response (base shear and inter storey drift ratio) of RC frames. On several platforms (for example, NICEE Workshop 2014), various stakeholders have expressed that it is a general assumption in design practice that infills with openings are less effective in imparting lateral strength and stiffness to the OGS frames, and hence, such frames can be analyzed and designed as bare frames. This leads to a common perception that presence of openings in infill walls of OGS frames reduce the seismic fragility of such frames. However, the above mentioned assumption is valid

only for FI frames since openings present only in the ground storey alters the lateral response of the FI frames significantly (Surendran and Kaushik 2012). It is required to be investigated whether there is an influence of openings in infill walls of upper stories on the overall seismic vulnerability of OGS frames.

(a) (b)

Figure 2.2 Collapse of OGS buildings during past earthquakes: (a) a three storey building in Port Blair, India after 26 December 2004 Sumatra earthquake (Kaushik and Jain 2007), and (b) a four storey building at Singtam market in Sikkim after 18 September 2011 Sikkim earthquake (Kaushik and Dasgupta 2013). Both buildings had big openings in infill walls of upper stories but still both collapsed.

2.2 Identification of damage

Seismic vulnerability models establish a relation between seismic hazard (i.e., seismic demand) and the resulting structural damage for a particular building stock. Hence, before vulnerability assessment, damage states (ds) or performance levels (PL) must be defined for a building class. In general, damage to a structure means the modification of its condition that affects the performance of the structure. The identification of damage can be done in different ways. Immediately after an earthquake the most easy and rapid assessment of damage is by visual inspection of the damaged site. Damage may be classified into two types- apparent damage and mechanical damage. The observed damage is usually defined as apparent damage, such as, cracks, spalling, separation of members, etc. Whereas mechanical damage implies some change in the mechanical property of the structure, e.g., change in the fundamental frequency, stiffness, available ductility, etc.

Building damage predictions are used to study expected damage patterns in a given region for different scenario earthquake. Building damage can best be described in terms of its components- structural and non-structural. Damage to non-structural components of buildings (i.e., architectural components, such as partition walls and ceilings, and mechanical or electrical systems) primarily affects monetary and societal functional losses and generates casualties of mostly light-to-moderate severity. Damage to structural components (i.e., the gravity and lateral-load-resisting systems) of buildings can be hazardous. Hazard mitigation measures are different for these two categories of building components as well. Hence, it is desirable to separately estimate structural and non-structural damage.

Various damage states or performance levels are proposed in the literature for different building typologies. Generally, damage state limits are kept dependent on the structural damage only even though the non-structural damage can be of equal importance and can be more drift or acceleration sensitive. It is due to the complexity in assessment of non-structural damage by conventional methods that their contribution in defining damage states are generally not considered. The degree of damage is generally a continuous parameter. However, for simplicity these are discretized into various discrete damage states. Each damage state varies within a range, the initial point of which is called as threshold damage. Damage assessment is required to estimate the probability of a given damage state or performance level to a particular building class. In other words, it is the numerical interpretation of the probable damage to a building due to a given hazard.

Several damage indices are mentioned in literature for the measure of damage after an earthquake. These damage indices are expressed in terms of strength parameters and parameters related to ductility and hysteretic energy dissipation. Under earthquake shaking, building damage state in the inelastic range relates well with storey drift since in the inelastic range the capacity of the structure remains constant or decrease but the storey drift increases. Hence, it is better to express damage in terms of deformation or storey drifts. One of the widely used damage index is the Park and Ang (1985) damage index. FEMA 273 (1997) defined different building performance levels based on the extent of damage (both structural and non-structural) to a building (Table 2.1).

Table 2.1 Relation between building damage and performance levels as defined in FEMA 273 (1997).

	Building Performance Levels			
	Collapse Prevention (CP) Level	**Life Safety (LS) Level**	**Immediate Occupancy (IO) Level**	**Operational (O) Level**
Overall Damage	***Severe***	***Moderate***	***Light***	***Very light***
General	Little residual stiffness and strength.	Some residual strength and stiffness left in all stories.	Structure substantially retains original strength and stiffness.	Structure substantially retains original strength and stiffness.
	Load-bearing columns and walls function. Infills and unbraced parapets failed or at incipient failure.	Gravity-load-bearing elements function. No out-of-plane failure of walls or tipping of parapets. Damage to partitions.	Minor cracking of facades, partitions, and ceilings as well as structural elements.	Minor cracking of facades, partitions, and ceilings as well as structural elements.
	Large permanent drifts.	Some permanent drift.	No permanent drift.	No permanent drift
	Some exits blocked.	-	Elevators can be restarted Fire protection operable.	All systems important to normal operation are functional.
	Building is near collapse.	Building may be beyond economical repair.	-	-
Non-structural components	Extensive damage	Falling hazards mitigated but many architectural, mechanical, and electrical systems are damaged.	Equipment and contents are generally secure, but may not operate due to mechanical failure or lack of utilities.	Negligible damage occurs. Power and other utilities are available, possibly from standby sources.

HAZUS (2013) methodology simply classifies the degree of building damage into four discrete damage states: Slight, Moderate, Extensive, and Complete damage. The damage scale of European Macroseismic Scale (EMS 98) (Grünthal 1998) is a modification of MSK 64 scale (Medvedev and Sponheuer 1969), and is designed to encourage co-operation between engineers and seismologists, rather than being for use by seismologists alone. The EMS is the basis for seismic intensity evaluation in European countries and is used in a number of countries outside Europe. Based on the type of

building, deformation and hence damage occurs in different way under earthquake loading. EMS 98 gives the damage description for two different classes of buildings- masonry and reinforced concrete as given in Table 2.2 and Table 2.3.

Table 2.2 Damage levels in MSK 64 and EMS 98 scale for masonry buildings (Grünthal 1998).

Classification of damage to masonry buildings	
Grade 1: 	**Negligible to slight damage** No structural damage, slight non-structural damage. Hairline cracks in very few walls. Fall of small pieces of plaster only. Fall of loose stones from upper parts of buildings in very few cases.
Grade 2: 	**Moderate damage** Slight structural damage, moderate non-structural damage. Cracks in many walls. Fall of large pieces of plaster. Partial collapse of chimneys.
Grade 3: 	**Substantial to heavy damage** Moderate structural damage, heavy non-structural damage. Large and extensive cracks in most walls. Roof tiles detach. Chimneys fracture at the roofline; failure of individual non-structural elements (partitions, gable walls).
Grade 4: 	**Very heavy damage** Heavy structural damage, very heavy non-structural damage. Serious failure of walls; partial structural failure of roofs and floors.
Grade 5: 	**Destruction** Very heavy structural damage. Total or near total collapse.

Table 2.3 Damage levels as in MSK 64 and EMS 98 scale for RC buildings (Grünthal 1998).

Classification of damage to Reinforced Concrete (RC) buildings	
Grade 1: 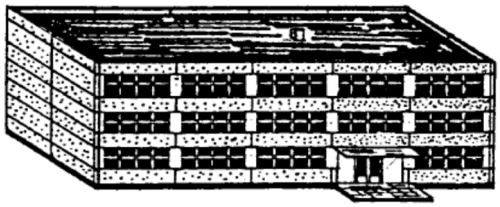	**Negligible to slight damage** No structural damage, slight non-structural damage. Fine cracks in plaster over frame members or in walls at the base. Fine cracks in partitions and infills.
Grade 2: 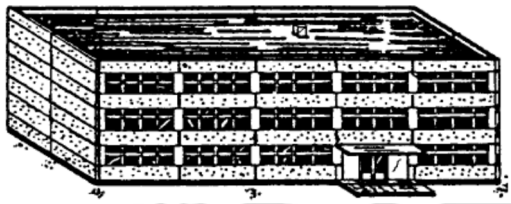	**Moderate damage** Slight structural damage, moderate non-structural damage. Cracks in columns and beams of frames and in structural walls. Cracks in partition and infill walls; fall of brittle cladding and plaster. Falling mortar from the joints of wall panels.
Grade 3: 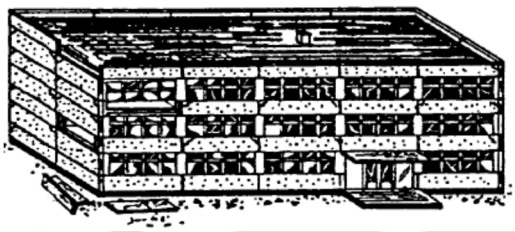	**Substantial to heavy damage** Moderate structural damage, heavy non-structural damage. Cracks in columns and beam column joints of frames at the base and at joints of coupled walls. Spalling of concrete cover, buckling of reinforced rods. Large cracks in partition and infill walls, failure of individual infill panels.
Grade 4: 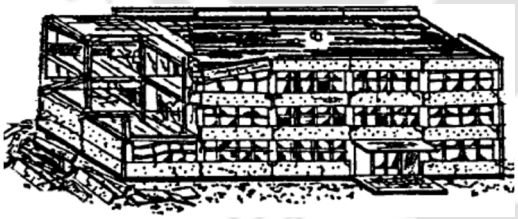	**Very heavy damage** Heavy structural damage, very heavy non-structural damage. Large cracks in structural elements with compression failure of concrete and fracture of rebars. Bond failure of beam-reinforced bars; tilting of columns. Collapse of a few columns or of a single upper floor.
Grade 5: 	**Destruction** Very heavy structural damage. Collapse of ground floor or parts (e.g., wings) of buildings.

Borzi et al. (2008) defined three different limit states based on sectional strains in the concrete and reinforcing steel at yield, as Light damage state, Significant damage state and Collapse damage state. After light damage state, the building is still considered usable without the need of seismic retrofitting. Beyond significant damage state, buildings are unsafe for use without retrofitting. More recently, Asteris et al. (2014) proposed a new damage index for masonry structures. This damage index (DI) is a ratio of percentage of the damaged area of the structure relatively to the total area of the structure. Based on this damage index, three structural performance levels were considered: Heavy damage (DI ≥ 20%), Moderate damage (10% < DI < 20%), and Insignificant damage (DI < 10%).

Rossetto and Elnashai (2003) proposed a new damage scale known as Homogenized Reinforced Concrete (HRC) damage scale. The scale is subdivided into seven damage states as none, slight, light, moderate, extensive, partial collapse, and collapse. The limit states are further defined in terms of HRC damage index (DI_{HRC}) as given by Eq. (2.1) to Eq. (2.4) for four main type of RC structures. Table 2.4 defines each damage state in terms of typical structural damage and non-structural damage expected, where, $ISD_{max\%}$ is the maximum interstorey drift ratio.

$$DI_{HRC} = 34.89 \ln(ISD_{max\%}) + 39.39, R^2 = 0.991 \text{ for ductile MRF} \quad (2.1)$$

$$DI_{HRC} = 22.49 \ln(ISD_{max\%}) + 66.88, R^2 = 0.822 \text{ for non-ductile MRF} \quad (2.2)$$

$$DI_{HRC} = 39.31 \ln(ISD_{max\%}) + 52.98, R^2 = 0.985 \text{ for infilled frames} \quad (2.3)$$

$$DI_{HRC} = 27.89 \ln(ISD_{max\%}) + 56.36, R^2 = 0.760 \text{ for shear-wall systems} \quad (2.4)$$

The damage levels or the performance levels can be associated with the pushover curves, also known as capacity curves, obtained from nonlinear static analysis of the building typology as shown in Fig. 2.3. More details about the nonlinear static analysis and resulting pushover curves will be provided in the section on seismic performance assessment. The probability of damage to buildings can be assessed by locating the performance point (PP) as the graphical intersection point of demand curve and capacity curve and is expressed through fragility curves. A very general relation between all these is shown in Fig. 2.3.

Table 2.4 Damage level in HRC scale for ductile, non-ductile and infilled moment resisting frame and RC shear wall structures, (Rossetto and Elnashai 2003).

DI_{HRC}	Damage State	Ductile MRF	Non-Ductile MRF	Infilled MRF	Shear-Wall
0	None	No damage	No damage	No damage	No damage
10	Slight	Fine cracks in plaster partitions/infills	Fine cracks in plaster partitions/infills	Fine cracks in plaster partitions/infills	Fine cracks in plaster partitions/infills
20	Light	Start of structural damage	Start of structural damage	Cracks at wall-frame interfaces	Start of structural damage
30		Hairline cracking in beams and columns near joints (<1mm)	Hairline cracking in beams and columns near joints (<1mm)	Cracking initiates from corners of openings	Hairline cracking on wall surfaces & coupling beams
40				Diagonal cracking of walls. Limited crushing of bricks at b/c connections	Onset of concrete spalling at a few locations
50	Moderate	Cracking in most beams and columns	Flexural and shear cracking in most beams & columns	Increased brick crushing at b/c connections	Most shear walls exhibit cracks
60		Some yielding in a limited number	Some yielding in a limited number	Start of structural damage	Some walls reached yield capacity
70		Larger flexural cracks & start of concrete spalling	Shear racking and spalling is limited	Some diagonal shear cracking in members especially for exterior frames	Increased diagonal cracking and spalling at wall corners
80	Extensive	Ultimate capacity reached in some elements-large flexural cracking concrete spalling & re-bar buckling	Loss of bonds at lap-splices, bar pull-out, broken ties	Extensive cracking of infills, falling bricks, out-of-plane bulging	Most shear walls have exceeded yield, some reach ultimate capacity, boundary element distress.
90		Short columns failure	Main re-bar may buckle or elements fail in shear	Partial failure of many infills, heavier damage in frame members, some fail in shear	Re-bar buckling, extensive cracking and through-wall cracks. Shear failure of some frame members
100	Partial collapse	Collapse of few columns, a building wing or single upper floor	Shear failure of many columns or impending soft-storey failure	Beams and/or columns fail in shear causing partial collapse. Near total infill failure	Coupling beams shattered and some shear walls fail
	Collapse	Complete or impending building collapse	Complete or soft-storey failure at ground floor	Complete or impending building collapse	Complete or impending building collapse

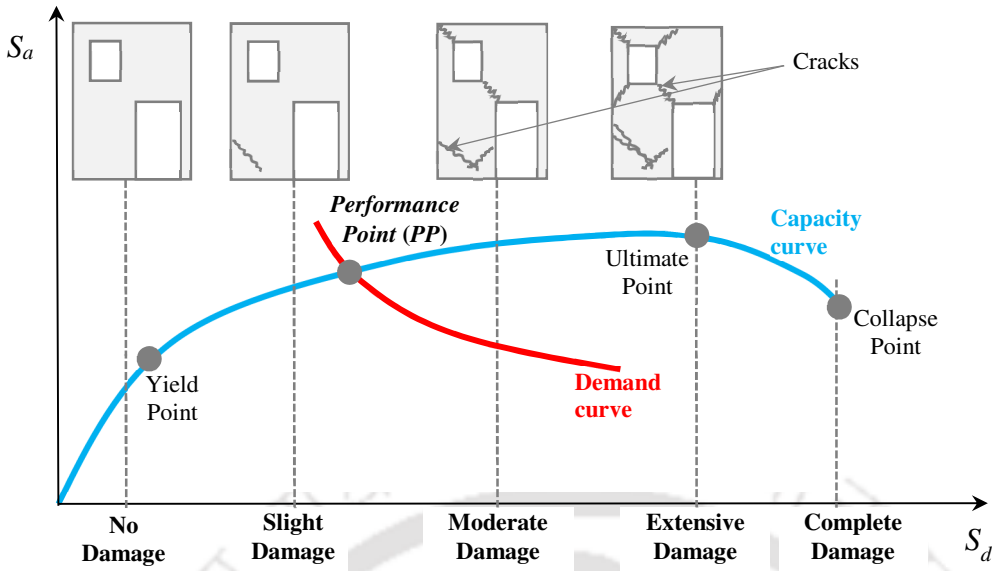

Figure 2.3 General relation between damage states, capacity curve and demand curve.

The HAZUS (2013) methodology considers uniform hazard response spectra with varying probability of exceedance obtained through probabilistic seismic hazard analysis (PSHA). Performance points (PP) are obtained as the points of intersection of response spectrums with capacity spectrum obtained from nonlinear analysis. These points define the thresholds for each damage states in the fragility or vulnerability curve. ATC 40 (1996) and FEMA 356 (2000) recommend values for nonlinear modelling parameters and inelastic deformation capacities and drift ratios. The interstorey drift (ISD) ratios of HAZUS (2013) are obtained for different building types based on material of construction and storey height. The percentage probability of damage for a particular type of building can be predicted by drawing vertical lines through the spectral displacements at PP on the fragility curves.

Lagomarsino and Giovinazzi (2006) obtained lognormal fragility curves as a function of target spectral displacement (S_{d*}) and defined displacement thresholds ($S_{d,k}$) and related the damage states directly to the pushover curves considering yield displacement (d_y) and ultimate displacement (d_u) as shown in Table 2.5. Similar damage state thresholds in terms of d_y and d_u are also defined in Barbat et al. (2008) for RC structures. The performance point (S_{d*}), in terms of displacement, is defined as a function of the demand and capacity curve parameters also accounting for the inelastic behavior of the structure by a closed analytical function as in Eq. (2.5).

$$S_{d^*} = \begin{cases} \left[1 + \left(\frac{S_{ae}(T)}{a_y} - 1\right)\frac{T_C}{T}\right] d_y & ;T < T_C \text{ and } \frac{S_{ae}(T)}{a_y} > 1, \\ \frac{S_{ae}(T)}{a_y} d_y & ;T_C \le T < T_D \text{ and } \frac{S_{ae}(T)}{a_y} \le 1, \\ \frac{S_{ae}(T_D)T_D^2}{4\pi^2} & ;T \ge T_D, \end{cases} \quad (2.5)$$

$S_{ae}(T)$, $S_{ae}(T_C)$, and $S_{ae}(T_D)$ are the seismic demand parameters and T, a_y, μ are the building capacity parameters. The damage state thresholds as given in Table 2.5 are based on expert judgment and have been verified based on the results of pushover analysis performed on prototype buildings, though details of this analysis are not reported.

Table 2.5 Damage states and corresponding damage state thresholds based on capacity curve parameters.

Damage state		Median value of spectral threshold displacements ($S_{d,k}$)	
		Lagomarsino and Giovinazzi (2006)	Barbat et al. (2008)
Slight	$S_{d,k1}$	0.7 d_y	0.7 d_y
Moderate	$S_{d,k2}$	1.5d_y	d_y
Severe	$S_{d,k3}$	0.5(d_y + d_u)	d_y + 0.25(d_u - d_y)
Collapse	$S_{d,k4}$	d_u	D_u

2.3 Damage Probability Matrix (DPM)

Seismic vulnerability assessments of buildings using deterministic evaluation of the level of damage to a particular building proves to be insufficient for large-scale seismic assessment of similar buildings subjected to a given hazard level or seismic demand. Therefore, a probabilistic representation of building performance considering the uncertainty in vulnerability evaluations is required for large-scale seismic assessment. This section discuss the various ways to express the deterministic damage evaluation in a probabilistic way considering the uncertainties related to earthquake demand and structural capacity. DPM specifies the probability of reaching or exceeding a damage state for a given earthquake intensity. Damage varies according to the characteristics of the ground motion even though its intensity is the same at a particular site. Uncertainties are associated both with seismic demand as well as with the structural properties of the building (Fig. 2.4). Hence, the damage is treated as a random variable and a certain probability distribution is assumed.

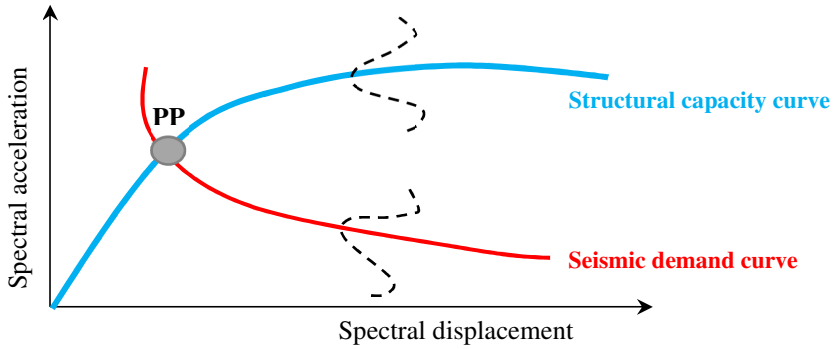

Figure 2.4 Uncertainties associated with the evaluation of Performance Point (PP).

The probability of damage to a particular typology of building will be the same under a given intensity of earthquake. This is the basic concept of constructing a DPM. The conditional probabilities can be defined as in Eq. (2.6), where, p_{ik} is the probability of reaching damage state d_i for ground motion intensity y_k, D is the damage random variable defined on damage state vector $\{D\} = \{d_0, d_1, ..., d_n\}$ and Y is the ground motion random variable.

$$p_{ik} = P[D = d_i \mid Y = y_k] \tag{2.6}$$

If the probability of complete damage is represented as $P[C] = P[C \mid Y]$, the discrete damage probabilities of different damage states – none (N), slight (S), moderate (M), extreme (E) and collapse (C) can be expressed as: $P[E] = P[C \mid Y] - P[E \mid Y]$, $P[M] = P[E \mid Y] - P[M \mid Y]$, $P[S] = P[M \mid Y] - P[S \mid Y]$, $P[N] = 1 - P[C \mid Y]$, respectively. DPM can be obtained either empirically by using past earthquake data and experiences, or analytically by performing nonlinear analysis for the structure, or by judgmental and hybrid methods. DPM through empirical or expert judgement can be regarded as a direct method of vulnerability assessment where damage to building typology is directly related to ground motion intensity. Selection of any one of the methods depend upon the damage data used for their generation.

2.3.1 Damage Probability Matrix from Expert Opinion

Damage probabilities based on expert opinion was first introduced in ATC 13 (1985) that essentially derived DPM for 78 structures, 40 of which refer to buildings, by asking 58 experts (noted structural engineers, builders, etc.) to estimate the expected percentage of damage that would result to a specific structural type subjected to a given intensity. Damage was described in terms of MMI scale considering the range VI to XII. The assessment of seismic risk and loss using ATC 13 approach was used by several

researchers, for example, for the city of Bogotá, Colombia (Cardona and Yamin 1997) to estimate and establish damage motion relationships. The primary drawback of this method is its subjectivity, as these are based exclusively on the subjective opinion of the experts. The DPMs based on expert opinions are also difficult to calibrate or modify in order to incorporate new data or technologies. Further, it is difficult to extend ATC 13 methodology to other building types and other regions, as well as to individual building characteristics. Nevertheless, it was the first relatively thorough study on earthquake damage and loss estimation and became the standard reference for many earthquake vulnerability assessments until the mid-1990s.

2.3.2 Damage Probability Matrix from Empirical Studies

Whitman et al. (1973) was the first to have systematically compiled statistics on both structural and non-structural damage to various building typologies from damage experiences after 1971 San Fernando earthquake. This has been widely accepted and adopted by people to define the probable distribution of damage. Each value in the matrix (as indicated by "…" in Table 2.6) expresses the probability that a certain building class will experience a particular level of damage as a result of particular earthquake intensity. The degree of damage is expressed in probabilistic terms. As a probability rule, the sum of each column must sum up to unity or 100%. The damage ratio is defined as the repair cost as a ratio of the replacement cost at the time of the earthquake. Apart from the damage data collected from the San Fernando earthquake, a questionnaire was developed to collect information on less damaged buildings. In constructing DPM each building is assigned a damage state based on damage cost and replacement cost (= building area × average building cost per unit area). Nine damage states were considered starting from 0 to 8. When the DPM is developed using observed damage of past earthquakes and applied to regions with similar characteristics to predict damage due to probable future earthquakes, a realistic indication of the expected damage is obtained and many uncertainties are inherently accounted for.

Major limitation of Whitman's DPM lies in the unreliability of the building data collected from surveys. The building data list may contain, say for a particular typology, buildings that do not belong to it, or it may have omitted or disregarded buildings, which should have been kept in the category due to restricted specifications about it. Further,

the actual damage costs are rarely available. If the data obtained for particular ground intensity is for a lesser number of buildings, the DPM constructed is meaningless.

Table 2.6 General format for constructing Damage Probability Matrix (Whitman et al. 1973).

Damage State	Structural damage	Non-structural damage	Damage ratio (%)	Intensity of earthquake				
				V	VI	VII	VIII	IX
0	None	None	0 - 0.05	…	…	…	…	…
1	None	Minor	0.05 - 0.3	…	…	…	…	…
2	None	Localized	0.3 - 1.25	…	…	…	…	…
3	Not noticeable	Widespread	1.25 - 3.5	…	…	…	…	…
4	Minor	Substantial	3.5 - 4.5	…	…	…	…	…
5	Substantial	Extensive	7.5 - 20	…	…	…	…	…
6	Major	Nearly total	20 - 65	…	…	…	…	…
7	Building condemned		100	…	…	…	…	…
8	Collapse		100	…	…	…	…	…

Eleftheriadou and Karabinis (2011) aimed at developing a methodology and obtaining the DPM and vulnerability curves for the empirical seismic vulnerability assessment of typical structural types, representative of the materials, seismic codes and construction techniques used in Greece and generally in Southern Europe. The work considered seismic demand in two forms-

i. The regional macro-seismic intensity (I),

ii. The ratio (a_g/a_o) of the maximum PGA of a certain earthquake event to the PGA that characterizes each municipality in the Greek hazard map. Intensities and PGAs are correlated using Eq. (2.7).

$$\ln(\text{PGA}) = 0.74I + 0.03 \tag{2.7}$$

Five damage state (ds) were considered (Table 2.7) and were given color codes. Central Damage Factor was calculated for each of the damage state. Frequency of different damage states for each structural type exposed to a specific seismic demand is obtained. Next, each element of DPM is obtained simply by cumulating the frequencies from the highest to the lowest level of damage. One matrix is constructed for each structural type expressing the distribution of damage in each intensity level. DPM were

not constructed for intensity less than VI, since for weaker intensities the building damage is almost practically zero. The assumption that the buildings not classified in structural types belong to the undamaged structures, combined with the fact that the non-surveyed buildings are considered undamaged, leads to underestimation of the probability of damage.

Table 2.7 Damage states description as given in Eleftheriadou and Karabinis (2011).

Damage State		Definition
None	ds0	No damage
Green	ds1	Slight damage
Yellow	ds2	Light- moderate damage
Red	ds3	Extensive damage-Partial collapse
Black	ds4	Collapse

2.3.3 Damage Probability Matrix from Analytical Studies

Singhal and Kiremidjian (1996) presented a method to estimate DPM based on nonlinear dynamic analysis of structures rather than based on empirical data. The damage probabilities were estimated from the responses obtained for three building classes (low, medium and high rise frames) based on Monte-Carlo simulation technique. The frames were subjected to an ensemble of ground motions to obtain the nonlinear responses. Again, primary limitation of the method is the subjectivity of the results due to use of particular ground motions.

2.4 Seismic Performance Assessment Methods

Seismic performance can be assessed with different levels of computational efficiency depending on available data and resources. Detailed nonlinear analyses (static or dynamic) are required to be carried out for assessing seismic capacity and performance of structures for a given hazard (demand). The present state-of-the-art for performance assessment methodologies is described in FEMA P-695 (2009). The procedures in FEMA P-695 are based on the concept of incremental dynamic analysis (IDA), which is a computationally intensive procedure that is rarely practical in non-research applications. It is a common practice to use simple nonlinear static analysis procedures or pushover analysis (PO) for performance evaluation of structure using Capacity Spectrum Method (ATC 40 1996), Displacement Coefficient Method (FEMA 356 2000, FEMA 440 2005), or the N2 method (Fajfar 2000) as discussed below. FEMA P-58 (2012) also summarizes

seismic assessment methods, for example, incremental dynamic analysis, limited-suite nonlinear analysis, and simplified nonlinear analysis (e.g., Dolšek and Fajfar 2005). First, a brief description of the simplified seismic assessment methods is provided in this section. This is followed by a concise review of the more recent and advanced seismic assessment methods.

2.4.1 Capacity Spectrum Method (CSM)

CSM, originally developed by Freeman (1998), requires construction of damped elastic response spectrum (or demand spectrum) and capacity spectrum in acceleration displacement response spectrum (ADRS) format using Eq. (2.8) as shown in Fig. 2.5.

$$S_a = \frac{V}{W * \alpha_1} \text{ and } S_d = \frac{\Delta_{roof}}{(PF_1 * \phi_{1,roof})} \tag{2.8}$$

where, α_1 and PF_1 are, respectively, the modal mass coefficient and participation factors for the first natural mode of the structure and $\phi_{1,roof}$ is the roof level amplitude of the first mode. Intersection of capacity and demand spectrum curves gives the performance point (PP) for the structure for a given hazard (Fig. 2.6). ATC 40 suggests three procedures (A, B, C) for using CSM; selection of anyone of which is a personal choice. The basic methodology of procedures A, B, and C is same, but differs in the assumption of post yield stiffness for deriving the bilinear capacity curve and in computational effort required. Determination of PP is an iterative procedure. An initial trial PP is determined from equal displacement approximation, and compared with the PP obtained from intersection of capacity spectrum and demand spectrum effectively damped for nonlinearity using the concept of effective viscous damping (β_{eff}). This procedure is iterated until PP obtained at a particular iteration is approximately equal (± 5% variation) to the PP obtained in the previous iteration.

Although the CSM is simple, its basic disadvantage is that the lateral force distribution for performing nonlinear static analysis of buildings is assumed that corresponding to the first mode of vibration only. Other higher dominant modes are not considered. Also, the PP obtained is dependent on elastic response spectra (rather than inelastic response spectrum) effectively damped for nonlinearity using the concept of effective viscous damping. To overcome such drawbacks, modified procedures are proposed in literature, e.g., Fajfar (2000) introduced the concept of inelastic spectra using

ductility dependent reduction factors. Chopra and Goel (1999a, 1999b) also introduced the idea of constant ductility dependent inelastic demand diagram and commented that deformation obtained by ATC 40 method is underestimated.

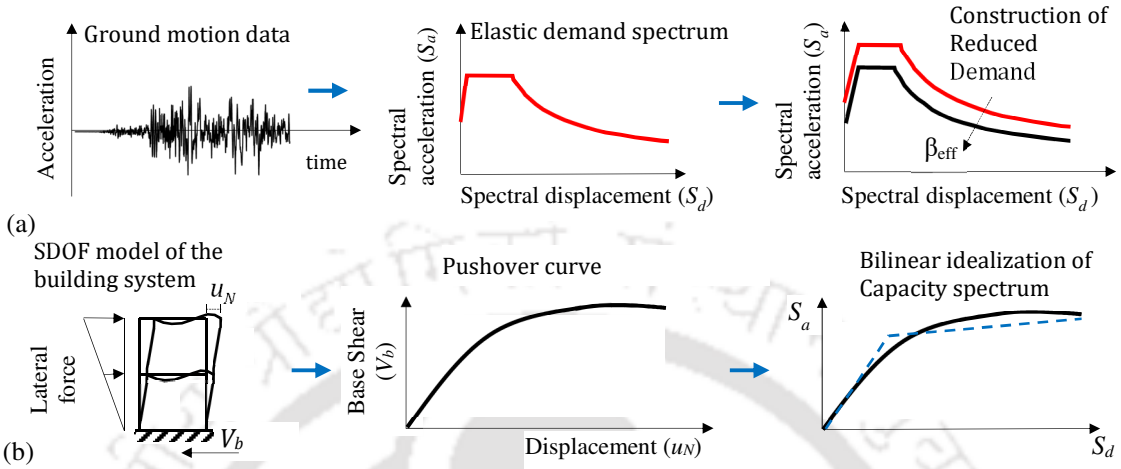

Figure 2.5 Steps in Capacity Spectrum Method (ATC 40 1996): (a) Construction of demand spectrum, and (b) Construction of capacity spectrum.

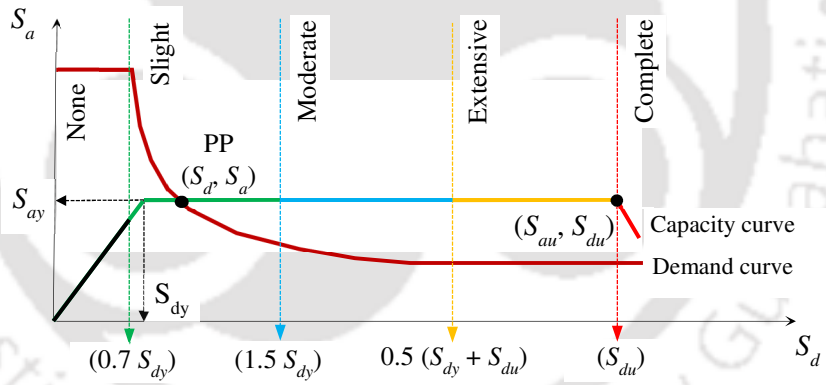

Figure 2.6 Plot representing capacity curve and demand curve (red) in ADRS format; performance point (PP) as obtained in CSM (ATC 40 1996) and associated damage state thresholds and quantification as per Lagomarsino and Giovinazzi (2006).

2.4.2 Displacement Coefficient Method (DCM)

DCM is a direct method as compared to CSM that modifies linear elastic response of the building (roof displacement) with the help of several coefficients (C_0, C_1, C_2, and C_3) to calculate a target displacement (δ_t) given by Eq. (2.9) (FEMA 356 2000). Unlike CSM, conversion of capacity and demand into ADRS is not required in DCM.

$$\delta_t = C_0 C_1 C_2 C_3 S_a \frac{T_e^2}{4\pi^2} \tag{2.9}$$

C_0 relates spectral displacement to likely building roof displacement, and C_1, C_2, C_3 take into account inelastic displacement, hysteresis effect, and P-delta effects, respectively. δ_t may be considered to be equivalent to the PP evaluated in CSM. The DCM is generally not preferred since the target displacement is heavily dependent on empirical relations for estimation of the coefficients.

2.4.3 N2 method

The N2 method (Fajfar and Gašperšič 1996 and Fajfar 2000) is a non-iterative method and is based on ductility dependent inelastic response spectrum. Originally, the method was developed for symmetric systems that oscillate predominantly in the first mode. Later on, it was extended to consider asymmetric buildings and buildings where higher modes are dominant. This method provides the user with graphical visualization of the performance of structure, though the graphical step is not necessary to obtain the seismic demand.

The method starts with determining the elastic response spectrum in acceleration displacement (A-D) format. Next, the base shear (V_b)–roof displacement (D_t) relationship for a multi degree of freedom (MDOF) is obtained from nonlinear static (pushover) analysis. For this, a displacement shape is assumed and lateral load distribution is determined based on the assumed displacement shape. Thus, load and displacement are mutually dependent in N2 method, which is not the case in case of ATC 40 methods. The V_b - D_t relationship obtained for the MDOF system is transformed to single degree of freedom (SDOF) system by dividing V_b and D_t by modal participation factor. The SDOF V_b - D_t relationship is approximated as elasto-plastic force deformation relationship and finally converted to A-D format which is called capacity diagram. The original method is applicable for those systems in which strain hardening has no practical influence on the results, so a simple zero post-yield stiffness is assumed. For a given demand curve (or elastic response spectrum), the seismic demand on the SDOF model is determined as the intersection of inelastic demand curve in A-D format and the SDOF capacity diagram. The inelastic demand curve is obtained in two steps. First, the reduction factor due to ductility (R_μ) is determined as the ratio of elastic to inelastic accelerations where the parameters are obtained using equal displacement rule. Next, the ductility factor (μ) is

determined using Eq. (2.10) in order to obtain the inelastic displacement demand (S_d) from elastic displacement demand (S_{de}) as in Eq. (2.11).

$$\left.\begin{aligned} \mu &= R_\mu && ; T^* \geq T_C \\ \mu &= (R_\mu - 1)\frac{T_C}{T^*} + 1 && ; T^* < T_C \end{aligned}\right\} \tag{2.10}$$

$$S_d = \frac{\mu}{R_\mu} S_{de} \tag{2.11}$$

Here, T_C is the characteristic period of the ground motion, and T^* is the elastic period of the idealized bilinear equivalent SDOF system. The above relations represent that the demand spectrum is reduced with R_μ if T^* falls in acceleration sensitive region of the demand curve, otherwise reduced with μ if T^* falls in velocity sensitive region. Although, the N2 method is simple, the estimates of inelastic displacements obtained for short period range are found to be less accurate. Moreover, the simplistic equations used for obtaining the inelastic demand spectra (in N2) is inappropriate for near fault ground motions, or soft soil conditions, or for hysteresis loops with significant strength deterioration. In contrast to N2 method, the CSM method considers a damping modification factor to enable simulation of imperfect hysteresis loops.

In addition to these three common methods, researchers have developed other methods for performance assessment, e.g., modified CSM (Chopra and Goel 2000). FEMA 440 (2005) evaluates the accuracy of CSM and DCM for estimation of displacement demand on inelastic single degree of freedom (SDOF) systems and suggests improvements over both the methods. It proposes simplified expressions for different coefficients used in DCM, and modified expressions for evaluation of effective natural period and effective damping for CSM while taking care of the ductility demand. Interestingly, only a minor difference was observed in the PP obtained using these different methods in the present study, when applied to regular frames with minor strain hardening in capacity curves. This shows that any of these methods can be used for performance assessment of regular symmetric buildings without compromising accuracy.

2.4.4 Nonlinear Dynamic Procedures

The structural response to a particular ground motion or a set of ground motions can be obtained by nonlinear time-history analysis, also known as nonlinear dynamic analysis. The structural response in dynamic analysis consists of the complete history of any particular response of the structure when a ground motion is applied at the base of the structure. The dynamic equation to be solved is given by Eq. (2.12).

$$M\,\ddot{u}(t) + C\,\dot{u}(t) + K\,u(t) = -M\,\ddot{u}_g(t) \tag{2.12}$$

Here, K is the stiffness matrix, C is the damping matrix, M is the diagonal mass matrix, u, $\dot{u}$ and $\ddot{u}$ are the displacement, velocity and acceleration of the structure at any instant t, in case for earthquake loading these are relative values with respect to ground, and $\ddot{u}_g$ is the ground acceleration. The solution of the above equation of motion can be found out by either direct integration method or by modal analysis method. Since the response of the structure wholly depends on the applied earthquake ground motion, it is very difficult to understand the seismic performance of the structure by doing just one time-history analysis. Therefore, a set of ground motions are applied at the base of the structure in order to systematically assess the seismic performance of the structure with varying earthquake intensity. Several methods have been used in the past for structural performance assessment based on nonlinear dynamic analyses using actual recorded as well as synthetic ground motions scaled for different intensity measures. Some of these methods, such as incremental dynamic analysis, multiple stripe analysis, cloud analysis, etc., are discussed next.

2.4.4.1 Incremental Dynamic Analysis (IDA)

Vamvatsikos and Cornell (2002) defined incremental dynamic analysis (IDA) as a parametric analysis method to estimate more thoroughly the structural performance under seismic loads. It involves subjecting a structural model to one or more ground motion records, each scaled to multiple levels of intensity, thus producing one or more curves of response parameterized versus intensity level. IDA also uses the same analogy of pushover analysis method where the seismic loading is scaled up to failure. The intensity levels should be selected in such a way that the structure should transform from linear elastic behavior to global collapse. Objectives of the IDA include understanding the structural response in relation to different levels of applied ground motion records including the rarer and severe ground motion levels (Vamvatsikos and Cornell 2002).

Incremental dynamic analysis can be performed on any structure using either a single ground motion with varying intensities or by using multiple ground motions. A brief review of both these methods are provided here.

i. Single-Record IDA

Incremental dynamic analysis involves performing a series of dynamic analysis of the structural model by monotonically increasing the intensity levels of the applied ground motion designed to force the structure from elastic range to global collapse. A Single-Record IDA study is a dynamic analysis study of a given structural model parameterized by the scale factor of the given ground motion time-history. It is simply known as IDA or dynamic pushover (DPO), and it involves a series of dynamic nonlinear analyses performed under scaled samples of an accelerogram, whose intensity measures are, ideally, selected to cover the whole range from elastic to nonlinear and finally to collapse of the structure. The purpose is to record damage measure of the structural model at each level of intensity measure of the scaled ground motion, the resulting response values often being plotted versus the intensity level as continuous curves. An IDA curve is a plot of a state variable (damage measure) recorded in an IDA study versus one or more intensity measures that characterize the applied scaled accelerogram.

'*The Hunt and Fill'* algorithm proposed by Vamvatsikos and Cornell (2002) is a key tool to fix the optimum number of intensity measure levels, and hence to optimize the number of analysis. Since the intensity measure level range is dependent on the accelerogram, it will tend to unbalance the distribution of runs. Hunt and fill algorithm is an enhancement of simple stepping algorithm by Yun et al. (2002) where the speed of convergence to the flat line is increased by increasing the step size within some tolerance, this is the '*hunting*' phase of the algorithm. Usually, IDA curves tend to become flat near the collapse point, so a finer discretization of intensity measure is required in this region.

Performance levels or limit-states are important ingredients of performance based earthquake engineering. Since IDA is one the available tools for Performance based analysis, it is required to define the limit state values on the IDA curve in order to understand the structural performance in a better way. In IDA the prediction of collapse is associated with the numerical instability in most of the programs. The non-convergence of the time integration scheme is generally treated as equivalent to the structural collapse. However, the accuracy with which the collapse can be predicted is well related to the

quality of the numerical model, the stepping of the integration, and even the round off error. Therefore, some basic rules are required to be framed for identifying the collapse point on the IDA curves. Two commonly used rules are damage measure (DM) based rule and intensity measure (IM) based rule as shown in Fig. 2.7.

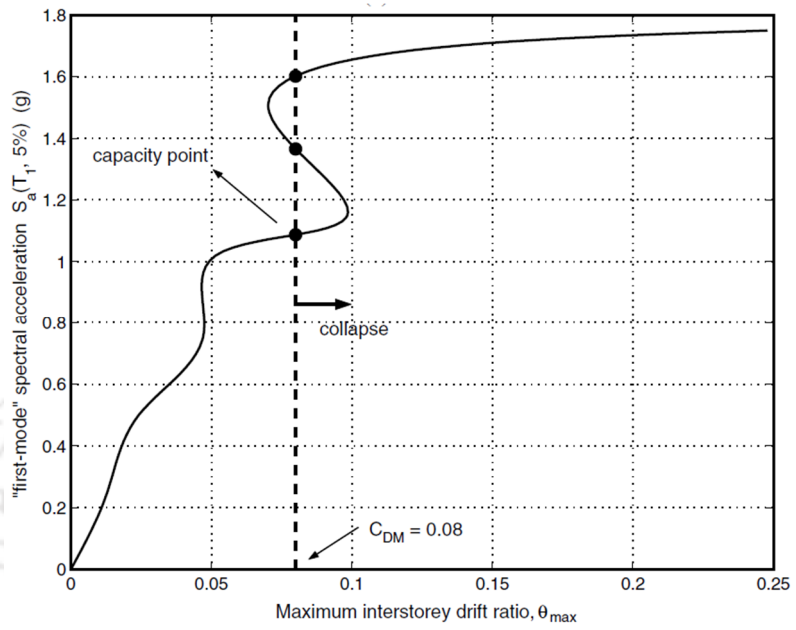

(a)

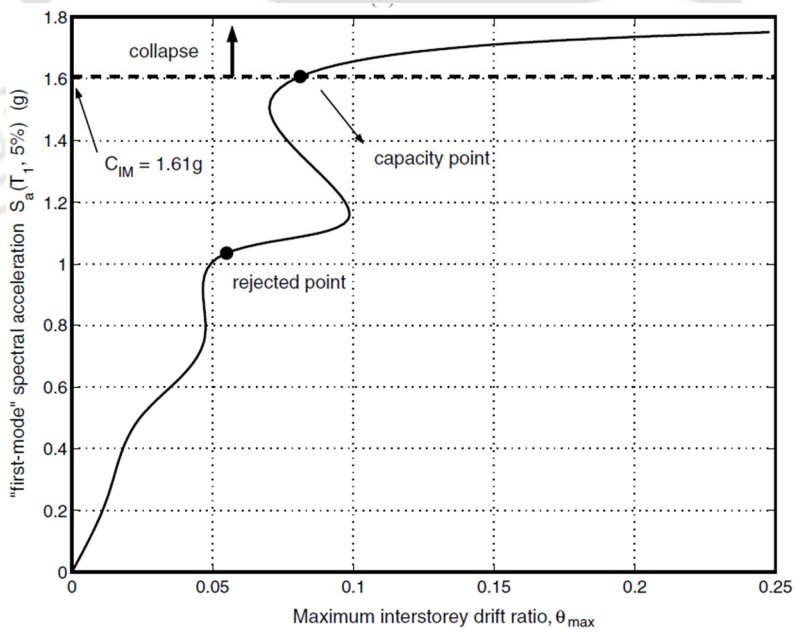

(b)

Figure 2.7 Identification of capacity points on IDA curves based on: (a) damage measure (DM) based rule and (b) intensity measure (IM) based rule (Vamvatsikos and Cornell 2002).

As the name suggests, degree of damage to the structure is used to identify the collapse point in DM based rule. When the DM increases beyond a certain value (C_{DM}) the structural model is assumed to be in the limit state corresponding to C_{DM}. The limit state values can be obtained through experiments, theory, or engineering experience and they may not be deterministic but can have a probability distribution. Sometimes IDA curves may have a *wave region*, and for a particular limit state, it may have two intersecting points on the curve (Fig. 2.7). This ambiguity can be handled by providing some specified rules like defining the limit state point as that corresponding to the lowest DM. This ambiguity is avoided in the IM based rule of assessing the collapse capacity by avoiding the multiple intersecting points. By having a single point (C_{IM}) on the IDA that clearly divides it into two regions, lower IM part is non-collapse region and upper IM part is collapse region. However, in case of multi-record IDA the limit state is required to be defined in each curve individually. FEMA 350 (2000) defines the collapse point as the last point on the curve with tangent slope equal to 20% of the elastic slope. As the possible *wave region* can provide more than one capacity point, in such cases the highest value is considered as capacity point.

ii. Multi-Record IDA

Since the structural response, and hence the IDA curve, is highly dependent on the characteristics of the ground motion records, single-record IDA may not be sometimes sufficient to characterize the complete behavior of the structure, especially those structures in which higher modes are predominant. Therefore, in multi-record IDA several accelerograms are used with varying intensities in order to interpret the complete behavior of structure under a wide spectrum of ground motions. A multi-record IDA is a collection of single-record IDA results with a common selection of IMs and same DM.

2.4.4.2 Multiple Stripe Analysis (MSA)

Multiple Stripe Analysis (MSA) is a nonlinear dynamic analysis procedure suitable for probability-based assessment of structures for multiple performance levels. Jalayer and Cornell (2009) classified the nonlinear dynamic analysis procedures into two groups. The first group, defined as *wide-range*, is suitable for making probabilistic assessments over a wide range of tolerable probability levels (e.g., MSA and IDA). Multiple stripe analysis is suitable for making probability-based assessments for a wide range of spectral acceleration values and/or limit states and IDA can be implemented in

order to locate the onset of global dynamic instability (collapse capacity) in the structure. The second group, defined as *narrow-range*, is suitable for making probabilistic assessments for a tight interval of tolerable probability values (e.g., Single stripe and double stripe analysis). These methods are found to be useful particularly when only limited number of dynamic analyses runs are feasible. The probabilistic performance objective for the assessments is defined by taking into account the uncertainty in the ground motion. Baker (2015) compared the efficiency of collapse fragilities obtained from incremental dynamic analysis and multiple stripes analysis. Multiple stripes analysis is seen to be more efficient than incremental dynamic analysis because analyses can be targeted at a limited number of important intensity measure levels, rather than requiring analysis at high or low intensity measure levels associated with collapse for some ground motions. However, it is noticed that some knowledge of the building's capacity must be available prior to analysis so that relevant portions of the fragility curve can be approximately identified.

MSA can be carried out both for the full range of ground motion intensities of interest and for a limited range of ground motion intensity levels. MSA, as suggested by its name, refers to a group of 'stripe' analyses performed at multiple spectral acceleration levels, where a stripe analysis consists of structural analyses for a suite of ground motion records that are scaled to a common spectral acceleration (Jalayer and Cornell 2009). The suite of ground motion records used for performing each stripe analysis should ideally be representative of the seismic threat at the corresponding spectral acceleration. The single stripe analysis, on the other hand, involves structural dynamic analyses for a set of records scaled to a common spectral acceleration value as described before. The output of single stripe analysis is referred to here as the 'stripe response'. Similarly, the common spectral acceleration value is referred to as the spectral acceleration of the stripe. The stripe response can be used to estimate the median and fractional standard deviation for structural response conditioned on the spectral acceleration of the stripe. The onset of 'collapse' in a structure for a ground motion record is identified as the point where the structural response (e.g., maximum interstorey drift) increases drastically when the spectral acceleration of the record is increased by a small amount. However, the single stripe response does not provide displacement versus spectral acceleration slope information. Therefore, a minimum number of two stripe responses are necessary for getting sufficient information about all the necessary parameters for probabilistic

assessment of structures. Therefore, the double stripe method, consisting of two separate single stripe analyses (the original stripe response plus an additional stripe response sufficiently close to the original stripe), is to be used for efficient structural assessment.

2.4.4.3 Cloud Analysis

The application of MSA and IDA are computationally demanding and time-consuming as the nonlinear dynamic analyses are required to be repeated for increasing levels of ground motion intensity considering scaled ground motion time-histories. In contrast, the cloud method is more efficient since it involves the nonlinear analysis of the structure subjected to a set of un-scaled ground motion time-histories (Jalayer et al. 2015). The cloud method has also been employed to model the record-to-record variability in ground motion, structural modelling uncertainties, and the uncertainties in material properties and construction details (Jalayer et al. 2007, Jalayer et al. 2011). Cloud analysis is based on simple regression in the logarithmic space of structural response versus seismic intensity for a set of registered records. One can substantially reduce the number of nonlinear dynamic analysis runs using the cloud method by choosing appropriate ground motion records. Therefore, its strong dependence on the suite of selected ground motion records is a big limitation of the method. For example, the resulting regression prediction (and also its dispersion) can change as a function of the range of ground motion intensities covered by the selected records (Jalayer 2003). So far, the cloud method has been used primarily for taking into account the uncertainties related to the record-to-record variability. But, a few past studies have also made efforts in taking into account in an approximate manner the epistemic uncertainties, i.e., uncertainties in capacity (Cornell et al. 2002, Jalayer and Cornell 2003, Jalayer et al. 2007). The effect of the epistemic uncertainties in these works is represented in the form of an overall increase in the dispersion for the probability of exceeding the limit state. However, these studies were not able to capture the bias in median limit state probability due the effect of epistemic uncertainties (Jalayer et al. 2015). The Bayesian cloud method combines cloud analysis and Monte-Carlo simulation in a Bayesian framework in order to take into account both the structural modelling uncertainties and record-to-record variability (Jalayer et al. 2015). Again, there are limitations of the Bayesian cloud analysis related to the number and the selection of the ground motion records.

The nonlinear dynamic methods such as IDA, MSA, and even cloud analysis to a certain extent are suitable for evaluating the relationship between engineering demand

parameter and IM for a wide range of IM values; however, their application can be quite time-consuming as the nonlinear dynamic analyses are usually repeated for several ground motions for increasing levels of intensity measure. Therefore, nonlinear static analysis procedures are hugely popular for seismic performance assessment of structures, especially the first-mode predominant structures. Once the seismic assessment is complete, the next step is to characterize the performance of the structures in a probabilistic manner by carrying out seismic fragility and vulnerability analysis. These concepts are discussed briefly in the next section on seismic fragility and vulnerability assessment.

2.5 Seismic Fragility and Vulnerability Assessment Methodologies

Vulnerability may be defined as the extent to which communities, structures, services or geographic areas are likely to be damaged or disrupted by the impact of a particular hazard, because of their nature, construction and proximity to hazardous terrains or a disaster prone area. Seismic vulnerability is a measure of the seismic strength or capacity of a structure. The seismic vulnerability of a structure can be described as its susceptibility to damage by ground shaking of a given intensity (Calvi et al. 2006). The aim of vulnerability assessment is to obtain the probability of a given level of damage to a given building type due to a scenario earthquake. The vulnerability of any structure is represented in the form of either Damage Probability Matrix (DPM) or vulnerability curves. The major objectives of vulnerability analysis on a large scale, such as that of a town are:

i. To plan preventive interventions for the seismic risk mitigation,

ii. To help the management of the emergency after a major earthquake, and

iii. To be aware of the impact of an earthquake to group of buildings in an area.

In assessing the vulnerability of an ordinary structure in the field, the first step is to assess the building type. Next, vulnerability models are utilized to represent mathematically these structural types. Vulnerability models are the tools to establish a correlation between hazard and structural damage (Guéguen 2013). Seismic hazard may be represented in terms of PGA or seismic intensity or the response spectrum. Damage is usually classified in terms of performance level of buildings. The review of the built

environment for seismic vulnerability estimation is normally carried out in the light of earthquake resistance of buildings, past earthquake damage history and repair thereof, construction practices being adopted, building typology, seismic zoning of the area, building samples, detailed survey of selected buildings, and creation of database and its quantitative and qualitative analysis.

The main steps of a vulnerability analysis (Guéguen 2013) thus can be summed up as follows:

i. Acquisition of the data available in the area of interest, identification of building classes and definition of the related vulnerability models,

ii. For each class, the definition of building parameters on which models are based; according to the data available, the parameters set can be single or differentiated for a micro-area,

iii. Partition of the territory into a number of zones, each characterized by a uniform hazard; disaggregation of the exposure data into different classes homogeneous for vulnerability,

iv. For each building class and micro-area, evaluation of the performance point, fragility curves and damage probabilities (taking into account more or less accurately the uncertainties involved).

Seismic vulnerability assessment mainly includes two broad approaches- quantitative approaches that include demand-capacity calculation for the structure and the qualitative approach that estimates structural scores based on different observed parameters for the building. A logical tree can be stated for assessing seismic vulnerability as in Fig. 2.8.

Several researchers attempted to develop and propose vulnerability assessment procedures that can be utilized for different types of data (for example, building type) available for buildings. There are two distinguished approaches for vulnerability assessment - the probabilistic approach and the deterministic approach. Probabilistic approach is preferred when past earthquake damage statistics are available, whereas a deterministic method depends on assessment of performance by buildings. This is done

by computing the Performance Point (PP) as the intersection point of ground motion demand response spectrum and capacity spectrum of the structure.

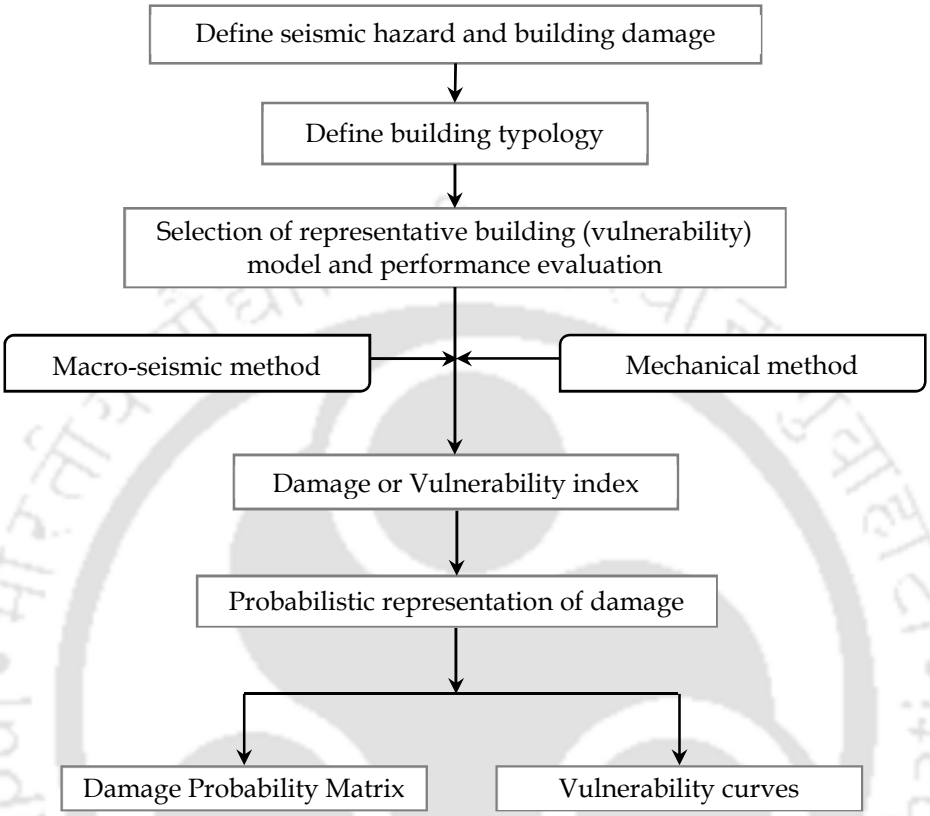

Figure 2.8 Diagrammatic representation of the steps involved in seismic vulnerability assessment of buildings.

Seismic vulnerability assessment of building typologies using advanced methodologies are of major importance for the reduction of seismic risk in urban areas. The development of an advanced and integrated methodological tool for the efficient seismic risk management of lifeline and utility systems is necessary for the establishment of efficient and effective mitigation schemes. A vulnerability assessment needs to be made for a particular characteristic of ground motion, which can represent the seismic demand of the earthquake on the building. The selected parameter should be able to correlate the ground motion with the damage to the buildings. Traditionally, macro-seismic intensity and PGA have been used for the purpose. More recent proposal is to relate seismic vulnerability of the buildings to spectral acceleration obtained for the ground motions. Each vulnerability assessment method models the damage on a discrete damage scale, which includes the MSK scale, the MMI scale, and the EMS 98 (Grünthal 1998).

Several methodologies have been proposed in the past literature for seismic vulnerability assessment of structures. Most of the methods are primarily based on following two approaches (Guéguen 2013):

i. Macro-seismic (observational) approach

It is an observed damage-based vulnerability method calibrated using post-earthquake data obtained from earthquake damage surveys. It is used when macro-seismic intensity hazard maps are available. For risk assessment of large areas, where the building information may be available only at a low resolution, macro-seismic intensity scales are most commonly used for assessing vulnerability. Traditionally DPMs are used to represent the damage in discrete form. Later fragility curves relating ground motion intensity to mean damage grade were introduced to represent vulnerability in a continuous form. Fragility curves are defined using vulnerability index and ductility index. The macro-seismic method was originally developed by Lagomarsino and Giovinazzi (2006) making use of classical probability theory and of the fuzzy-set theory for European buildings. Fragility curves and DPMs describe the conditional probabilities of sustaining different degrees of damage at given levels of ground motion.

ii. Mechanical approach

Mechanical models describe the structural response of a system by means of a capacity curve that provides essential information about the structural properties of a building, like stiffness, strength, and displacement capacity. This approach is applied when the hazard is provided in terms of peak ground accelerations and spectral values. The vulnerability of the buildings is defined in terms of a force-displacement curve called capacity curves, representative of inelastic equivalent single-degree-of-freedom (SDOF) system, within the mechanical method. For vulnerability assessment at large scale, capacity curve aims at idealizing the response of an entire structural inventory with similar behavior. Validation of the mechanical models is an important issue since direct comparison with actual damage is not generally possible unlike macro-seismic models. As a solution to this issue, the results of both the macro-seismic and mechanical models can be compared. This requires correlation between hazard parameters (for example, relation between macro-seismic intensity and PGA). Main advantage of the mechanical procedure is that the structural response is defined based on seismic input given by formal hazard analysis.

Dolce et al. (2006) classified methodologies for the evaluation of structural vulnerability in four groups:

i. *Direct*- This method assesses in a simple way the damage caused in a structure by a given earthquake,

ii. *Indirect*- This determines first a vulnerability index of the structure and then assesses the relationship between damage and seismic intensity,

iii. *Conventional*- This is essentially a heuristic method, introducing a vulnerability index independent of the damage prediction,

iv. *Hybrid*- This combines elements of the previous methods with expert judgments. Selection of one of these methods depends on the objectives of the study, the type of the results required, and on the available information.

Calvi et al. (2006) suggested a similar classification of methods for vulnerability assessment for use in loss estimation as Empirical, Analytical, and Hybrid. Various methods for the assessment of the vulnerability of buildings differ in expenditure and precision. The method to be chosen depends not only on the objective of the assessment but also on the availability of data and technology.

Based on the past literature, vulnerability assessment methods can be broadly categorized as:

i. Expert judgement methods

ii. Empirical methods

iii. Analytical or mechanical methods

iv. Hybrid methods

2.5.1 Expert Judgement Methods

The prime goal of the vulnerability assessment is to find the probability of damage that a particular existing building typology will experience in case of an earthquake of given intensity. When the use of empirical or analytical method is not feasible, opinions from experts are sought based on their expertise for vulnerability assessment. ATC 13

defines an expert as a person with high degree of knowledge in a particular area, which may be attained through organized research, field experience, or other means. In expert judgement method, first, the building typologies are defined (Fig. 2.9). A seismic intensity scale (for example, MSK or MMI) is chosen to define the intensity of earthquake. Next, a damage scale is defined to associate some damage level to buildings. These details are explained to the experts in detail after which they are given a set of questionnaire for obtaining probabilities of damage occurring in a building or a set of buildings under different ground motion intensity. The experts are asked to self-rate their experiences within 0 to 10, where zero means no experience in the field and 10 means highly experienced. Expert opinion can be taken in two ways:

i. Delphi method

ii. Consensus method

In Delphi method experts provide their individual answers or comments to the questionnaires solely based on their own experience in the field without any type of consultation with other experts. In contrast, in consensus method, the group of experts chosen are asked to arrive at a conclusion through discussion without anonymity. Combined efforts are put in and issues are settled through discussions in the consensus method. The main aim of any of these methods is to combine knowledge of an expert group in an unbiased manner. Responses of all the experts for the given questionnaire are collected and aggregated through statistical means to conclude. The results are resent to the experts and questionnaire process is iterated to revise the experts comments, if found necessary.

Drawbacks of expert opinion method

i. The weakest aspect of expert opinion method is the possibility of bias. Although questionnaire is completed in a highly controlled environment, biases can come into results due to various reasons, such as, selection of experts, personal/professional/political motivations, overconfidence of the experts, and time interval since last major destructive earthquake.

ii. The opinions are based on subjective judgement given by the experts based on their experience from past earthquakes and limited data.

iii. Bias may also be introduced because some experts are more vocal than the others are.

iv. Expert opinion based vulnerability assessment can only represent average conditions and may not be suitable for high intensity motions.

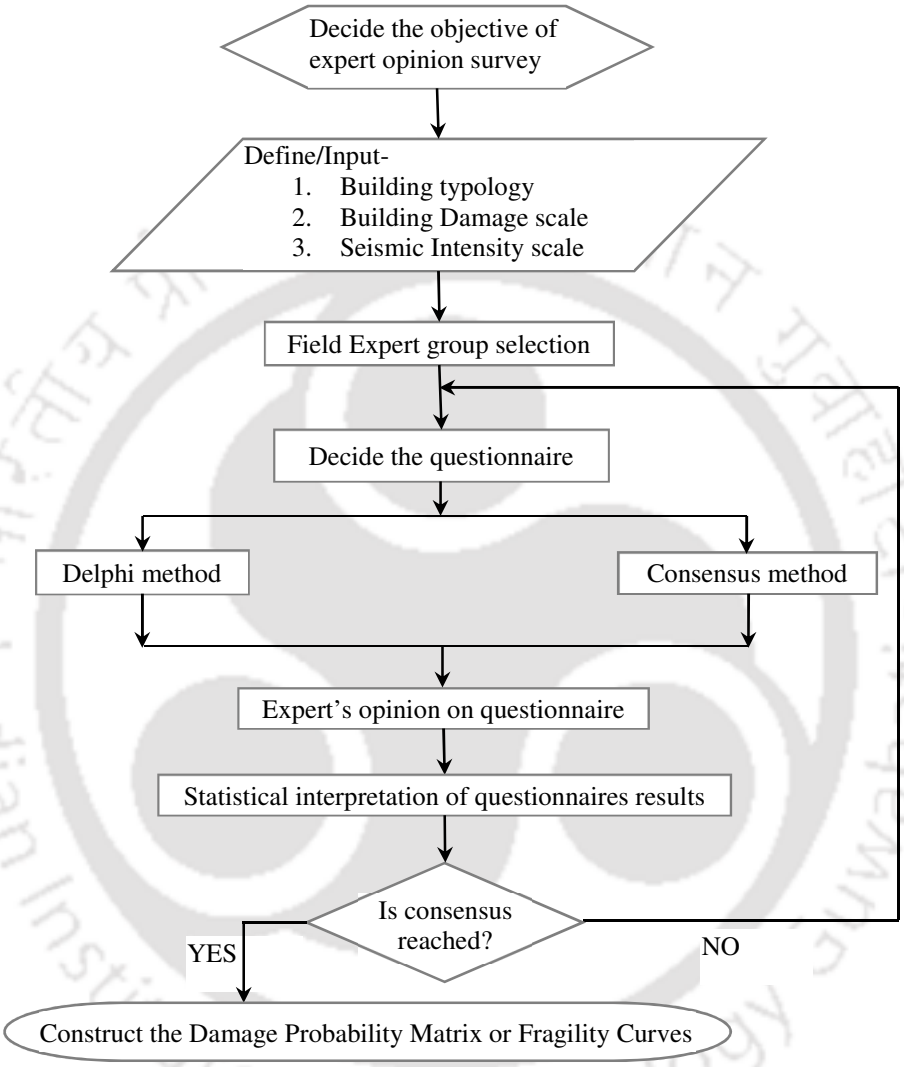

Figure 2.9 Flowchart for vulnerability assessment based on expert opinion.

2.5.2 Empirical Methods

Empirical method is a way of obtaining the required information by means of observation (direct or indirect) and experience. Empirical vulnerability assessment is based on the distribution of damage reported in post-earthquake surveys. The methods were initially developed as a function of macro-seismic intensities because of the fact that hazard maps were originally developed in terms of these scales. Empirical data can be analyzed quantitatively or qualitatively. This method can be used for seismic

vulnerability estimation of buildings if information on behavior of buildings after a damaging earthquake along with the earthquake data is available. As the results are directly related to the actual building damage, the vulnerability assessment is realistic. The process involved in empirical vulnerability assessment is shown in Fig. 2.10. There are basically two approaches for empirical study of seismic vulnerability: by constructing the damage probability matrix (DPM) or vulnerability curves. Empirical vulnerability functions can be constructed directly from past earthquake observations of losses collected over sites affected by different intensities of strong ground motion (Rossetto et al. 2013).

Drawbacks of empirical method

i. The empirical methods are mainly based on observed damage of the building stock. For defining vulnerability macro-seismic intensity scale is used to define ground motion input data, which is not a reliable measure of ground motion.

ii. Post-earthquake building damage statistics at sites are collected for multiple ground motions. Since large magnitude earthquakes are infrequent, the available data mostly represent small ground motions that result in low damage to buildings.

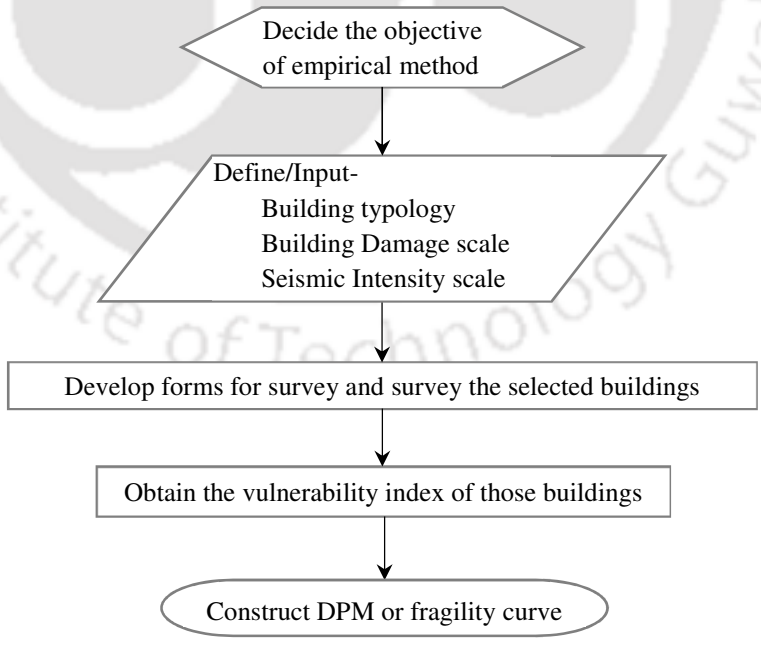

Figure 2.10 Flowchart for empirical vulnerability assessment of buildings.

2.5.3 Analytical or Mechanical Methods

The structural engineering community has developed a new generation of design and rehabilitation procedure that incorporates performance based engineering concepts. Damage control can only be achieved by introducing some kind of nonlinear analysis (static or dynamic) into the seismic design methods. As stated by Calvi et al. (2006), one of the main reasons for which the analytical/mechanical methodologies are becoming popular for use in risk and loss assessment is the technological advancements in the field of seismic hazard assessment, such as the derivation of seismic hazard maps in terms of spectral ordinates in place of macro-seismic intensity or PGA.

Most appropriate approach seems to be a combination of nonlinear static analysis and response spectrum analysis. Available simplified nonlinear analysis methods, referred to as nonlinear static analysis procedures (NSP), includes the capacity spectrum based methods (for example, ATC 40 1996, FEMA 273 1997) that use the intersection of the capacity ("pushover") curve and a reduced response spectrum to estimate maximum displacement; the displacement coefficient method that uses pushover analysis and a modified version of the equal displacement approximation to estimate maximum displacement; and the secant method that uses a substitute structure and secant stiffness. Some newer methods have also evolved from the basic procedures, for example, the N2 method based on capacity spectrum method.

The process involved in analytical vulnerability assessment of building typologies is shown in Fig. 2.11. In each of these methods, first a mechanical model needs to be defined that suitably represents a building stock. The nonlinear static analysis procedures involve the monotonic application of lateral forces of increasing amplitude or displacements to the mechanical model until the displacement of the control node in the mathematical model exceeds a target displacement (FEMA 273 1997). A detailed review of these performance assessment methods is already carried out in the previous section of this chapter. Structural response is obtained by means of a force-displacement curve, which is also known as pushover curve or capacity curve of the structure. Thus, it establishes a relationship of the structural capacity with the structural demand as discussed below. Damage assessment is carried out by comparing the capacity curve with the seismic demand (in the form of a response spectrum). Finally, the probability distribution of each damage levels can be obtained for different building typologies by

defining proper damage levels on the capacity curves. The only disadvantage associated with the method is that it is computationally intensive, time consuming, and needs a proper understanding of the physical behavior of the building subjected to ground motion of varying intensities.

Borzi et al. (2008) and Haldar and Singh (2009) obtained vulnerability curves for a random population of building using simplified pushover curves and displacement response spectra. Input ground motion parameter has been taken in terms of PGA. Displacement capacities from pushover curve and displacement demand from response spectrum are compared to obtain the vulnerability curves.

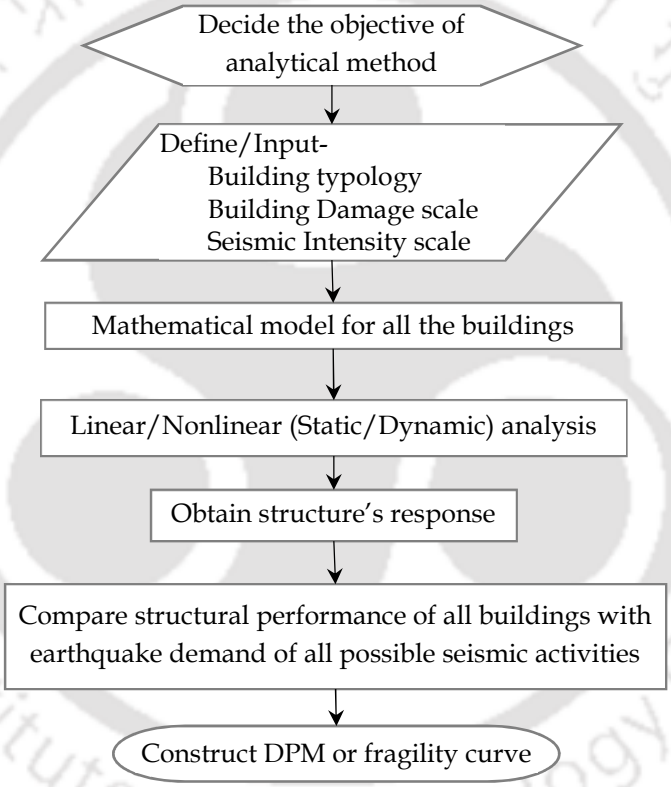

Figure 2.11 Flowchart for analytical vulnerability assessment.

2.5.4 Hybrid Methods

Hybrid methods combine post-earthquake damage statistics with simulated, analytical damage statistics from a mathematical model of the building typology under consideration. Thus, it can be a combination of expert judgement method, empirical method, and analytical methods or any two of them. Hybrid methods of performance assessment can be particularly advantageous when there is a lack of available damage data at certain intensity levels for the geographical area under consideration, and they

allow calibration of the analytical model to be carried out. Furthermore, the use of observational data reduces the computational effort that would be required to produce a complete set of analytical vulnerability curves or damage probability matrix (DPM). Kappos et al. (2006) derived vulnerability curves in terms of peak ground acceleration as well as spectral displacement. The authors considered several RC and URM buildings in Greece and analyzed to obtain pushover curves, and hence, the standard capacity curves. Analytical vulnerability curves are further calibrated using the damage database of the buildings in Greece.

2.5.5 Seismic Vulnerability Assessment using RVS

Rapid Visual Screening (RVS) is a quick and simple method for visual evaluation and collection of observed data of the building that requires only limited information. RVS is useful for all buildings except critical structures where detailed vulnerability assessment is always the requirement. Vulnerability assessment is a three level procedure that consist of the following (Jain et al. 2010, Sinha and Goyal 2004):

i. Rapid visual screening or Level 1 procedure involving physical screening of the building stock,

ii. Simplified Vulnerability Assessment or Level 2 procedure that requires simplified engineering analysis,

iii. Detailed Vulnerability Assessment or Level 3 procedure that is computationally extensive and requires nonlinear analysis to be carried out for the building model to evaluate its performance.

The RVS method was originally developed by the Applied Technology Council (ATC) in the late 1980's and published in 1988 in the Federal Emergency Management Authority (FEMA) 154 report. Later, it was modified in 2002 to incorporate latest technological advancements and lessons from earthquake disasters in the 1990s. The latest edition is FEMA P-154 (2015) that includes extensive updates, including improvements in the rapid visual screening methodology, the screening forms, and the underlying scoring that can be used for assigning a score to buildings for quantifying their seismic vulnerability. The rapid visual screening procedure, even though originally developed for typical constructions in US, has been widely used in many other countries after suitable modifications deemed necessary for local construction practices. The most

important feature about rapid visual screening procedure is that it permits seismic vulnerability assessment based on walk-around of the building stock in a region under consideration by a trained evaluator with the help of RVS team. RVS utilizes a scoring system that requires the evaluator to identify:

i. The primary structural lateral load-resisting system, and

ii. Building attributes that modify the seismic performance expected for this lateral load-resisting system. The inspection, data collection and decision-making process typically occurs at the building site, and is expected to take around 30 minutes for each building.

The RVS scores are based on the expected ground shaking levels in the region as well as the seismic design and construction practices for the city or region. Different codes and documents provide different methods for estimating the RVS basic score depending upon local building typologies, seismology, and other conditions (for example, FEMA 154 2002, Sucuoğlu et al. 2007, Jain et al. 2010, Ozhendekci and Ozhendekci 2012, FEMA P-154 2015).

If a building receives a score greater than a pre-decided cut-off score, the building is considered to have adequate seismic resistance and expected to have acceptable seismic performance, otherwise, the building is considered vulnerable and needs to be evaluated by a professional engineer having experience or training in seismic design. Use of higher cut-off value implies greater desired seismic safety. The RVS methodology is not intended for structures other than buildings. For important structures such as bridges and lifeline facilities, the use of detailed evaluation method is always recommended. Actual damage of buildings depends on a number of factors that are not included in the RVS procedure. As a result, RVS score should only be used as indicative to determine the necessity of carrying out further simplified or detailed vulnerability assessment of the buildings.

A fragility curve is the reformulation of the results of deterministic structural analysis in a probabilistic way. Like DPM, these are relations expressing the vulnerability as functions of certain parameters that describe the size of an earthquake. However, here damage probabilities are described in a continuous form (cumulative probability distribution function). A vulnerability curve graphically represents the relationship between probabilities of exceeding a particular level of damage versus a parameter

describing earthquake intensity measure (Fig. 2.12). Thus, a fragility curve for a particular damage state is obtained by computing the conditional probabilities of reaching or exceeding that damage state for a given deterministic estimates of spectral response. The conditional probability is defined in the same way as for DPM and can be expressed as in Eq. (2.13) (HAZUS 2013).

$$P[ds \mid S_d] = \Phi\left[\frac{1}{\beta_T}\ln\left(\frac{S_d}{\bar{S}_{d,ds}}\right)\right] \tag{2.13}$$

Eq. (2.13) represents the conditional probability $P[ds \mid S_d]$ of being in, or exceeding, a particular damage state (ds), given the spectral displacement at the performance point S_d. Φ is the standard normal cumulative distribution function and β_T is the normalized standard deviation of the natural logarithm of the displacement threshold ($\bar{S}_{d,ds}$) indicating uncertainties in capacity curve properties, damage levels, model errors and ground shaking.

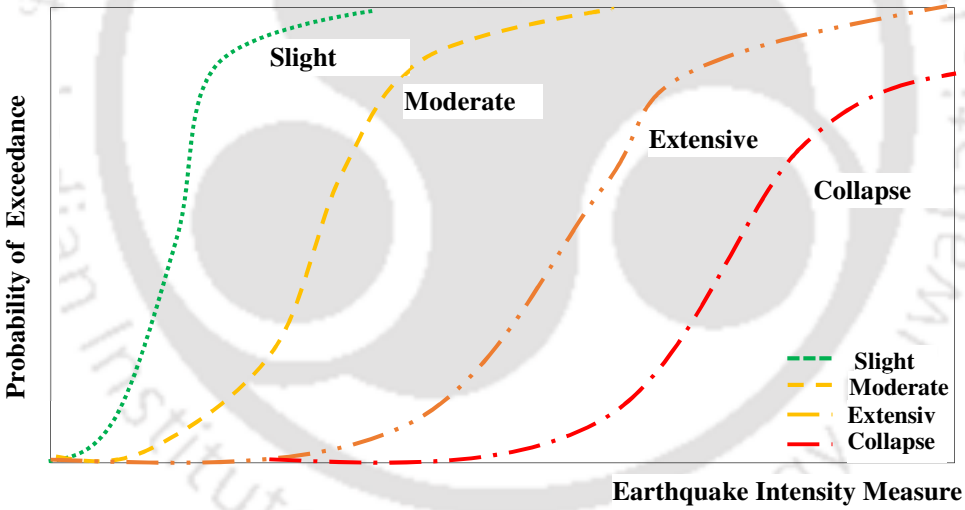

Figure 2.12 Example of fragility curves obtained for different damage states.

Shape of the vulnerability curves depends on the structural type because of the variations in their rate of accumulation of damage with increasing ground motion intensity (Fig. 2.12). The vulnerability assessment is carried out in terms of qualitative parameters by classifying the buildings in several vulnerability classes. A damage index is assigned to each class considering their typological, structural, geometric, and constructive characteristics. A simple mathematical model is then defined as a function

of the evaluated scores relating the seismic input (ground motion parameter) to the expected damage.

2.6 Summary and Gap Areas in the State-of-the-Art

Past literature shows that a lot of work has been carried out in identifying the vulnerable building typologies in different parts of the world, especially in the regions of high seismicity. Different group of researchers have suggested different interesting methods to identify limit states for the damage sustained by the buildings and corresponding damage thresholds reached by different building typologies so that a detailed seismic assessment of the buildings can be carried out for various limit states or performance levels. Several methods, ranging from empirical to nonlinear static analysis and nonlinear dynamic analysis, have been developed for seismic assessment of building typologies. A lot of work has also been carried out to optimize the efficiency and effectiveness of these structural assessment methods to suit a variety of needs, for example, to reduce the computational power and time required for detailed seismic assessment. Assessment has been carried out for different building typologies considering different engineering demand parameters (global and component level) and intensity measures for identifying the seismic demand. Determination of various uncertainties and their sensitivity become important when the seismic assessment of structures is carried out in probabilistic terms. Several approaches have been tried to estimate these uncertainties arising from the random nature of various parameters and their effect on the sensitivity of the seismic response of different building typologies. Using these details, seismic fragility and vulnerability of various building typologies has been assessed by different researchers using variety of methods. Methods have been made available for distinguishing the seismic fragility and vulnerability of different building typologies under different limit states.

Review of literature shows that though open ground storey (OGS) buildings have been identified as highly vulnerable building typology, not much work has been carried out on formal and detailed seismic fragility and vulnerability assessment of these buildings. Influence of openings in infill walls of OGS buildings on seismic response and vulnerability has not been studied with sufficient rigour. OGS buildings are vertically irregular due to severe reduction of lateral strength and stiffness at the ground storey level as the masonry infills are absent in the ground storey. It is very important to

understand which engineering demand parameters would be the most appropriate for realistic seismic fragility and vulnerability assessment of such vertically irregular buildings. Epistemic uncertainties associated with several material, geometric and loading parameters, and aleatoric uncertainties associated with ground motions are required to be evaluated for OGS buildings for further use in seismic vulnerability assessment. Moreover, one must recognize the importance of each of these building parameters on the sensitivity of seismic response of the OGS buildings before assessing the seismic vulnerability. A simplified procedure is required to be developed for seismic fragility and vulnerability assessment of OGS buildings that can be conveniently used by the design professionals. Development of some ready-to-use *design charts* or *fragility plots* may further assist the designers in quickly assessing the seismic vulnerability of OGS buildings and further help in achieving the performance objectives for the buildings. The primary objectives of the present study are derived from these gap areas and already summarized in Chapter 1.

❋ ❋ ❋

Chapter 3

SEISMIC PERFORMANCE ASSESSMENT

3.0 Overview

Open Ground Storey (OGS) buildings are most commonly constructed in many countries across the world. In such buildings, the ground storey is left open (i.e., without infill walls) primarily for parking purpose and other functional use. There is a need to understand and qualify such type of building construction for seismic resistance in earthquake-prone countries, like India. The presence of masonry infill walls only in upper stories make the ground storey quite flexible and weaker compared to the stiffer upper stories. As a result, the OGS columns are not able to resist the high displacement or ductility demand imposed on them during earthquakes, and the structural as well as non-structural components of the building may suffer severe damage or even completely collapse. Such buildings have performed quite poorly even during moderate earthquake shakings in the past. It is a common perception that the soft storey effect is reduced due to the presence of openings in the upper storey infills walls. This aspect has been investigated in the present study by carrying out an extensive parametric analysis by varying the central opening size in masonry infill panels of OGS and fully infilled (FI) frames. The study further evaluates a matrix of building models with number of bay varying from 1 to 6 and number of storey varying from 2 to 6, in both OGS and FI frames with and without central openings in infill walls. The matrix of building frames considered is intended to cover existing low-rise to mid-rise building typologies. Systematic nonlinear static and nonlinear dynamic analyses of the considered building frames are carried out to assess the seismic performance of the different frame configurations.

3.1 Details of Structural Systems

3.1.0 General

The present study includes three different configurations of reinforced concrete (RC) building frames. The mathematical modelling of RC frames are carried out in SAP2000 considering material nonlinearity. Modelling of RC beams and columns is quite well established as flexural members. Masonry infill panels can be modelled by the equivalent diagonal strut method, which is found to be sufficiently accurate in estimating the initial stiffness and lateral strength of the masonry infilled RC frames. The details of the structural modelling are discussed in the following sections.

3.1.1 Analytical Idealization of the Generic Buildings

An internal frame (Fig. 3.1) of a three-bay, four-storey (3B-4S) RC building, designed and detailed for the highest seismic zone as per the relevant Indian Standards (BIS 2016a, BIS 2016b), is considered. Three structural configurations representing both regular and irregular frames are considered for the 3B-4S RC frame as listed below:

a. Bare Frame (BF): Masonry infill walls are not provided in any storey (regular frame).
b. Open Ground Storey (OGS) Frame: Masonry infill walls are provided in all the stories except the ground storey (vertically irregular frame).
c. Fully Infilled (FI) frame: Masonry infill walls are provided in all the stories (regular frame).

Different number of bays (N_B) and stories (N_S) are considered for the building typologies intended to cover low- to mid-rise buildings, and with varying sizes of central opening in infill walls (*Op*). The openings considered account for the door and window openings present in the buildings. All the frames have a bay width of 3 m and a ground storey height of 4.4 m; all upper stories are 3.2 m high. Though ductile detailing is provided in the RC frame members, the frame is designed as a weak column-strong beam frame system to reflect the current design practice adopted by designers in India as well as in many other countries (Kaushik et al. 2009). The bare frame is modelled as per general design criteria of considering only the weight of masonry infills on the frame members. For the OGS frame, stiffness and strength of masonry infills are considered in the upper stories; however, the ground storey of the frame is kept open, i.e., without masonry infills.

The fully infilled (FI) frames are provided with masonry infills at all stories uniformly. Thus, both the strength and stiffness of masonry infill walls are considered while modelling for nonlinear analyses of FI frame. Typical structural plan, elevation, and member cross-sectional details of a 3 bay-4 storey (3B-4S) frame are shown in Fig. 3.1.

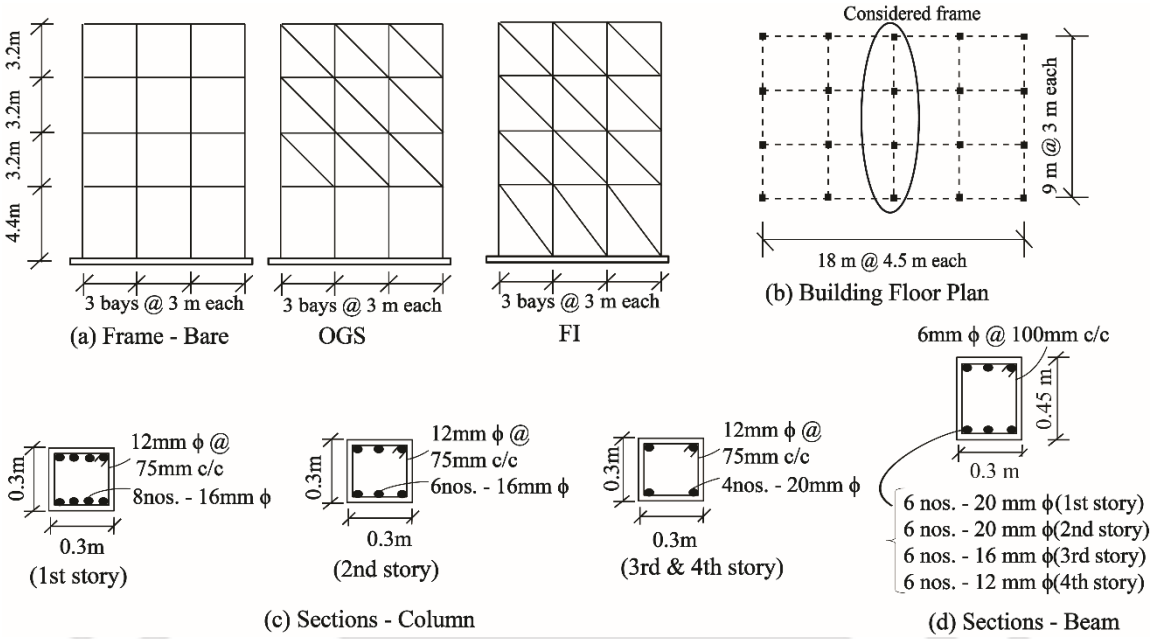

Figure 3.1 (a) Structural elevation of the considered frame – bare, OGS, and FI, (b) Building floor plan, and detailed sectional properties of (c) columns and (d) beams for the frames.

The RC frame is assumed to be fixed at the base and soil-structure interaction effects are not considered in the study. Columns and beams of the frame are modelled using two-noded frame elements with three degrees of freedom at each node. The mean compressive strength of concrete cubes of 150 mm size is considered as 25 MPa (Elastic Modulus: 25000 MPa), and the reinforcing bars have expected yield stress of 450 MPa (Elastic Modulus: 200 GPa). Poisson's ratio for concrete is taken as 0.15, and modulus of elasticity E_c of RC members of the frame is calculated using IS 456 (BIS 2000) as:

$$E_c = 5000\sqrt{f_{ck}} \text{ (MPa)} \tag{3.1}$$

where, f_{ck} is the characteristic cube strength of concrete in MPa.

Monolithic beam-column joints in RC frames are generally rigid (with some finite strength) as compared to columns and beams of the frame. This effect is simulated in the analytical models by defining end offsets in the RC joints with 50% rigidity (semi-rigid

joints) because of smaller size of joints. Infill walls are modelled as equivalent diagonal struts using two-noded beam elements. Several additional strut models have been proposed in the literature for infills; however, only single strut model is chosen in the present study because of its simplicity. The diagonal struts for masonry walls are modelled such that transfer of bending moments from RC frame elements to masonry is prevented. This is achieved by specifying moment releases at both ends of the strut elements. Therefore, in the plane-frame analysis, strut elements have only two degrees of freedom at each node: translations along two directions. Weight density and Poisson's ratio for masonry are taken as 18.0 kN/m^3 and 0.20, respectively. Modulus of elasticity of masonry E_m is taken from Kaushik et al. (2007) as:

$$E_m = 550 f_m' \text{ (MPa)} \tag{3.2}$$

where, f_m' is the compressive prism strength of masonry in MPa. In the present comparative study, weak masonry with f_m' as 4.1 MPa is used in the analyses; therefore, the modulus of elasticity of masonry comes out to be 2255 MPa.

An average value of strut width equal to one-fourth of the diagonal length of infill is used in the present study; this was also suggested by Paulay and Priestley (1992).

$$w_s = \frac{d_w}{4} \text{ (in m)} \tag{3.3}$$

where, d_w is the diagonal length of masonry wall. The thickness of strut is taken as the actual thickness of masonry walls (220 mm). The reduced width of the strut elements due to the presence of central opening in masonry infill walls is obtained using Eq. (3.4) (Surendran 2012), where r_0 is the ratio of opening area to the total area of the wall panel. Eq. (3.4) was developed based on experimental results of several frames with different opening sizes in masonry infill walls.

$$\text{Reduced strut width} = \left(1 - r_0^{0.675}\right) \times \left(\text{original strut width}\right) \tag{3.4}$$

Beams and columns of the frames are detailed to exhibit ductile response. Therefore, shear failure of the columns is not expected and not considered in the present study. There is a possibility of shear failure of the columns due to frame-infill interaction. However, this is a complex phenomenon, which is not taken care of by the simplified

diagonal strut modelling used in the present study. The masonry infill panels can fail in several failure modes under seismic action, for example, diagonal compression, crushing in the corners in contact with the frame, sliding shear along horizontal joints and diagonal tension. The present study, however, considers only the diagonal compression as the failure mode in infill panels that can be captured by the simplified equivalent diagonal strut model.

For the frames, first gravity load analysis, as a combination of dead and live loads (DL + 0.25×LL), is carried out before nonlinear static or dynamic analysis. P-delta effects are not included in the analyses, as the frames are not expected to undergo large deformations. Rayleigh damping (C_R) is assumed based on a modal damping ratio of 5% (Wilson 1996) and calculated using Eq. (3.5).

$$C_R = \alpha M + \beta K \tag{3.5}$$

where, a and β are scale factors calculated using Eq. (3.6).

$$\alpha = \frac{2\,(\xi_i \omega_j - \xi_j \omega_i)\omega_i \omega_j}{\omega_j^2 - \omega_i^2},\ \beta = \frac{2\,(\xi_j \omega_j - \xi_i \omega_i)}{\omega_j^2 - \omega_i^2} \tag{3.6}$$

Here, ω_i and ω_j are two of the Eigen frequencies of the system and ξ_i and ξ_j are their corresponding damping ratios, approximately equal to 0.05. The damping ratio for each mode i can thereafter be calculated using Eq. (3.7).

$$\xi_i = \frac{1}{2\omega_i}\alpha + \frac{\omega_i}{2}\beta \tag{3.7}$$

3.1.2 Nonlinear Material Properties for Static Analysis

In addition to the elastic material properties required in linear analysis, nonlinear material properties are required for nonlinear static analysis. In SAP2000 (CSI 2015), nonlinearity is modelled as lumped plasticity at desired locations on the structural members (Fig. 3.2(a)). Plastic hinges in RC members are assumed to form at a distance equal to half the average plastic hinge length (lp) from their rigid ends. It can be calculated by the following expression (Paulay and Priestley 1992):

$$l_p = 0.08L + 0.022 d_b f_y \text{ (in m)} \tag{3.8}$$

where, L is the length of the member in m (taken at the point of contra flexure from the end), d_b is the diameter of longitudinal reinforcement in m, and f_y is yield stress of longitudinal reinforcement in MPa. Plastic hinges (only flexural) are assumed to form at a distance of $l_p/2$ from the face of beams and columns. Flexural hinge properties involve axial force – bending moment interaction (P - M) as the failure envelope and bending moment - rotation (M - θ) as the corresponding load – deformation relation. Masonry infill walls which are modelled as equivalent diagonal struts and plastic hinges are assumed to develop at the center of struts along the length. Length of the plastic hinge in struts is assumed to be equal to three-fourth of the diagonal length of the strut. These assumptions are followed on the basis of results obtained in past analytical and experimental studies (Moghaddam and Dowling 1987, Kaushik et al. 2009). In addition, it is observed in the present study that variation in location of plastic hinge and its length in diagonal struts does not result in any significant variation in the nonlinear response of the frames. The struts are modelled as compression only elements, therefore, only axial hinges are assumed to develop in the masonry walls.

For simplified nonlinear static analysis, the P-M interaction surface and M-θ curves (flexural plastic hinges) for RC members are specified using auto hinge provided from tables 6-7 and 6-8 of FEMA 356 (2000). An idealized M-θ curve is shown in Fig. 3.2(b) showing the controlling points in the curve according to FEMA 356 (2000). The five points A, B, C, D, and E are used to define the backbone for hinge rotation behavior of RC members. Point A corresponds to the unloaded condition. Point B corresponds to the nominal steel yield strength. Point C has a resistance equal to the nominal strength. Line CD corresponds to initial failure of the member. It may be associated with phenomena such as fracture of the flexural reinforcement, spalling of concrete or shear failure following initial yield. Line DE represents the residual strength of the member. Point E corresponds to the deformation limit. Three more points – IO (Immediate Occupancy), LS (Life Safety), and CP (Collapse Prevention) are used to define the acceptance criteria of the hinge. For concrete, Mander's confined concrete model (Mander et al. 1988) is used to characterize the stress-strain curve. Fig. 3.3(a) shows a typical stress-strain curve for the RC column sections at III and IV storey of the frame. The idealized stress-strain model proposed by Kaushik et al. (2007) is used to model the material nonlinearity in masonry as shown in Fig. 3.3(b).

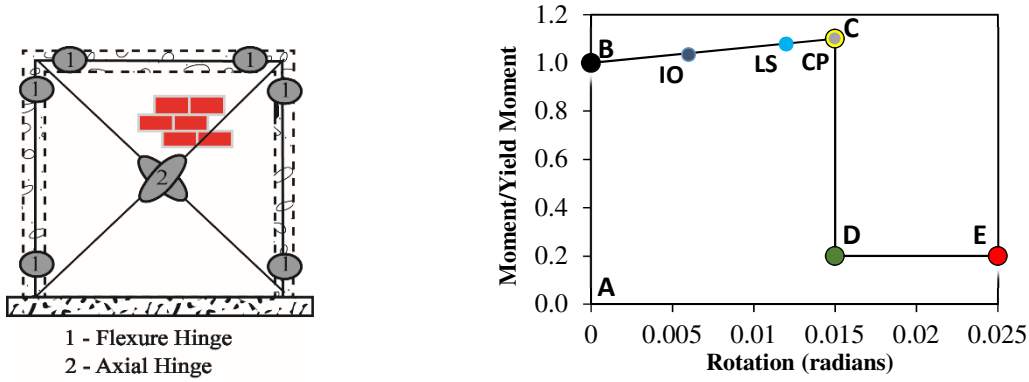

(a) (b)

Figure 3.2 (a) Location of the flexural hinge in RC members and axial hinge in the equivalent strut for masonry infill walls (b) Idealized moment-rotation curve for flexural members (FEMA 356 2000).

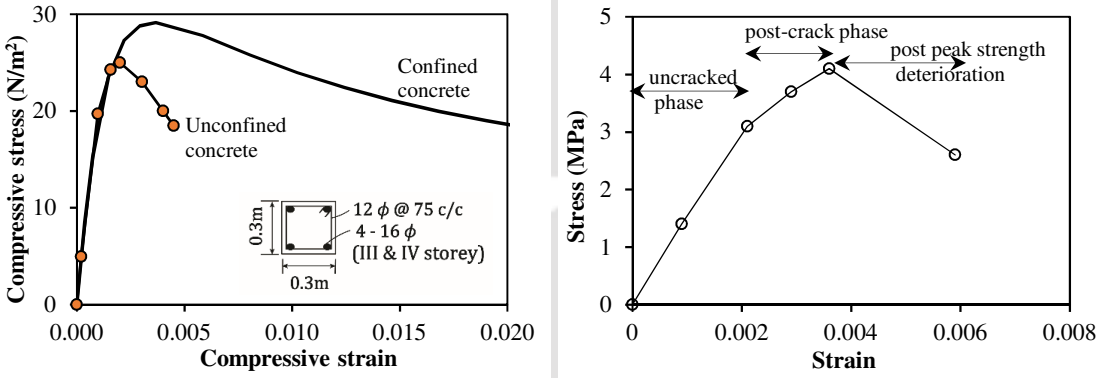

(a) (b)

Figure 3.3 (a) Mander's stress-strain curve for concrete (Mander et al. 1988) for the column sections at III and IV storey of the frames, (b) Idealized monotonic stress-strain model for weak masonry infill (Kaushik et al. 2007).

3.1.3 Nonlinear Material Properties for Dynamic Analysis

Fiber hinges obtained using section designer integrated with SAP2000 that enables the modelling and analysis of custom cross sections are used for defining the nonlinear hinges in RC members for nonlinear time-history analysis. Fiber hinges are ideal for dynamic behavior since they capture nonlinear hysteretic effects efficiently. In fiber hinges, the cross section is discretized into a series of representative axial fibers, which extend longitudinally along the hinge length. Depending on the material in its tributary area, each fiber has a stress-strain relationship. Integrating the behavior over the cross-section, then multiplying by hinge length provides axial force-deformation and biaxial moment-rotation relationships.

The Mander's model gives the stress-strain envelop in each of the concrete fibers in a section, however, its hysteretic characteristics, i.e., the strength and stiffness degradation for every loading and unloading, is defined by the Takeda hysteresis model. The Takeda model (Takeda et al. 1970) shown in Fig. 3.4(a) includes stiffness changes at flexural cracking and yielding, and strain-hardening characteristics. The Takeda model simulates dominantly the flexural behavior, and has a tri-linear envelope curve and is designed to dissipate energy even at low cycles once the cracking point has been exceeded.

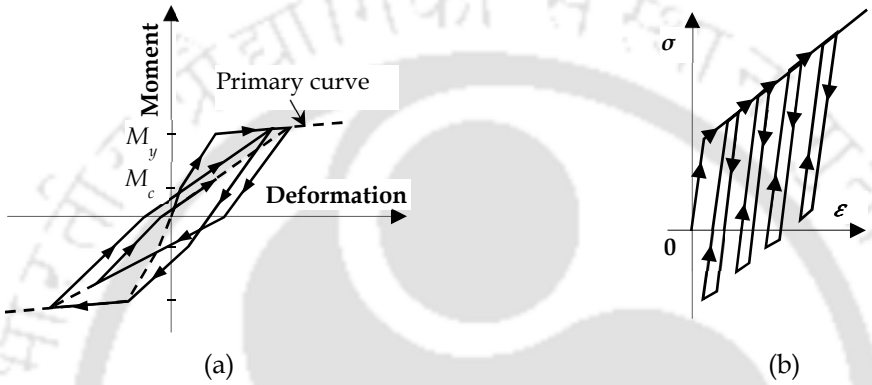

Figure 3.4 (a) Force-deformation relationship of Takeda's degrading stiffness model (Takeda et al. 1970), (b) Typical kinematic hysteresis model for reinforcing bars (Hahn et al. 1990).

Fig. 3.4(b) shows a typical kinematic hysteresis model used for reinforcing bars (Hahn et al. 1990), based on kinematic hardening behavior that is commonly observed in metals. This model dissipates a significant amount of energy and is appropriate for ductile materials. Upon unloading and reverse loading, the curve follows a path made of segments parallel to and of the same length, as the previously loaded segments and their opposite-direction counterparts until it rejoins the backbone curve when loading in the opposite direction.

Fig. 3.5 shows the Pivot hysteretic model (Cavaleri and Trapani 2014) used for the equivalent strut to model the hysteretic effects in masonry infill. The points S_1, S_2 and S_3 on the compression envelope represent, respectively, the yield, the peak and the restoring force corresponding to a reduction of 30% of the peak strength. δ_1 and δ_2 are the yield and peak displacements, respectively, and δ_3 is the final displacement after softening. I, II, and III define the yielding, peak and softening branches of the model. The Pivot model is based mainly on geometrical rules that define loading and unloading branches rather

than analytical laws. This reduces not only the computational effort but also the number of hysteretic parameters involved. Moreover, the Pivot model has great flexibility in modelling unsymmetrical tension–compression behavior, as in the case of infill (equivalent diagonal struts).

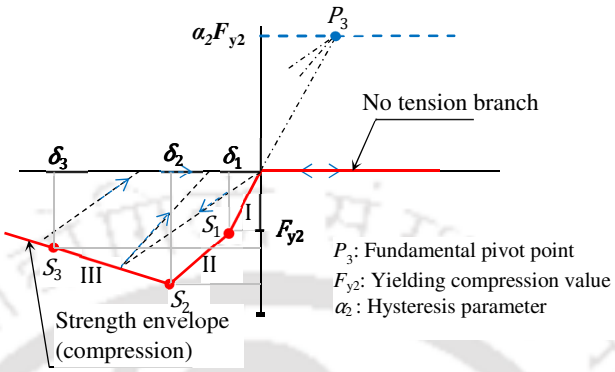

Figure 3.5 Hysteretic Pivot law particularization for the equivalent diagonal strut (Cavaleri and Trapani 2014).

3.2 Modal Analysis

Modal analysis, or the mode-superposition method, is a linear dynamic-response procedure which evaluates and superimposes free-vibration mode shapes to characterize displacement patterns. Mode shapes describe the configurations into which a structure will naturally displace. The natural period of vibration (T_N) for the first and second mode of the BF, OGS and FI frames are as listed in Table 3.1. There is a large difference in the natural time period of the FI frames and the bare or OGS frames due to the presence of infills in the ground storey that imparts large stiffness to the frame and reduces the time period. The modal mass participation ratios (Γ) give the relative participation of the mode that can be used for judging the significance of a vibration mode. It is observed that for all the three frames the first mode participation is very high as compared to the second mode (Mode 2). This implies that most of the response of the frames is concentrated in the first mode only. Thus, the frames considered are all first mode dominant structures.

Table 3.1 Table showing modal properties of the frames considered.

Frame	Mode 1		Mode 2		Floor Mass (Tonne)			
	T_N (s)	Γ	T_N (s)	Γ	Floor1	Floor 2	Floor 3	Floor 4
Bare frame	0.97	0.94	0.30	0.04				
OGS frame	0.78	0.98	0.11	0.001	43.7	43.7	43.7	32.9
FI frame	0.25	0.87	0.09	0.11				

3.3 Nonlinear Static Pushover Based Methods

3.3.0 General

The pushover (PO) analysis is a simple method that offers useful information on the expected behavior and lateral load-deformation capacity of a structural model. The structure is pushed based on the first mode deformation profile assuming the first mode to be the dominant mode. To provide some insight on the nonlinear behavior of the three models – bare, OGS, and FI frames, their static pushover analyses are carried out and results compared. SAP 2000 is used for the nonlinear static analyses, and then seismic performance assessment is carried out as per the procedure laid down in ATC 40 (1996), which is also recommended in ASCE (2013).

Nonlinear static analyses of the frames are carried out in order to obtain an estimate of the capacity of the frames. The capacity is defined in terms of a lateral force-displacement curve (Fig. 3.6) known as pushover curve. Fig. 3.6 shows PO curves obtained using FEMA 356 auto hinges (Fig. 3.6(a)) and fiber hinges (Fig. 3.6(b)). The FEMA 356 hinge underestimates the displacement capacity greatly as compared to the fiber hinges since the deformation limits set by FEMA 356 are very less compared to that set in the fiber hinges. The FEMA 356 auto hinges are simple to assign and requires less computational time as compared to the fiber hinges. However, fiber hinges give better results while performing nonlinear dynamic analysis. Thus, simple nonlinear static analyses are carried out considering FEMA 356 auto hinges, whereas, fiber hinges are used for dynamic analyses. It is observed that in both the methods, the initial stiffness of the OGS frame is slightly higher than that of the BF, but the peak base shear of both the frames are quite similar. This slight change in the initial stiffness is due to the presence of infill walls as equivalent diagonal struts in the upper stories of the OGS frame model. In contrast, the FI frame shows very high initial strength and stiffness as compared to both BF and OGS frame because of the presence of masonry infills in the ground storey of the FI frames. Most of the lateral load is initially resisted by the ground storey infills that act as compressive diagonal struts. The RC frame starts resisting the lateral loads after the masonry infill walls fail. Such lateral load sharing between the infill and the RC frame results in significant increase in initial lateral strength and stiffness of the FI frame in comparison to either the BF or OGS frame. Although masonry infills exist in both OGS and FI frames, the high lateral strength and stiffness are observed in FI frames only,

showing the importance of the presence of infills at the ground storey. In other words, the initial strength and stiffness of the frames are primarily influenced by the ground storey infills; the infills in the upper stories have very less influence on the overall behavior of the frame. At a lateral drift of around 0.015 in the FI frame, the ground storey infills fail, thus, a drop in strength is observed and subsequently, its strength becomes more or less similar to that of the BF or OGS frame. The presence of infill in the OGS frame has practically no influence on the strength and stiffness, and OGS frames can be treated similarly to BF as far as the base shear-roof drift relation is concerned. However, the OGS frames need special attention from the viewpoint of its failure, which is completely different from either the BF or the FI frame.

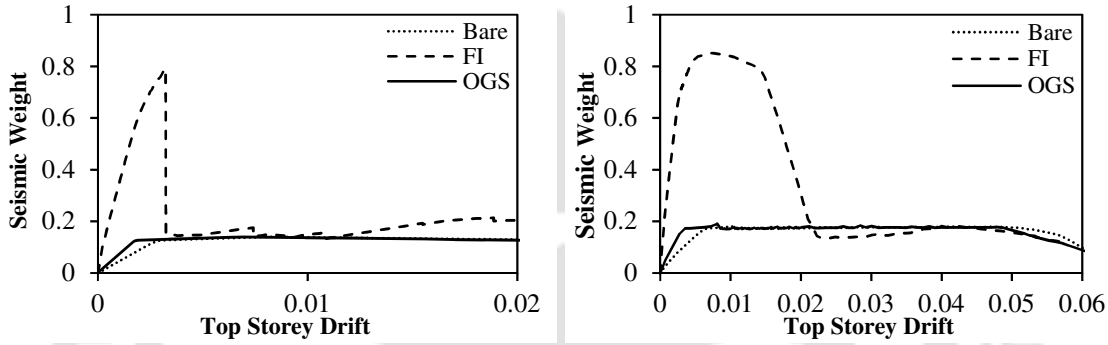

Figure 3.6 Nonlinear capacity curves for the frames using: (a) FEMA 356 hinges, and (b) fiber hinges.

3.3.1 Input Response Spectrum

The present study considers the seismic hazard in the form of response spectrum specified in the Indian seismic code (BIS 2016a) for assessing the seismic performance of the considered frames. The response spectrum is effectively reduced for hysteretic effects through standard procedures mentioned in ATC 40 (1996). To consider various levels of seismic intensity, peak ground acceleration (PGA) is varied from 0.1g to 1g by scaling the response spectrum. As discussed in Chapter 2, capacity spectrum method (CSM) is utilized in order to assess the seismic performance of the frames. The results of PO analyses and CSM are discussed next.

3.3.2 Influence of Central Opening Size in Masonry Infill

The PO curves obtained for 3B-4S OGS frames and FI frames with different *Op* are shown in Fig. 3.7(a) and Fig. 3.7(b), respectively, and are compared with the PO curve

obtained for 3B-4S bare frame in order to understand the influence of infill distribution on lateral load behavior. It is observed from the comparative PO curves that the peak lateral load carrying capacity of FI frames, even with *Op* up to about 50%, is much higher (nearly 4 to 5 times) than that of the OGS frames as well as the bare frames. In the case of FI frame, the presence of infills in the ground storey imparts tremendous stiffness and strength to the frame as seen from Fig. 3.7(b). Infills being brittle, fail after a certain level of deformation in the frame. Thus, the PO curve for any infilled frame initially shows very high lateral stiffness and strength that suddenly drops after reaching the ultimate capacity of the infills. This behavior of the FI frame is evaluated in the present study by increasing the opening sizes in the infill panels of all the stories. The sudden drop in strength and stiffness is observed in the FI frame until an opening of 50% is provided in the infill. When the opening size is further increased to about 60%, the stiffness and strength of FI frame under the action of lateral loads reduce gradually rather than exhibiting a sudden drop (Fig. 3.8). This is because of a balance achieved between the infill wall resistance and the RC frame resistance when 60% or more *Op* are provided in FI frame. Such a balancing behavior leads to sharing of lateral loads between the infill walls and the RC frame from the beginning. This, in turn, prevents the sudden drop in the lateral stiffness and strength as observed before.

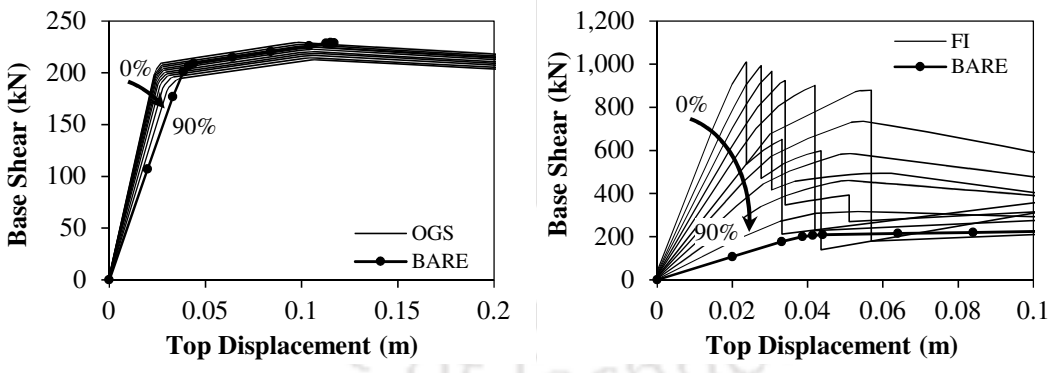

Figure 3.7 PO curves for 3B-4S: (a) OGS frame, and (b) FI frames with different central opening sizes.

Thus, globally, a relatively more ductile behavior is achieved for the considered frame as the opening size in infill is increased to about 60%. Therefore, it can be inferred that the performance of the FI frame with 60% *Op* is even better than the FI frame without *Op* as well as the bare frame. Two more examples of a 2B-2S and 6B-6S FI frame are shown in Fig. 3.9 to see the effect of opening size in infill. Though such a behavior is observed in

all the frames analyzed in the present study, the observed optimal value of *Op* must be used with caution as it may change due to presence of non-structural members and other components, which are not considered in the analysis.

On the other hand, the effect of *Op* is found to be negligible in the case of OGS frames as compared to the FI frames. There is hardly any change in lateral strength and stiffness of OGS frames with a change in *Op*. Thus, it is implied that the upper storey infills do not contribute significantly to the lateral stiffness and strength of the OGS frame. A similar observation is made for frames with other configuration of N_B and N_S. Since the study focuses primarily on OGS frames and the effect of openings is negligible on the behavior of OGS frames, further analyses are carried out only for 0% *Op*, i.e., no opening in infill, and 50% *Op*.

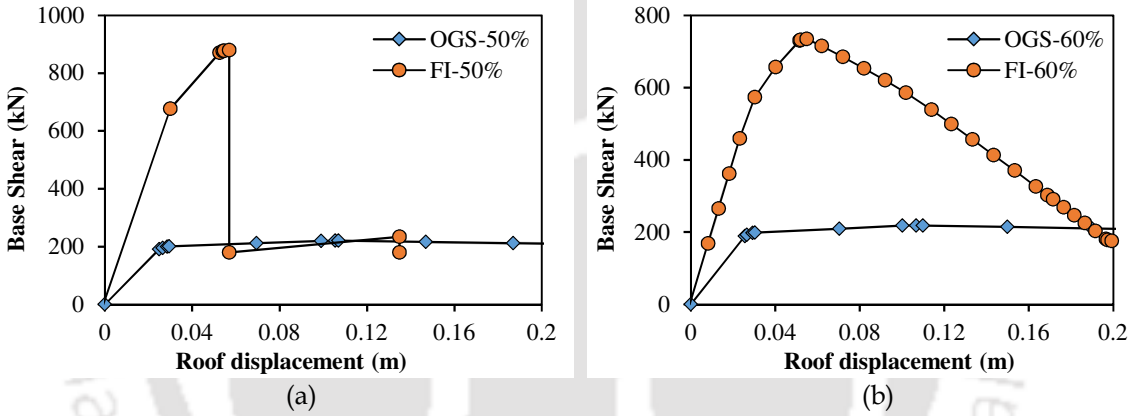

Figure 3.8 Effect of increase in opening size in infill of a 3B-4S OGS and FI frame from: (a) 50% to (b) 60%.

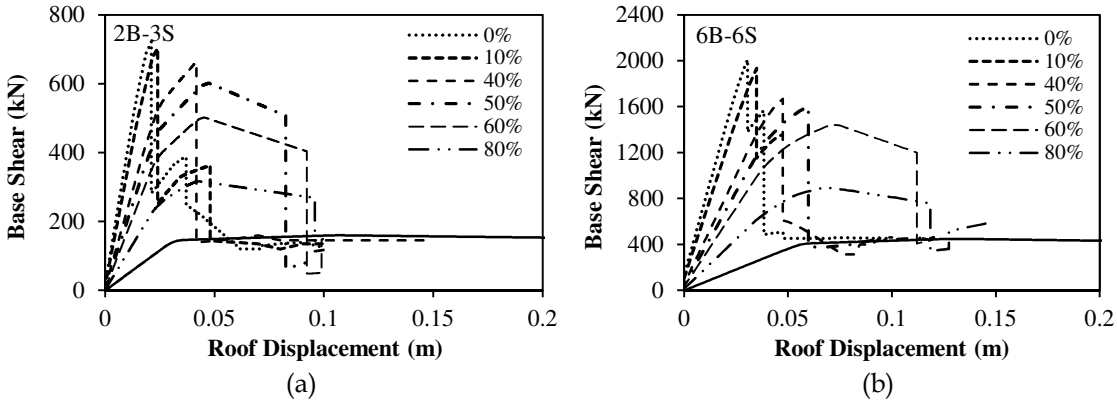

Figure 3.9 Effect of *Op* in infill on lateral load behavior of masonry infilled RC frames.

Fig. 3.10 shows response surface plot of performance points (PPs) in terms of spectral displacement (S_d) for 3B-4S OGS and FI frames with varying *Op* and PGA. The

PPs are obtained by carrying out CSM for the frames with increasing seismic intensity (PGA) and *Op*. With an increase in *Op* in OGS frames, spectral displacement demand (S_d) decreases marginally for a given PGA, whereas, it increases for FI frames. It is, however, noteworthy that the S_d obtained for OGS frames (with any *Op*) is always more than that for FI frames with same *Op* for a given PGA. A comparison of ductility demand (μ_D) for OGS and FI frames for three different *Op* also verifies this observation (Table 3.2). It is interesting to note that most of the FI frames (with 50-60% *Op*) are not expected to undergo nonlinear behavior for PGA of 0.36g (maximum design basis earthquake as per the Indian seismic code (BIS 2016a) for seismic zone V) as the μ_D is more or less equal to one. On the other hand, large ductility demand is imposed on OGS frames, most of which is concentrated in ground storey columns. A similar trend is observed in S_d and ductility demand (μ_D) for other PGA levels also.

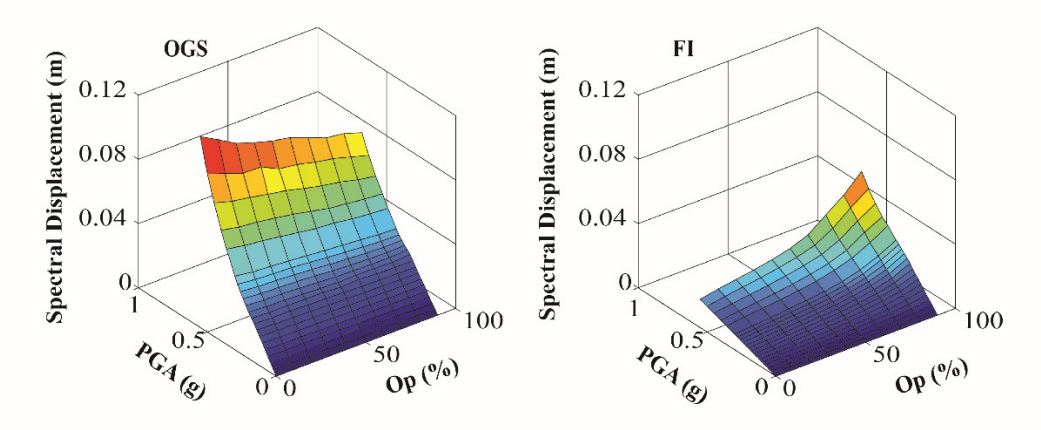

(a) (b)

Figure 3.10 Response surface plots of performance points in terms of S_d for: (a) OGS and (b) FI frames with different *Op* and PGA.

Table 3.2 Ductility demand (μ_D) on OGS and FI frames for a PGA of 0.36g.

Frames	0% *Op*			50% *Op*			60% *Op*		
	S_{dy} (m)	S_{du} (m)	μ_D	S_{dy} (m)	S_{du} (m)	μ_D	S_{dy} (m)	S_{du} (m)	μ_D
FI	0.013	0.012	0.96	0.018	0.018	1.00	0.019	0.021	1.08
OGS	0.021	0.059	2.81	0.021	0.051	2.43	0.021	0.05	2.38

Note: S_{dy} = spectral yield displacement and S_{du} = spectral ultimate displacement

Thus, from the study of opening size in masonry infill walls, it is inferred that the ground storey infill walls are the active participant in controlling the lateral load behavior of masonry infilled RC frames. Therefore, lateral load behavior of low-rise and mid-rise

OGS buildings remains unaffected by the amount of openings in infill walls. Also, the ductility demand imposed on columns of OGS frames for any level of seismic hazard is always much higher than that on columns of FI frames as well as BF with any opening size in the infill walls.

3.3.3 Influence of Change in Number of Stories

PO analysis and subsequent seismic performance assessment is carried out for the varying number of bays and stories in RC - OGS and FI frames. The number of stories (N_S) is varied from two (2S) to six (6S) for both OGS and FI frames considering 0% and 50% *Op*. The PO curves and capacity spectra are shown in Fig. 3.11 and Fig. 3.12, respectively, with varying N_S for 3B OGS and FI frames with 0% *Op*. PO curves for OGS frames indicate that there is a negligible decrease in initial stiffness but significant increase in lateral strength of the 3B frames with an increase in N_S. Capacity spectra show the dominating influence of mass in both OGS and FI frame, since spectral acceleration, S_a decreases with an increase in N_S. Thus, the effect of a change in mass is more significant than the change in stiffness due to varying N_S, keeping N_B constant. In case of FI frames, with an increase in N_S, both strength and stiffness decrease as shown in Fig. 3.11(b). Again, the decrease in initial stiffness is significant in case of FI frames as compared to the corresponding OGS frames, implying that the ground storey infill walls have a significant influence on the lateral load performance of the FI frames only. A similar trend in the PO curves and capacity spectra are observed for both OGS and FI frames with any other *Op* and N_B.

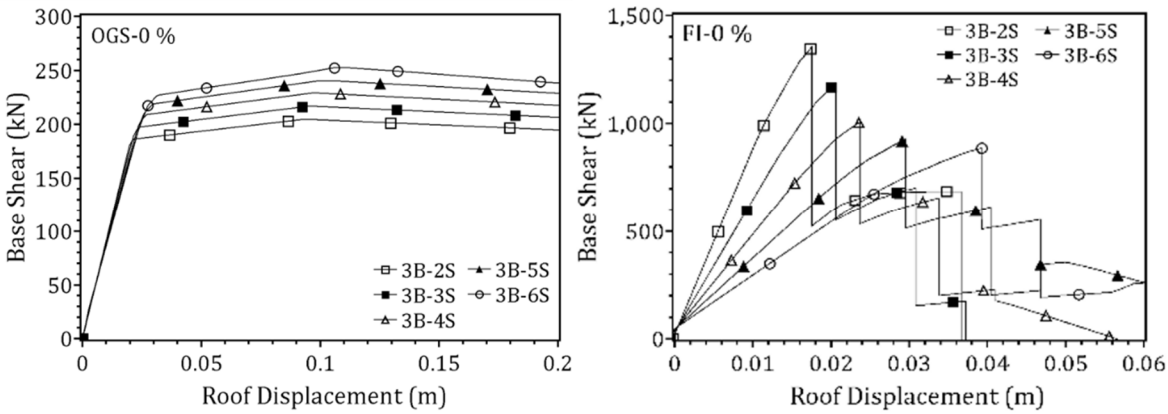

(a) (b)

Figure 3.11 Influence of variation in N_S on PO curve for: (a) OGS frames and (b) FI frames for a 3 bay (3B) frame with 0% *Op*.

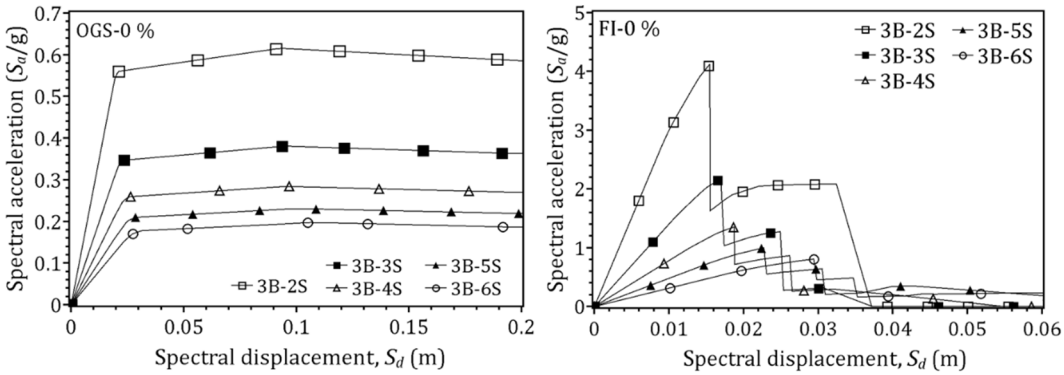

(a) (b)

Figure 3.12 Influence of variation in N_S on capacity spectra for: (a) OGS frames and (b) FI frames for a 3 bay (3B) frame with 0% *Op*.

3.3.4 Influence of Change in Number of Bays

The influence of variation in the number of bays (N_B) on the lateral load response of RC frames considering 0% and 50% *Op*, is studied by varying N_B from one (1B) to six (6B) for both OGS and FI frames. The variations in PO curves and capacity spectra due to change in N_B for a 4S frame are shown in Fig. 3.13 and Fig. 3.14, respectively. Fig. 3.13 indicates that with an increase in N_B for a given N_s (here 4S), both strength and stiffness increase for the OGS as well as FI frames. Capacity spectra (Fig. 3.14(a)) show the dominating influence of mass in the case of OGS frames since S_a decreases with increasing N_B, though the change in S_a goes on diminishing with increasing N_B. In case of FI frames, Fig. 3.14(b) shows that with an increase in N_B, S_a increases moderately for 1B and 2B frames after which the change is negligible. Clearly, the influence of mass is less on the lateral load behavior of both OGS and FI frames when N_B is varied in comparison to those cases where N_S is varied keeping the other parameter constant. Similar variations are observed in other frames considered in the study as well with any *Op* and N_S.

Thus, from the study of number of bay and storey variation, it is learned that both N_B and N_S are important decision variables in case of either OGS or FI frame. The influence of N_S as a seismic parameter is more as compared to N_B. Both N_B and N_S affect the building mass and stiffness and hence must be considered judgmentally. In case of both increase in N_B and N_S, the mass effect is more in OGS frame. In case of an increase in N_B, the stiffness effect is more in FI frame. Thus the infill panels, more specifically the one at the ground storey, plays a major role and must be considered for analysis of infilled frames.

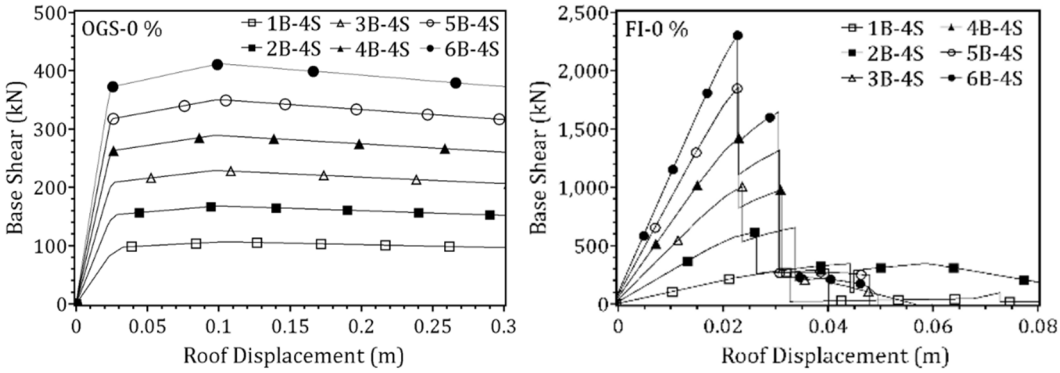

(a) (b)

Figure 3.13 Influence of variation in N_B on PO curves for: (a) OGS and (b) FI frames for a four storey (4S) frame with 0% *Op*.

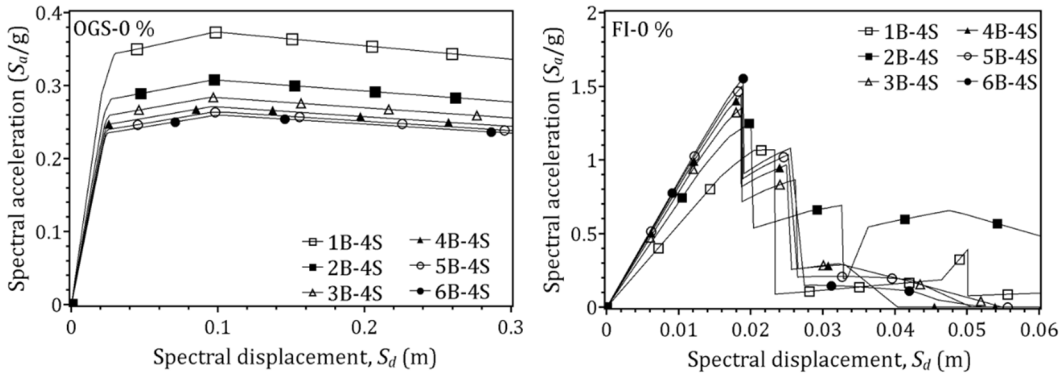

(a) (b)

Figure 3.14 Influence of variation in N_B on capacity spectra for: (a) OGS and (b) FI frames for a four storey (4S) frame with 0% *Op*.

3.3.5 Multiple Linear Regression

The influence of varying the building parameters on lateral response of different frame typologies is seen in the last section. In order to numerically interpret the effect of different parameters (i.e., N_B, N_S, *Op*, PGA, and natural period of vibration, T_N) on spectral displacement demand S_d (represented by performance point), multiple variable linear regression analysis (MLR) is carried out. MLR is a statistical technique that uses several explanatory variables to predict the outcome of a response variable by fitting a linear equation to the observed data. A regression equation describes how the mean response (Y) changes with the variables (X). The observed values vary about their mean and are assumed to have some standard deviation (ε) also known as residuals. Formally, the model for MLR, given n observations is expressed as:

$$Y_i = \beta_0 + \beta_1 X_{i1} + \beta_2 X_{i2} + \beta_p X_{ip} + \varepsilon_i \text{ for } i = 1, 2, \ldots, n \quad (3.9)$$

where, p represents the number of explanatory variables, and $\beta_0, \beta_1, \beta_p$ are the coefficients or parameters of the regression line to be estimated. This form of MLR model is also known as seismic demand model where the output corresponds to an engineering demand parameter.

The parameters, N_B, N_S, and Op are easy to identify through visual screening of a building, and they influence the performance of the building. In order to predict a more realistic S_d, the fourth parameter T_N, is considered that effectively include the effect of both mass and stiffness of the building concerned. T_N, however, requires modal analysis of the frames to be carried out. Thus, a two-level regression model is proposed for the estimation of the seismic performance (S_d) of the building frames: "Level I" and "Level II". The first level includes the parameters that does not require any *a priori* analysis. The second level requires modal analysis for the estimation of the time-period of the building. Based on the observation of the variation in S_d with respect to the intensity measure (PGA), three different ranges are considered for PGA: 0.02g to 0.3g, 0.3g to 0.65g, and 0.65g to 1g. The regression analysis is carried out separately for these different ranges of PGA, and coefficients are obtained for different parameters for the demand model shown in Eq. (3.9). The coefficients obtained from the multivariate regression analysis along with their standard error of estimate (SEE) and R-squared (R^2) value are given in Tables 3.3 and 3.4. The level I seismic demand model in the present study takes the form as shown in Eq. (3.10). Additionally, in level II demand model, the parameter, TP is considered with coefficient δ as given in Eq. (3.11).

$$S_d = K \times N_b^{\alpha} \times N_s^{\beta} \times (1.5 - Op)^{\gamma} \times PGA^{\theta} \tag{3.10}$$

$$S_d = K \times N_b^{\alpha} \times N_s^{\beta} \times (1.5 - Op)^{\gamma} \times PGA^{\theta} \times T_N^{\delta} \tag{3.11}$$

Table 3.3 Regression parameters for Level-I prediction.

Range	Frame	Coefficients					R^2	ε (m)
		K	α	β	γ	θ		
0.02g<PGA≤0.3g	BF	0.042	0.1	0.89	-	0.98	0.99	0.001
	OGS	0.040	0.1	0.77	0.3	1.00	0.99	0.001
	FI	0.004	-0.2	1.94	-1.16	1.00	0.98	0.001
0.3g<PGA≤0.65g	BF	0.067	0.16	0.97	-	1.57	0.99	0.004
	OGS	0.058	0.17	0.94	0.42	1.64	0.99	0.004
	FI	0.005	-0.13	1.8	-1.37	0.91	0.98	0.002
0.65g<PGA≤1g	BF	0.073	0.18	0.99	-	1.89	0.99	0.009
	OGS	0.058	0.2	1	0.5	2.00	0.99	0.009
	FI	0.005	-0.09	1.74	-1.52	1.02	0.97	0.002

Table 3.4 Regression parameters for Level-II prediction.

Range	Frame	Coefficients						R^2	ε (m)
		K	α	β	γ	θ	δ		
0.02g<PGA≤0.3g	BF	0.096	0.051	0.402	-	0.96	0.54	0.99	0.001
	OGS	0.093	0.052	0.338	0.475	0.987	0.564	0.99	0.001
	FI	0.327	-0.021	0.227	-0.18	0.999	1.731	0.99	0.0007
0.3g<PGA≤0.65g	BF	0.078	0.144	0.872	-	1.421	0.126	0.99	0.004
	OGS	0.072	0.153	0.836	0.466	1.646	0.136	0.99	0.004
	FI	0.082	-0.062	0.701	-0.666	0.938	1.153	0.98	0.0018
0.65g<PGA≤1g	BF	0.071	0.152	1.00	-	1.681	0.010	0.99	0.008
	OGS	0.059	0.198	1.007	0.481	1.921	0.010	0.99	0.008
	FI	0.013	-0.079	1.404	-1.265	1.029	0.373	0.97	0.0017

Both the Level-I and Level-II predictions are found to give a very good estimate for the spectral displacement demand of the building frames. The demand model will be further used in deriving the simplified fragility curves for the frames. Such predictive equations can be of a great help in determining seismic response without a need for performing rigorous nonlinear analysis when large building inventory is to be evaluated for seismic performance. This further aids in the rapid assessment of seismic fragility, and hence, vulnerability of structures in a large scale. As a case study, a school building located at Sankhu in Nepal is considered for analysis in SAP2000. The building was severely damaged during 2015 Nepal earthquake. CSM is used to estimate the performance point for the frame in the form of spectral displacement (S_d) for Indian standard response spectrum with varying PGA. The same has also been evaluated using the predictive demand model (both level I and level II) and the comparison are shown in Fig. 3.15. It is observed that the demand model gives a good estimate of the seismic displacement when compared with the analytical results obtained from SAP2000. The prediction of S_d using the proposed equation, however, needs to be validated with more analytical results.

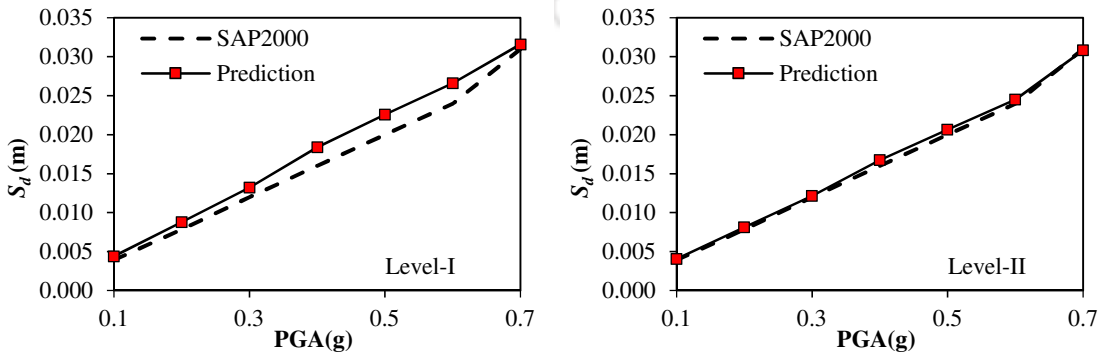

Figure 3.15 Seismic demand obtained from nonlinear static procedures and predictive seismic demand model for school building at Sankhu, Nepal.

3.4 Multiple Stripe Analysis (Nonlinear Dynamic Analyses)

3.4.0 General

The multiple-stripe analysis (MSA) is a nonlinear dynamic analysis method in which, "*stripes*" of structural response values are obtained by subjecting a structural model to a suite of ground motion records scaled to multiple levels of spectral acceleration varying from very low to a level until collapse is reached. Multiple-stripe analysis is a nonlinear dynamic analysis method that can be used for performance-based assessment of structures for a wide range of ground motion intensities and multiple performance objectives from the onset of damage through global collapse. Alternatively, the amount of analysis effort needed in the performance assessment can be reduced by performing the structural analyses and estimating the response at ground motion intensity levels of interest. MSA is better than using incremental dynamic analysis, since structural analyses are performed at a discrete set of IM levels, and different ground motions are used at each IM level.

3.4.1 Input Ground Motions

The sufficiency of the number and type of ground motion records required to be considered is a matter that needs special attention in seismic performance assessment as well as fragility analysis of structures since a large variability is generally associated with ground motion records. Each ground motion shows unique characteristics, leading to variability in the necessary outcomes of nonlinear dynamic analyses. The ground motions selected herein differ in their individual characteristics, such as frequency bandwidth, dominant frequency, energy content, and strong motion duration (defined as the time bounded by the 3% and 97% limits of the Arias Intensity) as listed in Table 3.5. Near-fault ground motion is usually characterized by a long-period impulsive motion in the horizontal direction, with a large amplitude both in displacement and in incremental velocity. This exposes the structures to high input energy in a very short duration resulting in unexpected damage, especially in taller structures in which higher modes of vibration are also dominant (Mazza and Vulcano 2010). However, the objective of the study is not to study the effects of near-fault ground motions on building frame responses. Therefore, the near-fault ground motion effects are not considered in the present study.

Table 3.5 Characteristics of ground motions considered for time-history analyses.

Sl. No.	Event	PGA (g)	Magnitude (M_w)	Band width	Dominant frequency (rad/sec)	Central frequency (rad/sec)	Arias Intensity (m/s)	Strong motion duration (sec)
1	1940 El Centro	0.35	7.1	0.94	9.20	30.00	0.16	24.02
2	1943 Indo-Burma	0.34	7.2	0.83	12.27	36.08	0.23	14.92
3	1978 Tabas	0.84	7.4	0.84	8.28	31.63	0.17	16.10
4	1985 Chile	0.71	7.8	0.99	11.85	48.12	0.31	33.81
5	1995 Kobe	0.82	6.9	0.88	9.12	14.75	0.13	8.56
6	1999 Kocaeli	0.25	7.6	0.94	7.17	12.68	0.22	36.83
7	1999 Duzce	0.97	7.2	0.92	18.33	37.28	0.32	12.60

Fig. 3.16 shows the acceleration time histories of the considered ground motions on the same scale. It is clear from the figure that each considered ground motion varies in terms of its modulation, peak ground acceleration (PGA), frequency content, and total duration. The Imperial Valley (El Centro), Indo-Burma and Duzce ground motions are similar with respect to their magnitude (Table 3.5), but they differ widely in their energy contents as represented by Arias Intensity, which corresponds to the total energy absorbed by the frequency ensemble of an undamped single degree of freedom (SDOF) system. For a given accelerogram of total duration T_d, the energy density or accelerogram intensity I_A is defined as the time-dependent integral of acceleration (a_g) and is obtained as in Eq. (3.11) (Koliopoulus et al. 1998). The maximum value of I_A is realized at the end of the accelerogram (i.e., setting t = T_d).

$$I_A = \int_0^t a(t)_g^2 dt \tag{3.11}$$

For each ground motion, the normalized energy density is plotted in Fig. 3.17(a) by normalizing the ground acceleration with respect to PGA in order to show the variation in the energy content of the ground motions. The Arias Intensity and the energy density function are suitable measures of the damage potential of a given strong ground motion record. The large difference in the considered ground motions is also depicted by the acceleration response spectra developed for each of the considered ground motions as shown in Fig. 3.17(b). The combined influence of the amplitude of ground accelerations, their frequency content, and the duration of the ground shaking on different structures is represented by means of response spectrum. The shape of the response spectrum and location of peaks are controlled by characteristics of site conditions (soil/rock) at the location of measurement, magnitude of earthquake, source

to site distance, etc. Fig. 3.17(b) also shows the natural time period of the three frames considered. The bare and OGS frames lie in the displacement sensitive zone, whereas the FI frame lies in the acceleration sensitive zone of the response spectra.

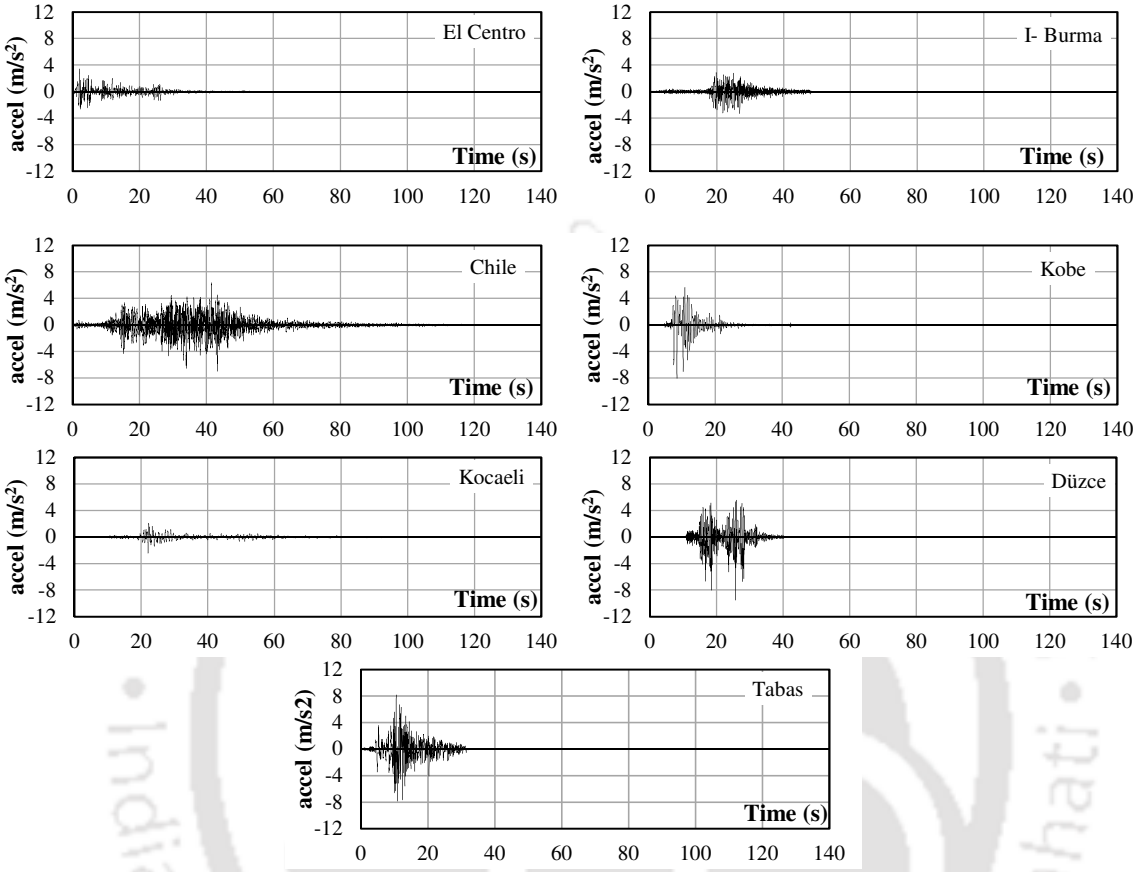

Figure 3.16 Acceleration time histories of the considered ground motion records.

In the present study, in order to capture the variability in the ground motion, each ground motion is treated as a Priestley process to generate samples of ground motion (Nithin et al. 2017). In each process, there is a deterministic frequency dependent envelope that remains constant over the samples of the process. Different samples of each ground motion are then created from the original ground motion where the sample to sample variation comes from different band-limited white noise signals associated with the frequency dependent envelope, which are different for different samples. Thus, a number of samples of the process are generated artificially. In the present study, for each process (or ground motion), 15 different samples are created, thus a total of 112 ground motions ($7 \times 15 + 7$) are considered. Samples generated for 1940 El Centro ground motion are shown in Fig. 3.17(c) in terms of dominant frequency of each sample obtained on the basis of Fourier spectrum. The figure clearly shows that there is a great variation in the dominant frequency of the generated samples. In order to evaluate the structural

performance under increasing ground motion intensity, each ground motion is again scaled for different PGA values ranging from 0.1g to 4g in increments of 0.1g until all the damage states are reached, and used for nonlinear time-history analyses of all the frames in SAP 2000.

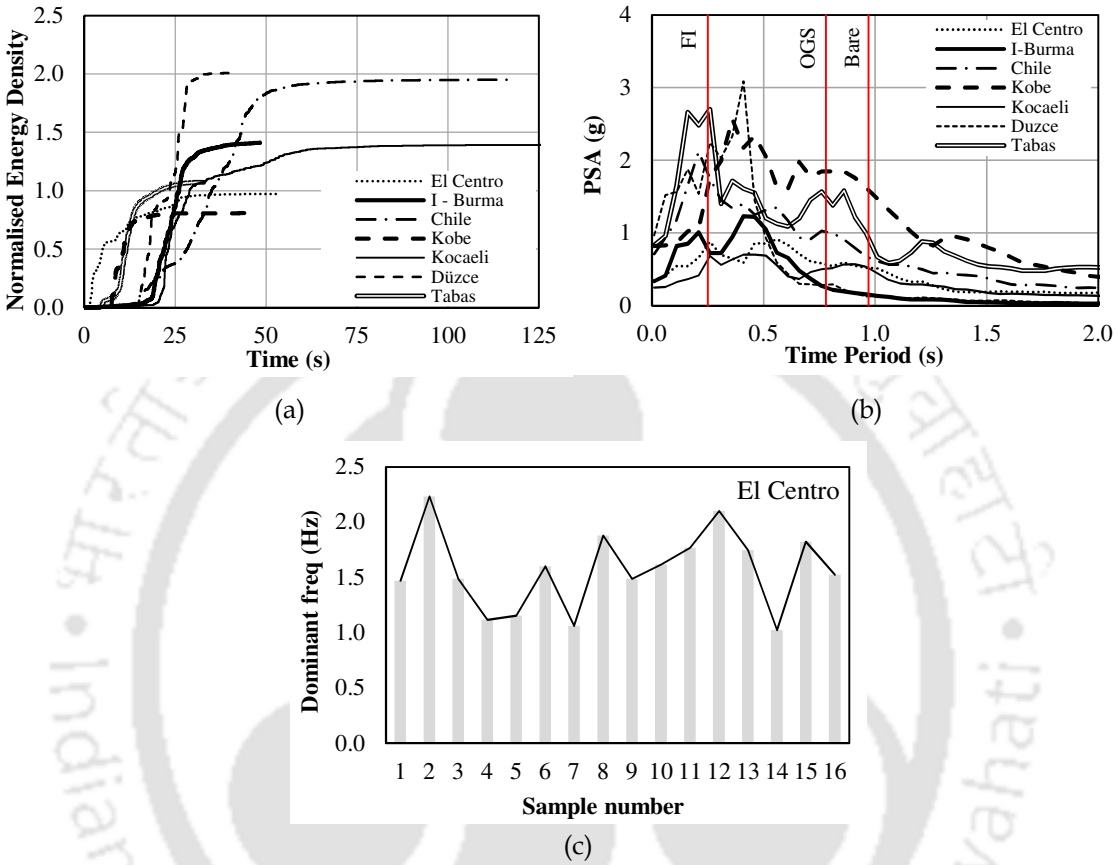

Figure 3.17 (a) Normalized energy density curves for the considered ground motions, (b) Response spectrum for the considered ground motions along with the first natural period of vibration of the frames considering all median estimates of parameters, and (c) Variation of dominant frequency of the samples of El Centro ground motion.

3.4.2 Fiber Sensitivity Analysis

A sensitivity analysis is a technique to understand the influence of different values of an independent variable on the output. As already mentioned in the previous sections, fiber hinges are used for the NLTHA. In order to test the sensitivity of various outputs obtained from NLTHA to the number of fibers employed for the fiber sections, a test is carried out by varying the number of fibers in the section, starting from a very low (3×3) number to a very high number (20×20). Fig. 3.18 shows the pushover curves obtained from the analysis of a 3B-4S bare frame by employing different number of fibers. It is

observed that initial slope of the PO curve remains unaffected by the number of fibers used. A minor variation is observed in the nonlinear region of the force-displacement plot that becomes stable after increasing the number of fibers to 10×10. Similarly, a comparison of displacement time-history is also made prior to and post failure of the RC columns in the bare frame (Fig. 3.19). A similar trend in the stability of number of fiber is observed, i.e., with 10×10 fibers, results are found to be stable and sufficient. Thus, from the fiber sensitivity analysis, a 10×10 number of fibers is fixed for further NLTHA.

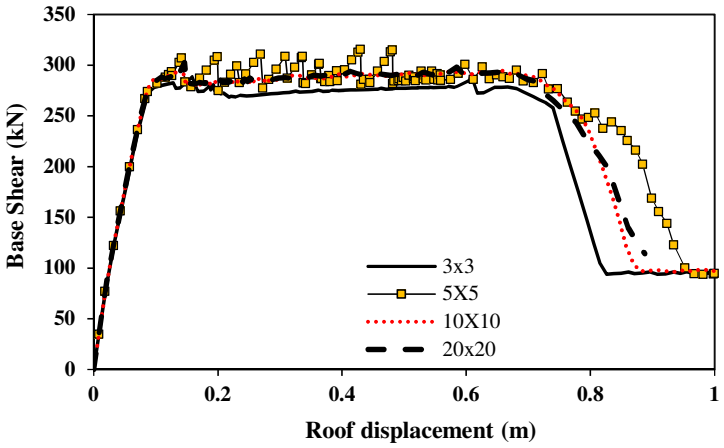

Figure 3.18 Comparison of pushover plots with a varying number of fibers for bare frame.

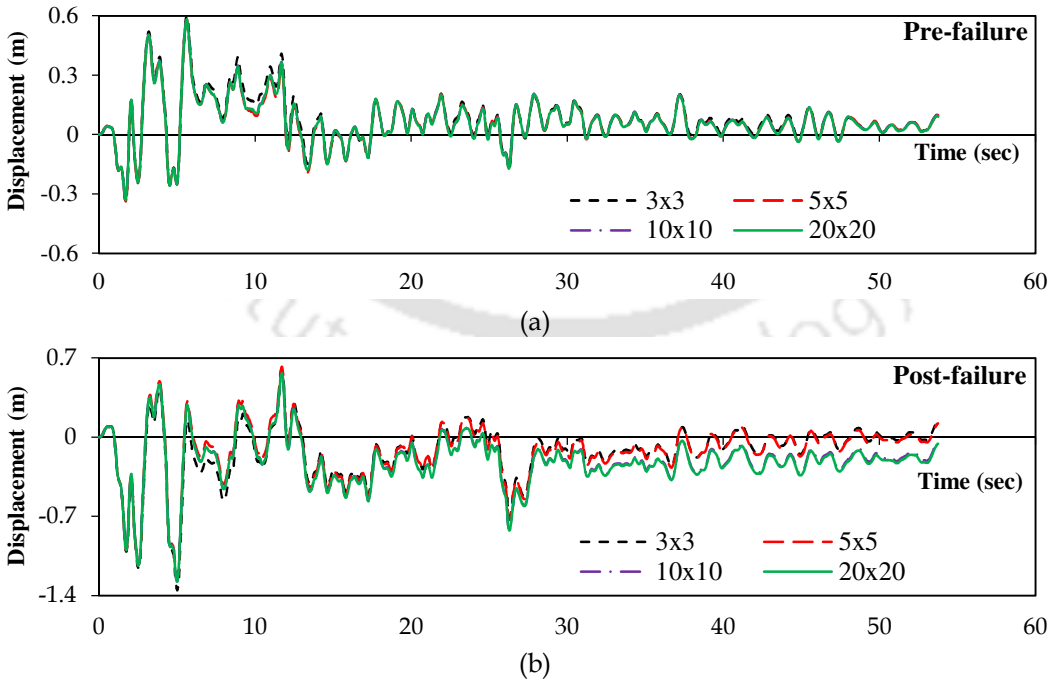

Figure 3.19 Comparison of displacement time-history plots with a varying number of fibers for bare frame: (a) pre-failure, and (b) post-failure.

3.4.3 Peak Interstorey Drift (ISD) Response

Interstorey drift of building structures can be defined as the normalized translational displacement between two consecutive floors. The peak interstorey drifts are evaluated at each floor level as the ratio of difference of storey displacements to the storey height. Interstorey drift is an important indicator of structural behavior in the performance-based seismic analysis. Fig. 3.20 shows the peak interstorey drift profiles of the bare, OGS and FI frames analyzed for 1940 El Centro ground motion.

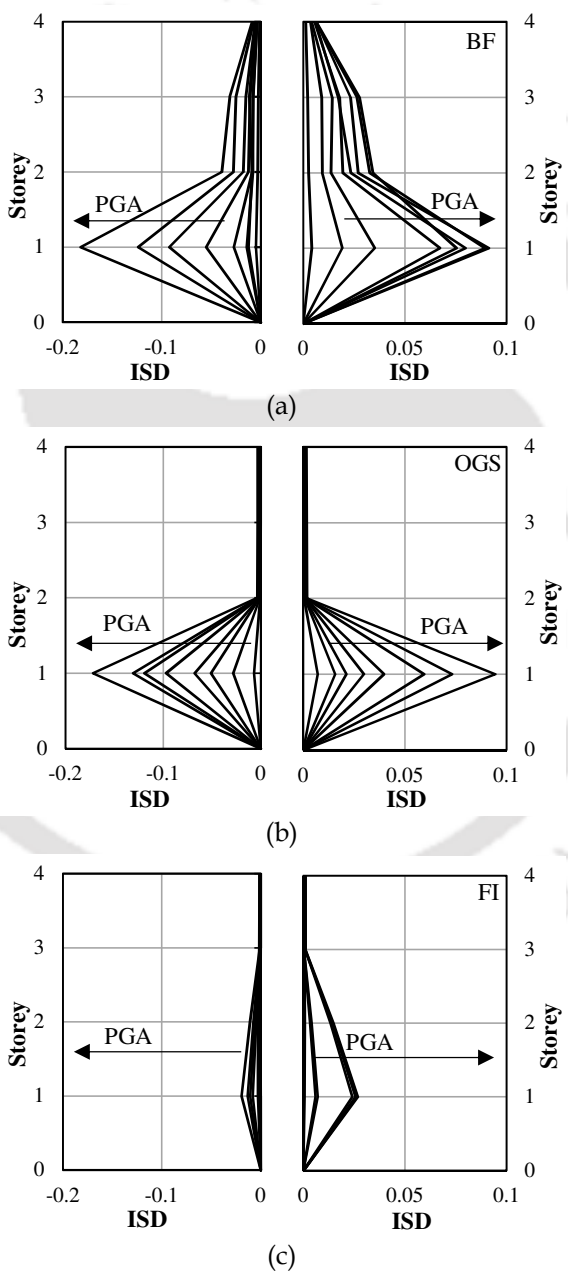

Figure 3.20 Peak interstorey drifts (ISD) profile with increasing PGA for 1940 El Centro ground motion for: (a) bare, (b) OGS, and (c) FI frame.

It is observed that in all the frames peak interstorey drift increases with increase in seismic intensity (i.e., PGA). The peak interstorey drifts are lowest in case of FI frames as compared to bare or OGS frames. In the bare frame, the ISD is highest at the ground storey and gradually decreases towards the top storey; thus, the lateral displacements, and hence, damage are uniformly distributed from bottom to top of the frame. In case of OGS frame also, the ISD is highest at the ground storey, however, there is a sudden drop of ISD at the upper stories. The ISD at the upper stories is almost negligible as compared to the ground storey ISD. Thus, in OGS frames, the damage is concentrated at the ground storey only, and failure of the OGS buildings is characterized by the failure of the ground storey columns. In FI frames, initially at lower values of PGA, the behavior corresponds to bare frame, but at increased intensity, the ISD profile becomes similar to OGS frames. It implies that, at the beginning before the failure of ground storey infills, the FI frames behave as a regular frame and the damage is uniformly distributed along all the stories. With increasing seismic intensity, the ground storey infills fail, and the behavior of the FI frame then resembles an OGS frame.

3.4.4 Derivation of Correlation on IM-EDP Pairs

In order to probabilistically assess the structural seismic performance for a given seismic hazard, it is necessary to know the relationships between ground motion intensity measures (IMs), and engineering demand parameters (EDPs). These relationships denoted as the probabilistic seismic demand models, PSDMs, are investigated here. Relationships between IM and EDP are obtained by statistically analyzing the results of nonlinear time-history analyses of structure responses under earthquakes of different intensity. Fig. 3.21 shows the multiple stripe analysis curves obtained from NLTHA using samples of 1940 El Centro ground motion by gradually increasing the seismic intensity (PGA) for each ground motion.

Nonlinear dynamic analyses of the frames considering the ensemble of ground motion give a median estimate and a standard deviation of the displacement response. The median estimate can be represented by a simple probabilistic seismic demand model (PSDM) using power's law relating seismic displacement demand (D in m) to the seismic intensity measure, IM (here PGA in terms of acceleration due to gravity):

$$D = a\,(\mathrm{IM})^{b}\,,\,\varepsilon \tag{3.12}$$

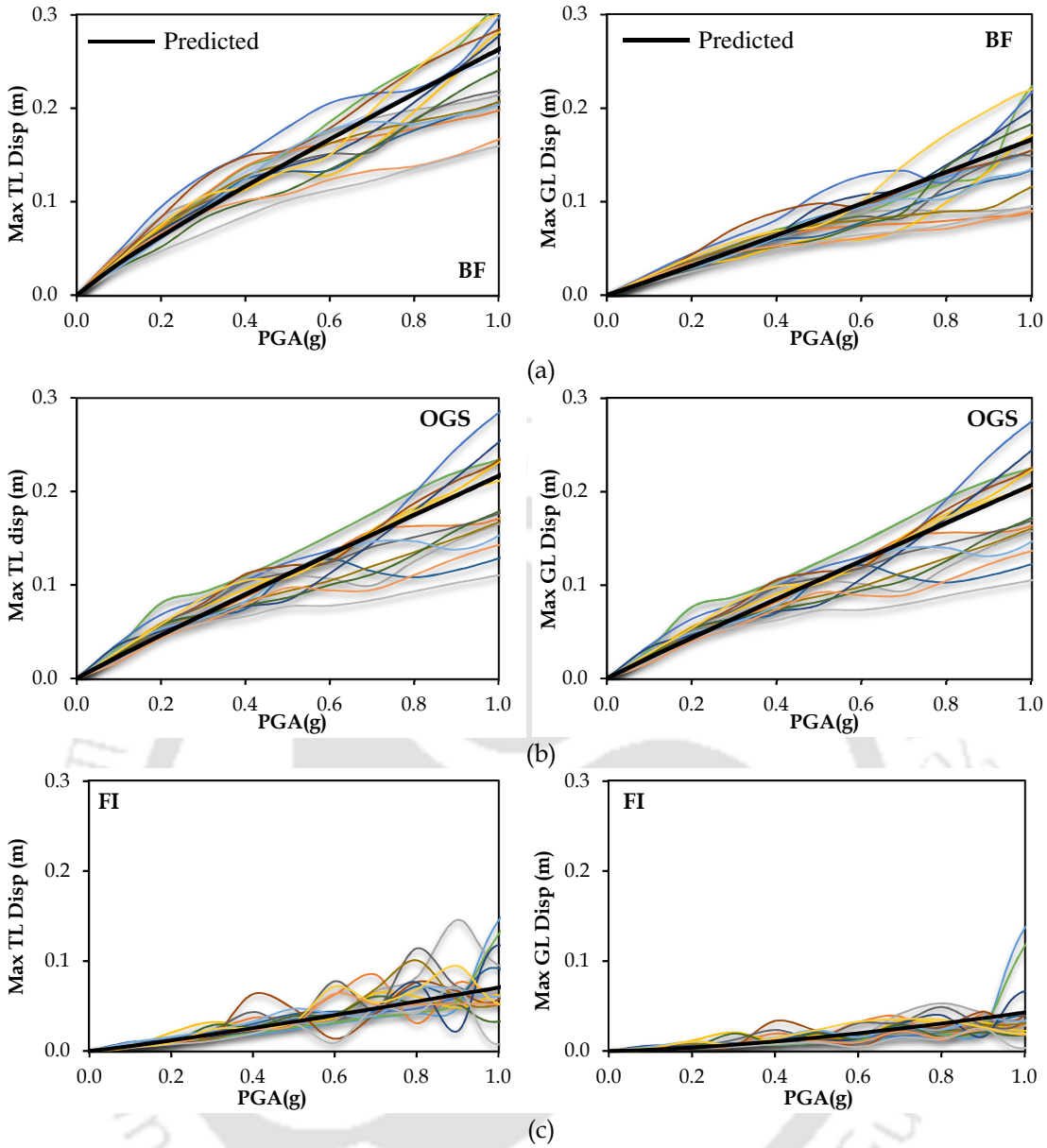

Figure 3.21 Multiple stripe analysis curves obtained using samples of 1940 El Centro ground motion for: (a) Bare (BF) frame, (b) OGS frame, and (c) FI frame.

The parameters *a* and *b* of the PSDM are determined by fitting the above model to the median values of the displacement demand obtained from nonlinear time-history analyses (Fig. 3.22). Fig. 3.21 also shows the demand model (solid black curve) considering all the samples of El Centro ground motion fitted based on Eq. (3.12). ε is a lognormal random variable with a median of 1.0 and logarithmic standard deviation $\sigma_{\ln\varepsilon} = \beta_{D|IM}$ that signifies the uncertainty in seismic demand due to record-to-record variability for a range of PGA. It is customary to assume that the logarithmic standard deviation determined from the regression of ln(*D*) on ln(IM) is constant over the range of IM of interest implying that the standard deviation in *D* increases with IM.

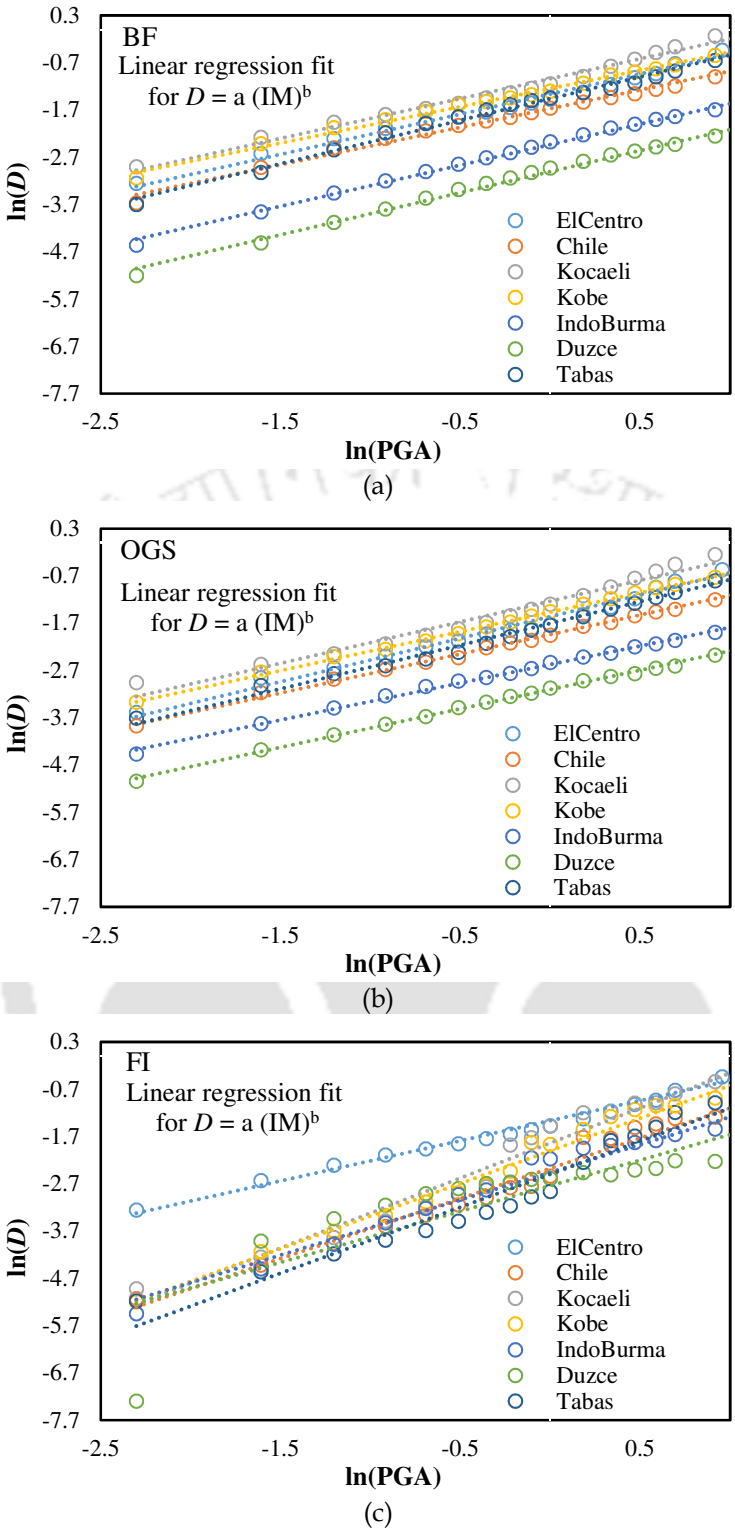

Figure 3.22 PSDM pairing: Top level (TL) displacement (median of all ground motions) with PGA as seismic intensity measure (IM) for: (a) BF, (b) OGS, and (c) FI frame.

The power's law parameters and their associated R-squared (R^2) values are as shown in Tables 3.6 and 3.7 for top level (TL) and ground storey level (GL) displacement, respectively. The parameters are also shown for the combined data of all the ground

motions and their samples. All the R^2 values in both Tables 3.6 and 3.7 are close to 1.0 implying a very good fit of the model. Fig. 3.22 also shows that the seismic demand model fits the data quite well. It is also observed that the fitting lines for most of the ground motions in case of FI frame are steep compared to both bare or OGS frames; this is also reflected by a higher value of the parameter b of the demand model. The seismic demand model can be used to predict the displacement demands in the frames given seismic intensity measure. Estimation of the lognormal standard deviation or uncertainty ($\beta_{D|IM}$) is a topic of research, which has been carried out in the present study for the three RC frames considering different EDPs, i.e., top or roof displacement and ground storey level displacement, and are discussed in next chapters.

Table 3.6 Parameters a and b of power's law approximation for median TL displacement.

Ground motions	Bare frame			OGS frame			Fully Infilled frame		
	a	b	R^2	a	b	R^2	a	b	R^2
El Centro	0.256	0.851	0.98	0.211	0.920	0.98	0.062	1.010	0.98
Chile	0.188	0.791	0.99	0.144	0.826	0.99	0.093	1.273	0.97
Kocaeli	0.354	0.842	0.98	0.292	0.877	0.97	0.159	1.482	0.97
Kobe	0.288	0.770	0.99	0.231	0.824	0.99	0.135	1.380	0.98
I-Burma	0.088	0.869	0.99	0.076	0.783	0.99	0.086	1.169	0.96
Duzce	0.050	0.891	0.99	0.045	0.816	0.99	0.082	0.568	0.97
Tabas	0.233	0.919	0.99	0.182	0.923	0.98	0.082	1.396	0.96
Combined	0.232	0.903	0.99	0.232	0.903	0.99	0.094	1.250	0.99

Table 3.7 Parameters a and b of power's law approximation for median GL displacement.

Ground motions	Bare frame			OGS frame			Fully Infilled frame		
	a	b	R^2	a	b	R^2	a	b	R^2
El Centro	0.162	1.007	0.98	0.201	0.933	0.98	0.022	0.988	0.92
Chile	0.107	0.876	0.99	0.136	0.846	0.99	0.058	1.707	0.93
Kocaeli	0.220	0.936	0.99	0.279	0.895	0.97	0.116	1.860	0.93
Kobe	0.175	0.846	0.99	0.220	0.835	0.99	0.093	1.795	0.94
I-Burma	0.033	0.945	0.97	0.071	0.798	0.99	0.053	1.516	0.95
Duzce	0.016	1.429	0.94	0.041	0.819	0.99	0.043	0.821	0.90
Tabas	0.144	1.074	0.99	0.173	0.946	0.99	0.046	1.785	0.91
Combined	0.141	1.023	0.99	0.169	0.909	0.99	0.064	1.690	0.89

3.4.5 Base Shear vs Roof displacement

The pushover curves obtained for the three frames using nonlinear static analyses are compared with that of the nonlinear dynamic analysis or response history output of the three frames plotted in terms of maximum roof displacement and corresponding base shear (Fig. 3.23). For obtaining the base shear - roof displacement curve from NLTHA, each ground motion is scaled at different PGA values. Finally, a median is considered for

the base shear force and displacement obtained from all ground motions at each PGA. It is to be noted that the comparison is done based on fiber hinge modeling. It is observed that the pushover curves of all the three frames match quite well with the response history output; in fact, the pushover curves represent more or less the envelop response for all the three frames.

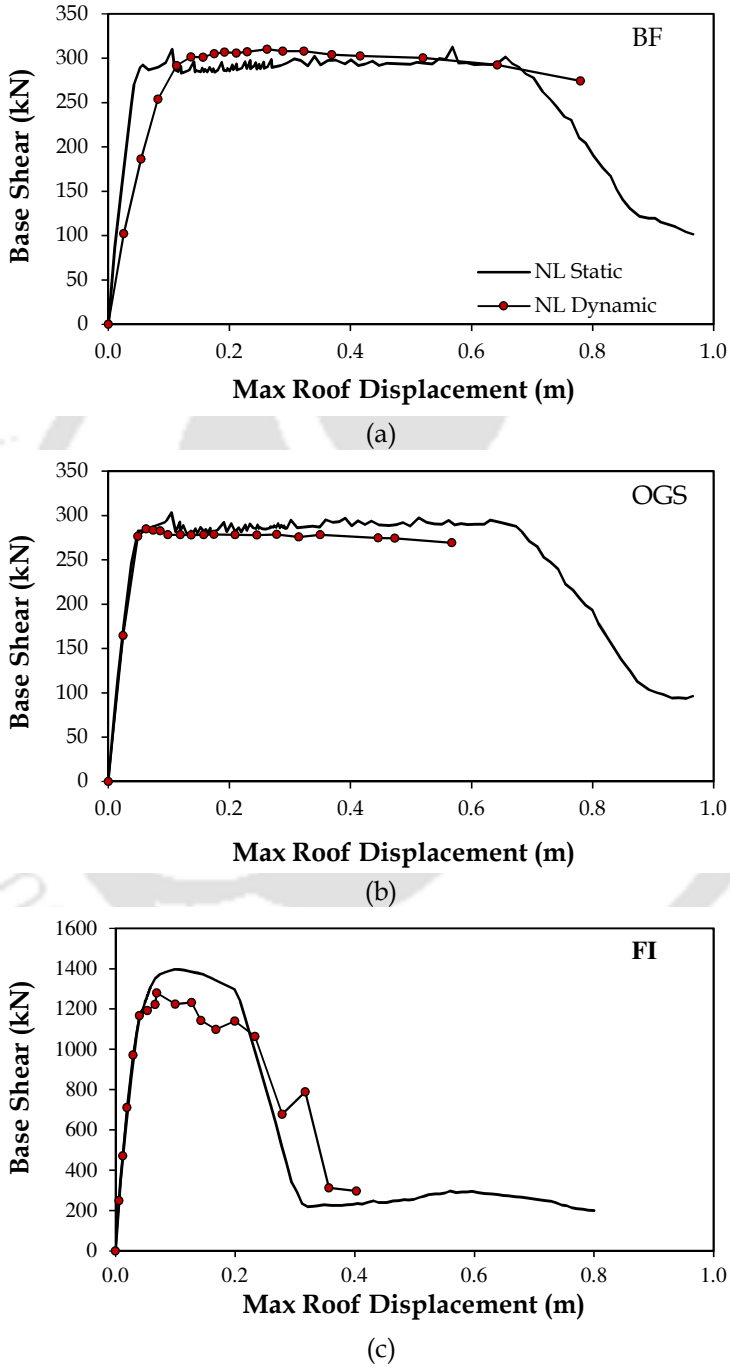

Figure 3.23 Comparison of capacity curves obtained from NL static analysis with median base shear-roof displacement curve obtained using dynamic analyses of: (a) bare, (b) OGS, and (c) FI frame.

3.5 Dynamic Amplification Factor

3.5.0 General

Nonlinear dynamic analyses carried out in the present study require huge computational effort and time, which is not always possible to realize for analyzing a large number of building models. However, under certain circumstances nonlinear assessment becomes necessary, for example when sufficient amount of statistical data is required for fragility assessment. In such a case, nonlinear static procedures can be performed and the resulting displacement demand (performance point obtained using CSM) can be modified by a suitable factor to obtain the nonlinear dynamic displacement demand. Such a factor is dynamic amplification factor (DAF). DAF is a dimensionless number, which describes how many times the seismic response obtained by static nonlinear analysis, should be multiplied in order to get the response under dynamic loads. A DAF higher than 1.0 implies dynamic response is higher, whereas, a DAF of less than 1.0 implies static response is higher. In order to capture the nonlinear static deformation response, capacity spectrum method is utilized. The CSM is carried out for different hazard levels in the form of response spectra. These response spectra are developed for the ground motions and samples of ground motions used in the nonlinear dynamic analyses of the frames.

3.5.1 Dynamic Amplification Factor for the Frames

The dynamic amplification factor is determined in the study as the ratio of the dynamic response to the static response of the building frames for a given seismic demand. The dynamic responses are obtained using the results of nonlinear time-history analysis conducted separately for two different cases: demand variation, and capacity variation. In order to capture the variation in the seismic demand, nonlinear dynamic analyses are carried out considering different ground motions (Table 3.5) and its samples with increasing seismic intensity as discussed in Section 3.4.4. The peak seismic responses are obtained for each seismic intensity and the median response is obtained. Corresponding nonlinear static analysis followed by CSM is carried out considering the same ground motions in order to obtain the median estimate. The DAF is then obtained as the ratio of the median responses from static and dynamic analyses at each seismic intensity measure level. The DAF in demand obtained for all the frame configurations are shown in Fig. 3.24(a) with respect to PGA.

The variation in capacity is related to the variation of uncertain parameters in geometry (sectional details), nonlinear material data and loading details related to the frame. Nonlinear time-history analyses are carried out for a number of sample frames modeled using the uncertain parameters using 1940 El Centro ground motion. Details regarding the variation of the uncertain data are provided in Chapter 5 (sensitivity analysis). The corresponding static responses (displacement demands) are obtained using the capacity spectrum method for the same ground motion as in NLTHA. Similar to demand variation, DAFs are obtained for the median responses at each level of the intensity measure (PGA). Fig. 3.24(b) shows the variation in DAF obtained for the three frames with respect to PGA by a variation in the parameters related to the capacity of the frames.

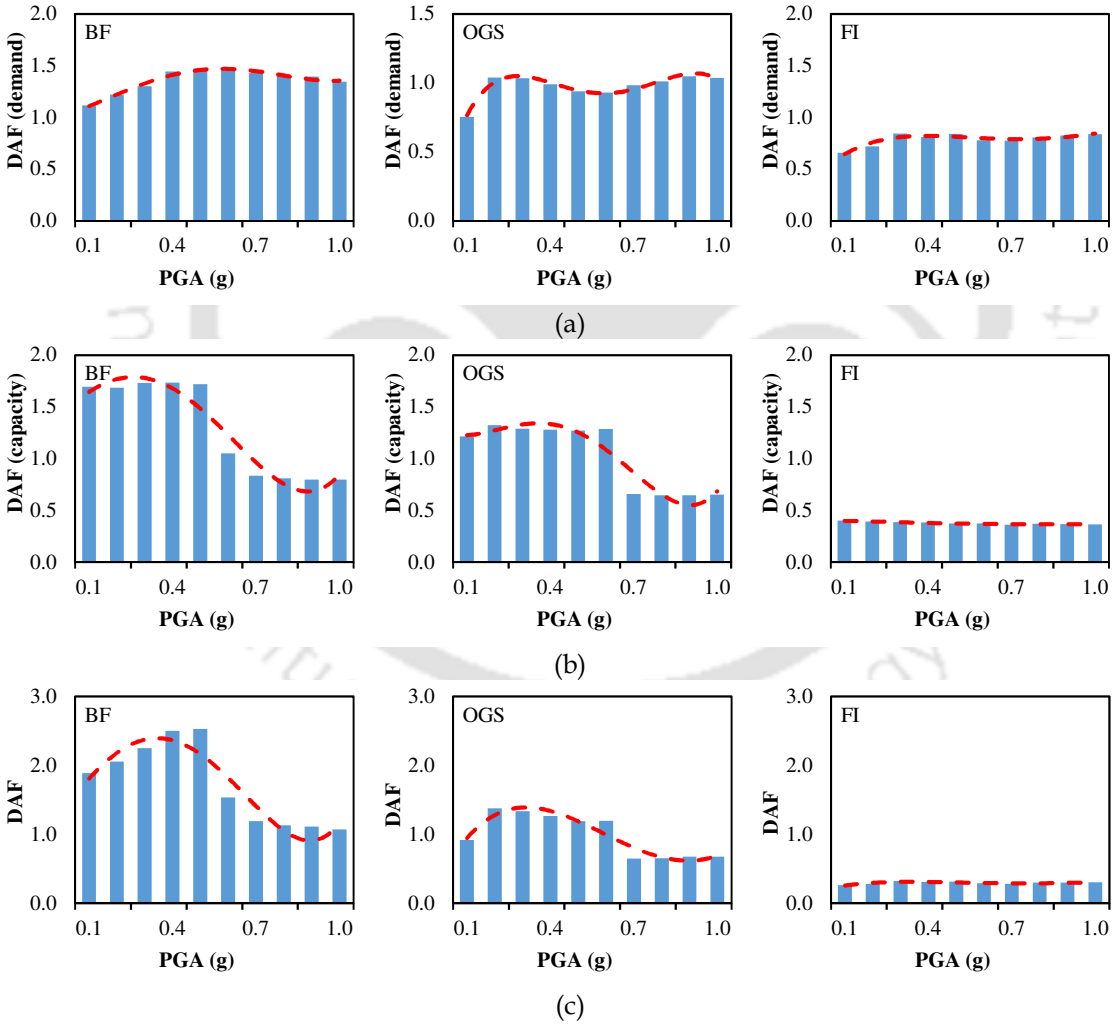

Figure 3.24 Dynamic Amplification Factors (DAF) obtained for the three frame configurations (Bare frame, OGS frame, and FI frame) with respect to: (a) demand, (c) capacity, and (c) combined response.

It is observed that the dynamic amplification factor values obtained for demand (seismic hazard) variation is nearly constant for different PGA range for all the three frame configurations. However, when a variation in the capacity of the frames is considered, DAF is high for lower values of PGA in bare and OGS frames, and it decreases with increasing PGA. In case of FI frame, the DAF is very low as compared to the other two frames and is more or less constant for all ranges of PGA. Combining the DAF for demand and capacity variation (Fig. 3.24(c) and Fig. 3.25), it is observed for all the ranges of PGA that the DAF is highest and greater than 1.0 for bare frame and lowest (< 1.0) for FI frame. This seems logical, since in bare frames dynamic response is higher because of the flexibility of the frame. In FI frames, mostly the DAF is less than 1.0, i.e., the static response is higher because of the higher stiffness of the FI frame. In OGS frame, static and dynamic responses are more or less similar (and the ratio is approximately 1.0) because, in addition to the ground storey flexibility, the OGS frames also have concentrated mass acting on all the upper floors that gives a balancing effect on the dynamic to static response.

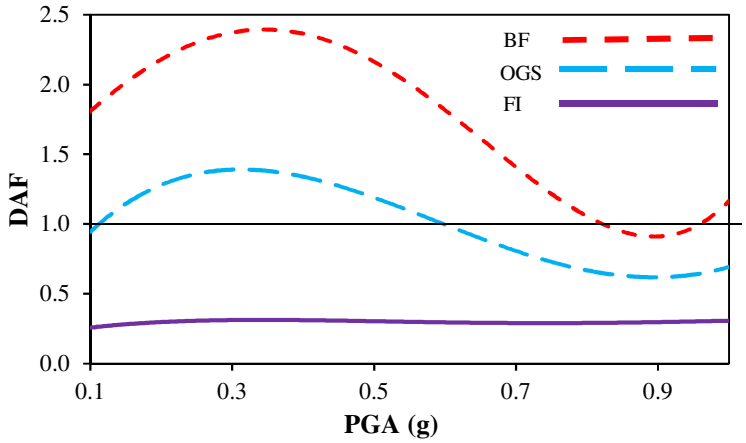

Figure 3.25 Combined DAF over a range of PGA for the three frames.

In addition to the continuous variation of dynamic amplification factor with respect to PGA, the values are averaged over a certain range of PGA values for simple application of the obtained DAF along with the demand model (Eq. (3.10)) as given in Table 3.8. An overall combined average for dynamic amplification factors is also provided over a PGA range of 0.1g to 1.0g. The combined average of the dynamic amplification factor is in the order, BF > OGS > FI, reflecting the structural type and behavior of the considered frames.

Table 3.8. Average Dynamic Amplification Factors obtained for the three frames for different PGA ranges.

PGA range	DAF for Bare frame		DAF for OGS frame		DAF for FI frame	
	Demand	Capacity	Demand	Capacity	Demand	Capacity
< 0.3g	1.21	1.7	0.94	1.28	0.74	0.39
0.3-0.65g	1.46	1.5	0.95	1.28	0.81	0.38
0.65-1.0g	1.39	0.81	1.02	0.65	0.81	0.36
Combined Average	1.72		0.99		0.30	

3.5.2 Application of Dynamic Amplification Factor

The nonlinear time-history analysis is the most desired method to predict the force and deformation demands in various components of the structure. However, the use of time-history analysis is limited because the dynamic response is very sensitive to the modelling and ground motion characteristics. It requires proper modelling of the cyclic load-deformation characteristics and careful consideration of the material degradation characteristics of all the important components. The computation time, time required for generation of input parameters, and interpreting the voluminous output of the analyses, make the use of the time-history analysis difficult for seismic performance evaluation. Nonlinear static analysis, on the other hand, is essentially a static analysis, in which the static loads are applied in an incremental fashion monotonically until the ultimate state of the structure, i.e., the structural failure defined by particular damage state or failure of certain structural members, is attained. The nonlinear material data are provided in the form of envelope or backbone curves obtained from cyclic tests or analysis. Thus, computationally the nonlinear static analysis are less demanding. In this regard, the DAF can be efficiently utilized which when multiplied by static response gives the dynamic response of the structure concerned.

The dynamic amplification factor obtained in the current study can be utilized for similar RC frame configurations to obtain the equivalent dynamic displacement response from static displacement response. The DAF for the frames are obtained over a range of PGA, implying a wide range of seismic hazard intensity can be considered for performance assessment of the framed buildings. The DAF provided would aid in seismic performance assessment more accurately by converting the static response to dynamic response, which is more realistic.

3.6 Summary and Conclusion

Masonry infilled RC frames with open ground storey are recognized as highly vulnerable seismically due to the soft storey effect. It is a common perception that the soft storey effect is reduced due to the presence of openings in the upper storey infills. This aspect has been investigated in the present study by carrying out an extensive parametric analysis by varying opening sizes in infill panels of OGS and fully infilled (FI) frames. Further, in order to cover existing low-rise to mid-rise building typologies, the number of bays and stories are also varied. Major conclusions drawn from detailed nonlinear static and dynamic analyses of the frames are enumerated below:

1. Influence of central opening size in masonry infill walls is studied, and it is revealed that central opening of any size has no effect on the lateral load performance of the OGS frames. In contrast, the performance of FI frames is greatly influenced by the opening size reflecting the significance of ground storey infills in lateral load behavior of such frames.

2. Study on variation in number of bays and stories in bare, OGS, and FI frames reveals that both these parameters are important decision variables that affect the seismic performance of RC buildings. The change in number of bays or stories affect the mass and stiffness of the buildings. In case of OGS frames, the mass effect is more, whereas, the stiffness effect is more in case of FI frames.

3. A multiple linear regression model for estimating the seismic displacement demand is developed based on the results of the nonlinear static analyses. The model gives good estimate as compared to the analytical results obtained using SAP2000.

4. Nonlinear time-history analyses show that the OGS frames have highest interstorey drift at the ground storey irrespective of the intensity of ground motion. In case of bare and FI frames, the distribution of ISD is uniform along the height. However, the FI frames start behaving like OGS frames at higher seismic intensities due to the failure of ground storey masonry infill walls.

5. Comparison of pushover plot obtained from nonlinear static analyses with the median base shear – roof displacement obtained from nonlinear dynamic analyses for the frames shows that the static analyses mostly gives an envelope curve for the lateral load capacity of the frames and can be efficiently used for the determination of the seismic demand.

6. Dynamic amplification factors are calculated for the considered frames, which can be used efficiently to obtain the nonlinear dynamic response from the nonlinear static response.

❋ ❋ ❋

Chapter 4

ENGINEERING DEMAND PARAMETERS

4.0 Overview

Engineering Demand Parameters (EDPs) are structural response quantities that can be used to quantify damage to structural and nonstructural components and systems. Engineering demand parameters forms an essential part of performance based seismic design of structures and estimation of seismic fragility functions. ATC 58 (2004) project task report lists different EDPs in use for predicting the earthquake performance of structural components and systems. It provides some discussion on needs and directions to define and quantify EDPs for comprehensive performance assessment of structures. Global demand parameters, such as, peak roof displacement or maximum drift over the height of the building, are commonly used to estimate seismic fragility. However, in case of buildings with vertical irregularities, the global demand parameters may not suffice since the maximum demand in such building is mostly concentrated at the level of irregularity (as discussed in Chapter 3). The present study focusses on one of the most common form of vertically irregular reinforced concrete (RC) buildings, known as, open ground storey buildings, where irregularity lies at the ground storey. Nonlinear dynamic analyses of RC frames with and without masonry infills subjected to a number of ground motions, each scaled for different PGA, are carried out in order to estimate the component level drift demands and global drift demands. The effectiveness of using component level engineering demand parameter in predicting the actual damage scenarios in such irregular buildings observed during past earthquakes in comparison to the damage predicted by the global engineering demand parameters is discussed in the chapter in detail.

4.1 Review of Engineering Demand Parameters

In order to specify the amount of structural and non-structural damage to structures, EDPs are identified. Several building codes and articles (FEMA 2000, Whittaker et al. 2004, Ramamoorthy et al. 2006, Jalayer and Cornell 2009, HAZUS 2013, Liu et al. 2016) suggest maximum roof displacement or global drift as a sufficient EDP to predict the building performance, and hence it's fragility. For all structural framing systems, interstorey drift is one of the traditionally used EDP, however, this is considered only at the top or roof level of the building frame. Contemporary probabilistic seismic analysis mainly focusses on global EDPs, owing to the high computational effort required for monitoring component level EDPs. Instead, a few researchers (Ruiz-Garcia and Miranda 2010) considered residual (permanent) drift demand as an efficient EDP for design of new buildings and for seismic assessment of buildings based on field observations. Prior to this, Ruiz-Garcia and Miranda (2006) showed height-wise distribution of residual lateral deformation demands in multi-storey degree of freedom systems.

Existing fragility assessment procedures, e.g., HAZUS (2013), require displacement thresholds to be defined for a frame-type specifying the limiting displacement capacity of the frame at various damage levels. Several documents and literature suggest such limiting displacement capacity values for different frame typologies. HAZUS (2013) defines these thresholds based on average interstorey drift ratio, which can be converted to corresponding top storey displacement by multiplying with the height of the building, thus showing a first mode deformation profile with highest displacement at the top. This procedure provides a good estimate of fragility for regular frames, but distort the true fragility of irregular frames, such as, an OGS frame.

Other works, such as, Kazantzi and Vamvatsikos (2015) recommended the use of storey level EDPs (peak interstorey drift ratio and peak floor acceleration at each floor) as adequate for assessing the structural and non-structural losses. Similarly, Freddi et al. (2017) highlighted that the global demand parameters, such as, maximum displacement or drift over the height of the building, is insufficient in predicting the response of structures that correlates well with the expected damage or failure pattern in low ductile RC frames. Ellingwood et al. (2007) suggested use of maximum interstorey drift angle as the demand variable due to its capability to provide an insight into the structural or local

collapse. Another study on multi-storey frames by Bai et al. (2011) developed probabilistic seismic demand models based on interstorey drift at each storey. It was concluded that the traditional demand model using the overall maximum interstorey drift could not capture the contribution from the storey responses.

4.2 Need of the Study

Reinforced Concrete buildings are among the most common type of construction typologies existing worldwide. RC buildings with masonry infill walls have undergone varying degree of damage during past earthquakes, therefore, seismic fragility assessment of such buildings becomes necessary to predict its damageability. RC frames with irregular distribution of infills are seismically even more vulnerable. For example, open ground storey buildings are vertically irregular buildings with no infills in the ground storey. As already discussed in Chapter 3, such buildings undergo large lateral deformation in the ground storey resulting in excessive ductility demand from ground storey columns eventually leading to their failure. The present study investigates the applicability of existing seismic fragility assessment methodologies with respect to different engineering demand parameters for RC frames with and without vertical irregularities (particularly the soft storey effect in the ground storey). The most common global EDP considered in a large-scale fragility assessment of building stock includes the peak roof or top storey displacement or the maximum interstorey drift over the height of the building. Here, the global displacement or drift response of the building is entirely defined by the top storey displacement assuming the first modal displacement pattern as dominant. However, such a methodology is insufficient to describe exactly the failure mechanism in building frames, particularly in case of irregular frames, such as, the open ground storey frames, where the failure is mostly concentrated at the level of irregularity. OGS columns lack adequate ductility capacity, stiffness, and strength needed to resist the high demand of storey shear. This leads to an undesirable column-sway failure mechanism in OGS buildings subjected to earthquake excitations, in which failure occurs mostly in the columns of the ground storey. In contrast, the infills present in the upper stories restrain the deformation of the upper stories, and thus, little damage is incurred in the upper stories of such buildings. The vulnerability of the open ground storey frames was observed by Mondal and Tesfamariam (2014) who reported that the infill thickness and vertical irregularity have significant influence on the response of RC frames. Similarly, the higher seismic vulnerability of vertically irregular masonry infilled frames

was also observed in several past studies (e.g., Dolšek and Fajfar 2001, Yuen and Kuang 2015, Choudhury and Kaushik 2018a).

Previous studies suggested various EDPs for fragility assessment of multistorey frames; however, such categorized EDPs are not available in the literature for irregular buildings. Hence, a component level fragility analysis with local demand parameters is carried out in the present study to estimate the realistic fragility of vertically irregular buildings. The present study clearly brings out the importance of a component level EDP in damage estimation of vertically irregular building frames with a focus on open ground storey frames. The roof level displacement as EDP may not always depict the true behavior of the frames. Instead, a component level EDP may be a better alternative for realistic seismic assessment of vertically irregular structures.

4.3 Estimation of EDPs for RC Frames with Infill

The primary objective of the study is to bring out a favorable engineering demand parameter that realistically defines the failure as well as the seismic fragility for RC frames with vertical irregularity. For this purpose, an internal frame (Fig. 3.1) of a three-bay, four-storey (3B-4S) RC building, designed and detailed for the highest seismic zone as per the relevant Indian Standards (BIS 2016a), is considered. As discussed in Chapter 3, three different structural configurations representing both regular and irregular frames are considered for the 3B-4S RC frame: Bare Frame (BF), Open Ground Storey (OGS) Frame, and Fully Infilled (FI) frame. Nonlinear dynamic analyses of the frames subjected to realistic ground motions are carried out in order to obtain the displacement demands on the frames at each storey level. The number of bays and stories in the frame, material properties and reinforcement detailing are decided based on the commonly constructed apartment buildings in India and many other countries. For the mid-rise buildings, the present configuration i.e., three bay four storey (3B-4S) can be considered as a median case building. The conclusions obtained for the 3B-4S representative sample are equally applicable to other mid-rise building frames.

Sectional details of various members as well as nonlinear data for the materials used for the frames are provided in Chapter 3. The frames are fixed at the base of ground storey columns. Beams and columns are modeled as line elements with concentrated plasticity defined using fiber sections. The beams and columns of the frames are detailed

to exhibit ductile response. Therefore, shear failure of the columns is not expected and not considered in the present study. There is a possibility of shear failure of the columns due to frame-infill interaction. However, this is a complex phenomenon, which is not taken care of by the simplified diagonal strut modeling used in the present study. The masonry infill panels can fail in several failure modes under seismic action, for example, diagonal compression, crushing in the corners in contact with the frame, sliding shear along horizontal joints and diagonal tension. The present study, however, considers only the diagonal compression as the failure mode in infill panels that can be captured by the simplified equivalent diagonal strut model. The materials considered in the analytical models are concrete, reinforcing steel and masonry infill, details of which are provided in Chapter 3. The ground motions considered in the present study for nonlinear dynamic analysis are also discussed in Chapter 3. The selected ground motions differ in their characteristics, such as, bandwidth, dominant frequency, energy content, and strong motion duration as listed in Table 3.5.

4.4 Nonlinear Dynamic Analyses

4.4.0 General

Nonlinear time-history analyses (NLTHA) of all the frame configurations are carried out for the selected ground motions scaled for large number of peak ground acceleration values in the range of 0.1g to 1g. The resulting output are plotted in terms of storey displacement and interstorey drift (ISD) demands at each storey of the frames for different ground motions scaled for different PGA for all the frames. Seismic response and behavior of the frames in terms of each engineering demand parameter is discussed in the next sections.

4.4.1 Considering Maximum Storey Displacement as the EDP

First, the maximum storey displacement obtained from NLTHA is considered as the engineering demand parameter, and the peak storey displacement demands of the OGS frames are compared with that of the bare frames in Fig. 4.1 for the ground motions considered at different PGA levels. In most ground motions and at any PGA, the top level (TL) peak displacement of BFs is either equal to or greater than that of the OGS frames. The storey displacement decreases from top to bottom stories in BF. However, in OGS frames, the peak displacement is achieved at the ground storey level (GL) itself and it is

maintained nearly constant in the upper stories. The difference in the peak storey displacement of BFs and OGS frames increases with increasing PGA. At ground storey, the OGS frames show higher displacement demand as compared to the bare frames. Since most of the lateral deformation in the OGS frames is concentrated in the ground storey level and there is insignificant relative deformation in the upper stories, the top displacement may not be the critical displacement to be considered in fragility assessment of OGS frames.

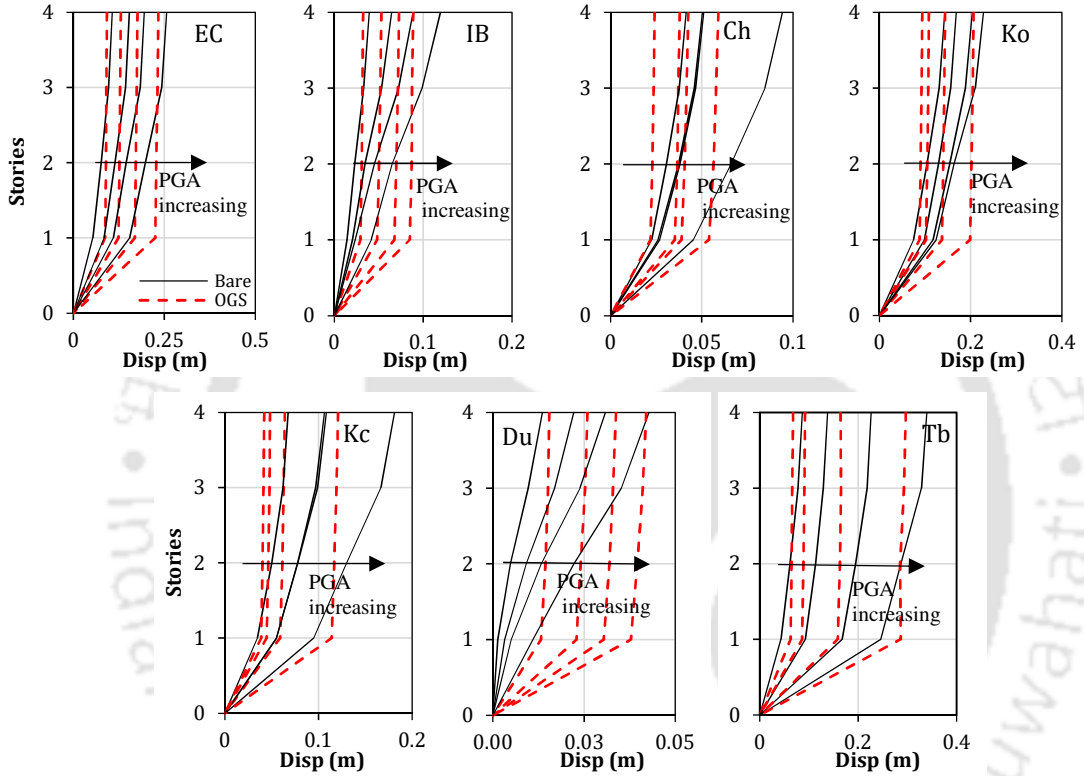

Figure 4.1 Peak storey displacement demands for Bare vs OGS frames for El Centro (EC), I-Burma (IB), Chile (Ch), Kobe (Ko), Kocaeli (Kc), Duzce (Du), and Tabas (Tb) ground motions for 0.3g, 0.5g, 0.7g and 1g.

Fig. 4.2 shows the comparison of deformation behavior of OGS frames with FI frames in terms of peak storey displacements. The FI frames deform gradually from bottom to top level. However, unlike BFs, the FI frames show a displacement pattern similar to that of OGS frames for some ground motions at higher PGA. This happens due to the early failure of the ground storey infills, after which the FI frames show irregular frame deformation pattern. Thus, considering peak storey displacement at top storey as EDP, it is difficult to recognize the location of failure in OGS as well as in the FI frames at higher seismic intensity measure levels.

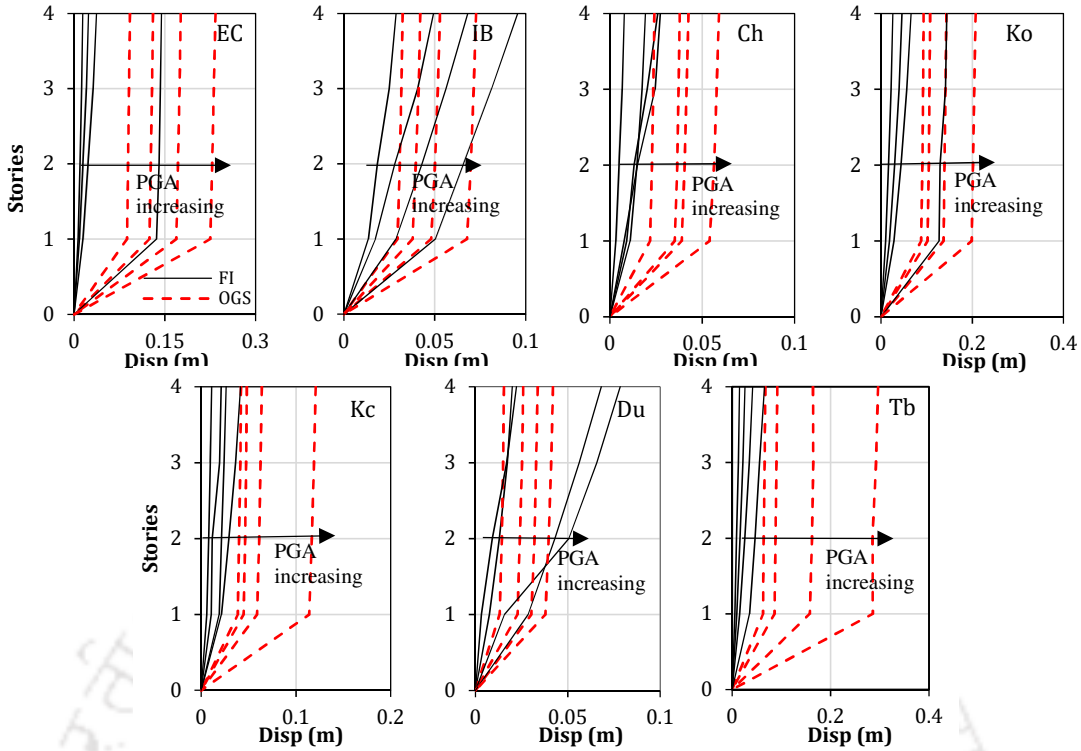

Figure 4.2 Peak storey displacement demands for FI vs OGS frames for El Centro (EC), I-Burma (IB), Chile (Ch), Kobe (Ko), Kocaeli (Kc), Duzce (Du), and Tabas (Tb) ground motions for 0.3g, 0.5g, 0.7g and 1g.

4.4.2 Considering Maximum Interstorey Drift (ISD) as the EDP

As an alternative to considering peak storey displacement as EDP, maximum interstorey drift is considered as EDP in the next set of NLTHA. Fig. 4.3 shows the storey-wise peak interstorey drift profile of BFs, OGS frames and FI frames obtained for the considered ground motions. The ISDs are computed as the difference of peak displacements between the adjacent stories normalized with respect to height of the storey considered. Fig. 4.3 shows that for any PGA, the OGS frames undergo a very high ISD demand in the ground storey compared to any other storey. Subsequently, a sudden reduction of ISD is evident from ground storey to upper stories in OGS frames. The ISD demand in the upper stories of OGS frames is almost nil, implying that there is no relative displacement in the upper stories. This happens because the infills present in the upper stories make the upper stories stiff in comparison to the ground storey, which is open. The complete upper stories, thus, move as a solid rigid mass with little or no relative deformation between the stories. Therefore, the relatively flexible ground storey columns are subjected to high ductility demand for which they are not generally designed. This leads to heavy damage in OGS columns, and hence, catastrophic failure of the OGS

frames. In contrast, the BFs mostly show a uniform ISD demand along the height as compared to OGS frames, indicating that the lateral forces are resisted uniformly by columns of all the floors. Fig. 4.4 shows that the ISD demands for FI frames are very less as compared to the OGS frames. Further, the FI frames also show more or less a uniform distribution of drift demands along the height of the frames. At higher PGA, however, some ground motions cause very high drift demands in the ground storey columns of the FI frames. Lateral behavior of FI frames for such ground motions is quite similar to OGS frames. As already discussed, this is basically the outcome of failure of ground storey infills at higher PGA.

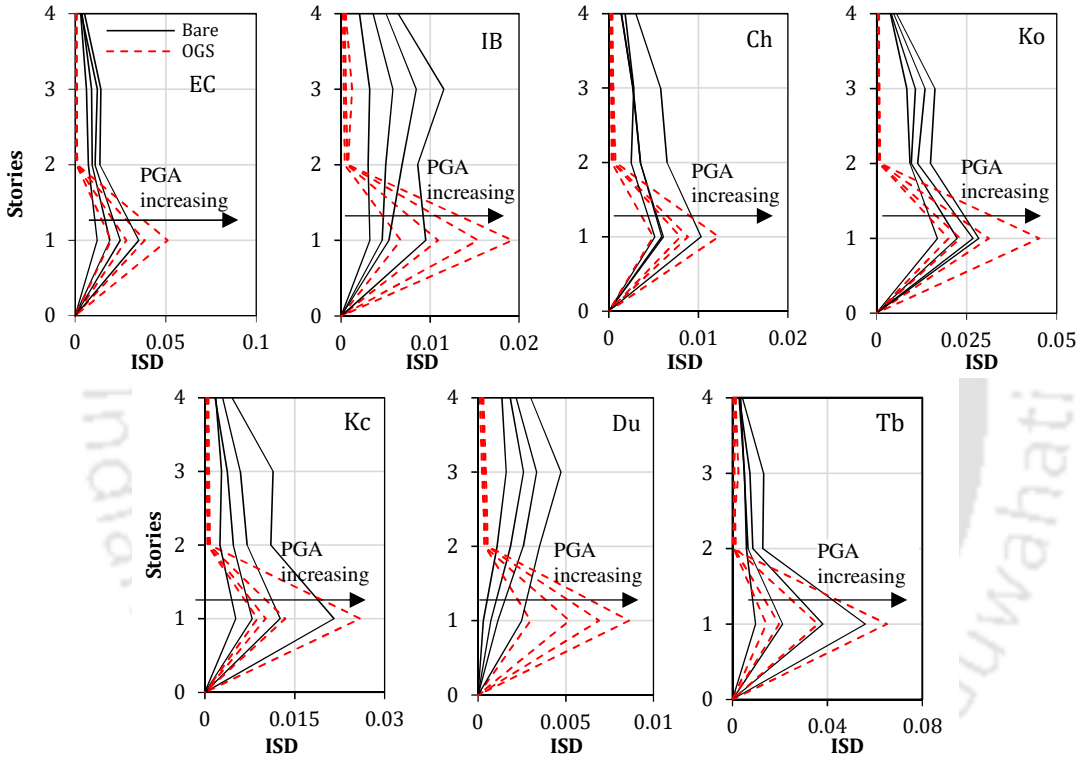

Figure 4.3 Peak interstorey drift demands for bare vs OGS frames for El Centro (EC), I-Burma (IB), Chile (Ch), Kobe (Ko), Kocaeli (Kc), Duzce (Du), and Tabas (Tb) ground motions for 0.3g, 0.5g, 0.7g and 1g.

Overall, it is observed from nonlinear dynamic analyses of the frames that the regular frames (BFs and FI frames) deform uniformly along the height of the building. However, for some ground motions in FI frames, the ground storey infills fail early leading to formation of a frame system similar to an OGS frame. Thus, the deformation behavior of the FI frames (after failure of infills) becomes similar to that of an OGS frame showing highest displacement at the ground storey and almost same and constant displacement at all the upper floors. This shows that the global displacement of the frame

is inadequate in predicting the local effect that takes place in the ground storey columns of both FI and OGS frames. The storey level performance or the local behavior is required to be well captured with the use of component level demand parameter, (e.g., GL-ISD) in order to estimate the seismic fragility satisfactorily. Thus, the choice of EDP must be emphasized for prediction of damage and localized failure pattern in irregular frames, and in those regular frames, which may become irregular during seismic excitation.

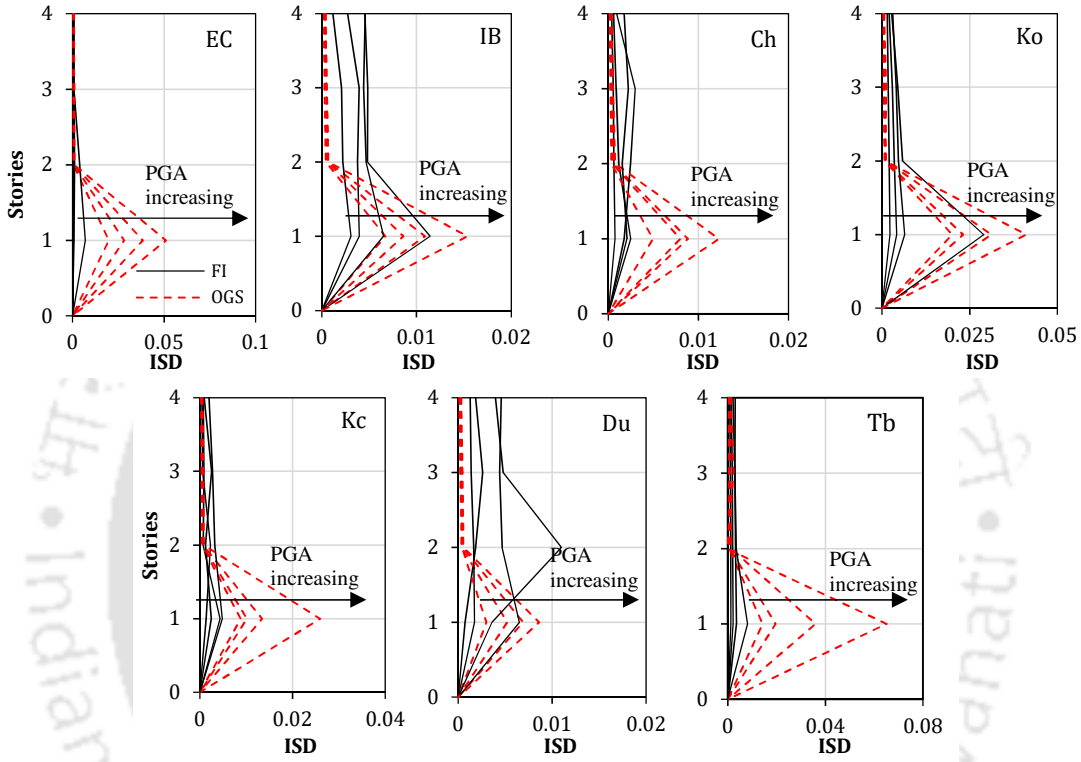

Figure 4.4 Peak interstorey drift demands for FI vs OGS frames for El Centro (EC), I-Burma (IB), Chile (Ch), Kobe (Ko), Kocaeli (Kc), Duzce (Du), and Tabas (Tb) ground motions for 0.3g, 0.5g, 0.7g and 1g.

It is clear from Figures 4.1 – 4.4 that the local level or component level demand parameter may be more efficient in portraying the realistic response of irregular frames. More specifically, the ground level displacement and ISD in case of OGS frame may be the more relevant EDP. Therefore, in Figures 4.5 - 4.11, the peak displacement and ISD demands at GL and TL are compared for all the frames under different ground motions with varying PGA values. Figures 4.5 – 4.11 clearly show that the peak lateral displacement of BFs is consistently more at TL for all earthquakes with all PGAs. Similarly, in case of FI frames, though the TL displacement is more than the GL displacement, the difference is not uniform and consistent as observed in BFs. As already discussed, this is because of the early brittle failure of masonry infill walls in ground

storey of FI frames under some ground motions. Contrastingly, there is practically no difference in the peak displacement at TL and GL in case of OGS frames for all the ground motions.

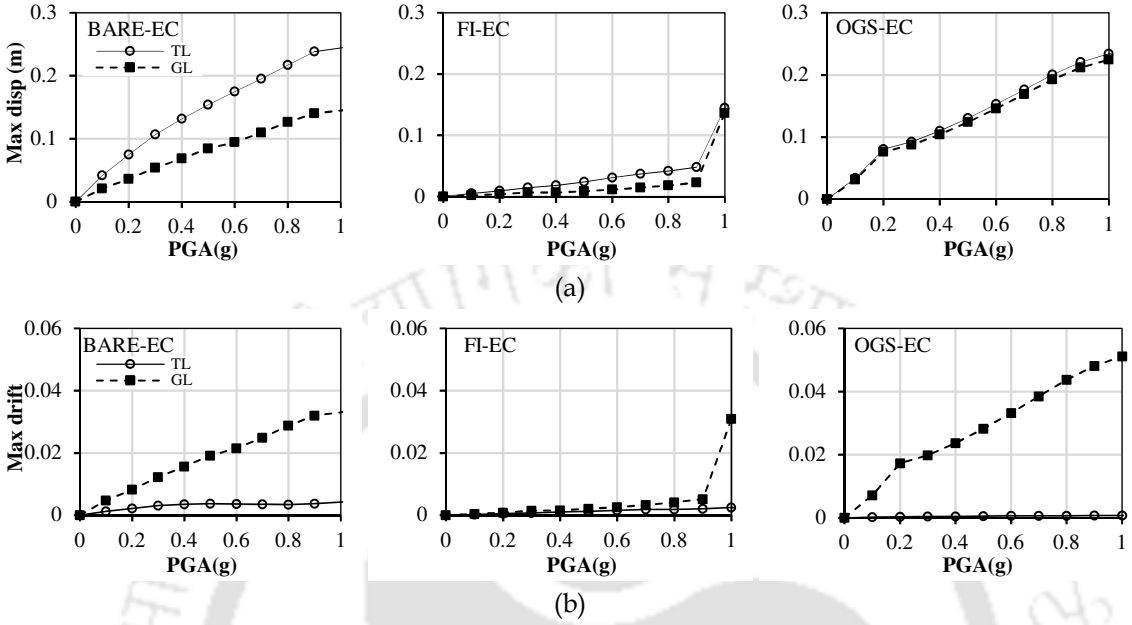

Figure 4.5 Variation of maximum: (a) displacement and (b) interstorey drift at top level (TL) and ground level (GL) for BF, FI frame and OGS frame for El Centro ground motion.

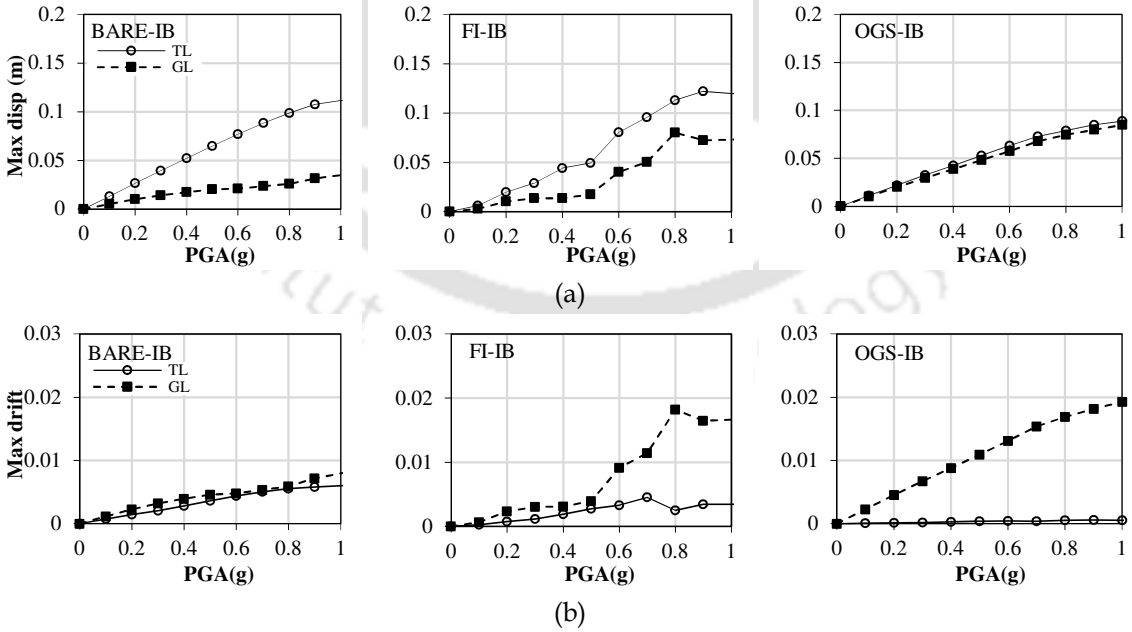

Figure 4.6 Variation of maximum: (a) displacement and (b) interstorey drift at top level (TL) and ground level (GL) for BF, FI frame and OGS frame for Indo Burma ground motion.

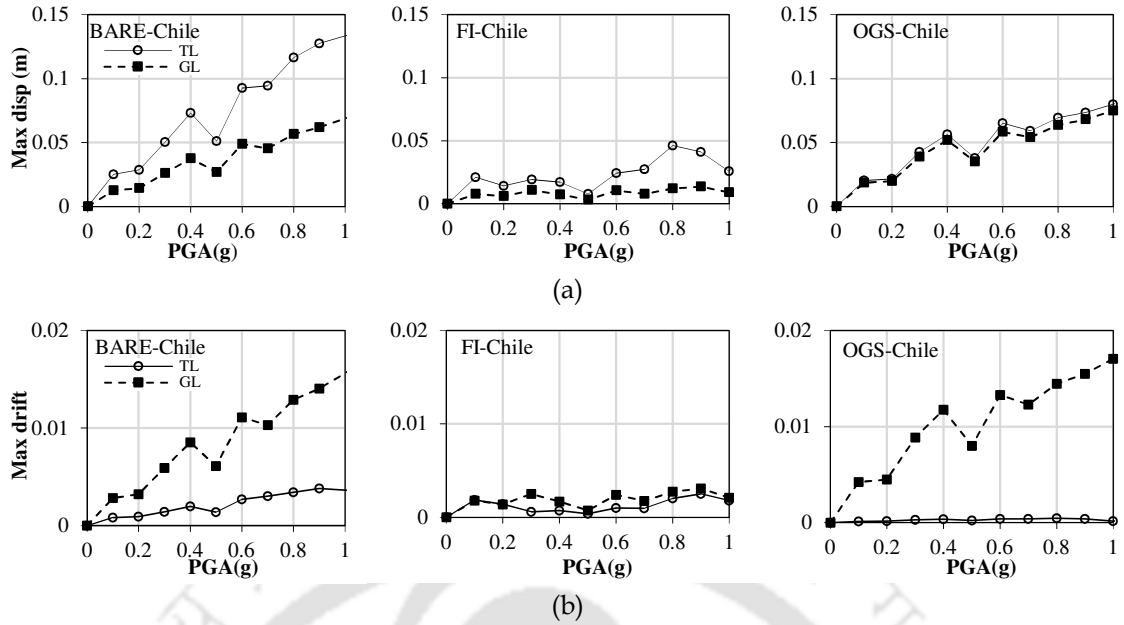

Figure 4.7 Variation of maximum: (a) displacement and (b) interstorey drift at top level (TL) and ground level (GL) for BF, FI frame and OGS frame for Chile ground motion.

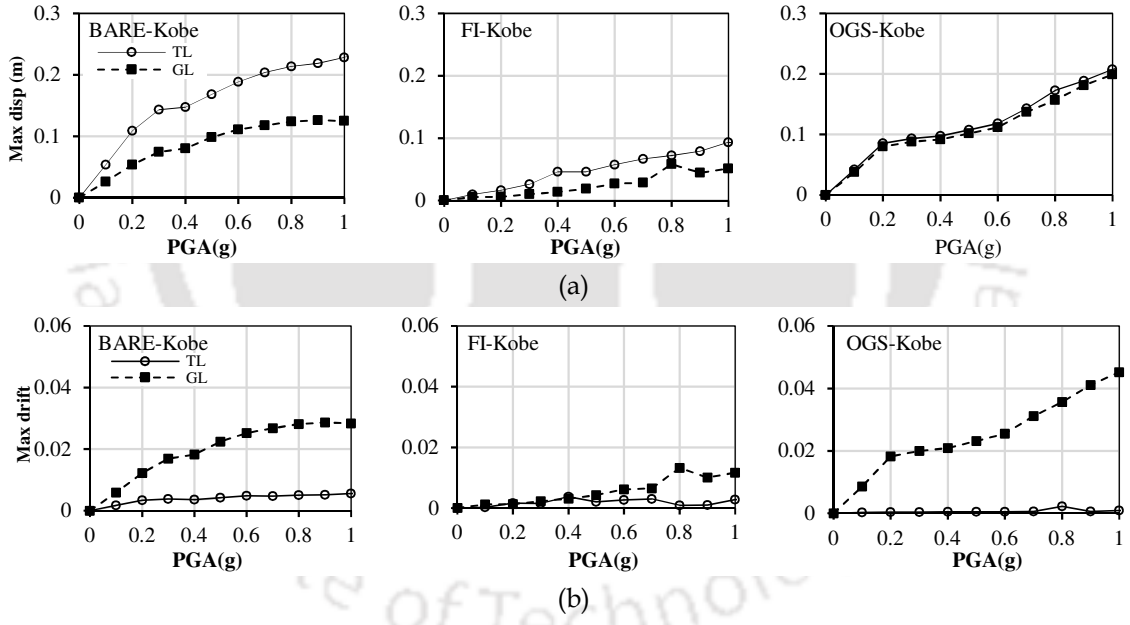

Figure 4.8 Variation of maximum: (a) displacement and (b) interstorey drift at top level (TL) and ground level (GL) for BF, FI frame and OGS frame for Kobe ground motion.

This clearly shows that the top level displacement of the frames can be conveniently taken as EDP for BFs and to certain extent for FI frames, since TL displacement is the critical displacement. But it is difficult to form such an opinion for OGS frame since both TL and GL show almost equal displacement and both the displacements appear to be critical.

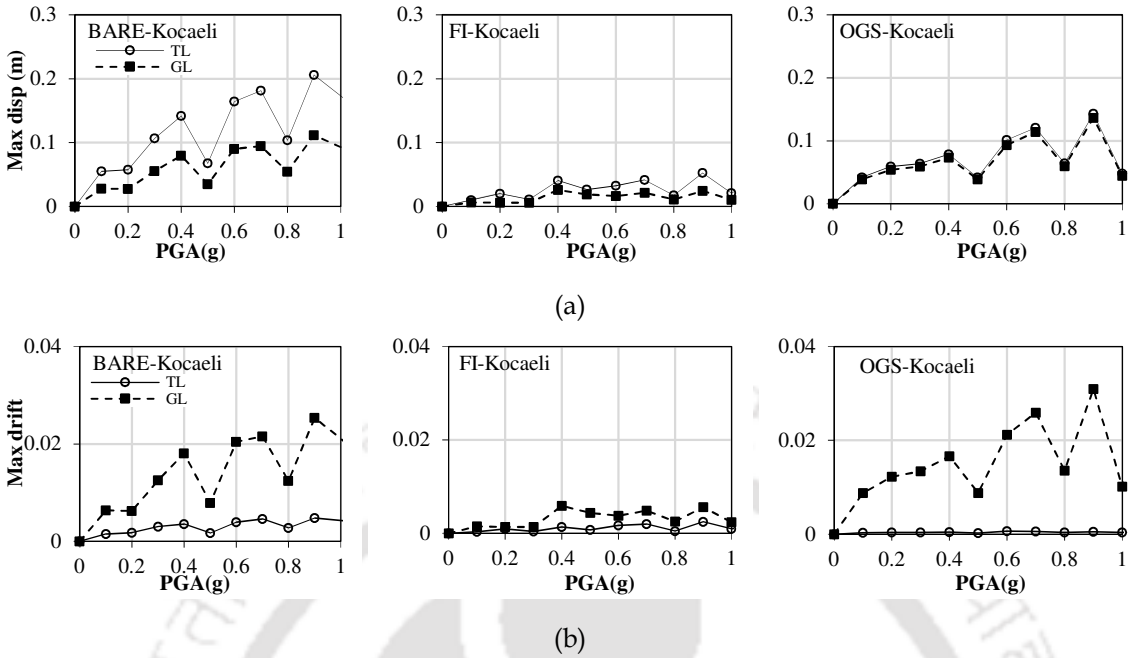

Figure 4.9 Variation of maximum: (a) displacement and (b) interstorey drift at top level (TL) and ground level (GL) for BF, FI frame and OGS frame for Kocaeli ground motion.

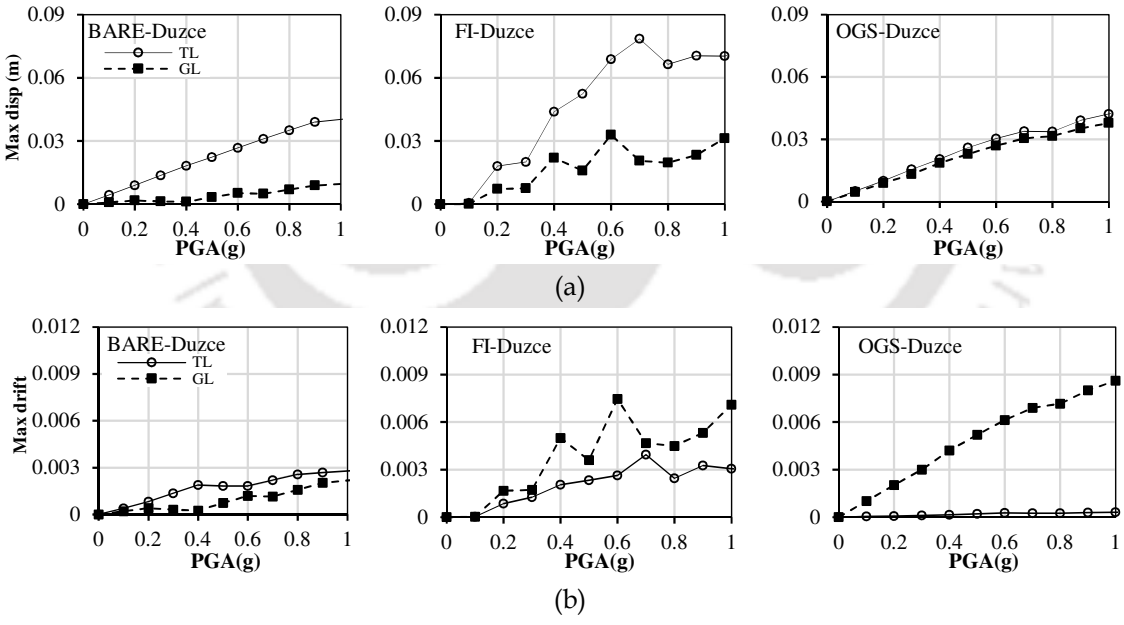

Figure 4.10 Variation of maximum: (a) displacement and (b) interstorey drift at top level (TL) and ground level (GL) for BF, FI frame and OGS frame for Duzce ground motion.

To look into the component level behavior, ISD is also plotted for TL and GL in Figures 4.5 – 4.11. Interestingly, the distribution of deformation of OGS frames changes completely on plotting the ISD demand; a very high GL-ISD demand is observed as compared to the TL-ISD. However, this difference is not much in case of FI frames or

BFs. Moreover, the TL-ISD in case of OGS frame is nearly zero. This proves that the ground storey columns are subjected to high ISD demand. In other words, there occurs a huge rotation in the columns of the ground storey of OGS frames, whereas, there is no rotation in all the upper storey columns. As already discussed, this is obvious due to the absence of infill in the ground storey of OGS frames. Clearly, the ground level columns are much more susceptible to damage compared to the top floor columns. This behavior is similar to the actual damage and failure observed in OGS buildings during past earthquakes, where huge rotation, and hence, damage was observed to be concentrated in the ground storey columns with a little relative deformation in the upper stories. This failure pattern of OGS frames is well captured analytically by considering the ISD at ground storey as the EDP.

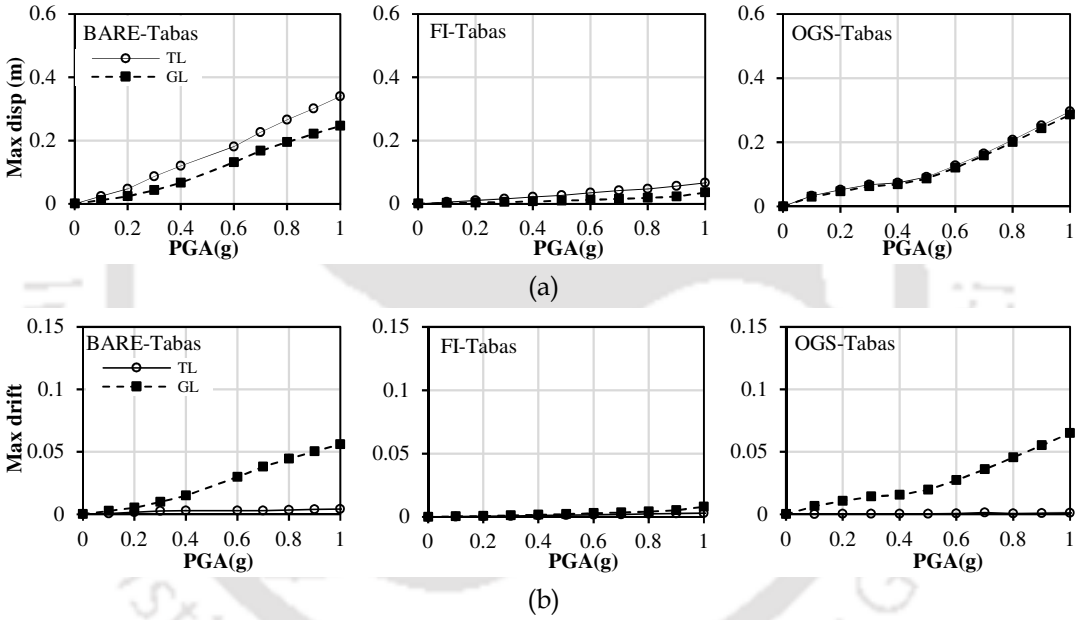

Figure 4.11 Variation of maximum: (a) displacement and (b) interstorey drift at top level (TL) and ground level (GL) for BF, FI frame and OGS frame for Tabas ground motion.

Therefore, from Figures 4.5 – 4.11 it is clear that the GL-ISD represents a better and realistic EDP for damage or fragility assessment of OGS frames for all ground motions at any PGA. On the other hand, for bare frames and FI frames (i.e., mostly regular frames) the GL-ISD or TL-ISD do not show a consistent variation across ground motions. For most of the ground motions considered, the TL-ISD and GL-ISD are nearly identical in case of FI frames, except at higher PGA, where the GL-ISD is higher as compared to TL-ISD. Therefore, peak lateral displacement at top storey may be used as EDP for damage or fragility assessment of regular frames. In case of BF, it is observed that for

some ground motions, GL-ISD is more critical than TL-ISD, similar to OGS frames. However, the value of TL-ISD for BF is considerable compared to TL-ISD for OGS frame, which is negligible. Thus, choice of a suitable EDP representing the true behavior or failure pattern is of concern particularly in case of irregular frames.

Fig. 4.12 shows the median of the frame responses obtained from NLTHA for all the ground motions. The maximum displacement at the top level or maximum drift over the height of the building (i.e., total drift at TL) are the two most commonly used EDPs for seismic performance assessment. For such EDPs, the BFs show maximum response (Fig.4.12 (b)) compared to FI or OGS frames. Similarly, when TL-ISD (Fig. 4.12(d)) is considered as EDP, the BF again shows highest response for all PGAs.

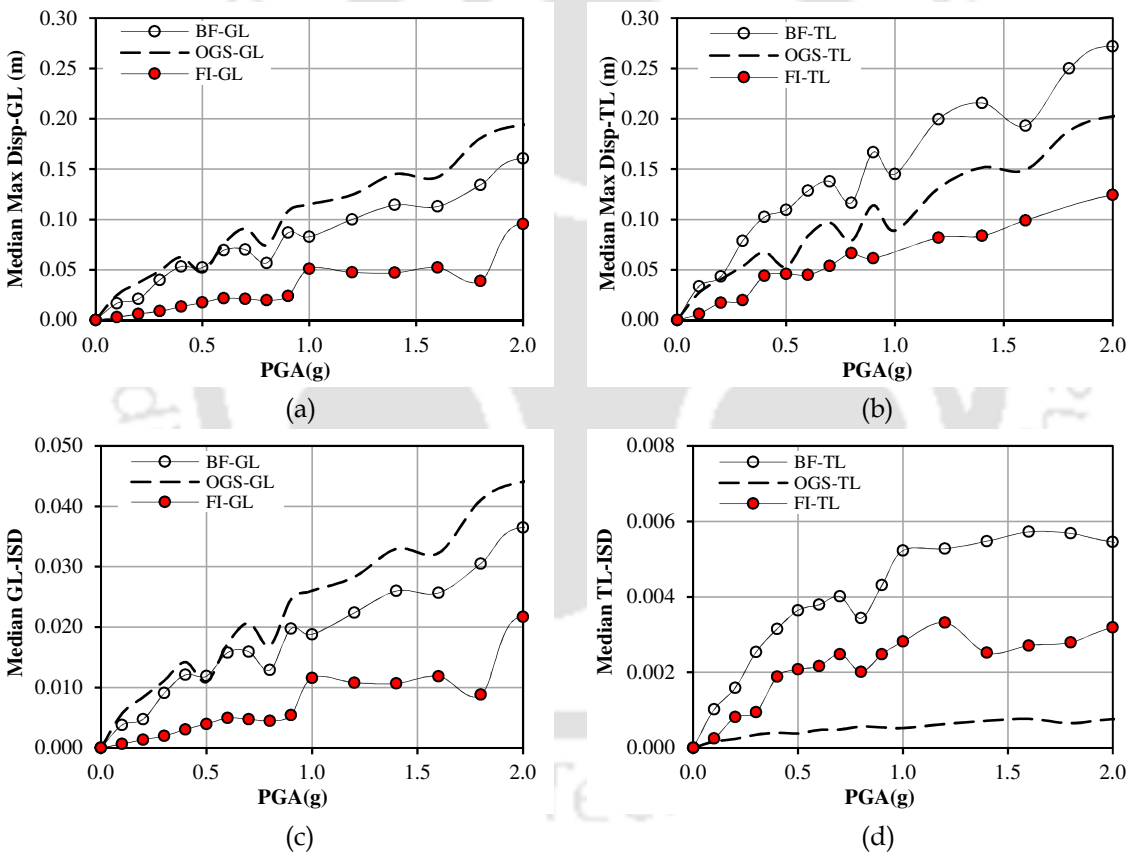

Figure 4.12 Median response at GL and TL obtained for BF, OGS frame and FI frame for all the ground motions.

Contrastingly, when displacement or GL-ISD (Fig. 4.12(a) and 4.12(c)) is considered as EDP, the OGS frames show the highest response. With respect to TL-ISD as the EDP, the OGS frames show the least response, which is in contrast to GL-ISD as EDP that shows the highest response. The displacement at GL or the GL-ISD thus shows

highest response for OGS frames, which is realistic and relates well to the past earthquake damage observed in such buildings.

4.4.3 Stiffness Factor

The stiffness factor (Fig. 4.13) or the stiffness degradation factor is defined as the ratio of the median stiffness at GL or TL (calculated as the median base shear divided by corresponding lateral displacement) to the maximum stiffness at the TL. The ratio is calculated based on the median values obtained from nonlinear time-history analyses considering all the ground motions and their samples (as discussed in Chapter 3). It is observed that in all the frames, the stiffness factor decreases with increase in seismic intensity measure (i.e., PGA) and it becomes constant after reaching a certain level of PGA. With increase in the seismic intensity, the frames undergo increase in displacement and plastic rotation occurs in the members of the frames. This increases the flexibility of the frames, and hence, the stiffness decreases.

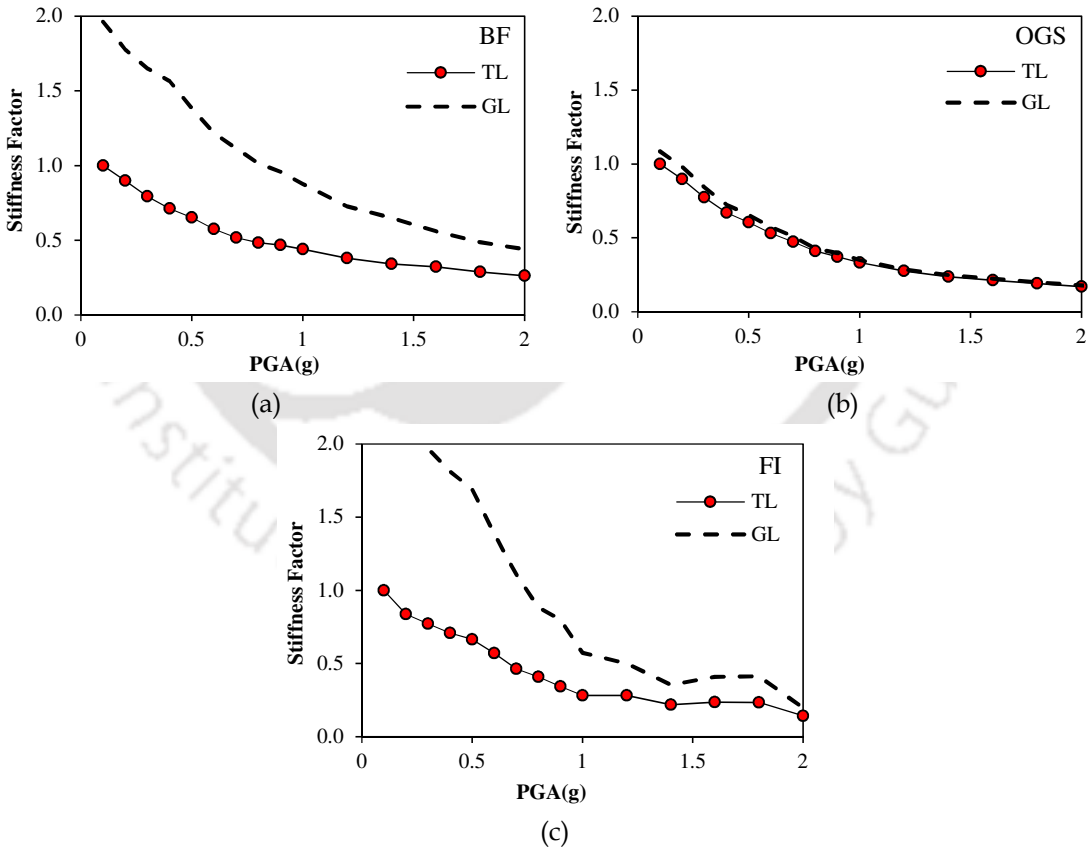

Figure 4.13 Comparison of stiffness factor at TL and GL for: (a) bare frame, (b) OGS frame, and (c) FI frame considering all the ground motions.

The initial stiffness demand at GL is much higher as compared to the stiffness demand at TL (nearly two times) in case of bare or FI frames. With increase in PGA, the GL stiffness factor reduces drastically and becomes equivalent to that of the TL stiffness factor. This implies that there is a uniform distribution of displacement demands in the bare or FI frame and that the displacement increases from GL to TL uniformly. However, in OGS frames, both the TL stiffness factor and the GL stiffness factor follow quite similar trend at all PGA levels. This proves that there is no relative deformation in the upper stories of the OGS frame and the variation in ground storey displacement itself represents the overall stiffness degradation in OGS frames.

4.5 Summary and Conclusion

The primary objective of the study is to establish a suitable engineering demand parameter for irregular building frames. Both global and component level demand parameters are evaluated for the three configurations of reinforced concrete frames (bare, OGS, and FI) by carrying out nonlinear time-history analysis considering seven ground motions. The major outcome of the study can be stated as below:

1 For regular frames, a global engineering demand parameter, such as, top or roof displacement or maximum interstorey drift at the top of the frame is sufficient to predict the damage, and hence, vulnerability of the frames to earthquake excitations.

2 In case of irregular frames, such as an OGS frame, where irregularity lies at the ground level, a component level EDP, i.e., ISD at the ground storey or displacement at the ground storey can conveniently predict the realistic deformations and, hence damage to the members in the frame.

3 Fully infilled frame is a specific case, where component level EDP needs to be considered only at high seismic intensity levels when the ground storey infills fail and the frame behavior becomes similar to the irregular OGS frames.

❄ ❄ ❄

Chapter 5

SENSITIVITY OF EDPS TO INPUT VARIABLES

5.0 Overview

Seismic fragility analysis involves probabilistic assessment of the seismic performance of structures. A large amount of uncertainty is involved in the estimation of seismic fragility. The probabilistic modelling framework for performance assessment of structures requires specifying the uncertainties in key input parameters in terms of probability distributions, sampling the distribution of the specified parameters in an iterative fashion, and propagating the effects of uncertainties through the analytical model. The objective of this work is to identify and statistically predict the influence of uncertainty in the independent input parameters on which the seismic performance of RC buildings (with and without infill walls) depends. Random samples of the uncertain parameters are used in parametric nonlinear dynamic analyses of three variants of typical three-bay, four-storey reinforced concrete frames, namely, bare frame, open ground storey frame, and fully infilled frame. The relative importance of the uncertainties in different input parameters on response sensitivity is discussed using different state-of-the-art statistical and graphical methods, such as displacement sensitivity radar charts, response sensitivity bar diagrams, tornado diagrams, Sobol' indices, Lasso regression, and weighted pie charts. The sensitivity of the seismic response of bare frames, open ground storey frames, and fully infilled frames is evaluated for different input parameters and compared in order to shortlist the parameters on which the seismic response of these frames mostly depends. Further, the influence of the input variables having high uncertainty on sensitivity of the seismic response of the frames is evaluated and discussed in the chapter.

5.1 Conceptual Background

Seismic vulnerability or fragility analysis is necessary for probabilistic seismic performance assessment of structures. The basic steps in fragility assessment include capacity and hazard estimation; a brief review of available analysis procedures for fragility assessment is given by Kaushik and Choudhury (2015). Structural analysis for capacity estimation of building frames includes a large number of assumptions related to the system parameters, and hence, involves a large uncertainty. The uncertainty arising from the variation in independent input parameters related to material, geometric, and loading properties that influence the capacity of the structure is known as epistemic uncertainty. The independent random input variables are chosen in such a way that they suffice the criticality of a problem. This leads to an assumption that all structural parameters are deterministic, and therefore, only their median values are generally considered in the analyses. However, the deterministic assumption may or may not suffice the purpose of analysis, i.e., the critical or median response may not be obtained considering all the median inputs. Thus, a probabilistic framework of seismic response assessment is essential in order to account for the variability or uncertainty associated with the random variables. Such a probabilistic assessment can be achieved through sensitivity analysis, which is a typical intermediate step in uncertainty analysis, aimed at identifying the input variables having a larger impact on the structural response (Celarec et al. 2012).

5.2 Need of the Study

Various past studies have carried out multiple parameter sensitivity analyses on different structural systems. The impact of input variable uncertainties on sensitivity in seismic response parameters have been studied for steel frames (Vamvatsikos and Fragiadakis 2010, Zona et al. 2012), masonry buildings (Rota et al. 2010), RC frames, wood frames (Aslani et al. 2012), gravity dams (Alembagheri and Seyedkazemi 2015), bridges (Padgett and DesRoches 2007), and steel jacket offshore platform (Eldin and Kim 2016). Mehanny and Ayoub (2008) considered different systems with the idealized single degree of freedom, and observed that the record-to-record variability is more considerable than the effect of uncertainty in the system parameters. Idealized systems for fourteen first mode-dominant structures with equal nominal relative lateral strength were considered in the study. Dolšek (2009) extended the incremental dynamic analysis with Latin

hypercube sampling to a set of reinforced concrete (RC) structures and showed that epistemic uncertainty does not have a significant influence on the seismic response parameters in the range far from collapse, but could have a significant influence on collapse capacity. It was also shown by means of Spearman correlation coefficient that of all the sources of epistemic uncertainty, damping and the ultimate and yield rotation in the columns have the greatest influence on the response of the RC structure. The uncertainties that influence the beams were not found to be so important for structures governed by the failure of columns. Kim et al. (2011) studied the sensitivity of design parameters, such as yield strength of beams, columns, and braces, live load, elastic modulus, and damping ratio of steel buildings subjected to progressive collapse. It was observed that the sensitivity of response depends on the collapse mechanism of the system. Limited studies (Celarec et al. 2012, Uva et al. 2012) on infilled RC frames were carried out in the past for examining the sensitivity of seismic response parameters to the uncertain modelling variables. However, only pushover analysis was carried out in these studies, because the use of nonlinear time-history analysis was computationally highly demanding. They observed that the parameters related to masonry infill have major influence on the response sensitivity of masonry infilled RC frames.

The sensitivity of a single input variable in the seismic response parameters is the simplest approach that can be used to study the influence of modelling uncertainty (e.g., Porter et al. 2002, Vamvatsikos and Fragiadakis 2010, Celik and Ellingwood 2010). Sensitivity analyses have been carried out in the past using different methods, such as tornado diagram analysis (TDA), first-order second moment (FOSM), Plackett-Burman design (Seo 2013) and Latin hypercube sampling (LHS) as discussed by Eldin and Kim (2016). TDA is a common tool for decision analysis, where the difference in the lower and the upper bound fractiles (known as swing) is evaluated to estimate the impact of a random input parameter on the output response. Porter et al. (2002) studied the sensitivity of seismic response of a high-rise non-ductile RC frame building to several parameters, and represented damage factors for the building using tornado diagrams. More recently, Seo and Linzell (2013) investigated on sensitivity of response of curved steel bridge to different parameters using tornado diagram analysis and provided insight into the seismic behavior of curved bridges. FOSM method uses a first-order Taylor series, and the first and second moments of the input variables to determine the random probability distribution of the response (Lee and Mosalam 2005, Baker and Cornell 2008,

Vamvatsikos and Fragiadakis 2010, and Celarec and Dolšek 2013). In both TDA and FOSM methods, the mean and standard deviation of the input parameter is predetermined, and based on that, the mean and standard deviation of the structural response is obtained. However, FOSM has been observed to lose accuracy when the relationship between input and response variables is nonlinear, which is a concern when modelling collapse (Gokkaya et al. 2016). LHS method uses stratification of the probability distribution function of a random variable. However, it gives only the relative importance of the input uncertain variables, and therefore, swing values cannot be obtained. Also, in case a large number of variables are involved, the number of simulations would be large and computationally intensive. Recently, Crozet et al. (2017) used Sobol' indices (Sobol' 1993) or variance-based sensitivity indices, given by Eq. (5.1), for sensitivity analysis of pounding between adjacent structures.

$$S_i = \frac{\mathrm{Var}[\mathrm{E}(Y \mid X_i)]}{\mathrm{Var}(Y)} \tag{5.1}$$

where, S_i represents the first order Sobol' index, Xi is the random input variable, Y is any output variable, Var is the variance, and $[\mathrm{E}(Y \mid X_i)]$ represents the expectance of Y conditioned on Xi. The Sobol' index can be determined up to any order based on the number of independent random variables. For considering qualitative variables in contrast to numerical variables, Soleimani et al. (2017) considered categorical regression model and carried out Lasso regression to evaluate the influential set of parameters out of a large number of covariates.

Review of past literature clearly shows that several methods, each having its own merits and demerits, have been adopted for sensitivity analysis of variety of structures without any consensus. Further, as discussed not many studies have been conducted on sensitivity analysis of masonry infilled RC frames. The choice of a proper engineering demand parameter (EDP) is important in seismic performance assessment of structures (Choudhury and Kaushik 2018b). The present study estimates the sensitivity of global seismic response (i.e., top or roof displacement) to uncertainty in various basic structural modelling parameters, such as those related to material (strength of concrete, steel, and masonry) and geometry (column dimensions). Three different types of structural frames are analyzed using nonlinear dynamic analysis: bare frame (BF - with no infills in any storey), open ground storey (OGS) frame (i.e., vertically irregular frame with infills only

in the upper stories keeping the ground storey open without infill), and fully infilled (FI) frames (with uniformly distributed infills in all the stories of the frame). Sensitivity analyses of the global response parameter to uncertain input variables are then carried out using different methods suggested in the literature for acceptable validation of the results. Sensitivity radar charts, response sensitivity bar diagrams, tornado diagrams, weighted pie charts, Sobol' indices, and Lasso regression coefficients are developed and compared for each of the random input variables for the three type of frames, and sensitivity determined.

This study thus focuses on estimating sensitivity of the global engineering demand parameters to identify random input variables whose further investigation may reduce the total uncertainty in the EDP. The results will be useful in determining the relative importance of the input parameters in fragility assessment of the considered frame configurations. The uncertainties associated with only the more important parameters can then be established with more rigour for a more accurate fragility assessment of structural systems. Computational efforts can be reduced by ignoring uncertainties in other random variables by treating them as deterministic and fixing their values at their best estimates. Different random input variables considered in the study are discussed in the next section.

5.3 Sensitivity Analysis

5.3.0 General

Sensitivity analyses are carried out for the three reinforced concrete frame typologies (Fig. 3.1) to find out the random input parameters on which the output or response sensitivity depends the most. The sensitivity analyses are accomplished based on the results obtained from modal analyses and nonlinear time-history analyses of the frames considering several ground motion records. The present sensitivity study identifies the uncertain input variables exhibiting strongest influences on the seismic demand of RC frame configurations using various state-of-the-art statistical and graphical techniques, such as radar charts, bar diagrams, pie charts, tornado diagrams, Sobol' Indices, and Lasso regressions techniques. The detail of each of these methods are discussed in this chapter and the results are presented in the following sections in order to comparatively assess the sensitivity for all the three frame configurations.

5.3.1 Uncertain Parameters Considered

Typical sources of uncertainty are those in ground motion and structural properties, known as aleatoric and epistemic uncertainties, respectively. The present study focusses mainly on sensitivity of response to various material, geometric, and loading properties i.e., the parameters responsible for epistemic uncertainties only. However, the sensitivity analyses are carried out for seven different ground motions to understand if there is any influence of different ground motion parameters on sensitivity of structural response. Ten structural parameters are considered as uncertain variables, namely, width of column (B_c), depth of beam (D_b), equivalent viscous damping (ξ), concrete compressive strength (f_{ck}), yield stress of steel (f_y), masonry prism strength (f_m'), unit weight of infill (γ_m) or infill load (IL), weight density of concrete (γ_c), width of equivalent diagonal strut used for modelling masonry infill walls (W_s), and ultimate strain at failure in masonry (ε_m). Width of the strut is different for ground ($W_{s\text{-}gr}$) and upper ($W_{s\text{-}up}$) stories. The statistical characteristics of each of the random input variables are presented in Table 5.1. The parameters related to the characteristics of masonry infill walls are considered only for FI frames, and not for the OGS frames, since their lateral load behavior is not affected by presence of infills in the upper floors (Choudhury and Kaushik 2017a). Random samples of each variable are generated based on their statistical characteristics.

As suggested in the literature (Table 5.1), a normal distribution is considered for the majority of the random variables, with the exception of the yield stress of reinforcing steel for which lognormal distribution is recommended (Ranganathan 1999). For each of the random variable, data is generated based on their corresponding standard deviations. Building mass and member dimensions are uncertain variables as the actual member dimensions (B_c, D_b) vary from those shown in the design documents, and unit weights (γ_c, γ_m) are imperfectly known. Moreover, material properties differ from those assumed in the analysis, e.g., actual stress-strain behavior at the element-fiber level differs from engineering idealizations. These independent material and geometric properties affect other dependent structural properties, for example, the concrete compressive strength affects the elastic modulus of concrete (E_c), and masonry prism strength affects the elastic modulus of masonry (E_m). Similarly, the parameters D_b and B_c affect the moment-curvature (or force-deformation) relationship of the structural members. A comprehensive discussion on uncertainty in viscous damping is presented by Porter et

al. (2002) and Celik and Ellingwood (2010). Uncertainties in structural strength and stiffness are considered at the stress-strain level. In constitutive models of reinforced concrete and masonry infill, three independent parameters are considered as random input variables: f_{ck}, f_y, and f_m' for strength uncertainty. The stiffness uncertainty is taken care of by using the dependent variables E_c and E_m. The masonry infill walls are modelled as diagonal struts for which the additional uncertain input variables considered are W_s and ε_m. Although, only the independent variables are monitored in the sensitivity analysis, the corresponding dependent variables are also given the due importance by varying their values appropriately in the analytical models.

Table 5.1 Considered uncertain input variables and their statistical characteristics.

Sr.	Variable	Probability Distribution	Mean	COV	Standard Deviation	Reference
1	f_{ck} (E_c)	*N*	25 MPa	0.124	3.11	Ranganathan (1999)
2	f_y	*LN*	450 MPa	0.038	17.26	Ranganathan (1999)
3	f_m' (E_m)	*N*	4.1 MPa	0.24	0.98	Kaushik et al. (2007)
4	ξ	*LN*	5%	0.76	3.8	Celik and Ellingwood (2010)
5	B_c	*N*	0.3 m	0.026	0.0079	Ranganathan (1999)
6	D_b	*N*	0.45 m	0.021	0.0094	Ranganathan (1999)
7	γ_c	*N*	25 kN/m^3	0.1	2.5	Ranganathan (1999)
8	γ_m (or *IL*)	*N*	18 kN/m^3	0.1	1.8	Kaushik et al. (2007)
9	$W_{s\text{-}gr}$	*N*	1.05 m	0.394	0.41	Basha and Kaushik (2015)
10	ε_m	*N*	0.0015	0.43	0.0006	Kaushik et al. (2007)
11	$W_{s\text{-}up}$	*N*	0.84 m	0.394	0.331	Basha and Kaushik (2015)

Note: *N* = Normal/Gaussian distribution, *LN* = Lognormal distribution, COV = Coefficient of variation, $E_c = 5000\sqrt{f_{ck}}$ and $E_m = 550 f_m'$

In the present study, the output is considered a known deterministic function of a variety of input variables. The sensitivity analyses are carried out based on the probability distribution of each of the input variables. Each variable is treated as uncertain but the simulation is controlled so that all the variables except one are taken at their median (50th percentile) value, and the response is evaluated establishing a baseline output. Then the output for a set of random input variables are determined, the input being the values based on their probabilistic distribution and coefficient of variation. The absolute value of the difference between the output from the two extreme cases (e.g., 16th and 84th fractile values) is a measure of the sensitivity of the output to that input variable. This difference is also called the swing (Porter et al. 2002). The process is then repeated, to determine the swing associated with the variability of all the other input variables. One can then determine the order of importance of the input variables to the sensitivity of the

output according to their swing. A larger swing in the seismic response to a particular input variable reflects more importance of that input uncertainty on the sensitivity of the seismic response.

5.3.2 Structural Modelling

A three-bay four-storey (3B-4S) reinforced concrete frame is considered as the base model (or mean model) where all the material and geometric properties and loading details are set to their median values. Three variants of the RC frame typologies (as discussed in Chapter 3) have been considered, namely, the bare frame (BF), open ground storey (OGS) frame, and fully infilled (FI) frame. The sectional details and member dimensions of the frame members are as shown in Fig. 3.1. The RC members are modelled as two-noded line elements and the masonry infill walls are idealized as single equivalent diagonal struts in SAP2000 (CSI 2015). The RC members are assumed to fail in flexural failure mode only as shear reinforcement with ductile detailing is provided in all the frame members as per the relevant Indian codes (BIS 2016b). Therefore, the RC members are provided with nonlinear flexural hinges defined using fiber modelling of the sections. The single equivalent diagonal struts are modelled with nonlinear axial hinges. The concrete compressive cube strength is taken to be 25 MPa (Elastic Modulus: 25000 MPa) and the reinforcing bars have expected yield strength of 450 MPa. Masonry prism strength is considered to be 4.1 MPa and elastic modulus is 2255 MPa. Weight of the masonry infill walls is considered as uniformly distributed load on the beams (weight density of masonry = 18 kN/m^3).

Mander's model (Mander et al. 1988) is used to characterize the stress-strain curve of concrete. The Mander model gives the stress-strain envelop in each of the concrete fibers in a section, and its hysteresis characteristics, i.e., the strength and stiffness degradation for every loading and unloading, is defined by the Takeda hysteresis model (Takeda et al. 1970). The hysteresis model is based on kinematic hardening behavior which is commonly observed in metals, is used for the reinforcing bars (Hahn et al. 1990). The idealized stress-strain model proposed by Kaushik et al. (2007) is used to model the material nonlinearity in masonry infill and the Pivot hysteretic model developed by Cavaleri and Trapani (2014) is used for modelling the hysteretic behavior of the equivalent struts for masonry infill.

5.3.3 Ground Motions Considered

The issue of adequately selecting and scaling an assemblage of ground motion records that could enable a dependable determination of structural behavior with fewer numbers of runs is of critical importance when ground motion variability is of concern. The primary objective of the present study is to understand the sensitivity of input modeling parameters on the response of the building frames. The intention is neither to perform an incremental dynamic analysis nor the multiple stripe analysis. Several past studies (e.g., Dymiotis et al. 1999, Rota et al. 2010, Kim and Han 2013) also considered three to seven real ground motions for determining displacement response from time-history analyses. Moreover, FEMA P-58 (2012) recommend using at least seven ground motions in order to reasonably estimate the median response over the height of the building. Thus, seven real-time ground motions without any modification in their inherent properties or scaling are used in the study.

Each ground motion differs in its characteristics, such as bandwidth, dominant frequency, energy content, and strong motion duration (considered the time bounded by the 3% and 97% limits of the Arias Intensity) as listed in Table 3.5. For each ground motion, normalized energy density curves and acceleration response spectra are plotted in Fig. 3.16(a) and Fig. 3.16(b) in order to show the variation in the ground motions. Nonlinear time-history analyses of are carried out for all the frames considering these ground motions, the results of which are discussed next.

5.4 Sensitivity from Modal Analysis

The modal analysis offers useful information on the expected behavior of a structural model. Modal analyses of the considered frames are carried out by considering all the uncertain parameters. Results of the modal analyses show that for bare frames (Fig. 5.1(a)), there is scarcely any difference in the time period due to change in the individual uncertain parameters, except for B_c and f_{ck}, which show a linear variation with a coefficient of variation of 8% and 6.5%, respectively. In OGS frames also (Fig. 5.1(b)), B_c and f_{ck} show the highest variation with coefficient of variation of 8.35% and 6.16%, respectively. For FI frames (Fig. 5.1(c)), the highest variation is observed in case of parameters related to infill, i.e., f_m' and W_s with COV of 21.2% and 25.15%, respectively. The modal characteristics give a preliminary indication of the parameters that may influence the nonlinear dynamic response of the frames.

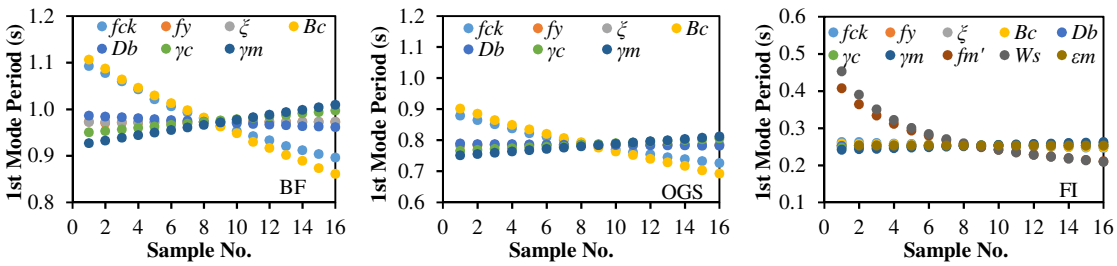

(a) (b) (c)

Figure 5.1 Sensitivity of natural period of vibration to random input variables for (a) bare frame, (b) OGS frame, and (c) FI frame.

5.5 Sensitivity from Nonlinear Time-History Analyses

5.5.0 General

For determining the sensitivity of output response to random input variables, the most commonly used global engineering demand parameter (EDP), i.e., displacement at the roof, is considered in all the time-history analyses. The results are categorized into various sections based on sensitivity analysis techniques, and compared.

5.5.1 Sensitivity of Response using Radar Charts

Radar charts, which graphically display multivariate data in the form of a two-dimensional chart, are presented in Figures 5.2 - 5.4, in which the three charts in each row represent the variation in displacement response of bare, OGS, and FI frames considering different samples (values) of an input parameter. The scatter in each chart represents the frame responses obtained from the nonlinear time-history analysis for the seven ground motions after normalization. Normalization of frame response is carried out with respect to the maximum value of displacement response obtained for each ground motion. The numbers at the bottom of each chart represent the coefficient of variation (COV) in frame response for the seven ground motions due to uncertainty in the considered variable. A higher value of COV means a higher variation in the response, and hence a higher sensitivity of the output. The numbers at the circumference of the radar charts represent the sample numbers of each uncertain parameter. The outermost circle of the chart represents the maximum frame response for a given ground motion with a value equal to one after normalization. A perfect circle formed by the scatter of the data points in the radar means there is a negligible variation in the output response due to any variation in the input parameter. In other words, it can be said that the frame response is insensitive

to any variation in the input data. On the other hand, if the scatter in the radar forms a spiral, it shows that the response varies significantly with respect to variation in the input, i.e., the response is highly sensitive to the uncertain parameter.

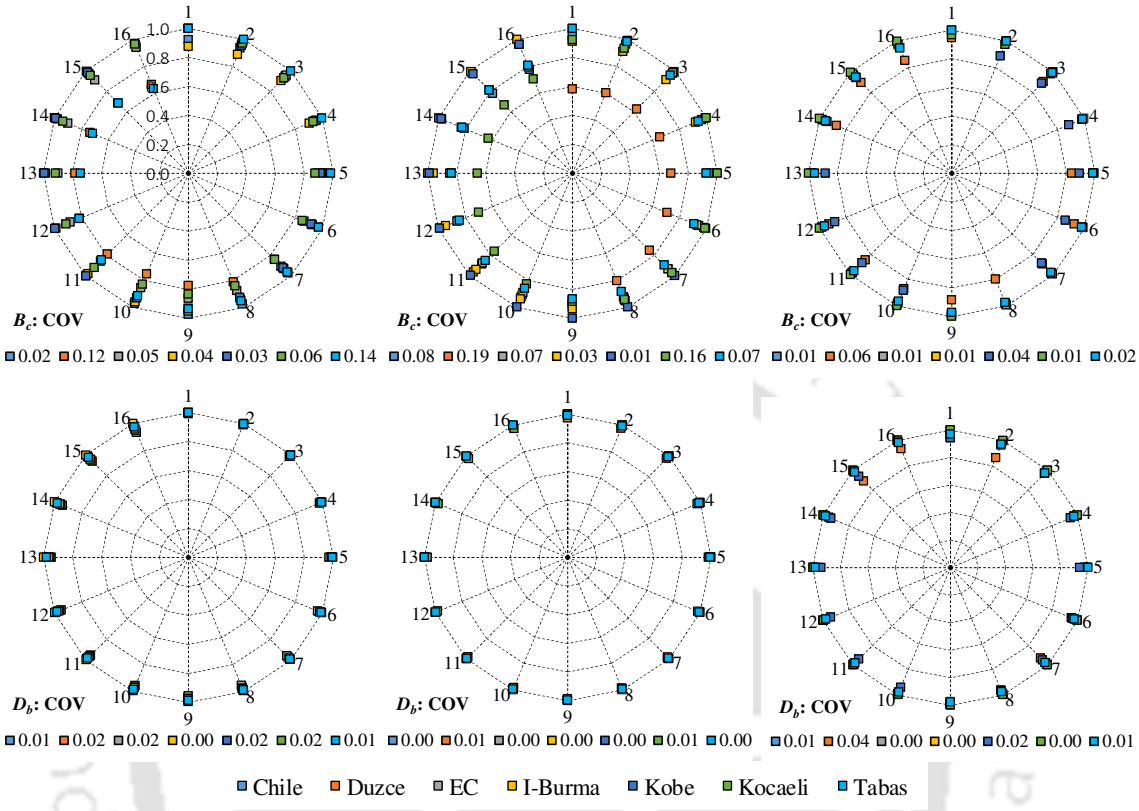

Figure 5.2 Displacement sensitivity radar charts for uncertain geometric input parameters with their COV for seven ground motions: (a) bare frames, (b) OGS frames, and (c) FI frames.

It is observed from the radar charts that for B_c, the scatters form spirals that tends to move inwards towards the center for several ground motions. As already discussed, formation of a spiral shows that the response is sensitive to the change in the variable. Scattering (formation of spirals) is highest in the OGS frames and least in the FI frames. A change in the value of width of column changes the sectional capacity, i.e., the yield and ultimate rotational capacities of the column members. This implies that the member section properties, i.e., the yield and ultimate curvature are sensitive parameters that yield a significant amount of variation in the response of OGS frames. There is no change in frame response due to a change in the input variable D_b for any ground motion in bare and OGS frames, i.e., the scatter forms a perfect circle. In FI frame, there is a slight variation in the response, however, the COV suggests that the values are negligible.

Comparing the sensitivity of D_b and B_c, it is inferred that the frame (bare, OGS or FI) response is more sensitive to any change in dimension of column rather than in beams. The yield and ultimate rotation in columns are important as influencing parameters.

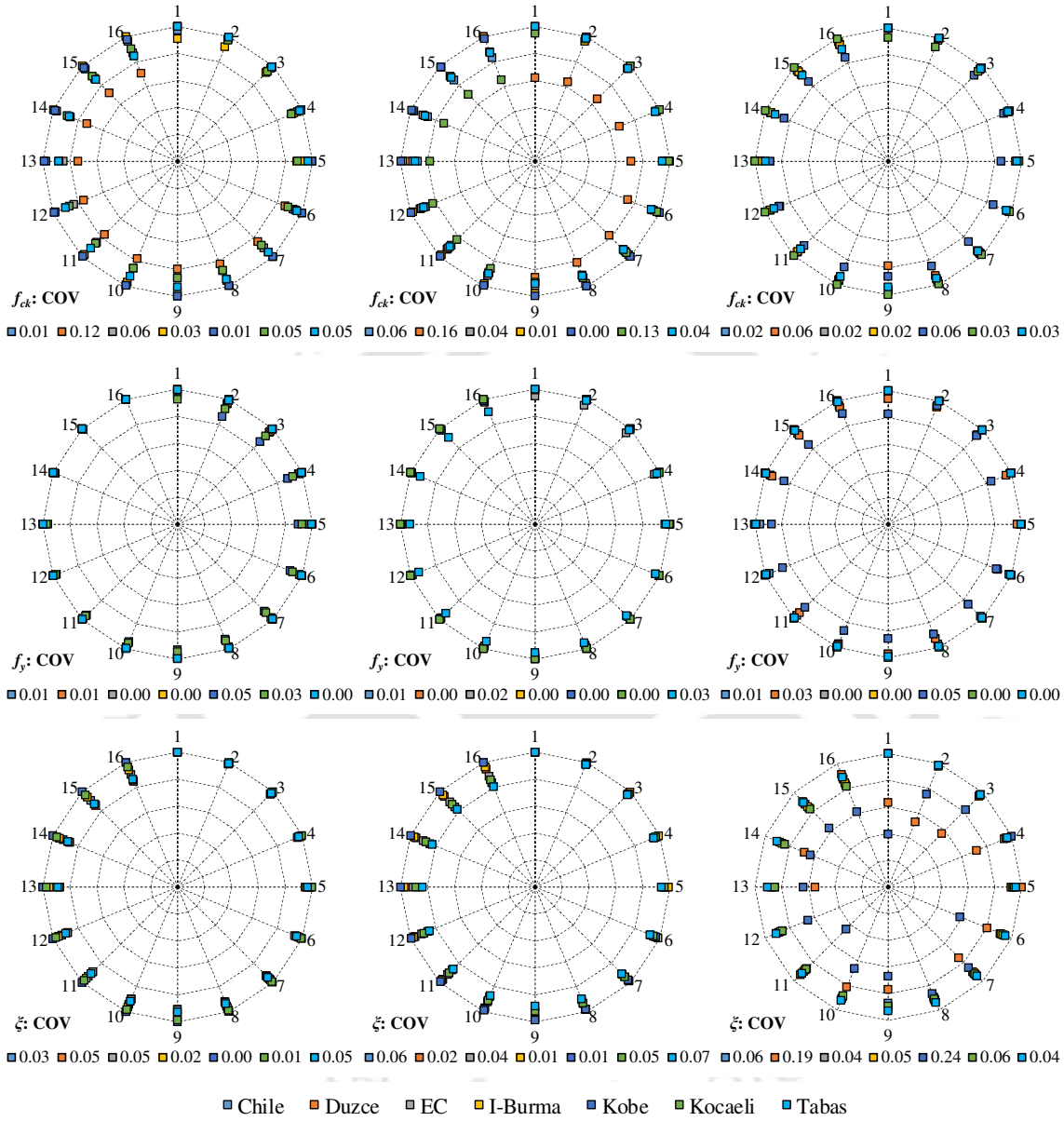

Figure 5.3 Displacement sensitivity radar charts for uncertain material input parameters with their COV for seven ground motions: (a) bare frames, (b) OGS frames, and (c) FI frames.

Significant variation in frame response (spirals in radar charts) is observed in the bare and OGS frames with a change in f_{ck} (Fig. 5.3). The value of COV ranges from 1% to 12% and 1% to 16%, respectively, in bare and OGS frames, indicating that there is little to moderate sensitivity in response of bare and OGS frames to change in f_{ck}. In fully infilled

frames, the COV is found to be negligible in the range of 2% to 6%. In case of f_y also, the scatters form almost perfect circle indicating that there is no sensitivity of bare, OGS or FI frame responses due to the change in f_y (the COV lies in the range of 1% to 5%). Lesser influence of f_y, as compared to f_{ck}, on sensitivity of seismic response of RC frames with different storey heights is also reported by Celik and Ellingwood (2010). The change in ξ shows the highest influence in response output of FI frames with a coefficient of variation as high as 24%. However, the effect of change in damping is negligible in response of BF and OGS frames with COV lying in the range of 1% to 7% only. There is a minor variation in the frame responses with respect to a change in the input parameter γ_c (Fig. 5.4). The response to infill load (γ_m or IL) variation also shows minor to moderate sensitivity with maximum COV of 3%, 9% and 12% in BF, OGS and FI frame, respectively.

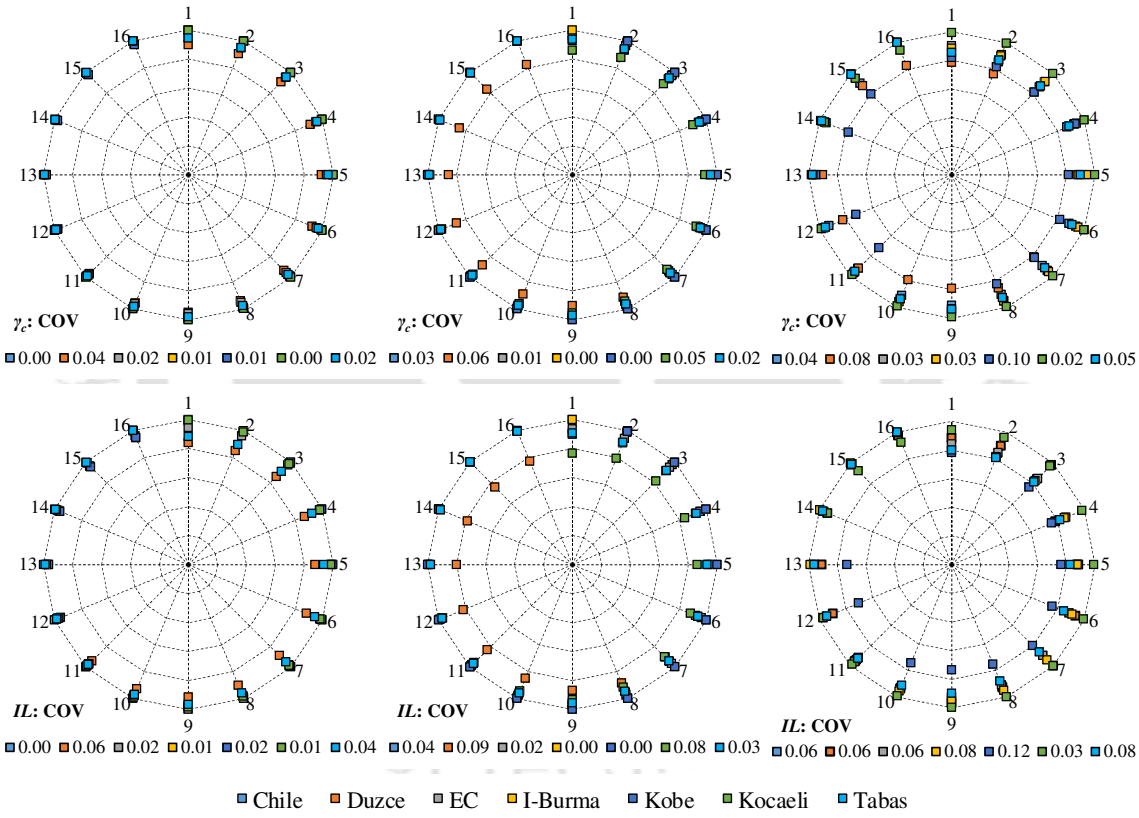

(a) (b) (c)

Figure 5.4 Displacement sensitivity radar charts for uncertain load input parameters with their COV for seven ground motions: (a) bare frames, (b) OGS frames, and (c) FI frames.

Three additional parameters (f_m', W_s, and ε_m) are considered in case of FI frames only, for which the variation in response due to input uncertainty are plotted as radar charts in Fig. 5.5. There occurs a large variation in the response due to uncertainty in f_m'

and W_s as seen from the formation of spiral in Fig. 5.5(a) and Fig. 5.5(b), respectively. Individual COVs for different ground motions are also very high with a maximum of 58% and 52% for f_m' and W_s, respectively. On the other hand, the variation in response due to a change in ε_m is negligible for most ground motions, except for the two cases where the COV is 11%. Thus, the effect of f_m' and W_s should be emphasized in the sensitivity of displacement response of FI frames.

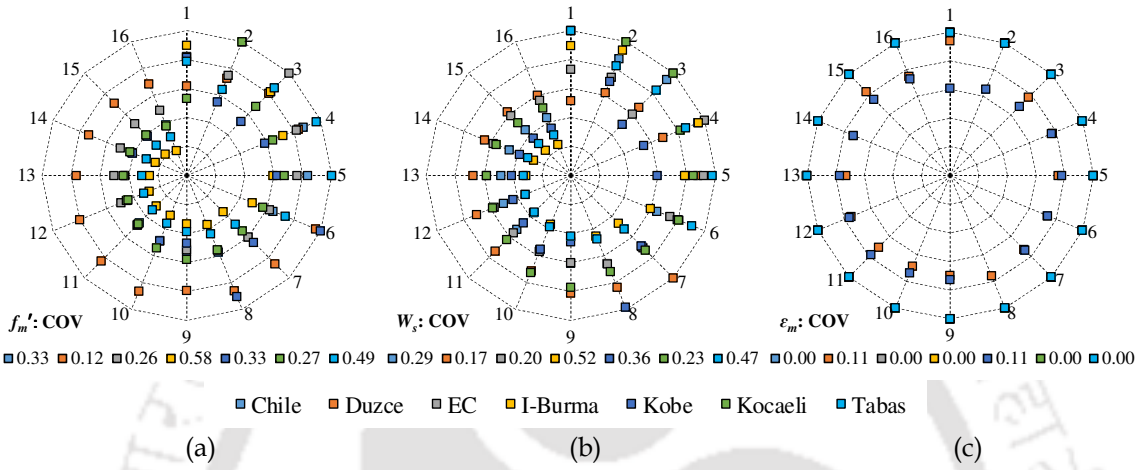

Figure 5.5 Displacement sensitivity radar charts for uncertain input parameters in FI frames: (a) f_m', (b) W_s, and (c) ε_m, with their coefficient of variation (COV) for seven ground motions.

5.5.2 Sensitivity of Response Using Bar Charts

It is equally important to understand the sensitivity of the structural response to variations in ground motions. Fig. 5.6 shows the bar charts for normalized roof displacement obtained for bare frames by varying different random input parameters. Normalization is done with respect to the roof displacement obtained from the median frame in which all the structural input parameters are set at their best estimate (i.e., median values). Each set of the bar chart in Fig. 5.6 represents the normalized displacement response obtained from nonlinear time-history analyses for a particular ground motion for different input parameters. The base line in each set of the bar chart has a value of 1.0 that represents the normalized displacement of the median model. Thus, each bar chart shows the variation in normalized roof displacement from the median estimate due to a variation in the random input parameter. It is observed that in most of the cases, the bars either reach a value of 1.0 (i.e., the median value), or oscillates around it often crossing the median value near the mid-sample range. This is due to the reason that near the mid-sample range lies the median model in which all the parameters are set

at their best estimates, and thus, gives normalized response near or equal to 1.0. However, it is not always necessary that the median parameter model result in the median seismic response as also observed by Vamvatsikos and Fragiadakis (2010).

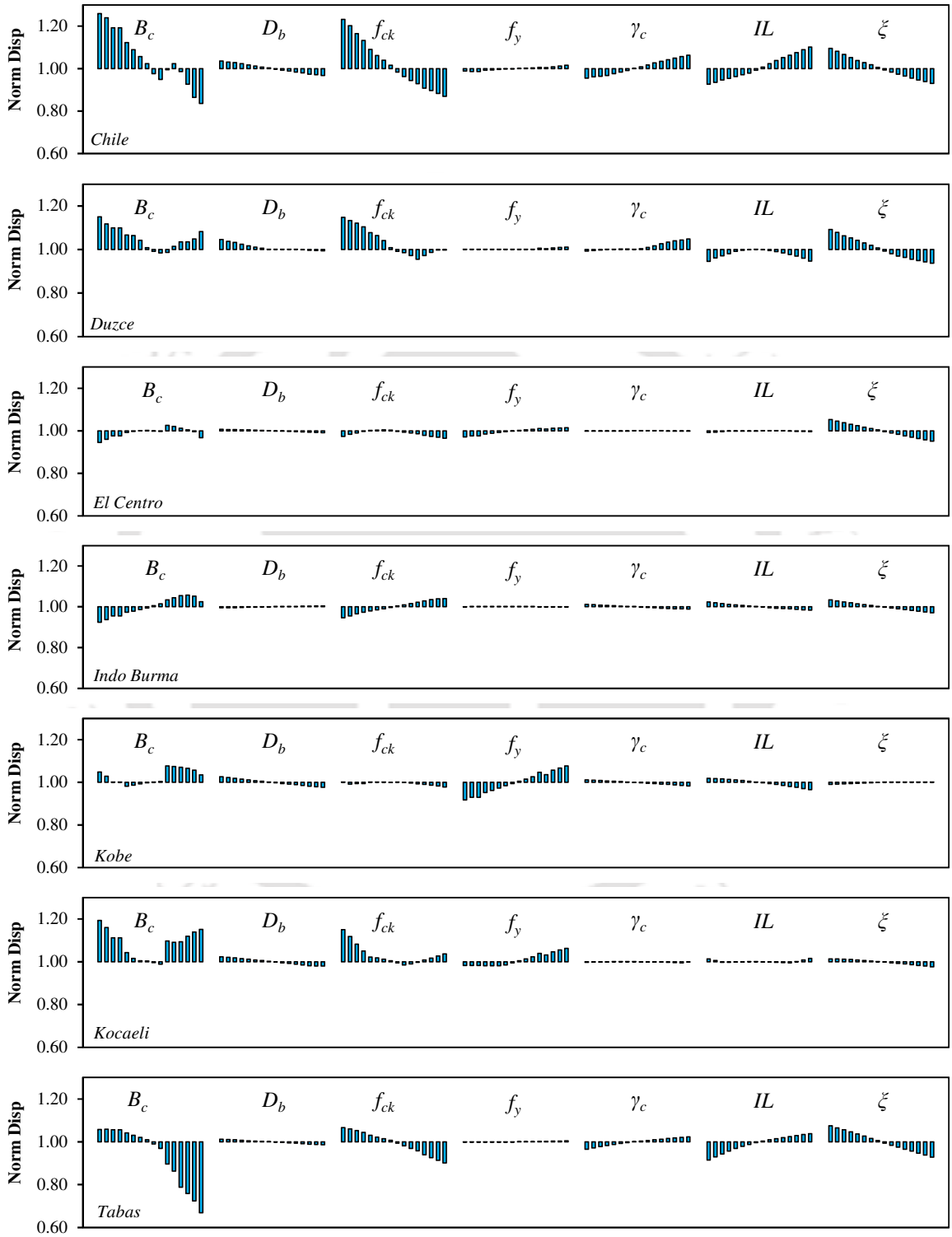

Figure 5.6 Response sensitivity bar diagrams for normalized top displacement in bare frames for different ground motions.

For majority of the ground motions, it is observed that a change in the parameters B_c, f_{ck}, IL, and ξ incurs a large variation in the estimates of roof displacement, i.e., values of the displacement response larger or smaller than 1.0 are obtained for the range of each input parameter considered (16 samples of each parameter). Varying the remaining parameters (D_b, f_y, γ_c) do not have much influence on the displacement response (i.e., their normalized displacement values are more or less equal to 1.0). Thus, it appears that in case of BF, of all geometrical properties, a change in column dimension is more influential than any dimensional change in beams. Liel et al. (2009) also conducted sensitivity analysis on a 4-storey RC frame and reported that the effect of column strength is more on the median collapse capacity compared to that of the beam strength. Out of the different material characteristics considered, the nonlinear displacements obtained are more sensitive to a change in f_{ck} and ξ, rather than f_y or γ_c.

Response sensitivity bar charts for normalized roof displacement are also obtained by varying different random input parameters for OGS frames (Fig. 5.7). Similar to the bare frame, for most ground motions, it is observed that the variation in parameters B_c, f_{ck}, IL, and ξ result in higher variation in response from the median estimate. A large oscillation in displacement response about the median value for these parameters indicates large deviations from the median estimate of displacement. Thus, it can be concluded that even though the structural behavior of bare frames and OGS frames differ significantly, the sensitivity of their global displacement response to random input parameters is quite similar. Column dimension, compressive strength of concrete, infill load, and system viscous damping are the major random input parameters affecting the sensitivity of global response of OGS frames.

In addition to the random input parameters considered for the bare and OGS frame, three additional parameters – ultimate strain in masonry (ε_m), compressive prism strength of masonry (f_m'), and width of equivalent diagonal strut (W_s) – are considered for sensitivity analysis of FI frames. Response sensitivity bar diagrams for fully infilled frames for different ground motions are shown in Fig. 5.8. Interestingly, for the FI frame, comparing all the random input parameters together, there is practically no variation in response output due to a change in the parameters B_c, D_b, f_{ck}, f_y, γ_c, IL, ξ, and ε_m. The most influential parameters for FI frames are f_m' and W_s indicating that uncertainty in these parameters has a major impact on the displacement response of FI frames. It can be

inferred from the results that the structural parameters (f_m' and W_s) related to infill primarily affects the response of FI frames.

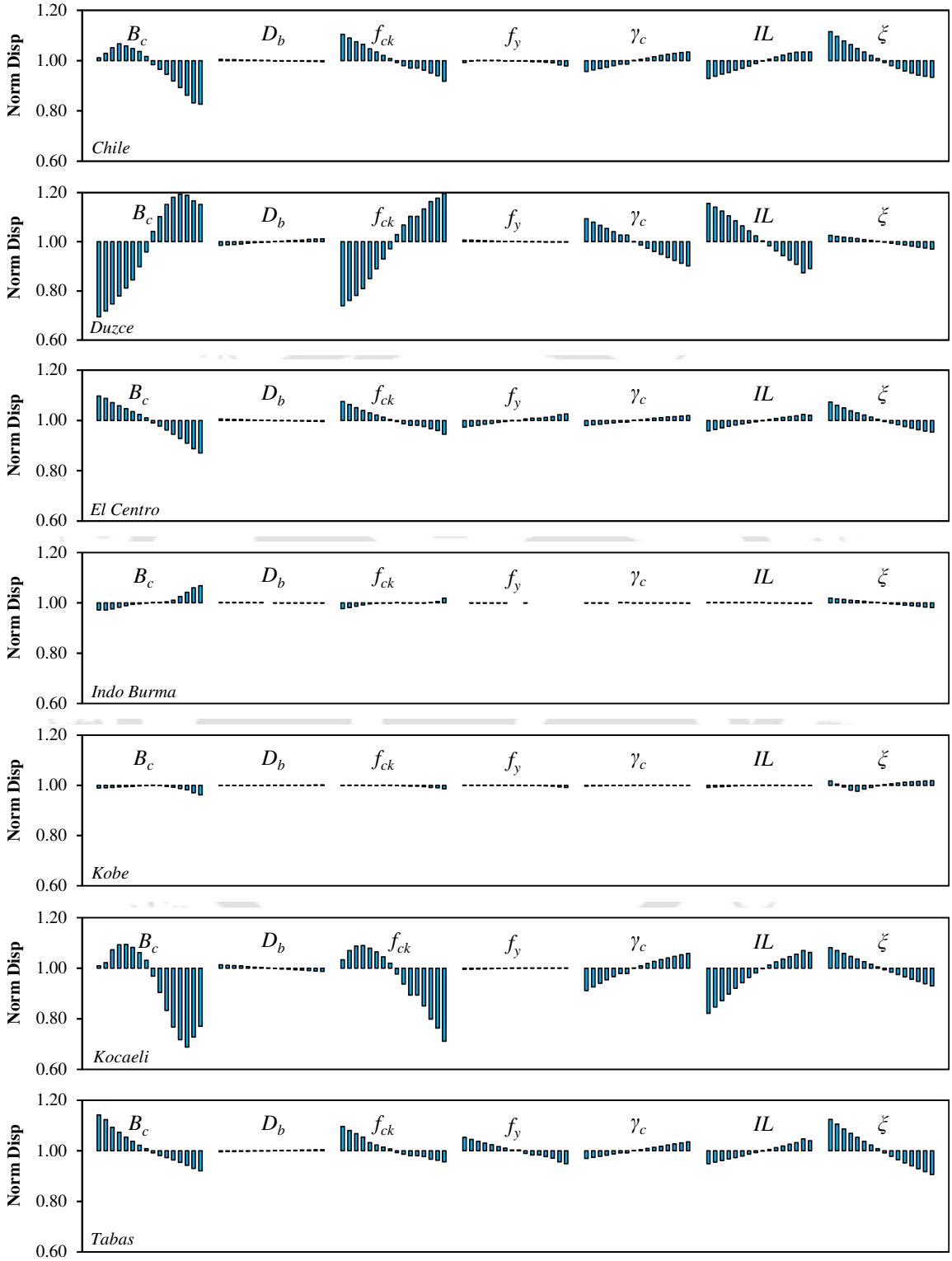

Figure 5.7 Response sensitivity bar diagrams for normalized top displacement in OGS frames for different ground motions.

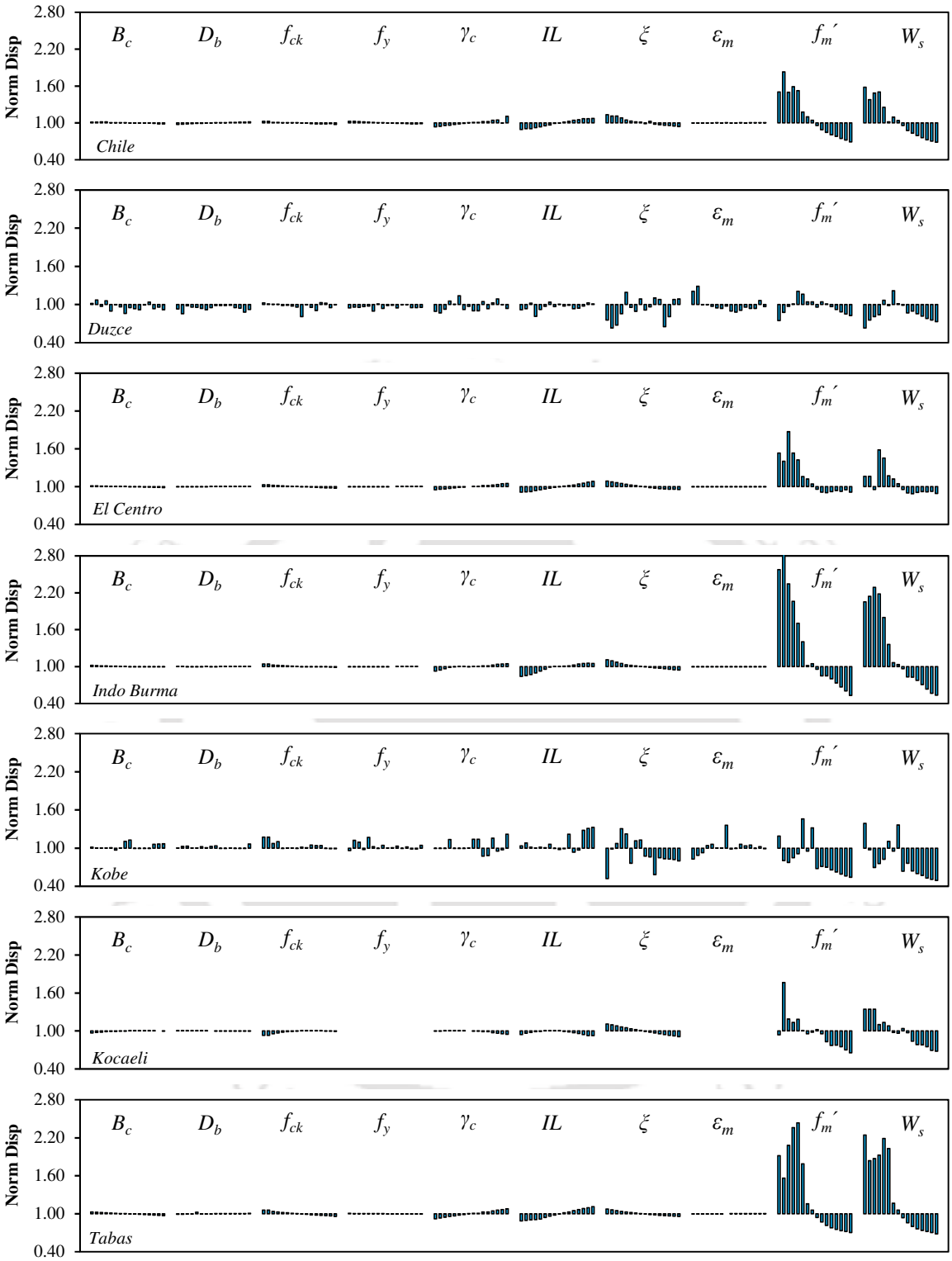

Figure 5.8 Response sensitivity bar diagrams for normalized top displacement in FI frames for different ground motions.

It is also interesting to note that in both bare and OGS frames, the response sensitivity of different parameters changes drastically for different ground motions. As mentioned already, B_c, f_{ck}, IL, and ξ show highest sensitivity in bare and OGS frame, more

specifically for Duzce, Kocaeli, and Chile ground motion. This is possibly due to the reason that these ground motions have high energy density (Arias Intensity in the range of 0.17 m/s to 0.32 m/s) values as compared to the other ground motions considered. On the other hand, for FI frames the response sensitivity is dominantly highest for f_m' and W_s only for all the ground motions without displaying much dependence on the energy content of the ground motions. Thus from these observations, it is clear that for relatively flexible systems (such as, bare and OGS frames), the sensitivity of displacement response is more for those ground motions, which have higher energy density. In contrast, for stiffer systems (such as, the FI frame), response sensitivity is independent of the energy content of the ground motion.

In OGS frame, the highest median frame response is obtained for Tabas (0.13 m) and Kobe (0.11 m) probably due to their high PGA values of 0.84g and 0.82g, respectively (Table 3.5). However, the sensitivity of response to different parameters for these ground motions is lesser than that for the other ground motions as shown in Fig. 5.7. Again, in BF the median frame response for Kobe (0.216 m) is higher than that for Chile (0.15 m), but the sensitivity of response to parameters is highest for Chile and lowest for Kobe (Fig. 5.6). Apparently, the sensitivity of the frame response is not dependent on the peak response of the frames or PGA of the ground motion. Similarly, in case of FI frame, the displacement response of the median frame is highest for Duzce (0.07 m) ground motion, whereas, sensitivity is least for the same (Fig. 5.8). Thus, although the number of ground motion considered is limited in the study, it can be concluded that the record-to-record variability can be obtained by concentrating more on energy characteristics of the ground motion. Increasing the number of records would have resulted in more elaborate description of record-to-record variability. However, the present study is concerned more on the sensitivity of the frame response to epistemic uncertainties.

5.5.3 Sensitivity Based on Tornado Diagram Analysis

Tornado charts (Porter et. al. 2002), as shown in Fig. 5.9, are also used for testing the sensitivity of response to different input parameters for the three frames, and for validating the sensitivity results obtained using radar charts and bar diagrams. Tornado diagrams have been effectively used in the past for seismic demand sensitivity analyses of buildings (Porter et al. 2002, Lee and Mosalam 2005, Seo and Linzell 2013). These diagrams are composed of set of flat bars corresponding to each parameter, where bar

length represents the variation in average maximum seismic responses caused by variation in each individual parameter. The extreme ends of the tornado show the 16th and 84th percentile values for the output response due to the variation in different random variables.

Based on tornado diagram analysis, it is validated that the basic parameters that influence the structural performance of a bare frame are B_c and f_{ck}. In OGS frames also, B_c shows the highest influence on the sensitivity of displacement response. Other parameters influencing the OGS frame response are f_{ck} and ξ similar to that for the bare frame. Additionally, for OGS frames, the infill load (IL) acting on the members of the frame also seems to be equally important as viscous damping (ξ). Celik and Ellingwood (2010) also observed with the help of tornado diagrams that structural damping and concrete strength are the key parameters influencing the sensitivity of response of RC frames designed for gravity loads in low-seismic regions. The effect of uncertainty in damping and ultimate and yield rotation in columns is also shown to be significant on RC frame responses by Dolšek (2009).

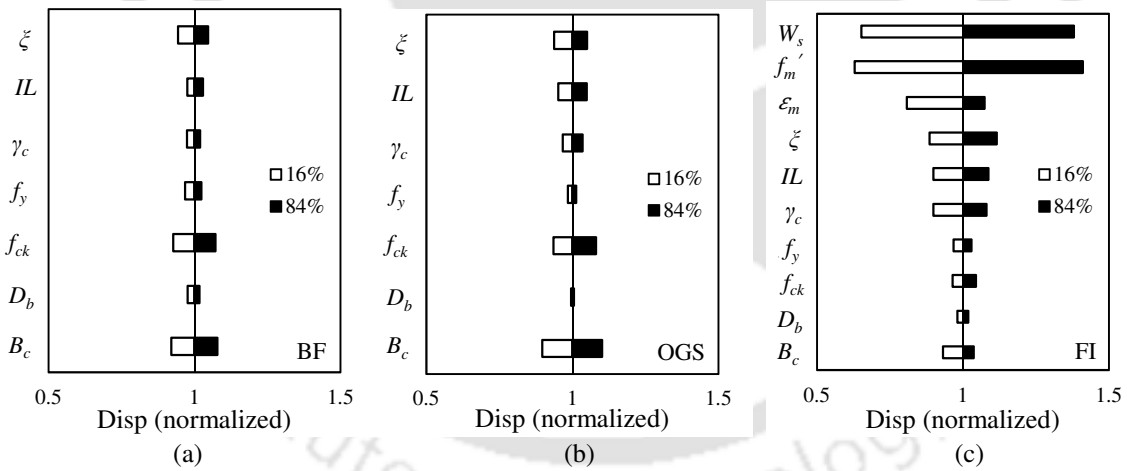

Figure 5.9 Tornado diagrams for displacement response sensitivity for (a) bare frame, (b) OGS frame, and (c) FI frame. (Figure shows the 16th and 84th percentile values of response for each uncertain parameter. The displacements are normalized with respect to the maximum response obtained for each ground motion).

In the present study, additionally the infill load (IL) acting on the members of the OGS frame also seems to be equally important as viscous damping. Other factors, such as W_s and ε_m are not considered for the OGS frame since the upper floor infills do not affect the overall performance of the frame (Choudhury and Kaushik 2018a). On the contrary, the parameters, such as, f_m' and W_s show the highest sensitivity on the response

of FI frame. This observation is further supported by the swings calculated for the three different frames for all the random input parameters (Table 5.2). The swing values, which can be used to quantitatively assess the sensitivity, are calculated as the difference between the extreme ends of the tornado diagram, i.e., the difference between the 16th and 84th percentile values in percentage. A high value of swing represents a higher sensitivity of the parameter on the output response. Highest swing is observed for parameters f_m' and W_s in case of FI frame; these swing values are about 7 times higher than that for B_c, and about 3 times higher than that for ε_m and ξ. This clearly implies that one has to be very careful with the values of f_m' and W_s when analyzing FI frames.

Based on the swing values reported in Table 5.2, the order of response sensitivity to different random input parameters of the different frames is as below-

BF: $B_c > f_{ck} > \xi > f_y > IL > \gamma_c, D_b$

OGS: $B_c > f_{ck} > \xi > IL > \gamma_c > f_y > D_b$

FI: $f_m' > W_s > \varepsilon_m > \xi > IL > \gamma_c > B_c > f_{ck} > f_y > D_b$

Table 5.2 Swing values obtained for different frames for considered random input variables.

Parameters	Swing values		
	BF	**OGS**	**FI**
B_c	16	20	11
D_b	4	1	4
f_{ck}	14	15	8
f_y	6	3	6
γ_c	4	7	18
IL	5	10	19
ξ	10	11	23
ε_m	NA	NA	27
f_m'	NA	NA	78
W_s	NA	NA	73

Note: NA = not applicable

The uncertain parameter, which has the greatest effect on the seismic response quantities, can vary from structure to structure since the structural collapse mechanism depends on the design process (Celarec and Dolšek 2013). Nevertheless, it is clearly observed that the order of response sensitivity to random input variables is similar in bare and OGS frame, i.e., parameters B_c and f_{ck} shows the highest sensitivity in output response. However, in FI frame, uncertainty in the parameters related to infills have

dominating influence on the sensitivity of displacement response. This is in agreement with Celarec et al. (2012) where results of nonlinear static analysis indicated that in fully infilled RC frames, uncertainty in the characteristics of the masonry infills has the highest impact on the response parameters.

5.5.4 Comparative Sensitivity for the Three Frames

The comparison of displacement response sensitivity due to input variation across different frames is shown in the bar charts of Fig. 5.10. The bars represent the coefficient of variations (COV) in the displacement response considering all the ground motions. Interestingly, it is observed that the parameters B_c and f_{ck} show highest sensitivity to the displacement response of the OGS frames. For all the other parameters, i.e., D_b, f_y, γ_c, IL, and ξ, FI frame comparatively shows a higher sensitivity. Out of different parameters, masonry prism strength (f_m') shows the highest sensitivity with a coefficient of variation of 37%, closely followed by W_s with a COV of 33%. The order of response sensitivity in bare, OGS, and FI frames along with their COVs is listed below (also shown in Fig. 5.10):

BF: $B_c(9) > f_{ck}(8) > \xi(5) > IL(3) > f_y(2) > \gamma_c, D_b(2)$

OGS: $B_c(12) > f_{ck}(10) > IL(6) > \xi(5) > \gamma_c(4) > f_y(2) > D_b(1)$

FI: $f_m'(37) > W_s(33) > \xi(14) > \varepsilon_m(13) > IL(9) > \gamma_c(7) > B_c, f_{ck}, f_y(5) > D_b(2)$

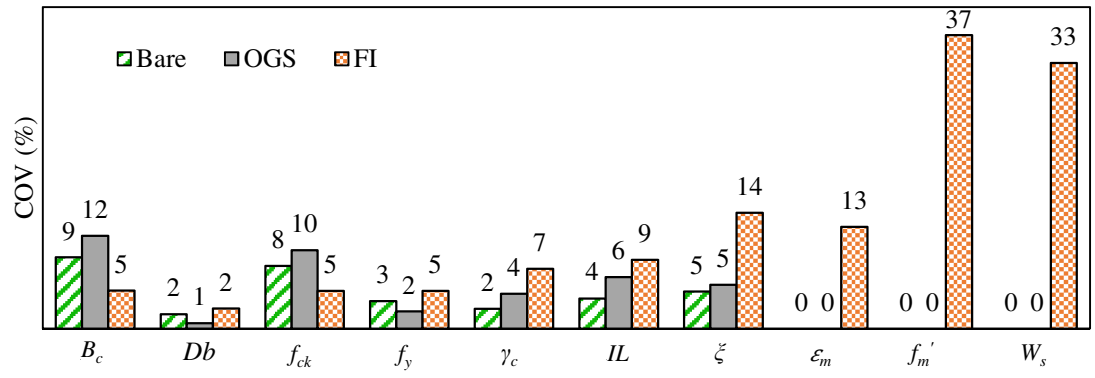

Figure 5.10 Bar charts showing the comparison of sensitivity of response to different parameters with respect to Bare, OGS, and FI frames.

Thus, it is clear from Fig. 5.10 that in FI frames, the parameters related to infills are the most sensitive input, and therefore, their uncertainties should be appropriately taken care of. These parameters are masonry prism strength, width of strut, and ultimate strain in masonry. The input uncertain parameters that mostly affect the response in OGS and BF are similar, i.e, width of column, concrete compressive strength, and damping. To

reduce the overall uncertainty in performance assessment, the focus should be on reducing the uncertainty in these parameters.

5.5.5 Sensitivity Based on Sobol' Index

The Sobol' index is a sensitivity index expressing the share of variance of response or any output data resulting from a given input or combination of input. Sobol' sensitivity analysis determines the contribution of each input parameter and their interactions to the overall model output variance. The Sobol' first-order sensitivity index gives a measure of the contribution of a given variable on a function or output without taking into account its interactions with the other variables. The higher the sensitivity indices value, the more influential respective model parameters are. Each parameter is a random variable ranging over some finite interval, with all the parameters mutually independent. The Sobol' method is based on decomposition of variance of any output variable obtained from the analysis considering random input parameters. The variance is decomposed into contributions from effects of single parameters, combined effects of pairs of parameters, and so on. The Sobol' first-order sensitivity index for a set of parameters is defined as in Eq. (5.1).

This index is evaluated for the three frame configurations considering all the independent random variables as already discussed. Fig. 5.11 shows the variation in Sobol' index obtained for all the parameters of the frames. The figure also relates the Sobol' index to the structural response under different ground motions, which is not seen in the results of sensitivity analyses carried out using the other methods. Thus, Fig. 5.11 gives the overall distribution of the sensitivity of the response of the three frames to different parameters for all the ground motions. As a general observation, significant impact of variation in compressive strength of concrete (f_{ck}) and width of column (B_c) is observed on the seismic response of bare frame and OGS frame (Figures 5.11(a) and 5.11(b)) since the value of Sobol' index is very high for these parameters compared to that for the other parameters. Additionally, in OGS frame (Fig. 5.11(b)), ξ also has an importance relative to the other parameters as indicated by the higher value of Sobol' index. In FI frames (Fig. 5.11(c)), f_m' and W_s hold the major position with the highest sensitivity index compared to any other random variables; an exception is system damping (ξ) for which two ground motions show sensitive index comparable to that of f_m' or W_s.

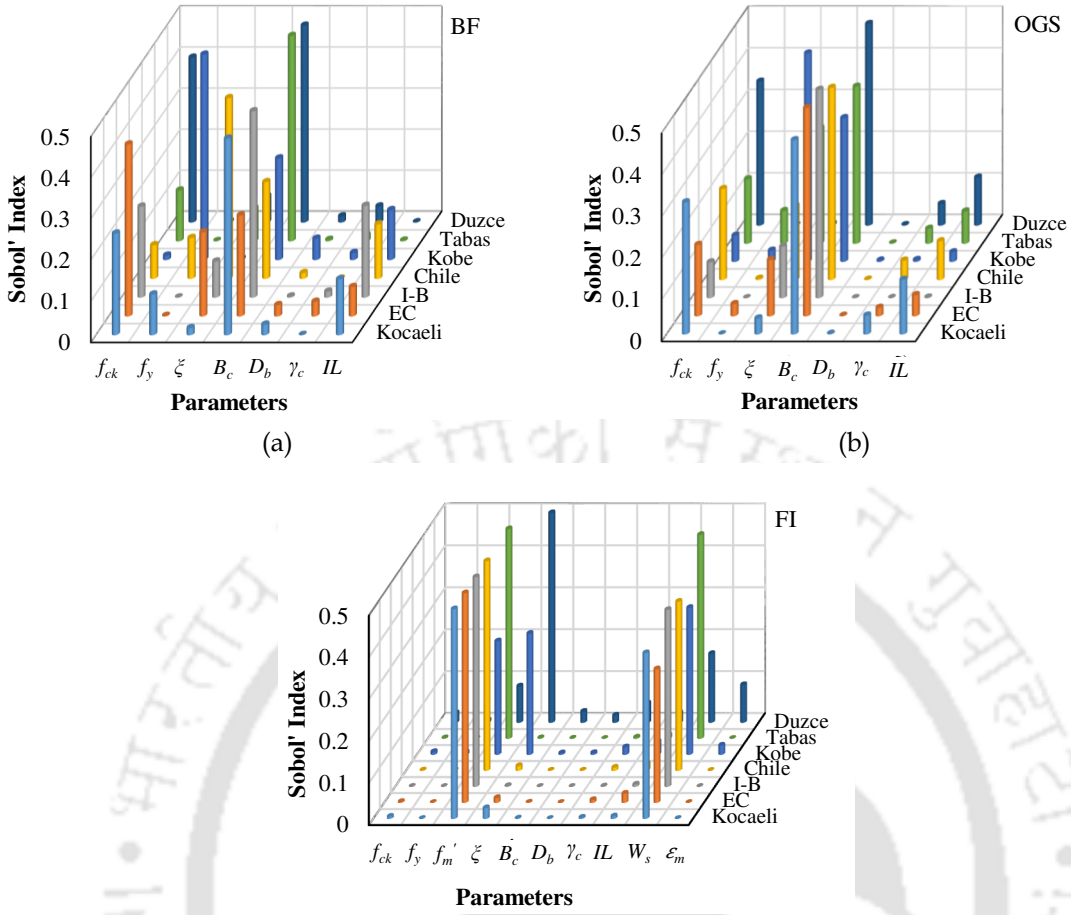

Figure 5.11 Sobol' first order sensitivity index for different parameters for the (a) Bare frame, (b) OGS frame, and (c) FI frame.

5.5.6 Sensitivity Based on Lasso Regression

In the present study, Lasso (least absolute shrinkage and selection operator) regression technique is also used for carrying out a sensitivity study to assess the effect of varying the list of modelling variables (Table 5.1) on the displacement response of the considered RC building frames. The method involves penalizing the absolute size of the regression coefficients such that some coefficients are shrunk and others set to zero, thus, retaining the good features of both S*ubset selection* and *Ridge regression* (James et al. 2013). Lasso is a regularization technique mainly applicable to the problems with a large number of covariates from which the influential set needs to be determined (Tibshirani 1996). A regularization or tuning parameter (λ) controls the amount of regularization. For generalized linear models, and for a non-negative value of λ, Lasso solves the following problem (Eq. 5.2):

$$\min_{\beta_0,\beta}\left(\frac{1}{N}\text{Deviance}(\beta_0,\beta)+\lambda\sum_{j=1}^{n}\left|\beta_j\right|\right) \tag{5.2}$$

The function Deviance in this equation is the deviance of the model fit to the responses using intercept β_0 and predictor coefficients β. N is the number of observations, parameters β_0 and β are a scalar and a vector of length n, respectively. $\sum_{j=1}^{n}|\beta_j|$ is the penalty term used for regularization. Fig. 5.12 shows the count of non-zero Lasso coefficients for different parameters plotted with respect to λ for bare, OGS, and FI frames. In order to obtain the count of non-zero coefficients, Lasso regression is first carried out separately for all the seven ground motions. For each random parameter, the Lasso coefficients are evaluated at different values of λ, which is determined by cross-validation.

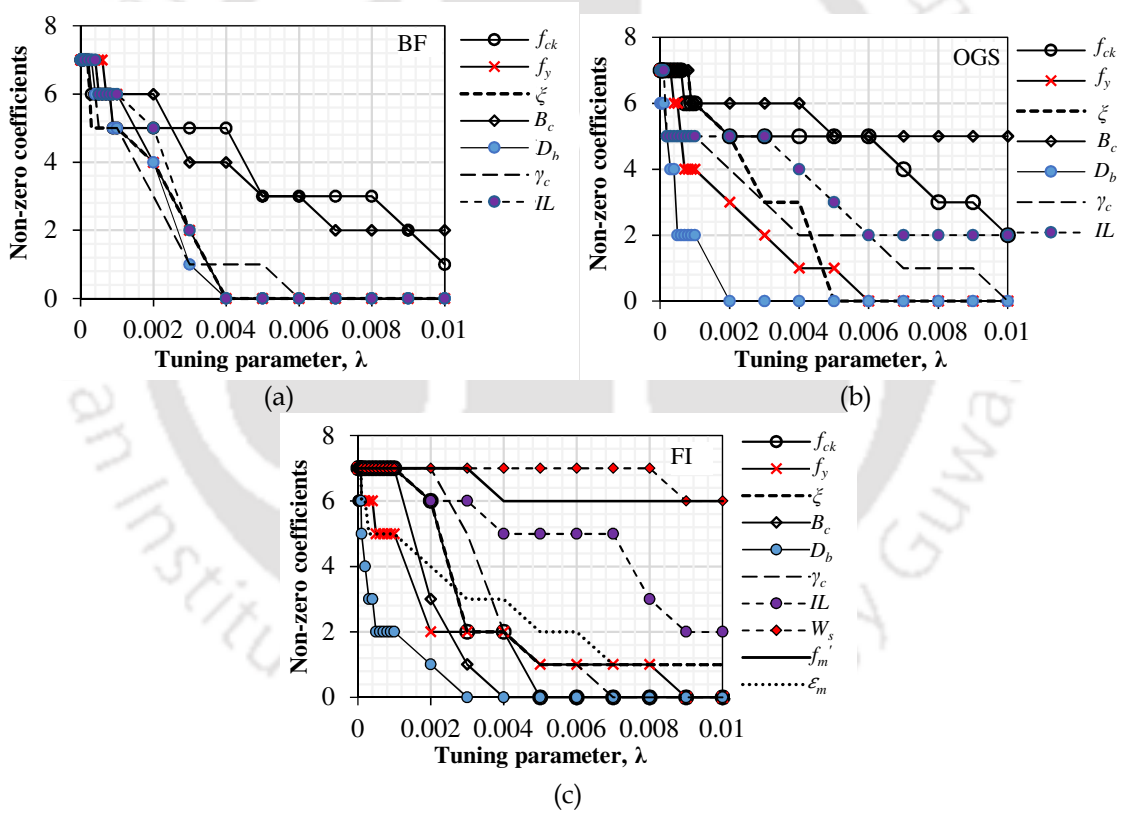

Figure 5.12 Significance of random variables on the displacement response using Lasso regression for the considered frames: (a) bare frame, (b) OGS frame, and (c) FI frame.

As the value of λ is increased, the values of the coefficients reduce and eventually some coefficients tend to zero value. The parameters with zero coefficient are the ones with negligible influence on the model. Thus, the remaining parameters with non-zero

coefficients are selected as the subset of the original set of parameters influencing the output. It is observed that for the bare frame, except for f_{ck} and B_c, all parameters cease to give non-zero coefficients at a λ value of 0.006. In case of OGS frame also, highest number of non-zero coefficients are obtained for B_c and f_{ck}. This again confirms that B_c and f_{ck} are the most important random variables in case of bare and OGS frames affecting the sensitivity of displacement demand on the frames. This observation is in agreement with the results obtained from the Sobol' index and tornado diagram analysis. f_y and D_b are the least significant parameters in all the frames since their coefficients quickly reduce to zero. For FI frames, the Lasso regression shows that W_s, f_m', and IL are the primary parameters whose uncertainty contribute majorly to the displacement response.

5.5.7 Weightage of Input Uncertainty to Output Sensitivity

So far, the sensitivity of different parameters to the seismic response of the three frames is evaluated using independent approaches and the most important or the sensitive parameters are shortlisted. However, it is also important to understand the relative weight each input uncertainty has on the output sensitivity. The pie diagrams in Fig. 5.13 show the weight (relative COVs) of uncertainty in individual random input parameters versus the sensitivity in the output response. The weighted sensitivity in the displacement response of the frames is obtained as the weighted ratio of the maximum COV for the individual parameter to the maximum COV of all the parameters for all the ground motions. This type of normalization gives a weighted comparison of all the parameters. Fig. 5.13(a) shows the weightage of uncertainty in each input variables considered in the study. The chart shows very less variation in parameters B_c, D_b, f_y, γ_c, γ_m, IL, and f_{ck} in comparison to parameters ξ, ε_m, f_m', and W_s for which the weightage is quite higher.

It is observed that even though some input parameters show a very less COV, their influence on the displacement response is very high and the vice versa. This is in contrast with Celarec and Dolšek (2013) who observed that a large coefficient of variation in the random input variable has significant impact on the results of sensitivity or uncertainty analysis. For example, the weightage of width of column (B_c) on response is 30% and 31% in bare and OGS frame, respectively, even though the weightage of uncertainty in the input variable B_c is only 1%. This shows that the displacement response of bare or OGS frame is highly sensitive to any change or variation in the dimension of

column of the frame members. Thus, even though minor variations are practically observed in some parameters, such as, the width of column, their influence on the structural performance can be very high that cannot be ignored. On the contrary, the beam parameter, i.e., the depth of beam (D_b), also having a weightage of 1% in input uncertainty, do not show any significant sensitivity in the response of any of the frames showing a weightage of only 2% to 5% in response sensitivity. The uncertainties that influence the beams are not so important, since the lateral load response of the frames is primarily governed by the characteristics of the columns. Similarly, f_{ck} also shows a high input to output sensitivity in OGS and BF, i.e., even though the input weightage is not so high (only 6%), the output response weightage is very high (26%).

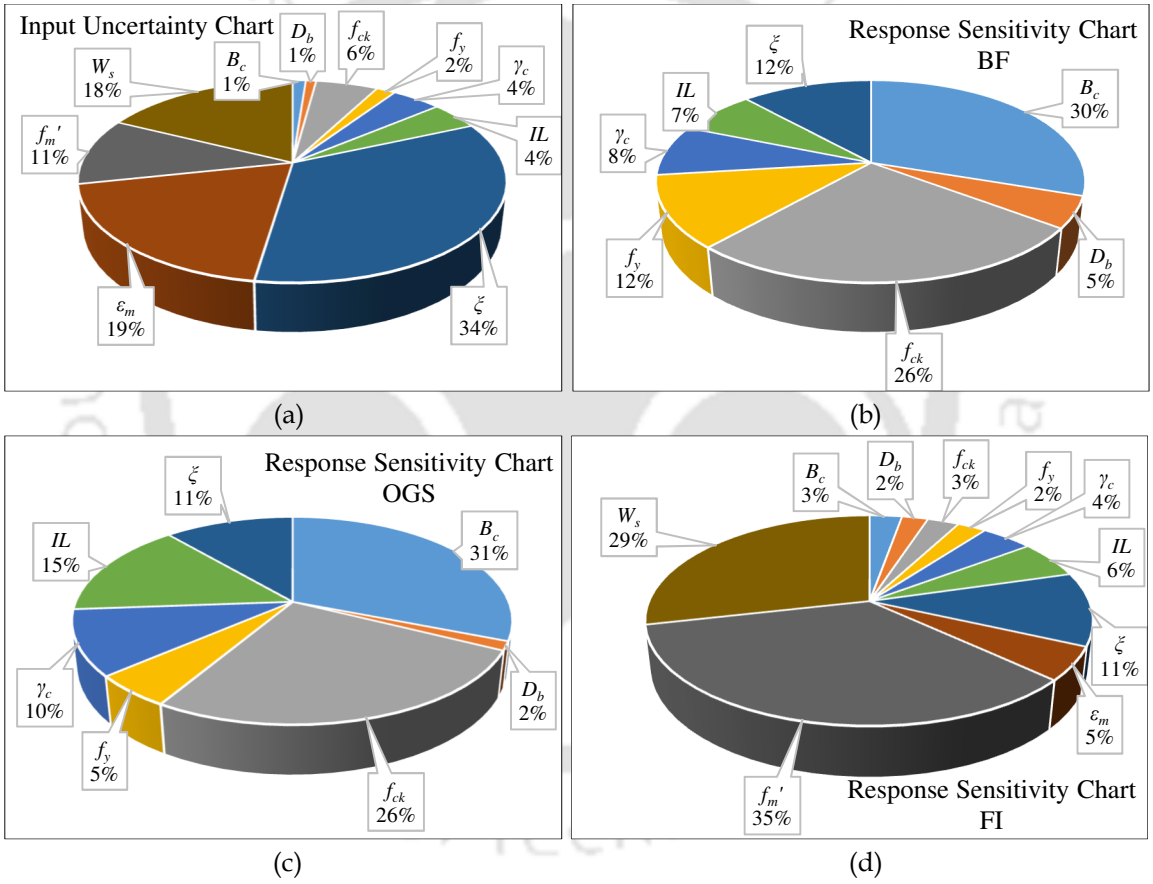

Figure 5.13 (a) Weightage of different parameters in different random input variables, (b) Response sensitivity chart for Bare frame, (c) Response sensitivity chart for OGS frame, and (d) Response sensitivity chart for FI frame.

Infill load (IL) may be important in case of OGS frames as it shows a weightage of 15% in response sensitivity as compared to its input uncertainty of just 4%. In FI frames, as already discussed in the previous sections, the input parameters that chiefly dominate the sensitivity of output response are those related to infill. These parameters (W_s and f_m')

contribute to a total of 64% (29%+35%) weightage in sensitivity out of all the parameters (Fig. 5.13(d)), even though their combined input uncertainty is 29%. Uncertainty in other input variables, such as, f_y, γ_c, ξ, and ε_m have relatively lesser influence on the roof displacement although the weighted uncertainty in some of these variables is very high (e.g., 34% in ξ and 19% in ε_m).

5.6 Sensitivity of Other EDPs

Use of local EDPs, such as the interstorey drifts, have been found to be important for member capacity evaluation, investigation of failure criteria, and fragility estimation of irregular buildings, especially those designed for gravity loads (Dymiotis et al. 1999, Freddi et al. 2017). Open ground storey frames are found to have severe vertical irregularities in the form of drastic reduction of stiffness and strength in the ground storey. However, as observed from Chapter 4, the displacement in OGS frames at the roof and the ground storey level is more or less similar. Therefore, the sensitivity of the response should not change for OGS frames even if the global roof displacement is chosen as EDP. Lee and Mosalam (2005) also observed that the sensitivity of local and global EDP to some random variables is similar for RC shear wall buildings. Moreover, most of the national codes have design provisions related to global roof displacement as the EDP.

In order to understand the role of EDP on the response sensitivity to different input parameters, in addition to studying the sensitivity of the commonly used global EDP (eg., top displacement) to random input parameters, some local EDPs (eg., interstorey drift at top level and ground storey level) are also considered in the present sensitivity study. . It is observed that the parameters on which the sensitivity of the EDPs depends do not change even if different local EDPs are used. That means the response (global or local) of bare and OGS frames is highly sensitive to uncertainty in fck and B_c. Similarly, the global or local response of fully infilled frame depends mostly on the uncertainty in f_m' and W_s.

5.7 Summary and Conclusion

The primary objective of the study is to gain an insight into the sensitivity of the displacement response of three building configurations to basic uncertain input variables. Using ground motions of various peak intensities and energy characteristics, it is shown by nonlinear response history analysis that the sensitivity global building response to

uncertain input parameters is very high. On the other hand, it is also observed that the seismic response output of these frames is not sensitive to some commonly used parameters. Following conclusions can be drawn for the investigated frames:

1 Independent sensitivity tests (modal analyses, sensitivity radar charts, response sensitivity bar diagrams, tornado diagram analysis, Sobol' indices, Lasso regression, and weighted pie charts) show that the uncertainty in compressive strength of concrete and width of column plays a major role in the sensitivity of seismic response of bare frames and open ground storey frames. However, in fully infilled frames, the width of the diagonal strut and the masonry prism strength play the vital role in the sensitivity of the output.

2 The response of the frames in which the infill walls are placed uniformly in all stories (FI frame), is most affected by the uncertainty in parameters related to infill characteristics. On the other hand, the infill parameters do not affect the response of the frames in which either the infills are provided in vertically irregular or non-uniform fashion (OGS frames), or not provided at all (BF). Thus, even though the OGS and FI frames are both infilled frames, their seismic response and sensitivity to random input variables depend on the collapse mechanism of the structure, and hence, can differ significantly.

3 It is observed from the radar charts that some ground motions, especially those with high input energy, can significantly affect the sensitivity of the response of the frames. Results show that for some ground motions, uncertainty in viscous damping also has a considerable effect on the sensitivity of response of all the frames.

4 The seismic response of all the frames is found to be least sensitive to uncertainty in the yield stress of steel and depth of beam as these parameters have lowest values of swing, Sobol' indices, and Lasso coefficients.

5 The magnitude of uncertainty in input parameters may not solely decide degree of their sensitivity in the output response, as some of the input

parameters with higher uncertainty are found to have a negligible effect on the output sensitivity, and vice versa.

The overall conclusion of the study is that sensitivity analysis is a prerequisite for carrying out a probabilistic assessment of structures. It is established from the results of the study that an input parameter with high uncertainty may not always produce the highest sensitivity in the response of structures. The response sensitivity of fully infilled frames is found to depend significantly on the parameters related to infill, such as masonry prism strength, whereas column dimension and concrete compressive strength are the chief contributors to the response sensitivity of relatively flexible (bare and OGS) frames. To some extent, system viscous damping has an influence on all the types of frames considered in the study. The sensitivity of frame response is also more reliant on the energy density of ground motion rather than its peak ground acceleration value. Thus, the record-to-record variability in structures can be obtained from ground motion records with varying energy density. The significant parameters determined from the sensitivity analysis are recommended to be carefully used for the evaluation of total dispersion in response resulting from the epistemic uncertainty.

❄ ❄ ❄

Chapter 6

TREATMENT OF UNCERTAINTIES IN EDPS

6.0 Overview

Assessment of seismic fragility of buildings involves large uncertainties including irreducible aleatoric and inherent epistemic uncertainties in seismic demand and capacity, respectively. These uncertainties are considered in the present study to investigate their effects on the damage state dependent fragility estimates of reinforced concrete buildings. Three configurations of reinforced concrete building frames with and without masonry infill walls - bare, open ground storey, and fully infilled frames are examined. Random samples of basic uncertain input variables related to material, geometry, and loading are generated based on Latin Hypercube Sampling to estimate the epistemic uncertainty. Several ground motions and their frequency envelope dependent samples are considered for determining the aleatoric uncertainty and its influence on the response of the frames in all the damage states. RC building categories and associated uncertainties specified in the literature are evaluated for sufficiency to predict damage and failure pattern in the frames.

6.1 Need of the Study

Performance-based earthquake engineering is marked by the presence of large uncertainties from two basic sources: (1) widely recognized record-to-record variability in ground motions, and (2) the inherent variability in random system parameters. These sources of uncertainties are generally categorized as either aleatoric or epistemic (Kiureghian and Ditlevsen 2009). Uncertainties are characterized as epistemic if the modeler sees a possibility of reducing them by collecting more data or by refining models.

Such models generally include several random parameters related to material, geometry, and loading. Uncertainties are categorized as aleatory if the modeler does not foresee the possibility of reducing them. Thus, the uncertainty in seismic demand arising from the variability in ground motion records can be termed as aleatoric. In addition, there are modeling uncertainties in simulating the structural response, which relates to the analysis method and the extent to which the idealized model accurately represents the real behavior. The primary objective of the present study is to estimate the total uncertainty in the inelastic displacement demand for first mode-dominant RC building frames.

It is important to determine the structural capacity and demand accurately for the assessment of collapse risk of existing structures or even design new structures with certain levels of margin against collapse. This is possible through quantification of uncertainties associated with various sources. Although over the last decade, an increasing emphasis has been placed on the explicit quantification of uncertainties, several challenges still need to be met if the completeness of uncertainty consideration is to be achieved. Probabilistic estimation of seismic performance is an active area of research with several past studies (e.g., FEMA P-695 2009, D'Ayala et al. 2015) suggesting methodologies and approaches for it. Past studies suggested various methodologies to account for the uncertainties using both nonlinear static and dynamic or incremental dynamic analyses. For example, Kosič et al. (2014) introduced a pushover-based seismic risk assessment procedure that involves uncertainty analysis at the level of a single-degree-of-freedom (SDOF) model. The procedure was demonstrated only for RC frames, but it is applicable to any building structure within the limitations of pushover analysis. Baker and Cornell (2008) proposed the use of a combination of numerical integrations and first-order second-moment (FOSM) approximations to incorporate both epistemic and aleatoric uncertainty and account for their effects on the output variables. On the other hand, a few studies (Fajfar and Dolšek 2012, Choudhury and Kaushik 2018a) adopted default values of dispersion to be used in order to determine the probability of exceedance of a given limit state.

Several studies exist for the estimation of uncertainty due to record-to-record variability and variation in capacity parameters; however, these are subjected to limitations. Ibarra and Krawinkler (2011) found that the uncertainty in deterioration parameters has important effects on the variance of collapse capacity; however, the study considers only SDOF systems with different periods of vibration ranging from 0.1s to 4s.

Dymiotis et al. (2001) examined the behavior of fully infilled frames and open ground storey (OGS) frames and found that the OGS frames were more vulnerable considering the material uncertainty; however, the uncertainties were not quantified. Kwon and Elnashai (2006) and Aslani et al. (2012) presented uncertainty analysis for wooden, steel, and RC frames, but infills walls were disregarded in the analysis. Sensitivity analyses have been carried out in the past for infilled frames (e.g., Celarec et al. 2012, Choudhury and Kaushik 2018c) using nonlinear analyses results, but the net effect of the most sensitive parameters on the response remains to be quantified. Gokkaya et al. (2016) illustrated the incorporation of the modeling uncertainty in structural model parameters through nonlinear dynamic analyses to probabilistically assess the storey drifts and collapse risk of RC building without infill walls.

Some studies (e.g., Porter et al. 2002; Lee and Mosalam 2005; Mehanny and Ayoub 2008) indicated that uncertainties of the structural system have limited effect on the estimation of seismic performance. While a few others (e.g., Celarec and Dolšek 2013) pointed out that consideration of epistemic uncertainties can have a significant effect on the estimation of seismic performance and risk of RC frame structures. It was further reported by Gokkaya et al. (2016), for RC moment frames designed for a high-seismic site, that the average effect of modeling uncertainty on collapse fragility can be represented by either a shift in median by –5% combined with an added modeling dispersion of 0.33, or no shift in median and an added modeling dispersion of 0.40. Thus, there is a lack of consensus on the use of uncertainty analysis in fragility estimation. Moreover, it is observed from the literature survey that not many studies have been carried out for uncertainty evaluation for masonry infilled RC frames with and without vertical irregularities.

6.2 Uncertainty in Assessment of Vertically Irregular RC Frames

Seismic performance of RC buildings with masonry infill walls depends on the distribution of infills: a regular distribution of infills improves the seismic behavior, whereas vertically irregular distribution can lead to soft storey mechanisms. The ground storey infills play a major role in the seismic resistance of masonry infilled buildings. Failure of the ground storey infills triggers the soft storey effect that can be detrimental to the ground storey columns. Comprehensive analytical and experimental research has already been carried out for investigating the seismic performance and fragility of such

frames. However, the performance greatly depends on assumptions in design and modelling of the frames. For instance, the masonry infills in RC frames can be most simply modelled as a single equivalent diagonal strut or by using complex FEM models. Another typical assumption in the design of infilled frames is that the infill walls are non-structural, and therefore, high lateral stiffness and strength imparted to the frame by the infills is neglected. Thus, there exists a significant uncertainty in the consideration of input parameters in structural modelling and performance assessment of masonry infilled RC buildings.

The total uncertainty arises due to variability in the estimation of capacity, demand, and modelling, and can be determined as the square root of sum of squares (SRSS) of all these uncertainties (Vamvatsikos and Fragiadakis 2010). Usually, such uncertainties are not properly accounted for owing to the requirement of heavy computational demand for carrying out a large number of simulations. Uncertainty decreases with the increase in calculation effort in analysis and modeling type. Naturally, it is a matter requiring resolution as to what is the limit up to which the uncertainty in the structural properties and ground motions needs to be considered, which in turn directly influences the seismic fragility. In order to resolve this issue, an exhaustive uncertainty analysis is carried out in the present study. Three different configurations of a three-bay four-storey RC frame with and without infill are considered for analysis:

(a) Bare frame (BF) with no infill in any of the storey,
(b) Open ground storey (OGS) frame with infills in all the stories except the ground storey, and
(c) Fully infilled (FI) frame with regular distribution of infill throughout the stories.

Epistemic uncertainties arising due to different random system parameters are considered mainly for material used in construction (RC, rebar and masonry), geometry (member dimensions), and loading (self-mass of concrete and masonry elements). Aleatoric uncertainties arising from the frequency distribution, energy content, and other characteristics of ground motions used in the study are investigated for several ground motions (natural and synthetic). The results obtained will provide insights into fragility assessment of RC buildings with and without masonry infill walls considering aleatoric and epistemic uncertainties. These details regarding the estimation of both the type of uncertainties are provided in the next sections.

6.3 Uncertain Input Parameters in Structural Capacity Evaluation

6.3.0 General

Structural capacity is dependent on the assumption in several building parameters related to material, geometry and loading that bring uncertainty into the analysis. Usually, seismic performance assessment involves estimation of the seismic capacity of the structures based on the mean or median value of these parameters. However, the underlying uncertainty in the assumption of the mean parameters propagates into the capacity estimation, and finally affects the seismic fragility of the structure. Such uncertainty is, however, reducible and can be estimated based on knowledge of the system parameters. In order to evaluate this uncertainty, present study includes the basic system parameters as discussed in Chapter 5. The statistical characteristics of each of the random input variables are presented in Table 5.1. The parameters related to the characteristics of masonry infill walls are considered only for FI frames, and not for the OGS frames since their lateral load behavior is not affected by the presence of infills in the upper floors only (Choudhury and Kaushik 2018a). Results of the sensitivity analysis required to be carried out in order to understand the relative importance of these parameters on seismic response are already reported in Chapter 5.

6.3.1 Generation of Data (Sampling)

Sampling is a statistical procedure, which involves selecting a limited number of observations, states, or individuals from a population of interest. A sample is assumed to be a representative of the whole population to which it belongs. The most comprehensive, but at the same time a computationally expensive, way of sampling is the Monte Carlo simulation, which generates a random sample of multiple independent variables from the probability distribution for that input variable. Because it relies on pure randomness, it can be quite inefficient; one might end up with some points clustered closely, while other intervals within a space may not get any samples. Monte Carlo simulation can be further improved by replacing the classic random sampling of the population with Latin Hypercube Sampling (LHS). LHS is a special case of stratified sampling proposed by McKay et al. (1979) that aims to spread the sample points more evenly across all possible probability values. It partitions each input distribution into P intervals of equal probability and selects one sample from each interval. It shuffles the sample for each input so that there is no correlation between the inputs (unless one wants a correlation). The P values thus obtained

for one uncertain parameter are paired in a random manner (i.e., equal likely combinations) with P values of other uncertain parameter. LHS allows efficient estimation of the quantity of interest by reducing the variance of classic Monte Carlo sampling. While random sampling produces standard errors that decline with $\sqrt{P}$, the error in LHS goes down much faster, approaching the rate of $\sqrt{P^3}$ for linear functions, i.e., the desired confidence in results can be achieved by a factor of P^2 (Vamvatsikos and Fragiadakis 2010). More than 50% of the computational efforts can be saved by using LHS instead of simple Monte Carlo sampling (Olsson et al. 2003).

In LHS, representative samples for each random input variable are generated. The domain of each variable is divided into equiprobable disjunct intervals of the probability, N_{sim}. It is strictly observed that one sample is chosen from each interval. The variables are generated using the most common strategy to determine the samples of random input variables, i.e., by inverse transformation of the cumulative distribution function in the middle of the j^{th} strata (Dolšek 2009) as shown in Eq. (6.1).

$$x_{j,i}=F_i^{-1}(p_{j,i})=F_i^{-1}\left(\frac{j-0.5}{N_{sim}}\right), i=1,...,N_{var}, j=1,...,N_{sim} \tag{6.1}$$

where, $x_{j,i}$ is the j^{th} sample value of the i^{th} random variable X_i, $p_{j,i}$ is the probability that the variable X_i is less or equal to $x_{j,i}$, $F_i^{-1}(p_{j,i})$ is the inverse of the cumulative distribution function of the variable X_i evaluated at probability $p_{j,i}$, and N_{var} is the number of random variables. The correlation between random variables generated based on Eq. (6.1) may not always be same as the target or prescribed correlation. The difference between the two correlation matrices can be minimized by permutation of the elements of the generated sample matrix. The difference between the generated and the prescribed correlation matrix is represented by a norm, E, defined as in Eq. (6.2), where, $S_{i,j}$ and $K_{i,j}$ are, respectively, generated and prescribed correlation coefficient matrix between the random variables X_i and X_j.

$$E = \frac{2}{N_{var}(N_{var}-1)}\sqrt{\sum_{i=1}^{N_{var}-1}\sum_{j=i+1}^{N_{var}}(S_{i,j}-K_{i,j})^2} \tag{6.2}$$

When the norm E (error) is reasonably low, it is assumed that the sample of random variables is optimum. The norm E is calculated based on the repeated trials for different sizes of the sample N_{sim}. The maximum difference between the generated and prescribed

correlation coefficients (E_{max} = max($S_{j,i}$ – $K_{j,i}$)) are presented in Table 6.1. Based on the norm E and E_{max}, a set of 25 samples is found to be optimum after which the error (norm) stabilizes in case of both infilled and non-infilled frames. Also, the sample size N_{sim} is greater than twice the size of the variable N_{var}; this is considered sufficient for accurate results (Dolšek 2009). Random samples based on the distribution of the parameters are then created that have no correlation with each other.

Table 6.1 E and E_{max} for the generated and target correlation coefficients for random input variables obtained for different sample sizes $N_{sim.}$

Frame	N_{sim}	10	15	20	25	30	40	50	60	200
Bare and OGS frame	E (norm)	0.004	0.004	0.003	0.002	0.002	0.001	0.001	0.001	0.001
	E_{max}	0.075	0.062	0.047	0.021	0.016	0.016	0.009	0.008	0.008
FI frame	E (norm)	-	0.003	0.002	0.001	0.001	0.001	0.001	0.001	0.001
	E_{max}	-	0.103	0.064	0.049	0.046	0.041	0.030	0.031	0.030

Fig. 6.1 shows the generated samples for the variables before and after error optimization. Fig. 6.1(a) and Fig. 6.1(c) show the relation between sample data for compressive strength of concrete (f_{ck}) and yield stress of reinforcing steel (f_y), whereas Fig. 6.1(b) and Fig. 6.1(d) show the relation between viscous damping ratio (ξ) and width of columns (B_c). The correlation coefficients (both Pearson and Spearson as indicated in the figures) for both the distributions are very small that show the data are almost independent and uncorrelated as prescribed. Similar results (correlation coefficients) are also obtained for all the other random input parameters considered in the study. The sample data for input parameters are then used to prepare the N_{sim} number of models for carrying out nonlinear time-history analyses in SAP 2000 (CSI 2015) for all the ground motions.

6.4 Ground Motions Considered

Seismic performance of buildings is highly dependent on the characteristics of the ground motion records chosen, so a sufficiently large number of records are required in order to cover the entire range of possible building's response to ground motion records. The selected number of ground motions should be sufficient to provide stable estimates of the median capacities. Uncertainties in ground motion intensity (generally known as aleatoric uncertainties) are commonly represented by a site-specific hazard curve, which relates spectral intensity to the frequency of exceedance. The additional uncertainties

associated with frequency content and other attributes of the ground motion records are termed as 'record-to-record' variabilities (Liel et al. 2009). Usually, the analyst requires employing a significantly large number of ground motion records representative of the location of the assessed building or a class of buildings. However, this is always not possible due to lack of real ground motion data from the same location. In the present study, nonlinear time-history analyses are carried out considering seven earthquake ground motions namely, El Centro (1940), Indo-Burma (1943), Tabas (1978), Chile (1985), Kobe (1995), Kocaeli (1999), Duzce (1999) as shown in Fig. 3.15. In order to capture the variability in the ground motion, synthetic samples of each ground motion are created. This is already discussed in Section 3.4.1 of Chapter 3.

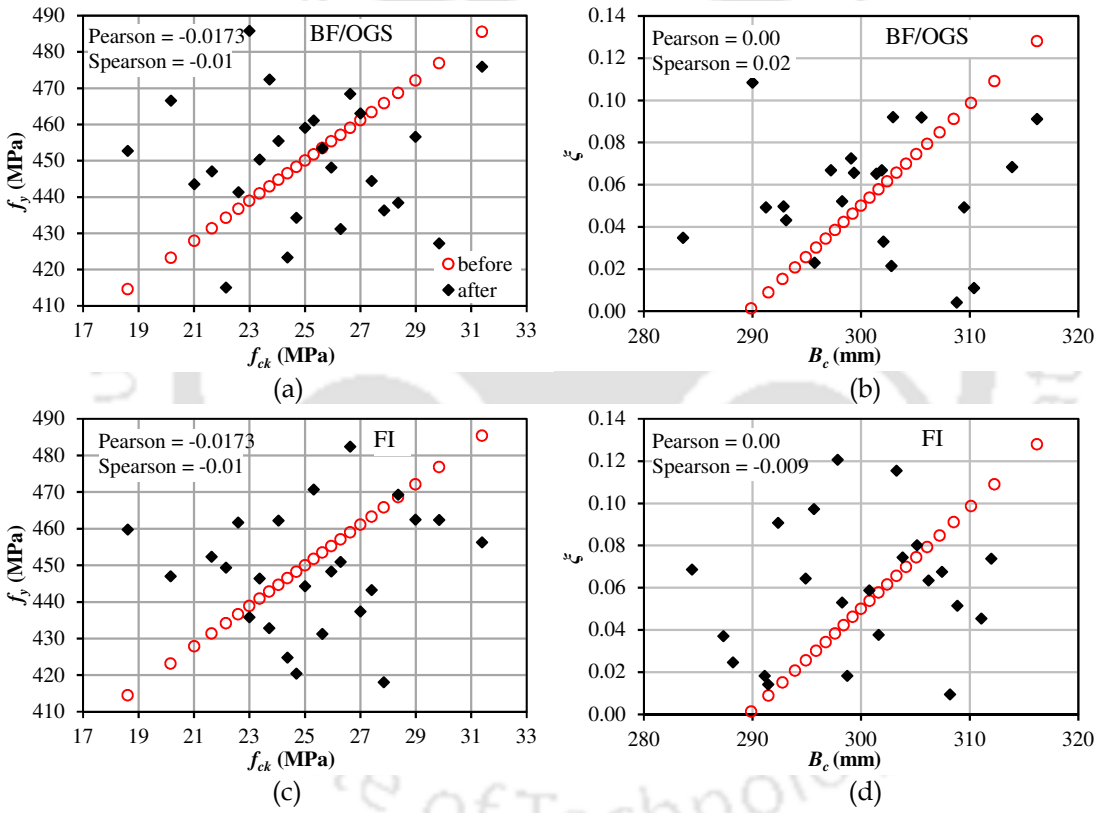

Figure 6.1 Comparison between sample values of the selected random input variables before and after optimization of the sample matrix. The comparison is made between f_{ck} and f_y, and ξ and B_c for: (a), (b) bare and OGS frame and (c), (d) fully infilled frame.

For each ground motion, 15 different samples are created, thus a total of 112 records (7×15+7) including real ground motions and their samples are considered; each ground motion is again scaled for different PGA values ranging from 0.1g to 4g in increments of 0.1g until all the damage states in the buildings are reached. The number of ground motions considered is, therefore, reasonably high in order to obtain the ground

motion record-to-record and sample-to-sample variability in the inelastic displacement response. The ground motions and generated samples of ground motions are used for the estimation of engineering demand parameters (EDP), and the uncertainty for each damage state. For the estimation of uncertainty in capacity, the El Centro (1940) ground motion scaled for different PGAs is used bringing out the variance due to epistemic uncertainties at different levels of intensity measures (IM) by varying the random input parameters. Record-to-record variability is evaluated from nonlinear time-history analyses of the "mean frames" (in which the mean values of all the random variables are considered) using all the seven ground motions and their samples scaled for different PGAs.

6.5 Choice of IM vs EDP

Development of probabilistic seismic demand model (PSDM) is an essential first step in the generation of seismic fragility curves. Single variable PSDM relates a particular IM to an EDP. PGA is one of the most important ground motion parameters that is also easily understood by the design professionals. Several other IM parameters, like spectral acceleration at first natural period ($Sa(T_1)$), are also used in the past (e.g., Celik and Ellingwood 2010). However, it is rightly pointed out that PGA is the optimal choice when hazard computability is considered (Padgett et al. 2008). Therefore, PGA is considered as the IM in the present study and results are compared for two different EDPs. The choice of an EDP is a matter that needs special attention. Different approaches involve the use of different categories of EDPs for response assessment. For example, global EDPs, that give information on system behavior, and local EDPs, which are believed to be more accurate in describing the response of frame members. A few studies (Dymiotis et al. 1999, Freddi et al. 2017) highlight that local EDPs are required to evaluate the failure criteria, and estimate fragility of RC frames. Whereas, a few other studies (Lee and Mosalam 2005) also suggest that sensitivity, and hence uncertainty, of local and global EDPs is similar for some random input variables. It is already observed in Chapter 4 that the OGS frame is a very interesting case that is vulnerable to soft storey mechanism. Hence, evaluation using both local and global EDPs is of importance in case of the irregular OGS frames. Thus, for estimating the nonlinear response of the building frames using time-history analysis, global (top level (TL) displacement) and component level (ground storey level (GL) displacement) EDPs are chosen.

6.6 Probabilistic Performance Evaluation

6.6.0 General

Using the random data of system parameters generated with LHS, independent models for bare, OGS and FI frames are created in SAP 2000 (CSI 2015). The bare frame consists of flexural members (beams and columns) modelled as 2D elements with concentrated plasticity at the member ends for a definite plastic hinge length. Additionally, the OGS and FI frames have masonry infills wall panels modelled as equivalent diagonal strut members. The diagonal struts are modelled to fail only in axial compression with the plastic hinge located centrally for a definite length. Details regarding the section, material and loading are provided in Chapter 3. For each model, the values of the random input parameters (Table 5.1) that affect the capacity of the frames are varied using the data obtained from LHS. Both nonlinear static (pushover) and dynamic analyses are carried out for the frames and their displacement responses are compared for probabilistic performance evaluation.

6.6.1 Nonlinear Static Analysis

The nonlinear pushover (PO) analysis is a simple method that offers useful information on the expected behavior of a structural model. The structure is pushed based on the first mode deformation profile assuming the first mode to be the dominant mode. To provide some insight on the nonlinear behavior of the range of models generated, their static pushover curves are obtained and plotted as shown in Fig. 6.2. The maximum and minimum strengths vary within 250kN to 350kN for both the BFs and OGS frames. The peak lateral strength of FI frames is comparatively much higher and has a wide range varying from 1000kN to 4000kN. The median (50^{th}), 16^{th}, and 84^{th} percentile curves are also plotted showing the obeserved variation in the data. The PO curves reveal that none of the frames is initially affected by the variation in the random input parameters in the linear range before reaching the yield point. The effect of material, geometric, and loading uncertainties is indeed significant in the post-yield stage in all the frames. For BF and OGS frame, the variation in maximum and minimum lateral load carrying capacity in terms of seismic weight is similar (15% to 23%). In case of FI frame, the post-yield variation in the lateral resistance is much larger (60% to 250%) as compared to the BF or OGS frame. This could possibly be due to the presence of equivalent diagonal struts, in FI frames having parameters with highly uncertain characteristics (f_m' ε_m, and W_s). The

frame response is significantly affected by a change in the properties of the equivalent strut. It is a matter of further investigation if similar behavior is obtained in nonlinear response history analysis.

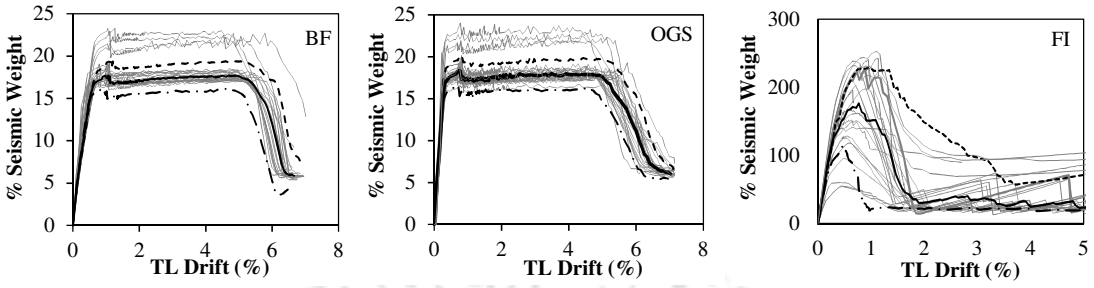

Figure 6.2 Pushover curves with median (50th), 16th, and 84th percentile curves showing variation due to epistemic uncertainty for the three frames: (a) BF, (b) OGS, and (c) FI. The lateral load resistance is normalised with the total seismic weight and plotted on the Y-axis.

6.6.2 Nonlinear Response History Analysis

Nonlinear time-history analysis (NLTHA) or dynamic analysis provides extensive knowledge of the frame seismic behavior under earthquake excitation. Fig. 6.3 shows the displacement response (at both GL and TL) obtained using NLTHA for El Centro ground motion scaled for different PGA values (0.1g to 4g) until all the damage states of interest are reached. The median (50th), and 16th and 84th percentile curves demonstrating the variation in the response with respect to different scaled PGAs of the ground motion are shown in each figure.

It follows from Fig. 6.3 that initially the variation in the displacement demand in both TL and GL is very less indicating the pre-yield state of the frame as represented by the PO curves also. With increasing seismic intensity (i.e., PGA) the frames attains nonlinearity and the variation in the demand increases as observed from the percentile curves. Interestingly, in OGS frame, the median and the standard deviation curves are more or less similar at the TL and GL. This indicates that the median estimates and uncertainty at TL and GL are similar in case of OGS frame, and hence global EDP (TL displacement) suffices for the estimation of OGS frame response. In case of both BF and FI frames the displacement response at GL is obviously significantly lesser than that at the TL. The BFs show gradual change (or increase) in the displacement response (both at GL and TL) with increasing PGA. however, in case of FI frames, there is a sudden change

in the slope of the line representing the response. This change in the slope marks the failure of masonry infill walls in the ground storey of FI frames after which the FI frames becomes flexible. As observed in the pushover analysis, the variation in the EDPs is maximum in case of FI frames. in the next section, an attempt will be made to estimate the uncertainties associated with these EDPs in different frames.

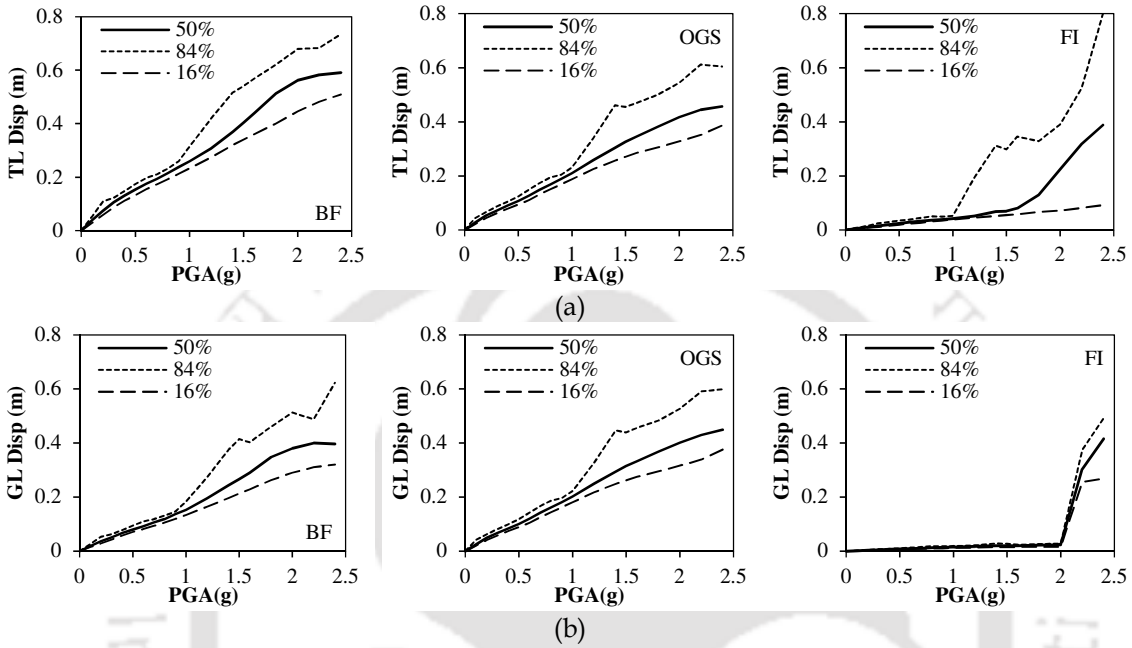

Figure 6.3 Variation in displacement with PGA considering epistemic uncertainty in NLTHA for the three frames-BF, OGS, and FI for: (a) TL displacement, and (b) GL displacement.

6.7 Estimation of Uncertainties in EDPs

6.7.0 General

The uncertainty in the material, geometric, and loading characterization and the uncertainty in ground motion are the basic sources affecting the overall uncertainty in the estimation of seismic response of a structure. These sources are quantified in the present section for the three frame typologies considering different EDPs.

6.7.1 Epistemic Uncertainty

Epistemic uncertainty depends on how well the material and sectional properties of the members of a model and various loads are simulated. The properties, such as, weight density, the strength of concrete or rebars are random characteristics that vary from source to site. Such randomness can be physically reduced and quantitatively

identified through uncertainty analysis of the random input variables by using either nonlinear static or dynamic analysis. In the present study, nonlinear response history analysis is carried out in order to determine the displacement demand on the frames. Any variation in the obtained displacement demand for the frames is due to the randomness in the input parameters. This variability is determined as the lognormal standard deviation considering all the N_{sim} models, and is called the epistemic uncertainty or the uncertainty in capacity (β_C).

The epistemic uncertainty arising due to variation in input parameters is shown for the three frames in Fig. 6.4 and Fig. 6.5 with respect to PGA and median displacement, respectively. It is observed that even though all the three frames are categorized as RC frames, the uncertainty in their response vary significantly from each other. The uncertainty in response increases with increasing PGA or median displacement. At lower values of PGA (here up to about 1g), the uncertainty in the estimation of displacement response of all the three frames at both TL and GL is very low. At higher values of PGA, however, the value of β_C for the three frames increases considerably with highest β_C for the FI frame (about 0.5) and lowest for the OGS frame (about 0.25). At a PGA value of 3g, the maximum uncertainty in BF is 0.4 and 0.3, respectively, considering TL and GL displacement as EDP. An uncertainty value of 0.25 for code-designed buildings and 0.3 for pre-code buildings is recommended to account for the variability in the capacity curves as defined in HAZUS obtained from pushover analysis of the building models. However, there is neither any categorization of building category for OGS frames in HAZUS nor it does mention any local EDPs.

The median displacement and the corresponding logarithmic standard deviation (or uncertainty) is plotted in Fig. 6.5 for the three frames. The median displacement is estimated as the median of all the displacement response obtained from the 25 different models for each frame type at different PGA. The basic observation is that the uncertainty in response of FI frame at any displacement value is always higher compared to that observed in case of the BF or OGS frame. The maximum uncertainty in the response of FI frame considering both TL and GL displacement is approximately equal to 0.6. In OGS frame also, the maximum uncertainty for TL and GL displacement is similar, and is nearly equal to 0.4. This is not so in case of BF, where the uncertainty related to the TL-EDP is higher (0.5) compared to GL-EDP (0.4).

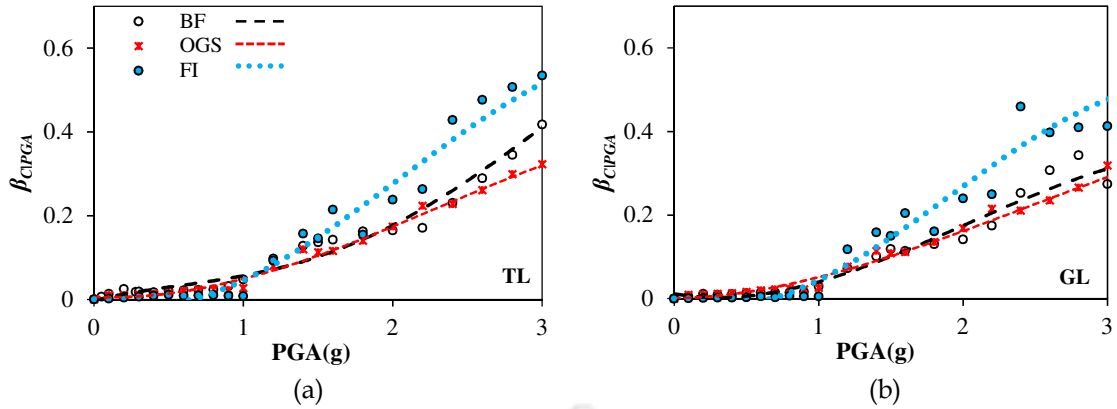

Figure 6.4 Epistemic uncertainty in response with respect to PGA at (a) top storey level and (b) ground storey level.

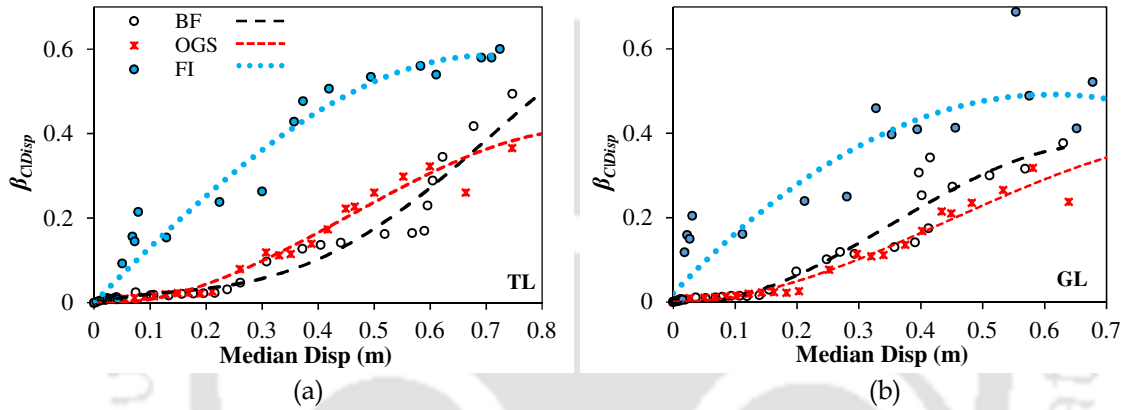

Figure 6.5 Epistemic uncertainty in response with respect to median displacement at (a) top storey level and (b) ground storey level.

To estimate the seismic fragility based on different damage state levels as prescribed in literature (eg., HAZUS) or for developing continuous fragility flow plots (Choudhury and Kaushik 2018a), the uncertainty in capacity estimation for a chosen displacement threshold (i.e., the median value) can be obtained directly from Fig. 6.5. It is clear from Fig. 6.4 and Fig. 6.5 that the epistemic uncertainty in both TL and GL displacement response is always higher for FI frames considering either PGA or median displacement as intensity measure. It is also important to note that the epistemic uncertainty in response estimation of OGS frame is mostly the lowest except for some intermediate values of median TL dispalcement where the uncertainty in response of BF is slightly lesser. Clearly, the uncertainty is a function of frame typology and it depends more on the characteristics and distribution of masonry infills in the frame.

In Chapter 5 sensitivity analyses was carried out considering variability in the uncertain input parameters and highly sensitive parameters having highest swing values

were identified. For BF and OGS frames, f_{ck} and B_c were found to have highest swing values, and for FI frame, W_s and f_m' were the parameters showing highest sensitivity. A separate set of uncertainty analysis is, therefore, carried out considering only these parameters to understand their influence on the estimated uncertainty. Again, 25 different sets of models are prepared by varying only the selected variables for carrying out nonlinear time-history analyses considering El Centro ground motion. The comparison of epistemic uncertainty considering all variables and only selected variables is shown in Fig. 6.6 plotted with respect to PGA.

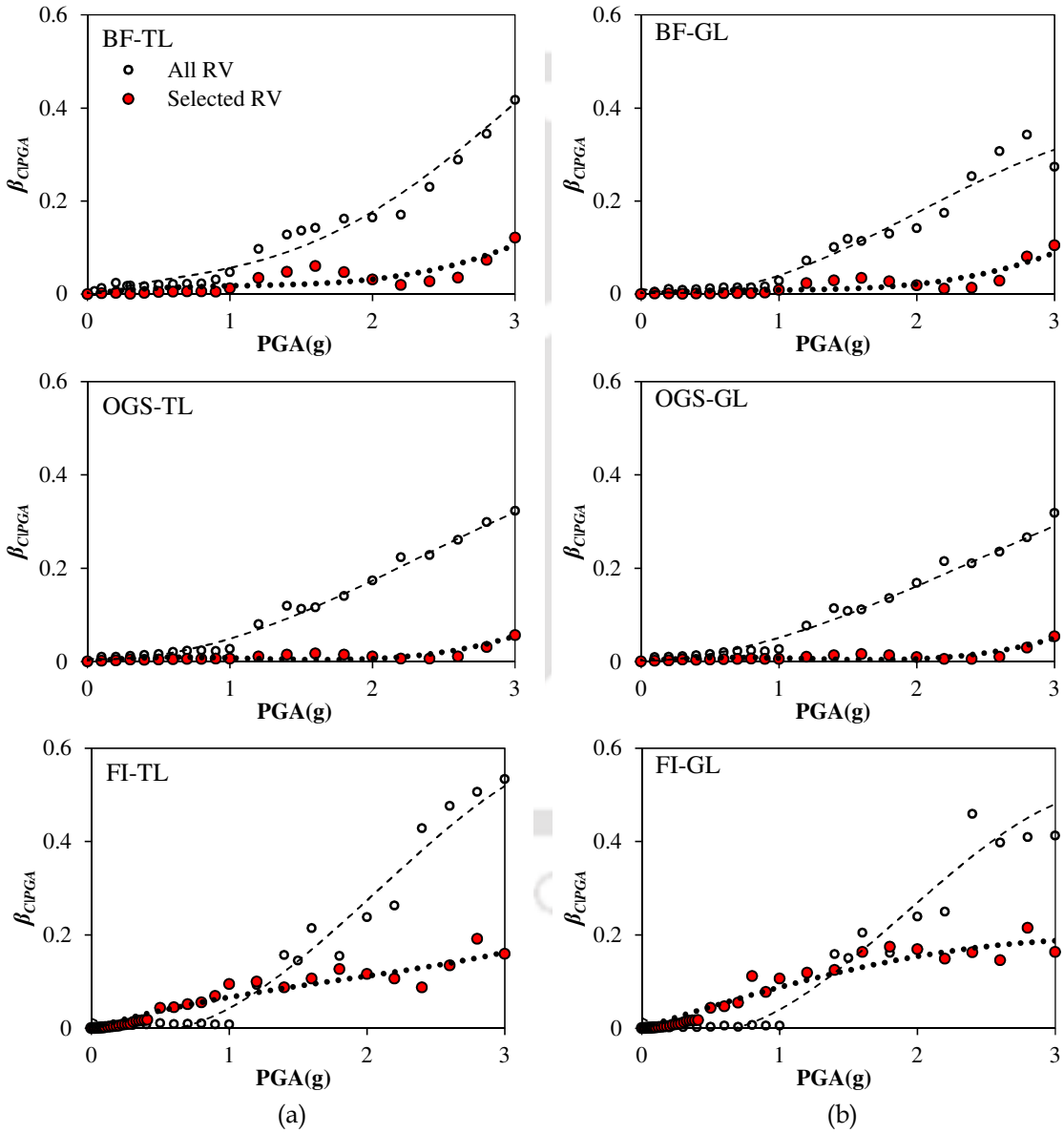

Figure 6.6 Epistemic uncertainty in response with respect to PGA considering all random variables (RV) and selected random variables for the three frames at (a) top storey level and (b) ground storey level.

Fig. 6.6 shows that there is no definite pattern in the difference in uncertainty when only selected parameters are considered versus when all the parameters are considered. In case of BF, the estimated uncertaintyconsidering selected parameters is always less (about one-third of the value obtained by considering all the random variables). In case of OGS frames, the uncertainty obtained by considering all the variables is significantly higher at higher PGA (beyong 1g). For lower values of PGA the uncertainty follow the trend of BF. In case of FI frames, the uncertainty obtained considering only selected variables is even more than that obtained considering all the variables upto about PGA of 1.3g, beyond which the trend reverses. Thus, epistemic uncertainty increases the overall uncertainty by significant amount even if only selected random variables are considered in the analyses. Thus, it is extremely important to consider the epistemic uncertainty correctly and it cannot be simply ignored in the process of seismic fragility assessment.

6.7.2 Aleatoric Uncertainty

Uncertainty in response due to variable seismic demand is supposedly irreducible since they exist in nature and they are inherent to the process involved (Porter 2016). Such uncertainties can be estimated by considering ensemble of ground motions with different characteristics. Nonlinear dynamic analyses of the frames considering the ensemble of ground motions give a median estimate and a standard deviation of the displacement response. The median estimate can be represented by a simple PSDM using power's law relating seismic demand to the seismic IM by Eq. (3.12) as discussed in Chapter 3. The uncertainty in the seismic demand can be characterized by the PSDM by considering a random variable with median of unity and logarithmic standard deviation ($\sigma_{ln\varepsilon}$). The $\sigma_{ln\varepsilon}$ defines the uncertainty in demand ($\beta_{D|IM}$) given an intensity measure.

The lognormal standard deviation or uncertainty ($\beta_{D|IM}$) is estimated for the three frame configurations considering different EDPs, i.e., TL and GL displacement as shown in Fig. 6.7. Each figure shows the uncertainty ($\beta_{D|IM}$) in response from sample-to-sample variation in individual ground motion (dotted lines) and the combined uncertainty for all ground motions and their samples (solid line with marker) varying with respect to PGA. It is observed that the variation in uncertainty ($\beta_{D|IM}$) from different ground motions increases with increasing seismic intensity (PGA) of ground motion. For the bare frame, at TL the combined value of aleatoric uncertainty for all ground motion lies in the range

of 0.1 to 0.3, whereas, the uncertainty at GL lies in the range of 0.2 to 0.3 for a PGA ranging from 0.1g to 3g. Thus, the aleatoric uncertainty with respect to PGA does not show much variation for different EDPs in case of BF.

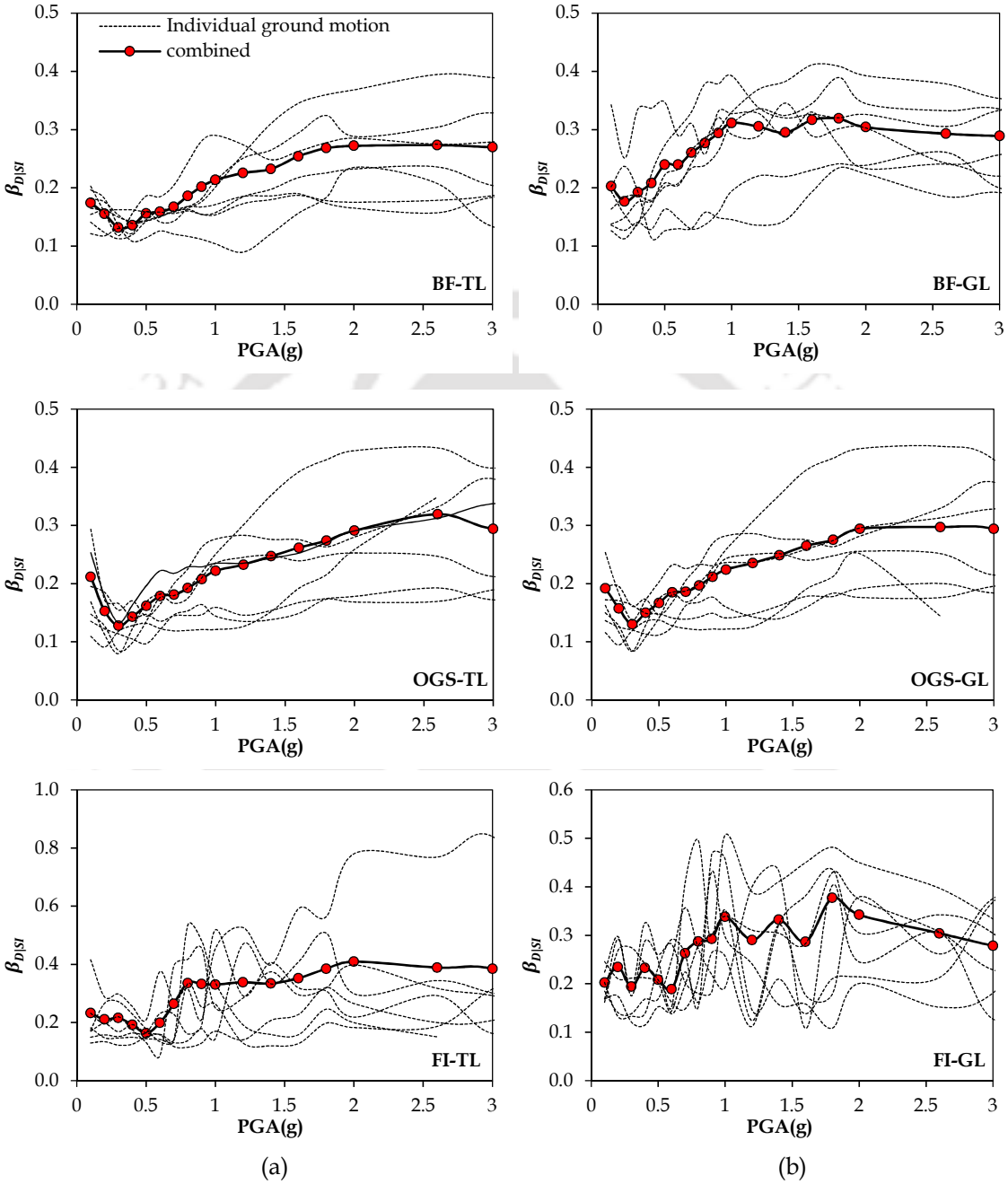

Figure 6.7 Aleatoric uncertainty in response with respect to PGA at (a) top storey level and (b) ground storey level.

In OGS frame also, the uncertainty for TL and GL-displacement are quite similar and lies in the range of 0.1 to 0.3, similar to bare frame. The TL and GL-displacements show similar uncertainty due to the well-established concept that the GL and TL-

displacements are similar in OGS frames since the whole upper stories move laterally as a single unit without any significant interstorey drift under an earthquake excitation (Choudhury and Kaushik 2018a). The highest variability due to aleatoric uncertainties is obtained in FI frames varying from 0.2 to 0.4 for both TL and GL displacement. The obtained results are, however, found to be contrasting to the observation made by O'Reilly and Sullivan (2017) where, the record-to-record variability was found to be lowest for FI frames constructed in Italy. Such contrasting observations may result from large variability in the material properties of masonry constructed in different places.

Fig. 6.8 shows the aleatoric uncertainties ($\beta_{D|IM}$) obtained for the three frames for individual sets of ground motion with respect to the median displacement (median of the displacements obtained using the samples of ground motion for each PGA). The combined curve of uncertainty in the figure (solid line with marker) is the combination of all the ground motions and their samples plotted with respect to both the EDPs: median displacement and drift. The variation in uncertainty ($\beta_{D|IM}$) from different ground motions follow similar trend as in Fig. 6.7, and increases with increasing displacement demand on the frames for all the EDPs.

Fig. 6.9 shows that the aleatoric uncertainty is always highest in case of the FI frame for both engineering demand parameters (TL and GL). The high variability in the aleatoric uncertainty values in FI frames obtained using individual ground motions as compared to the BF or OGS frame is perhaps due to the brittle failure of the ground storey infills of the FI frame. The uncertainty in the TL-EDP is almost similar in both BF and OGS frame, however, uncertainty in the GL-EDP in case of bare frame is higher as compared to the OGS frame. Fig. 6.10 further clarifies the observed difference in the uncertainty considering the EDPs: TL-displacement and GL-displacement. In BF the uncertainty in GL-displacement is high as compared to that of the TL-displacement. For FI frame, though there is no definite pattern, the uncertainty obtained by considering TL-EDP is lesser for small displacement (upto about 0.1m) after which the trend reverses. In case of OGS frame, there is no difference at all in the uncertainty of the two EDPs, i.e., the uncertainty in TL-displacement and GL-displacement are exactly equal. Therefore, care must be taken in the consideration of correct EDP, since uncertainty seems to depend on the considered EDP.

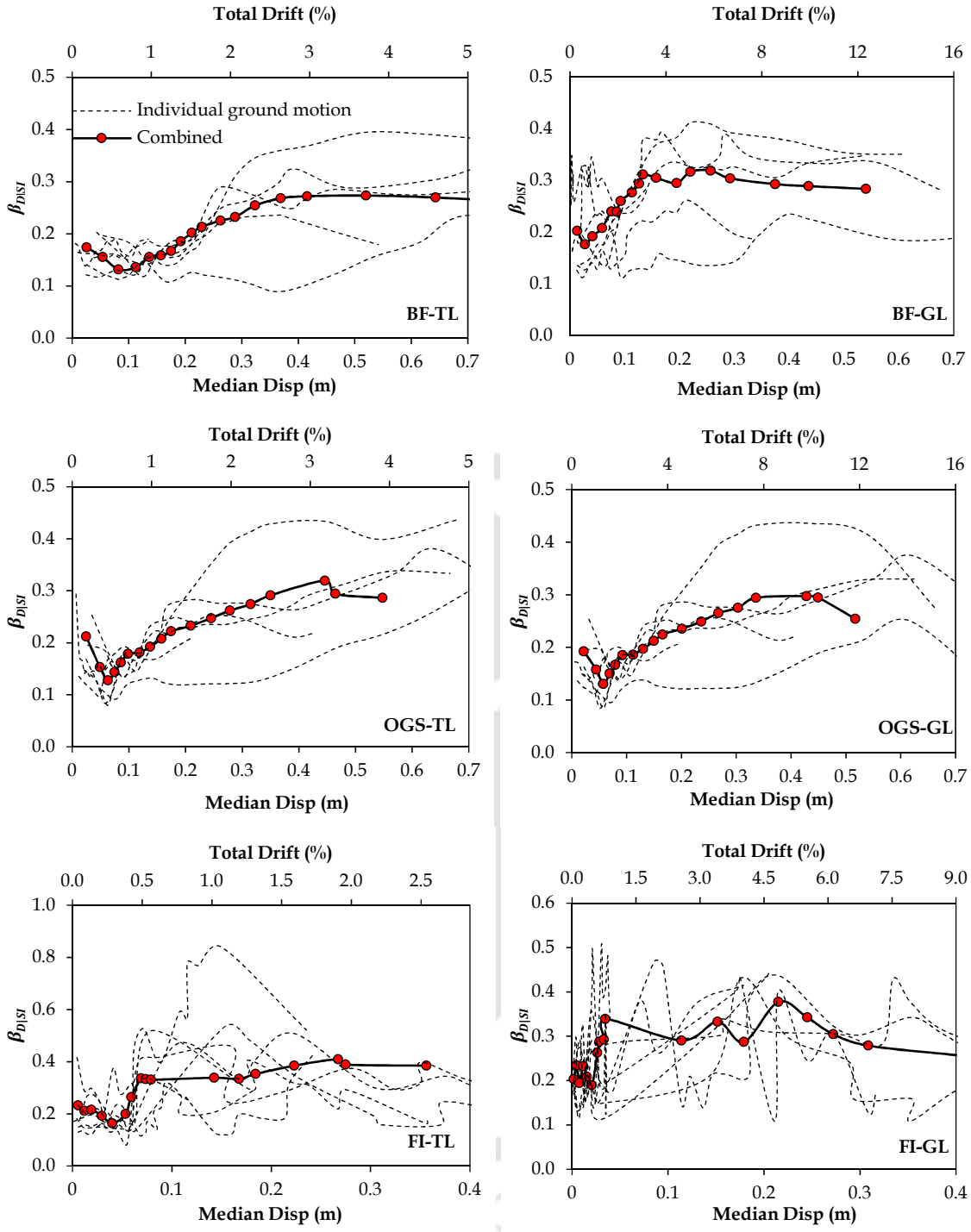

Figure 6.8 Aleatoric uncertainty in response with respect to median displacement and total drift at (a) top storey level (TL) and (b) ground storey level (GL).

The uncertainty arising due to random characteristics of each ground motion in seismic demand is combined for each PGA level and a single average value of uncertainty is obtained for each of the three frames as shown in Table 6.2. It is observed that for both the TL and GL displacement the uncertainty in demand is highest in FI frame.

Interestingly, the uncertainty for OGS frame is similar for both TL and GL displacement because the OGS frames displace laterally by similar amount at both TL and GL. There is no relative displacement between the top storey and the ground storey due to the absence of infill in the ground storey of the OGS frame. The dispersion values reported in O'Reilly and Sullivan (2017) for collapse fragilities arising from record-to-record variability considering $Sa(T_1)$ as the EDP for 2- and 3-storey frames are also shown in Table 6.2.

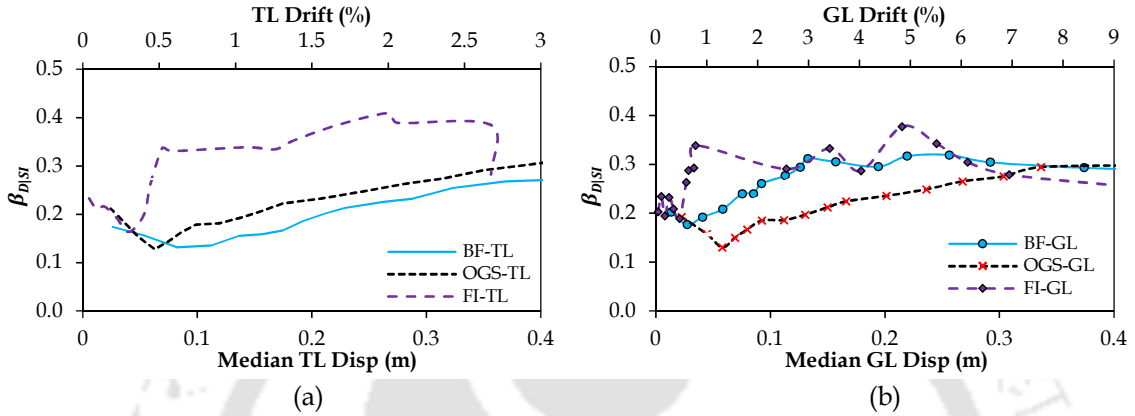

Figure 6.9 Comparison of aleatoric uncertainty with respect to median displacement and drift at (a) top storey level and (b) ground storey level for the three frames.

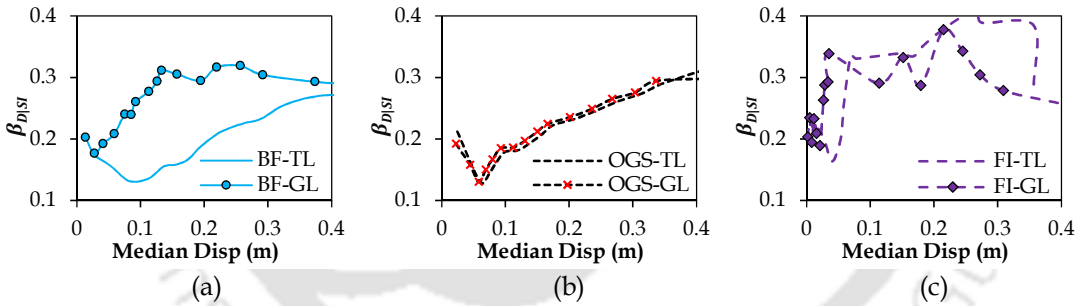

Figure 6.10 Comparison of aleatoric uncertainty in TL and GL response with respect to median displacement of (a) bare, (b) OGS, and (c) FI frame.

As seen in Table 6.2, the dispersion values reported by O'Reilly and Sullivan (2017) remain almost constant with increase in the number of storey in case of BF and OGS frame, whereas, it increases significantly in case of FI frames. It was also pointed out by Aslani et al. (2012) that aleatory uncertainty associated with RC buildings increases with the number of stories. Celarec and Dolšek (2013), however, observed no significant difference or practically identical dispersion values in displacement for RC 3-storey and 4-storey contemporary buildings, and it was in the range of 0.31 to 0.34. HAZUS (2013), on the other hand, recommends a value of 0.45 at shorter period and 0.50 at long period for describing the variability of the demand spectrum. These suggested values are quite

high as compared to those obtained in the present study. Studies such as FEMA P-695 (2009) suggests β_{RTR} (record-to-record variability) in the range of 0.20 to 0.40 for various structures; these values are well in accordance with the present study.

Table 6.2 Aleatoric uncertainty ($\beta_{D|IM}$) in the estimation of displacement response due to randomness in ground motion records.

Frames	Average from samples of Ground Motion							Combined Average	β_{RTR} ($Sa(T_1)$)*	
	ElCentro	Chile	Kocaeli	Kobe	Indo Burma	Duzce	Tabas		O' Reilly and Sullivan (2017)	
	4 - storey								3-storey	2-storey
	Top Storey Level (TL) Displacement									
BF	0.23	0.18	0.15	0.24	0.17	0.17	0.26	0.21	0.30	0.34
OGS	0.25	0.20	0.17	0.25	0.15	0.17	0.29	0.23	0.38	0.37
FI	0.49	0.26	0.27	0.30	0.22	0.20	0.27	0.30	0.32	0.17
	Ground Storey Level (GL) Displacement									
BF	0.28	0.19	0.17	0.31	0.26	0.30	0.31	0.27	-	
OGS	0.25	0.20	0.15	0.25	0.16	0.16	0.29	0.23	-	
FI	0.37	0.26	0.23	0.28	0.27	0.27	0.25	0.28	-	

*$\beta_{RTR}(Sa(T_1))$ is the uncertainty associated with the record-to-record variability with $Sa(T_1)$ as EDP.

6.7.3 Total Uncertainties

For all practical purposes, the SRSS rule for combining aleatoric and epistemic uncertainty is considered accurate as the sources of uncertainty are uncorrelated (Aslani et al. 2012, Vamvatsikos and Fragiadakis 2010). FEMA P-58 (2012) also recommends calculating the total dispersion from SRSS of dispersion in a design equation to predict failure demand, dispersion in material strength and uncertainty associated with construction quality. Therefore, in the present study, the total uncertainty (β_T) is calculated as the SRSS of β_C, β_D, and β_M as shown in Eq. (6.3).

$$\beta_T = \sqrt{\beta_C^2 + \beta_D^2 + \beta_M^2} \tag{6.3}$$

β_M represents the modelling uncertainty and a value of 0.2 is generally considered based on the assumption that the modeling process yields an estimate of building frame response that, with 90% confidence, is within ±30% of the actual value (Celik and Ellingwood 2010). The uncertainty in demand (β_D) accounting for the aleatoric randomness is considered from Table 6.2. The total uncertainty thus, determined for each frame is shown in Fig. 6.11 with respect to both PGA and the median drift at top level. It is observed that the total uncertainty depends heavily on the aleatoric uncertainty arising due to the record-to-record variability.

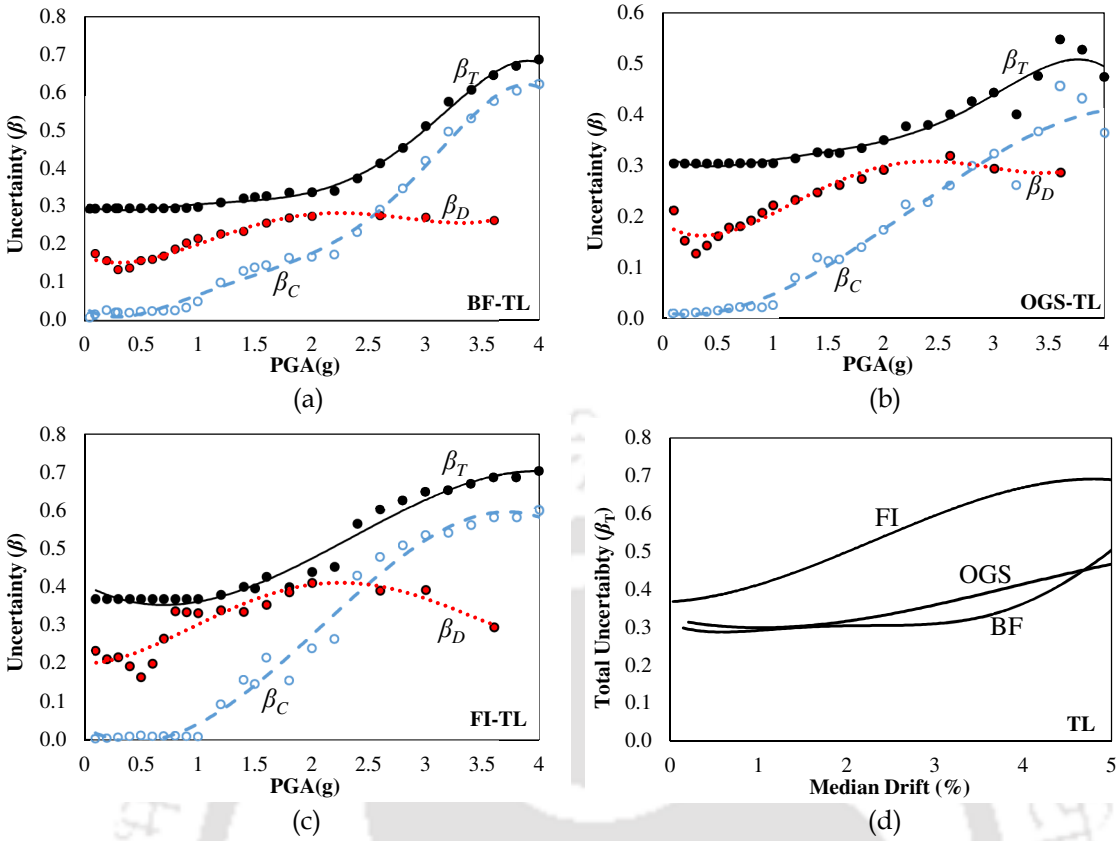

Figure 6.11 Combination of aleatoric, epistemic and modelling uncertainty in TL displacement response with respect to PGA for (a) BF, (b) OGS frame, and (c) FI frame, and (d) variation in total uncertainty with respect to median drift at TL.

Fig. 6.11(a), Fig. 6.11(b), and Fig. 6.11(c) show that the epistemic uncertainty due to capacity variation is significant only at high seismic intensity levels. It is clear from Fig. 6.11(d) that for a given intensity level (drift), the uncertainty for FI frame is highest. At low drift thresholds, the BF and OGS frames show almost similar trend of uncertainty, but it changes at higher drift level. These total uncertainty values can be used for different damage states in the estimation of fragility as discussed in the next section.

6.8 Uncertainty for Damage State Definition

Estimation of seismic fragility requires prior knowledge of uncertainty associated with different EDPs for different damage states. Different codes and literature give different values of total uncertainty for different damage dependent limit states. For example, FEMA P-58 (2012) suggests a default value of 0.6 for β_T for all damage states, however, these values are not categorized for different types of RC buildings. HAZUS (2013) suggests uncertainty values for RC buildings designed to old, moderate, and

modern codes with and without masonry infill walls (denoted as C1M and C3M, respectively), but vertical irregularity in such buildings is not accounted for.

Based on the damage states defined by Barbat et al. (2008), the median drift values for different damage states (Slight, Moderate, Extreme, and Complete) are determined in the present study and the corresponding total uncertainty values for the three frames are given in Table 6.3. For the sake of comparison, the damage state drift thresholds and corresponding uncertainty values for different damage states mentioned in HAZUS (2013) are also presented. All the frames are categorized into two broad types: RC moment resisting frames (RC) and RC frames with unreinforced masonry infill walls (RC-URM). According to HAZUS, C1M represents the RC frame of medium height (4-7 stories) that is comparable to the bare frame considered in the present study; C3M represents RC-URM frames of medium height. OGS and FI frames being infilled frames are compared with the C3M category of HAZUS. In case of the C3M category, HAZUS does not suggest any values for the median drift threshold value and β_T for high and moderate code level. It is observed that the median drift threshold values obtained in the present study for the bare frame is mostly higher than that for the C1M values. However, HAZUS overestimates the uncertainty values for bare frame for all the damage states.

Table 6.3 Comparison of median and uncertainty (beta) values in displacement response at TL for different frame typologies.

Building Type		Design Level	Slight		Moderate		Extensive		Complete		Collapse *	
			Med	β_T	Med	β_T	Med	β_T	Med	β_T	β ($Sa(T_1)$)	
			4 storey								3 storey	2 storey
RC	C1M	High	0.33	0.68	0.67	0.67	2.00	0.68	5.33	0.81		
		Moderate	0.33	0.70	0.58	0.70	1.56	0.70	4.00	0.89		
		Low	0.33	0.70	0.53	0.74	1.33	0.86	3.33	0.98		
	Bare	Present	0.49	0.30	0.71	0.30	1.80	0.30	5.06	0.50	0.45	0.44
RC-URM	C3M	Low	0.20	0.85	0.40	0.83	1.00	0.79	2.33	0.98		
	OGS	Present	0.31	0.30	0.45	0.30	1.42	0.30	4.34	0.45	0.47	0.44
	FI	Present	0.20	0.40	0.29	0.40	0.51	0.40	1.19	0.50	0.37	0.22

Note: Med = median drift threshold value, Present = present study. *The values are taken from O'Reilly and Sullivan (2017)

Although OGS and FI frames are treated under the category RC-URM in HAZUS, as there is no other category where infill frames can be put, the physical behavior and failure pattern of these two frames vary greatly. This difference in behavior is not reflected in the HAZUS building typology definition of RC-URM. As observed from Table 6.3, the median drift thresholds obtained in the present study for the FI frame are

significantly less than the values obtained for the OGS frames for all the damage states. The uncertainty values defined in HAZUS are very high for RC-URM category, compared to the uncertainty values obtained in the present study. The total uncertainty in the estimate of spectral acceleration at first natural period, $\beta(Sa(T_1))$ for the collapse damage level for 2- and 3- storey RC buildings as suggested in O′ Reilly and Sullivan (2017) are also presented in Table 6.3. It is observed that the uncertainty values recommended in that study were more or less similar for the bare and OGS frame for any number of storey, and these values match quite well with the uncertainty values obtained in the present study for complete damage state. However, the uncertainty values proposed by them for FI frames increase significantly with increase in number of storey; and these values are much smaller than the uncertainty values obtained in the present study for FI frames for complete damage state. Thus, a consistency is observed in the values of total uncertainty obtained in the present study and some of the past studies for bare and OGS frames; the uncertainty values, however, differ significantly in case of FI frames.

6.9 Summary and Conclusion

A complete statistical analysis for the three frames are carried out using the results of nonlinear dynamic analyses. Estimates of both epistemic and aleatoric uncertainty stemming from various sources are provided in terms of PGA and median drift thresholds. Uncertainty analyses reveal that:

1 Ground motion variability is a major contributor to the total uncertainty in all the frames. On the other hand, uncertainty in the material, geometric, and loading parameters is significant only for higher damage states for all the three frame configurations.

2 Various documented building typologies, such as, those in HAZUS for masonry infilled RC frames, are not sufficient to consider the effect of vertical irregularities, arising due to irregularly distributed infills in the OGS frame. The uncertainty values suggested in the literature need revision to include the vertically irregular framed structures.

❄ ❄ ❄

Chapter 7

SEISMIC FRAGILITY ANALYSIS

7.0 Overview

Seismic fragility analysis is the key component for seismic vulnerability and risk assessment methodologies. A common nontechnical definition of fragility is "the quality of being easily broken or damaged" (Porter 2016). The concept of a seismic fragility function in earthquake engineering dates at least to Kennedy et al. (1980), who defined fragility function as a probabilistic relationship between frequency of failure of a component of a nuclear power plant and peak ground acceleration in an earthquake. More broadly, one can define a fragility function as a mathematical function that expresses the probability that some undesirable event occurs as a function of some measure of environmental excitation. As discussed in Chapter 2, one can distinguish three general classes of fragility functions by the method used to create them: empirical, analytical and expert opinion or judgement based method. In this chapter seismic fragility of RC building frames with masonry infill walls is assessed based on the results of nonlinear analyses carried out in the previous chapters for seismic performance assessment, and for establishing sensitivity and uncertainty related to several building parameters.

7.1 Formulation of Seismic Fragility

The most common form of a seismic fragility function, given the damage state thresholds and variability associated with the damage states, is the lognormal cumulative distribution function (CDF) as shown in Eq. (7.1). $P[x \geq \theta_d \mid IM]$ represents the conditional

probability of exceedance of the EDP (here, x) with respect to θ_d, given the seismic intensity measure (IM), such as PGA. Φ represents the standard normal cumulative distribution function, θ_d is the median (threshold) value of EDP, (e.g., interstorey drift, spectral displacement) considered for different damage states, and β_T is the normalized standard deviation of the natural logarithm of the threshold (θ_d). Lognormal standard deviation values (β_T) describe the total variability (or uncertainty) associated with each fragility curve for a particular damage state. Assessment of seismic fragility of buildings involves large uncertainties including irreducible aleatoric and inherent epistemic uncertainties in seismic demand and capacity, respectively. These uncertainties are considered in the present study as discussed in Chapter 6 to investigate their effects on the damage state dependent fragility estimates of reinforced concrete buildings.

$$P[x \geq \theta_d \mid IM] = \Phi\left(\frac{\ln(x/\theta_d)}{\beta_T}\right) \tag{7.1}$$

A fragility curve can also be built by fitting a statistical model to data on building damage at different values of the IM. Such statistical models are generally fitted to the probability of exceedance for a particular IM, which is calculated as in Eq. (7.2), where, N_F is the number of analysis cases where the considered EDP exceeds the limit, and N_T is the total number of analysis cases at that IM level. Comparing Eq. (7.2) with Eq. (7.1), a particular IM level represents a specific damage state. The median and standard deviation of the statistical models can be estimated by different parameter estimation techniques, such as maximum likelihood. Seismic fragility results considering both the formulations are presented in the following sections.

$$\text{Probability of exceedance at an IM level} = \frac{N_F}{N_T} \tag{7.2}$$

7.2 IM vs EDP in Fragility Assessment

Selection of relevant seismic intensity measure and the possible response outcome, also called as engineering demand parameter (EDP), from nonlinear analysis is of utmost importance in fragility analysis. A seismic demand model as discussed in Chapter 3 mostly describes the relationship of IM to EDP. An IM is a ground motion parameter, which is considered representative of the earthquake damage potential with respect to the specific structure. Chapter 4 extensively scrutinized the concern on choice

of EDPs for fragility estimation, especially for vertically irregular masonry infilled frames. In addition, the issue of choice of an IM is already discussed in Chapter 6 for the estimation of uncertainty considering different damage states. Present study considers PGA as the intensity measure and various global and local EDPs for the estimation of seismic fragility at different damage states as discussed in the following sections.

7.3 Damage Dependent Limit States

Seismic damage assessment is the numerical quantification of probable damage to a building due to a given hazard. Damage states are specified in order to physically categorize the degree of damage to members of a building. Chapter 2 already discusses about several damage indices suggested in the past literature in terms of different parameters (e.g., strength, ductility, energy dissipation). Damage states were expressed in the past (Lagomarsino and Giovinazzi 2006, Barbat et al. 2008) in terms of capacity curve parameters, such as, yield displacement (d_y) and ultimate displacement (d_u). Other parameters, such as, maximum base shear capacity (Silva et al. 2014) or interstorey drift ratio (HAZUS 2013) have also been used to quantify the damage in buildings. Fig. 7.1 shows graphically discrete damage states for RC building frame on an idealized pushover curve, thresholds of which are demarcated by vertical lines based on yield and ultimate displacement as given in Barbat et al. (2008).

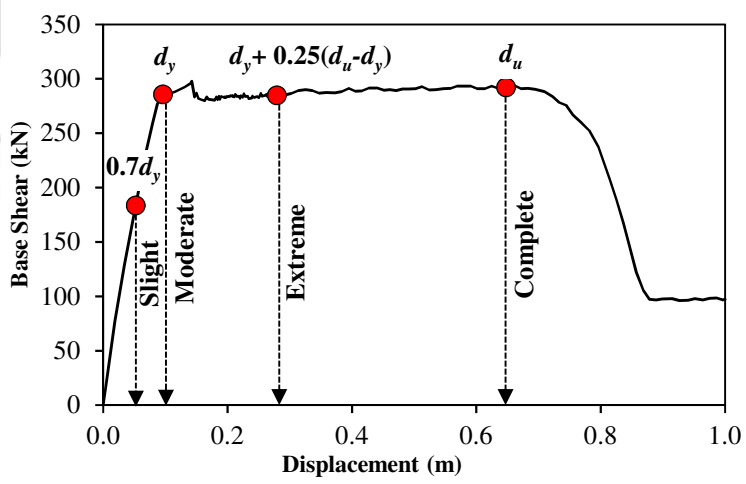

Figure 7.1 Discrete damage states defined on an idealized capacity curve based on Barbat et al. (2008).

For the RC building typologies in the present study, four sequential damage states based on (Barbat et al. 2008) are considered as Slight (S), Moderate (M), Extreme (E), and

Complete (C). These damage states are quantified based on the yield and ultimate displacement of the building frames. The yield displacement (d_y) is defined as the displacement at which the initiation of the first plastic hinge in any ground storey columns take place. For bare and OGS frames, failure point or ultimate displacement (d_u) is defined as the displacement when at least 50% of the ground storey columns exceed hinge rotation corresponding to life safety (LS) limit state as defined in Chapter 3 (Fig. 3.2). The LS limit state corresponds to a displacement or damage level in which the columns reach a deformation equal to three-fourth of the deformation specified for collapse prevention level, i.e., before the shear strength of columns is reached (FEMA 356 2000). For fully infilled (FI) frames, failure of the ground storey infill walls is an additional criterion considered to obtain the ultimate displacement capacity of the frame. The criterion of 50% or more "failures" of columns in a storey is an assumption to strike a balance between the usual over conservative approach, according to which failure coincides with failure of the first lateral load resisting member, and the reality witnessed after earthquakes that buildings do not collapse even after a number of lateral load resisting members fail (Kappos et al. 2006).

For the fragility analysis considering different EDPs, the damage states specified in HAZUS (2013) for mid-rise RC buildings are used in the present study; slight (S), moderate (M), extreme (E), and complete (C) are the four damage states for which the average interstorey drift thresholds (Δ_{ds}) are specified (Table 7.1). The frames considered are categorized under two different model building types of HAZUS: the BFs are classified as C1-M frames and both FI and OGS frames are classified as C3-M type frames designed for low code seismic level, where M stands for mid-rise buildings. For the estimation of fragility for each damage state, both the displacement threshold values and uncertainty values are required. The uncertainty values available in the literature and obtained in the present study are already discussed in Chapter 6; their effect on seismic fragility is scrutinized in the next section.

Table 7.1 Average interstorey drift (ISD) thresholds (Δ_{ds}) as specified in HAZUS (2013).

Damage States	Δ_{ds}	
	C1	C3
Slight (S)	0.0033	0.002
Moderate (M)	0.0053	0.004
Extreme (E)	0.0130	0.010
Complete (C)	0.0330	0.023

7.4 Treatment of Uncertainties in Fragility Estimation

7.4.0 General

Uncertainty estimation is essential, since it influences the seismic fragility as observed from Eq. (7.1). Chapter 6 already discusses the various sources from which the uncertainty in fragility estimation arise. Empirical values of epistemic and aleatoric uncertainty were quantified with a view of assessing the seismic fragility of the considered RC frames. In addition, comparison of the empirical values of damage state thresholds and uncertainties available in literature with those obtained in the present study suggests that the fundamental behavior of the considered frames differs from those available in the literature. Thus, this section investigates the extent to which the uncertainty influences the seismic fragility of the considered RC frames.

7.4.1 Influence of Total Uncertainty

Estimation of uncertainty in the seismic fragility analysis with some degree of confidence is extremely difficult due to unavailability of highly variable material properties (e.g., masonry) geometry, and material, large variation in construction methods, and scarcity of ground motion records. Therefore, a preliminary analysis is carried out for a 3B-4S RC bare frame, considering a range of β_T values (0 to 1.2) for which fragility is estimated using Eq. (7.1) as shown in Fig. 7.2. The horizontal line with markers (Fig. 7.2(a)) represent the probability of exceedance of a damage state with zero uncertainty, i.e., the probability values are either zero or one. Spectral displacement at 50% probability value represents the damage state median value (damage threshold) which is around 0.6m in the presented figure. At any displacement demand, before reaching the median displacement value, the seismic fragility increases with an increase in the uncertainty value, whereas, the trend reverses after the median point is crossed.

Also, it is observed that as the value of β_T increases, the curve flattens, implying a wider range of demands (S_d) over which there is a significant probability that the considered damage state will initiate or exceed. Further, the difference between the discrete cumulative probabilities at a given displacement demand (S_d) decreases with increasing values of total uncertainty. The cumulative difference becomes very less after an uncertainty value of about 0.7 is reached. This can be more clearly observed in the Fig. 7.2(b), where the term {P[β_{T1}] - P[β_{T2}]} in the Y-axis represents the difference in discrete

cumulative probability of exceedance of a damage state between two consecutive total uncertainty values (β_{T1} and β_{T2}). Thus, Fig. 7.2(b) represents the difference of P[ds | S_d] value between any two consecutive curves of Fig. 7.2(a) for different values of S_d. The variation of {P[β_{T1}] - P[β_{T2}]} is shown with respect to total uncertainty values (β_T). Clearly, at an S_d value of 0.6 (threshold value), the difference {P[β_{T1}] - P[β_{T2}]} is equal to zero at all the values of uncertainty as observed from the figure, since it is the median value. For all other values of S_d, the difference {P[β_{T1}] - P[β_{T2}]} is non-zero except for some S_d value at very small values of β_T (< 0.2). The rate of change of {P[β_{T1}] - P[β_{T2}]} with respect to β_T becomes very less for all S_d after reaching a β_T value of around 0.7.

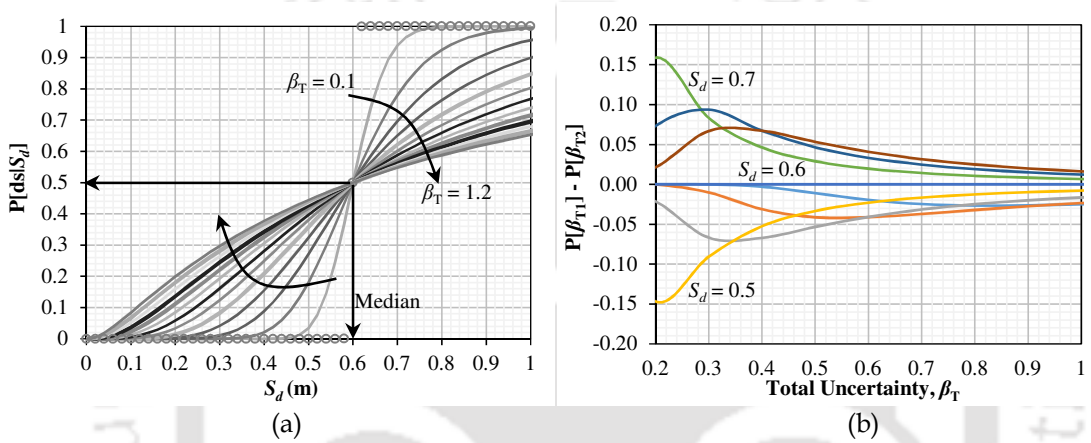

Figure 7.2 (a) Effect of total uncertainty (β_T) on construction of fragility curves, (b) Difference in discrete cumulative probabilities of exceedance with respect to total uncertainty for different S_d values.

While FEMA P-58 (2012) suggests a default value of 0.6 for β_T for all damage states, HAZUS (2013) suggests values of 0.75, 0.70, and 0.65 for buildings designed to old, moderate, and modern codes, respectively. These uncertainty values are obtained as a combination of uncertainty arising from variation in capacity, seismic demand, and modelling uncertainties, thus taking care of all the parameters affecting fragility estimates. The suggested values of β_T for mid-rise RC bare frames (C1M) designed for moderate code level is 0.7 for all damage states except for the complete damage state for which the value is 0.89 (HAZUS 2013). However, β_T for masonry infilled RC frames designed for moderate code is not specified in HAZUS (2013). It is also to be noted that the consideration of different variability associated with each damage state in the analysis may result in unrealistic fragility curves (for instance, intersecting curves) in cases where median values are closely spaced (Gueguen 2013).

Thus, considering all the above observations and code recommendations, comparative seismic fragility analysis for the considered frame configurations are carried out for a β_T value of 0.7 as an approximate value of uncertainty for all the damage states. The seismic fragility can also be estimated for other values of uncertainties based on code recommendations. However, the code specified values of uncertainties are very high and lack specific values of uncertainties for masonry infilled RC frames. In addition, there is no specific building category provided for vertically irregular OGS frames. Thus, as discussed in Chapter 6, detailed analysis for the estimation of uncertainty for the three RC frame configurations was carried out considering all the sources of uncertainty. Seismic fragility for different frame configurations is assessed in the next section considering the obtained values of epistemic and aleatoric uncertainties.

7.4.2 Influence of Epistemic and Aleatoric Uncertainties

The two basic sources of uncertainty are investigated in the Chapter 6 from which it is clear that aleatoric uncertainties arising due to variation in ground motion characteristics are rather more influential as compared to the epistemic uncertainties. Nonetheless, the epistemic uncertainties becomes important at higher values of PGA, i.e., at higher damage states. Thus, this study is dedicated to the evaluation of the impact of different sources of uncertainty on the structural fragility of different RC building frame typologies with special consideration on vertical irregularities. Considering the damage states suggested by Barbat et al. (2008), seismic fragilities for the four damage states (Slight, Moderate, Extreme, and Complete) are evaluated for the three RC frame typologies considering aleatory as well as epistemic uncertainty. In addition, the fragility is also plotted for the combined uncertainty (Fig. 7.3). Epistemic and Aleatoric uncertainties considered in the seismic fragility analysis are specified in Table 6.2 and Fig. 6.4 and 6.5.

The three curves intersect at a point that represent 50% probability of exceedance, i.e., the median or threshold of the damage state. At slight damage state when the displacement threshold is very less, it is observed that consideration of only epistemic uncertainty overestimates the fragility beyond the threshold point. It is interesting to note that there is a little difference in the seismic fragility estimated considering only the uncertainty in the ground motion and a combination of variability in ground motion and capacity. A similar trend is observed for the moderate and extreme damage states also.

However, in the complete damage state, both epistemic and aleatoric uncertainties contribute almost equally to the total uncertainty. In general, it can be inferred that the uncertainty in the parameters related to geometry, material and loading does not have a significant influence on the fragility estimates for lower drift thresholds (or damage states) and the inclusion of only ground motion uncertainty may be adequate. For complete damage fragility however, the contribution from both epistemic and aleatoric uncertainties must be accounted for. Similar observations were also reported by Padgett and DesRoches (2007) for fragility estimates of bridge structures.

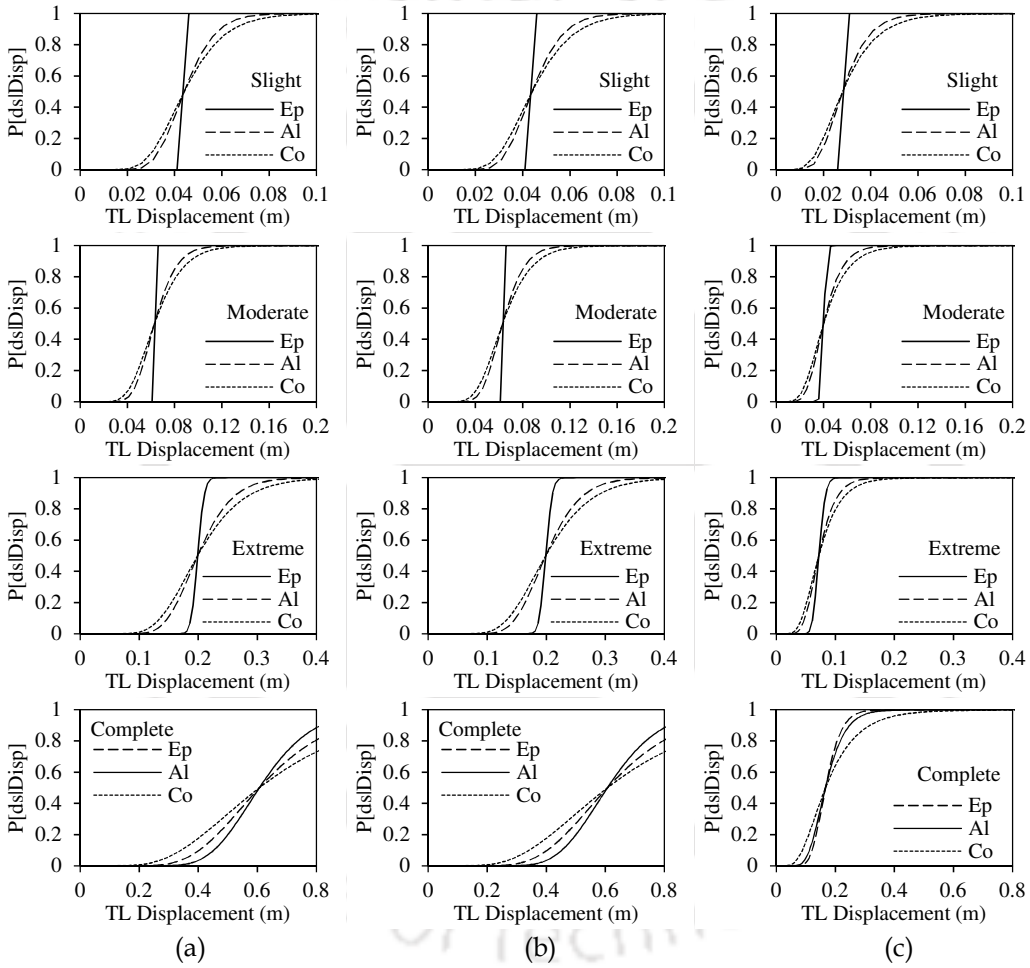

Figure 7.3 Comparison of seismic fragility estimates considering different sources of uncertainty-epistemic (Ep), aleatoric (Al) and combined (Co) for (a) Bare, (b) OGS, and (c) FI frames. P[ds|Disp] is the conditional probability of exceedance of a damage state (ds) given displacement.

Fig. 7.4 shows the comparison of the seismic fragility curves obtained using the parameters specified in HAZUS (2013) with those obtained using the uncertainty and threshold values estimated in the present study considering TL displacement as the EDP.

Apparently, the fragility of high code designed C1M frames is consistently low, whereas, the low code designed frames have the highest fragility. In comparison, the bare frames analyzed in the present study show altogether a different fragility, mostly intersecting all the other fragility curves. Therefore, it is clear that more studies are required to provide data for updating existing building typology models and associated uncertainties.

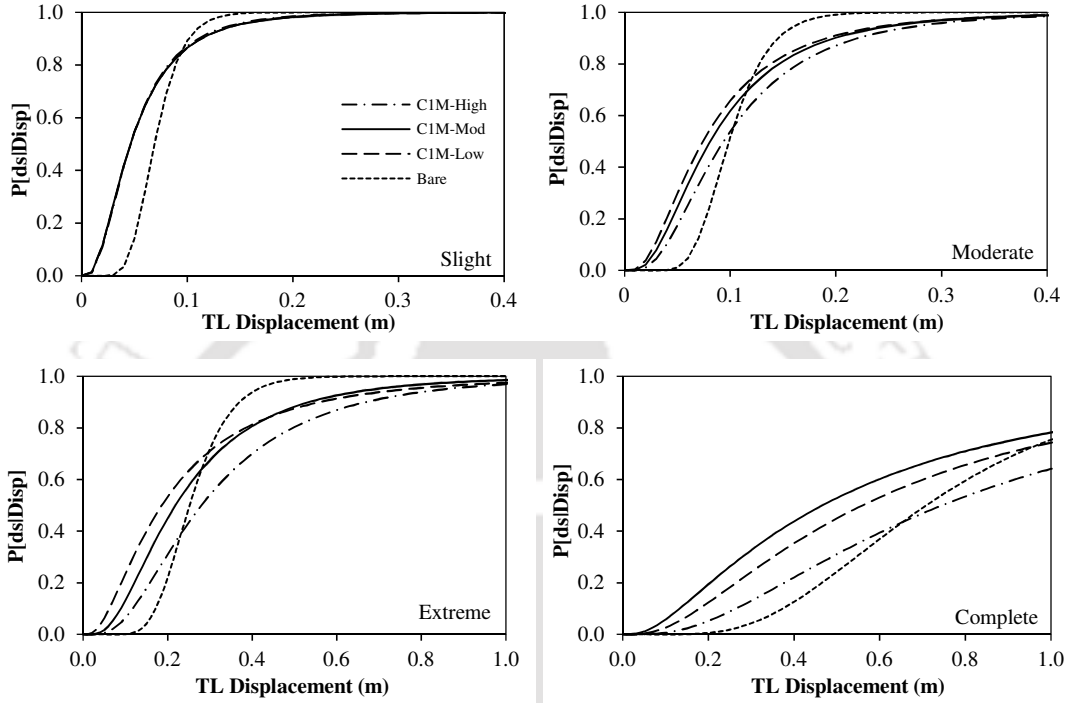

Figure 7.4 Comparison of seismic fragility derived based on HAZUS (2013) and present study for RC moment resisting frames without infills.

The seismic fragility of the RC-URM mid-rise frame for low design code level (HAZUS 2013) is also compared with the fragility of two variants of infilled frames (OGS and FI frames) considered in the present study (Fig. 7.5). It is observed that with displacement demand as the intensity measure, the seismic fragility of FI frame is much higher than that for the OGS frame for any given damage state. This is reasonable since the physical behavior of the two frames is completely different, i.e., the FI frames are much stiffer than the OGS frames. It is observed that if PGA is used as IM, the seismic fragility of FI frames becomes lowest among the three frames. This issue will be discussed in greater detail in Section 7.5.1. Nevertheless, the frame typology C3M specified in HAZUS (2013) for infilled frames is unable to reflect the true behavior of the two infilled frame typologies. Thus, the HAZUS specified typology for masonry infilled RC frames is not sufficient to cover the entire range of the buildings.

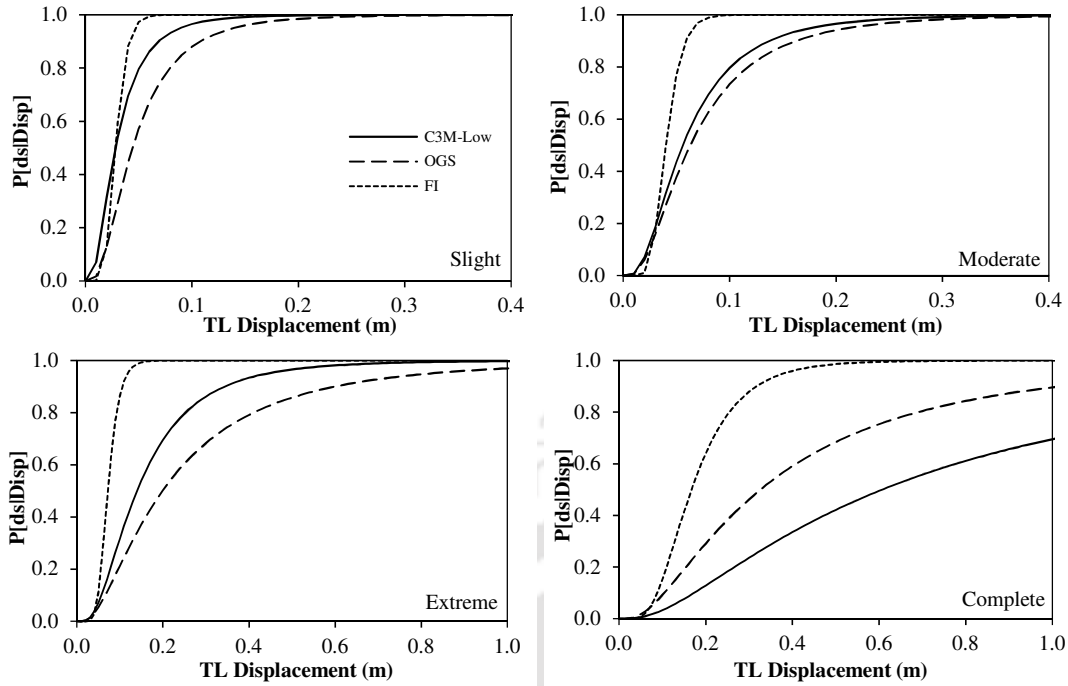

Figure 7.5 Comparison of seismic fragility derived based on HAZUS (2013) and present study for RC frame buildings with unreinforced masonry infill walls.

The differences between the HAZUS based and NLTHA based fragilities in this study are attributed to the fact that the deformation limits (thresholds) in the HAZUS are conservative, and the logarithmic standard deviations are substantially higher (as shown in Table 6.3), often exceeding 90%, while those in the present study are on the order of 50% or less. It should be noted that HAZUS is aimed at regional loss estimation rather than individual building assessment, and the large logarithmic standard deviations reflect the considerable variation in construction that exists within each building category. Thus, it is not surprising that a HAZUS analysis may lead to an erroneous appraisal of individual building performance, as it was not developed for that purpose. Results of fragility analysis considering different damage state dependent thresholds and uncertainty for different EDPs are discussed in the next sections.

7.5 Seismic Fragility Assessment

7.5.0 General

Seismic fragility of the RC fame typologies (bare, OGS and FI frames) are obtained using both nonlinear static analysis and nonlinear dynamic analysis in this section. Various comparative results are plotted for the three frames, and the influence of different type of analysis procedures (nonlinear static and dynamic) on fragility assessment are

shown. Also, the effect of varying the central opening size and number of bays and stories, as detailed in Chapter 3, are shown here in terms of seismic fragility. The influence of different uncertainty values on seismic fragility is already reflected in the previous section; therefore, comparative results are plotted for seismic fragility considering different uncertainty values obtained in previous section and those obtained in Chapter 6, wherever necessary.

7.5.1 Comparative Seismic Fragility of the Frames

This section explores the comparative seismic fragility curves for the 3B-4S RC frames: bare, OGS, and FI, modelled considering fiber hinges. For each of the frame, damage state thresholds are decided based on Barbat et al. (2008), which depend on d_y and d_u of the frames as already discussed. Fig. 7.6 shows the comparative seismic fragility curves for the three frames for the different damage states. It is observed that the seismic fragility of the three frames are very different from each other. For a given seismic displacement demand, the FI frame have the highest and the bare frame have the lowest seismic fragility. In fact, the probability of reaching or exceeding the complete damage state is very high in case of FI frame as compared to the other two frames. This is because the seismic fragility is inversely proportional to the seismic displacement capacity of the frames. Since the ductility of the FI frames is the least, their displacement capacity is also less, and hence, have the highest seismic fragility for a given displacement demand.

However, with respect to PGA (Fig. 7.7), the trend in the seismic fragility of the three frames is altogether different as compared to that with respect to displacement demand. The bare and the OGS frames have the highest seismic fragility, whereas, the FI frame have the lowest fragility when plotted with respect to PGA. At each damage state, initially at lower PGA (i.e., seismic intensity level), the seismic fragility of FI frame is much less than that of the OGS frame. This implies that the seismic force resistance of the FI frames is much higher and better than the OGS or bare frame initially i.e., when the infill walls are intact. The ground storey infills in the FI frame imparts tremendous strength to the frame to resist the seismic force. However, at higher PGA, the seismic fragility of the FI frame tends to increase and becomes similar to that of the OGS frame. This certainly happens after the failure of the ground storey infills in the FI frame, after which the seismic behavior of FI frame becomes similar to the OGS frame and their

fragility appears similar. Influence of central opening size in infill, number of bays and stories, analysis type, and EDPs on seismic fragility assessment will be discussed next.

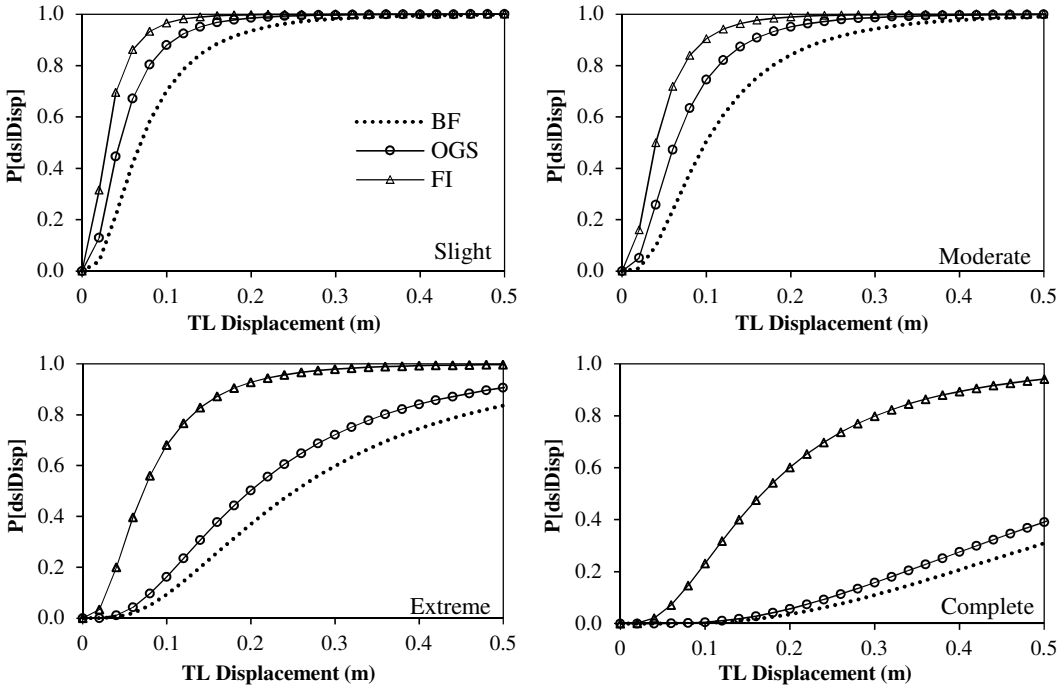

Figure 7.6 Comparative seismic fragility curves for the three frames for different damage states (Barbat et al. 2008) with respect to TL displacement.

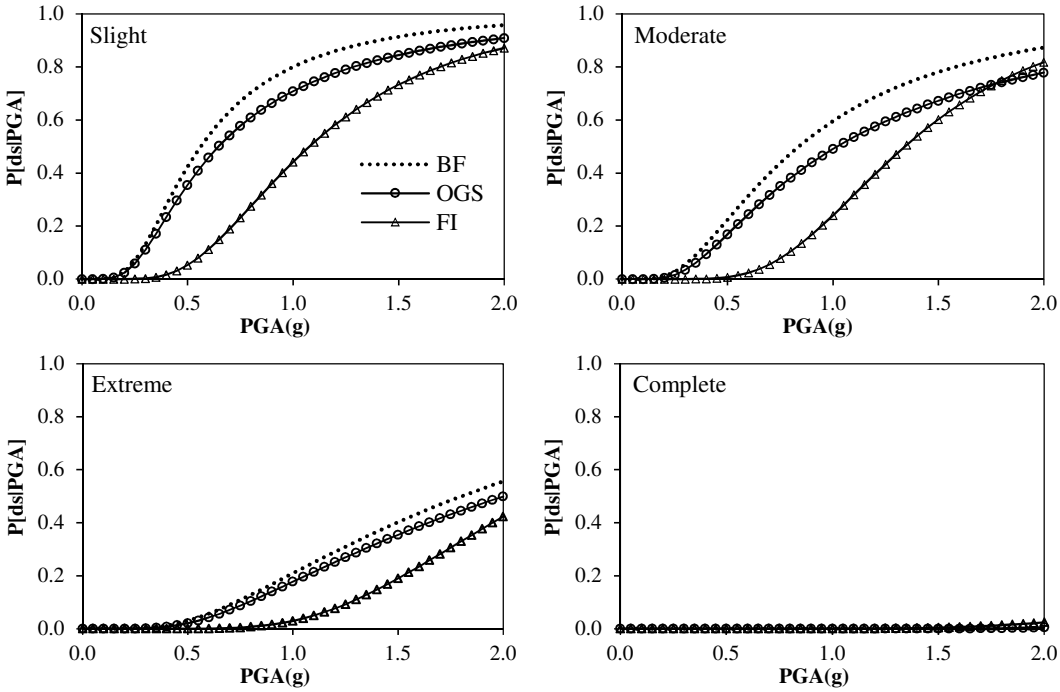

Figure 7.7 Comparative seismic fragility curves for the three frames for different damage states (Barbat et al. 2008) with respect to PGA. P[ds|PGA] is the conditional probability of exceedance of a damage state (ds) given PGA.

7.5.2 Influence of Central Opening Size in Infill

As already discussed in Chapter 3, presence of openings in infill walls have a significant influence on lateral capacity of FI frames but not on that of the OGS frames. Fig. 7.8 shows the fragility curves obtained for 3B-4S OGS and FI frames with different *Op* plotted with respect to S_d. These fragility curves are also compared with those obtained for 3B-4S bare frame. It is observed that in both the OGS and FI frames, though the seismic fragility decreases with increasing *Op*, the decrease is not considerable in case of OGS frames. The fully infilled frames are very stiff and hence undergo significantly lesser lateral displacement compared to the relatively flexible bare and open ground storey frames. As seen in Chapter 3 from the comparison of pushover curves also, the lateral load behavior of FI frames changes drastically with increase in opening sizes in infills (Fig. 3.7(b)). There occurs a significant reduction in both the lateral strength and stiffness of the FI frames with increasing central opening size in infill walls. Since there is a large change in the flexibility of the frames with changing opening sizes in infills, there occurs a large change in the displacement capacity (or ultimate displacement before failure) of the frames.

The displacement capacity of the fully infilled frames with larger central opening size in masonry infill is higher compared to one with a lesser opening size. Again, a greater displacement capacity implies lower fragility. In contrast, in OGS frames, the change in central opening size in infills does not affect the overall performance of the frame. There is an insignificant reduction in the stiffness as well as strength of OGS frames with increase in opening size in infills of upper stories (Fig. 3.7(a)). This implies that the displacement capacity, and hence the seismic fragility of the OGS frames, do not alter much due to opening size.

Further, although from the pushover curves, it appears that the lateral load carrying capacity of the bare and OGS frames is nearly the same (Fig. 3.7), OGS frame even with 90% *Op* are found to be more fragile compared to the bare frame. Thus, the common conception among different stakeholders that increase in opening in infill of OGS frame reduces its seismic vulnerability is not correct. On the other hand, seismic fragility of FI frames with any *Op* is higher than that of the bare frame for slight, moderate, and extreme damage states. However, for complete damage state, fragility of FI frames with about 60% *Op* nearly coincides with that of the bare frame.

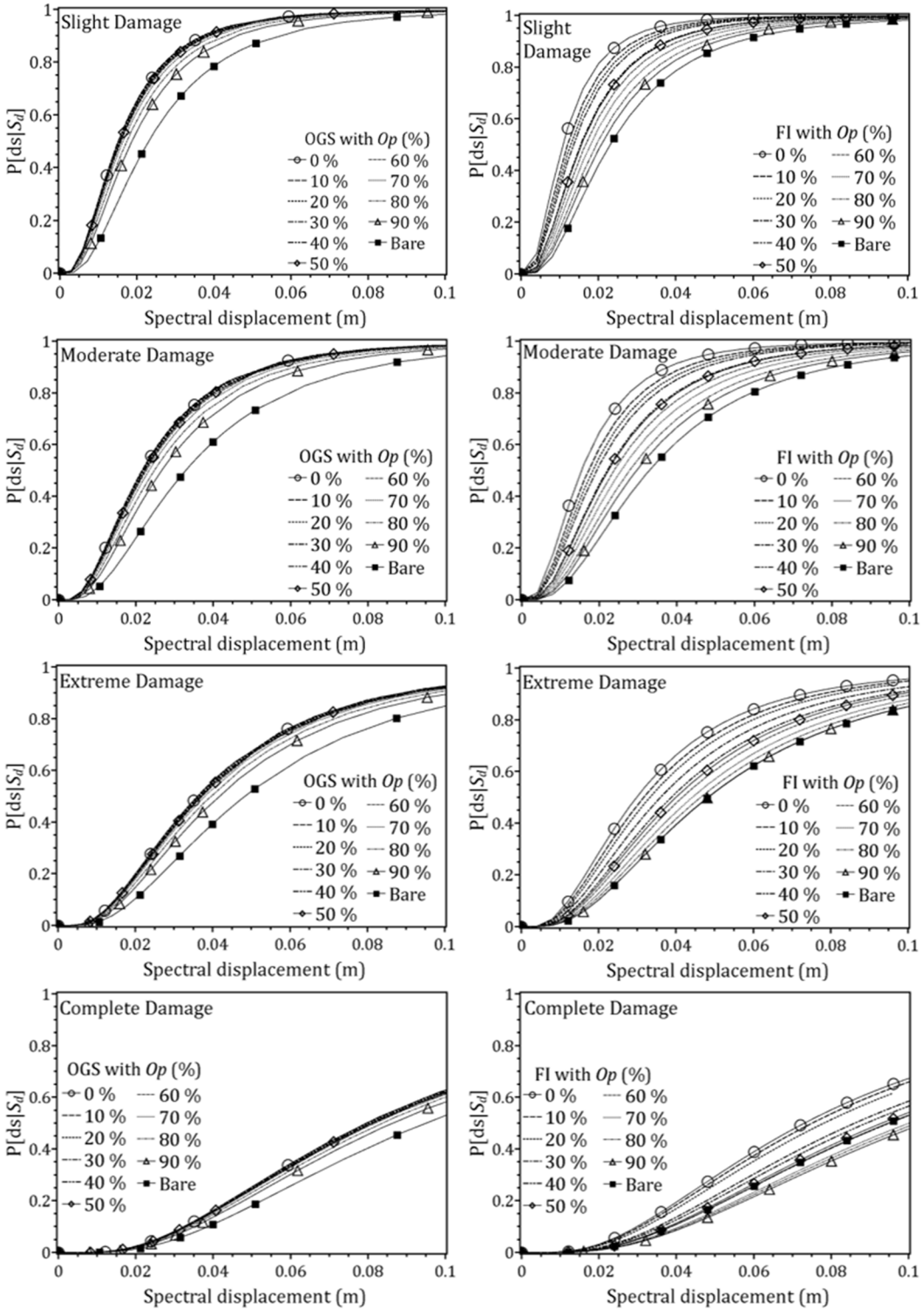

Figure 7.8 Comparison of fragility curves for 3B-4S (a) OGS and (b) FI frames with varying *Op*. For comparison, the seismic fragility of bare frame is also shown.

The faster rate of reduction in the fragility of FI frames with increasing *Op* relative to OGS frames is because of faster rate of increase in displacement threshold ($\bar{S}_d$), which in turn, depends on d_y and d_u of FI frames. With an increase in *Op*, both d_y and d_u increase

in OGS and FI frame (Fig. 7.9), however, the rate of increase is much higher in FI frame. When the *Op* is increased from 0% to 90%, the increase in d_y is 93% and 23%, and increase in d_u is 42% and 9% in case of FI and OGS frames, respectively. The d_y and d_u values of FI frame exceed those of OGS frame after *Op* of about 50% and 20%, respectively. In fact, the d_u value in the FI frame with 60% *Op* is similar to that in the bare frame value due to which their fragility also coincides. Beyond 60% *Op*, the d_u value in FI frame exceeds the bare frame value, and hence, the fragility of FI frame is lower than that of the bare frame.

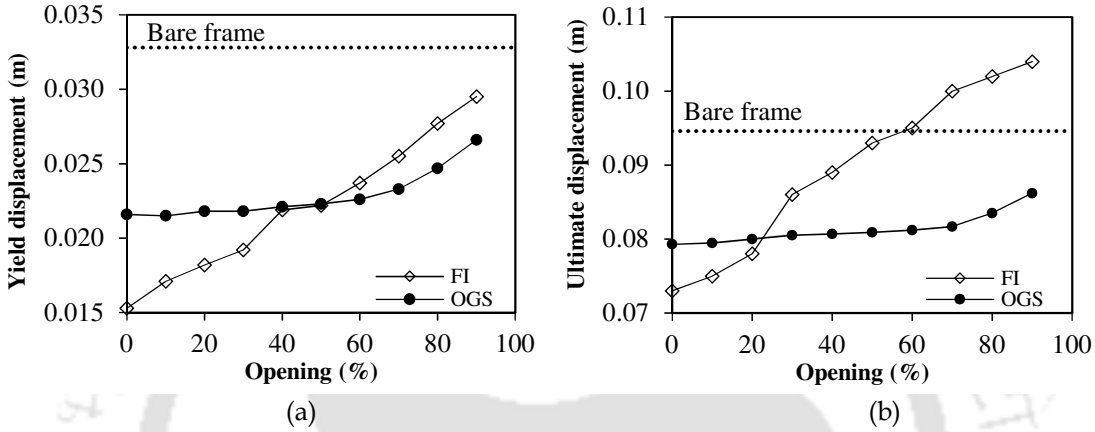

Figure 7.9 Variation in (a) yield displacement, and (b) ultimate displacement with *Op* for OGS and FI frame.

From the fragility analyses of OGS and FI frames, it is observed that for any combination of N_B and N_S, the FI frames have a faster rate of reduction in seismic fragility compared to the corresponding OGS frames. In addition, as already discussed, because of higher displacement threshold values for FI frames with higher central opening sizes, the fragility of complete damage for FI frames with different N_B and N_S reduces even below the fragility of bare frame when 50% to 60% *Op* is provided in FI frames. This is not so in the case of OGS frames, and thus, the fragility of OGS frames always remains higher than that of the bare frame with any *Op* and for any combination of N_B and N_S when assessed with respect to S_d.

7.5.3 Influence of Number of Bays and Number of Stories

Seismic fragility curves are developed for the bare, OGS, and FI frames in order to study the influence of varying the number of bays and number of stories. Fig. 7.10 shows the seismic fragility distribution with respect to both PGA and S_d for a 3B RC bare frame with varying number of stories (2S-6S). Fig. 7.11 also shows similar fragility curves for a 4S RC bare frame with varying number of bays (1B-6B). It is clear from the figures

that for bare frames at any damage state, the influence of change in number of stories is more than a change in number of bays. With respect to PGA, the influence of either change in number of bays or stories on seismic fragility increases with severity of the damage states. With respect to S_d, the influence of change in number of stories on seismic fragility remains more or less same for different damage states; however, there is only a marginal influence of varying the number of bays on seismic fragility with respect to S_d. Seismic fragility increases with increasing number of stories when observed with respect to PGA. On the other hand, fragility decreases with increasing number of stories when observed with respect to S_d for all the damage states. For an increase in number of bays, seismic fragility increases both with respect to S_d and PGA, even though the increase is minimal with respect to S_d. With an increase in number of stories, the structural flexibility increases, which increases the displacement capacity. Hence, with respect to displacement (S_d), the 3B-6S bare frame shows the lowest fragility. Stiffer frames (with lower number of stories) can take up higher force as compared to the flexible ones (with higher number of stories). Thus, with respect to PGA, the frame with lowest number of storey shows the least fragility. On the other hand, given a constant number of storey, addition of bays in a building frame increases the stiffness of the building and decreases the displacement capacity. Hence, the 6B-4S bare frame shows the highest fragility when compared to other 4S frames with lower number of bays.

Fig. 7.12 and Fig. 7.13 show the comparative fragility curves for OGS and FI frames with varying number of stories. In both OGS and FI frames, for a given damage state with respect to spectral displacement demand, the seismic fragility is observed to decrease with increasing number of stories; this observation is similar to that of the bare frames, however, the variation in fragility is more in case of FI frame. On the contrary, with respect to PGA seismic fragility increases with increasing number of stories for the reason already discussed. The effect of a change in the number of bays in seismic fragility of OGS and FI frames is also shown in Fig. 7.14 and Fig. 7.15. It is observed that the increase in number of bays does not influence the seismic fragility of either OGS or FI frames significantly for a given displacement demand (Fig. 7.14). With respect to PGA however, seismic fragility of OGS frames is observed to increase with increase in number of bays. In case of FI frames, seismic fragility decreases with increase in number of bays, although marginally.

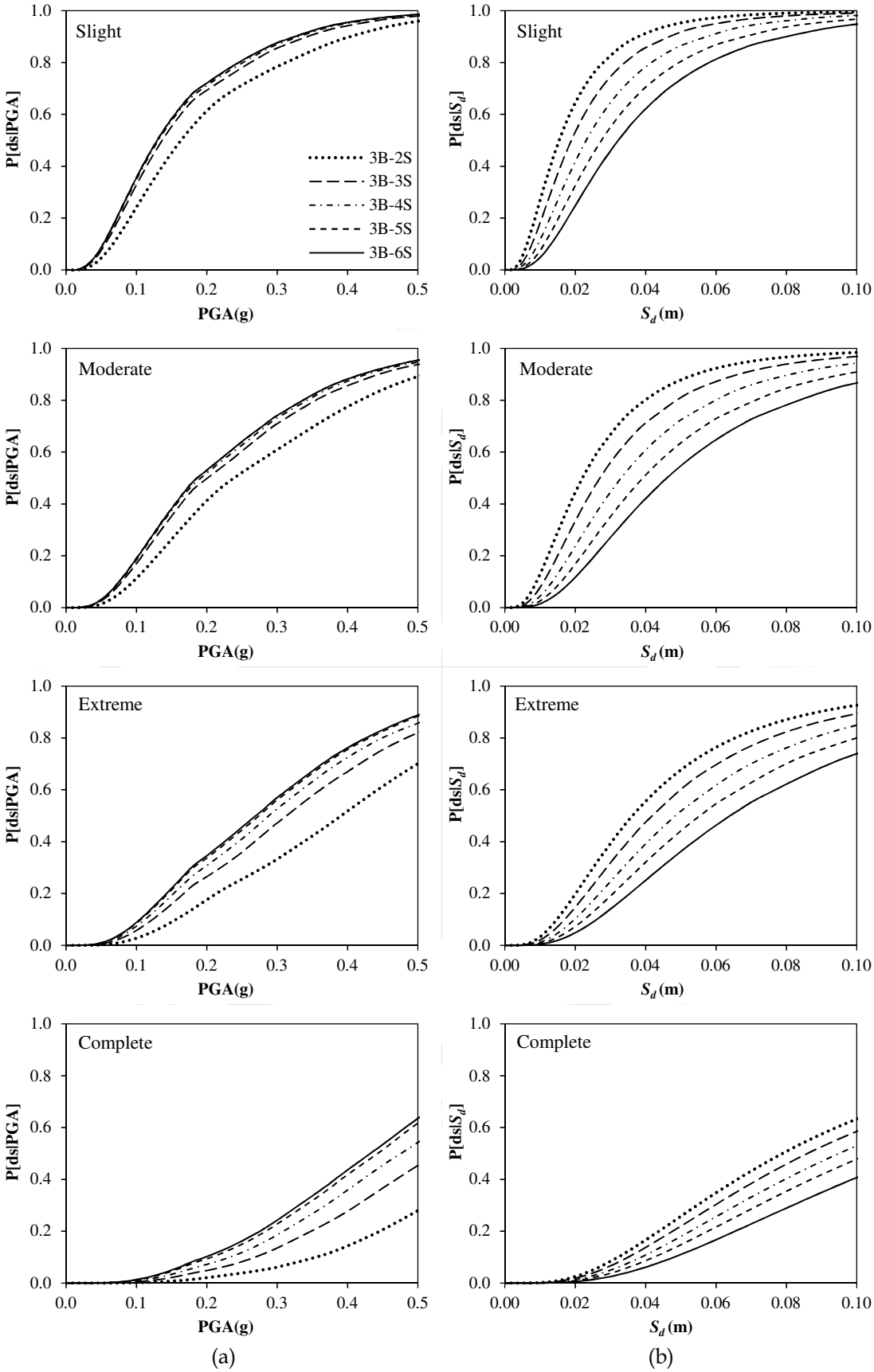

Figure 7.10 Comparison of fragility curves for 3B-RC bare frame with varying number of stories (2S to 6S) with respect to (a) PGA and (b) spectral displacement (S_d).

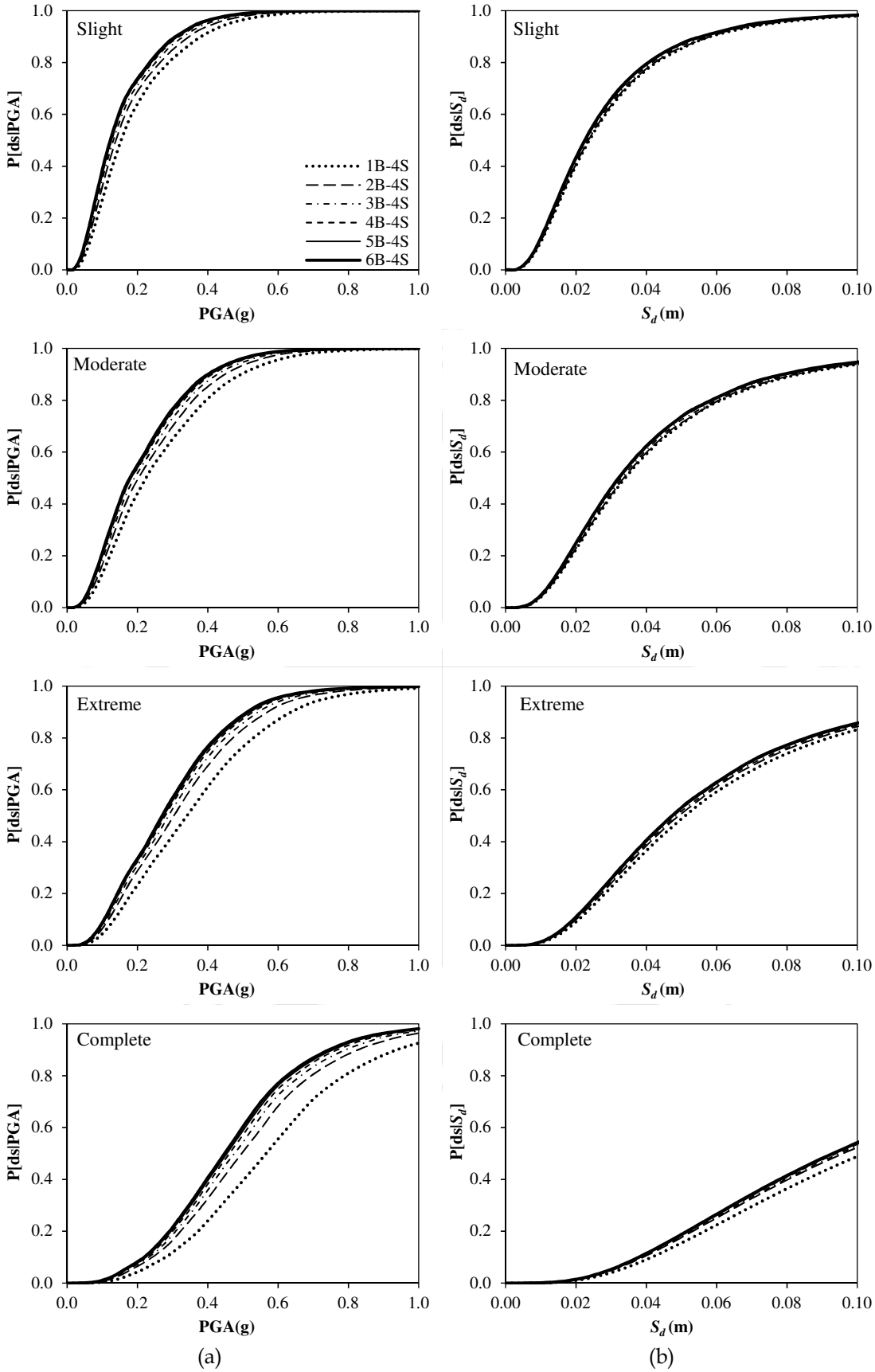

Figure 7.11 Comparison of fragility curves for 4S-RC bare frame with varying number of bays (1B to 6B) with respect to (a) PGA and (b) spectral displacement (S_d).

In order to show the combined influence of variation in number of bays and number of stories on seismic fragility of OGS frames, fragility contour plots are developed for the four damage states. The influence is shown for two PGA values specified for seismic zone IV and V (highest seismic zones in India) in the Indian seismic code (BIS 2016a) considering *Op* values of 0% and 50%. Fig. 7.16(a) shows a contour plot for seismic fragility obtained for OGS frames without any opening (0% *Op*) with respect to N_B and N_S for a PGA of 0.36g. Seismic fragility for a given PGA is found to increase with increasing N_B and N_S in any damage state, however, the change is marginal with respect to N_B. At the considered PGA level of 0.36g, almost all the configurations of frames with different combinations of N_B and N_S have high probability of undergoing slight and moderate damage, but the probability of undergoing complete damage is more for frames with higher N_B and N_S. Similar trends are observed for OGS frames with other *Op* and PGA levels, for example, as shown in Fig. 7.16(b) and Fig. 7.16(c) for OGS frame with 0% opening and PGA of 0.24g, and for OGS frame with 50% opening and PGA of 0.36g, respectively. Comparing Fig. 7.16(a) and Fig. 7.16(b), it can be inferred that change in opening from 0% to 50% in OGS frames decreases the seismic fragility marginally for any combination of bay and storey at a given PGA.

7.5.4 Influence of Analysis Type

Seismic fragility assessment can be carried out using the engineering demand parameters obtained either from nonlinear static analyses or from nonlinear dynamic analyses of the buildings. It requires large number of analysis runs (static or dynamic) to satisfactorily estimate the structural response to different earthquake excitations considering a range of relevant building parameters. Nonlinear dynamic method of analysis is computationally very expensive and requires much more input data than that required in case of nonlinear static method of analysis. Therefore, large amount of uncertainties are associated with nonlinear dynamic analysis results. Due to these reasons, nonlinear static pushover analysis methods are sometimes preferred for assessment of lateral load behavior of buildings. It will be interesting to study the difference in seismic fragility obtained using results of nonlinear static and nonlinear dynamic analysis methods. Such a study will help to develop a method for converting fragilities obtained using static analysis methods to that corresponding to dynamic analysis methods.

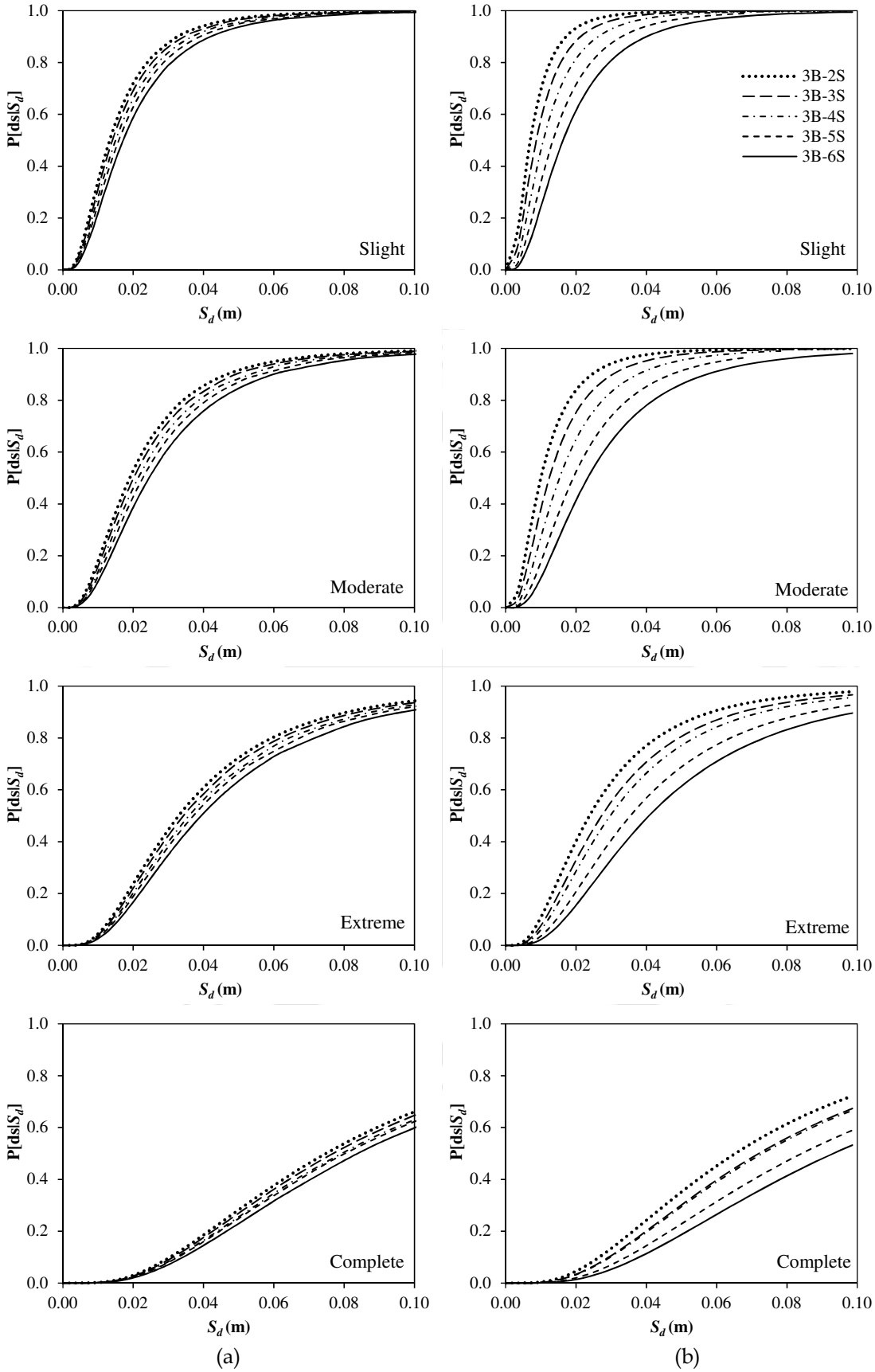

Figure 7.12 Comparison of fragility curves for 3B-RC frame with varying number of stories (2S to 6S) for (a) OGS and (b) FI frames with respect to spectral displacement (S_d).

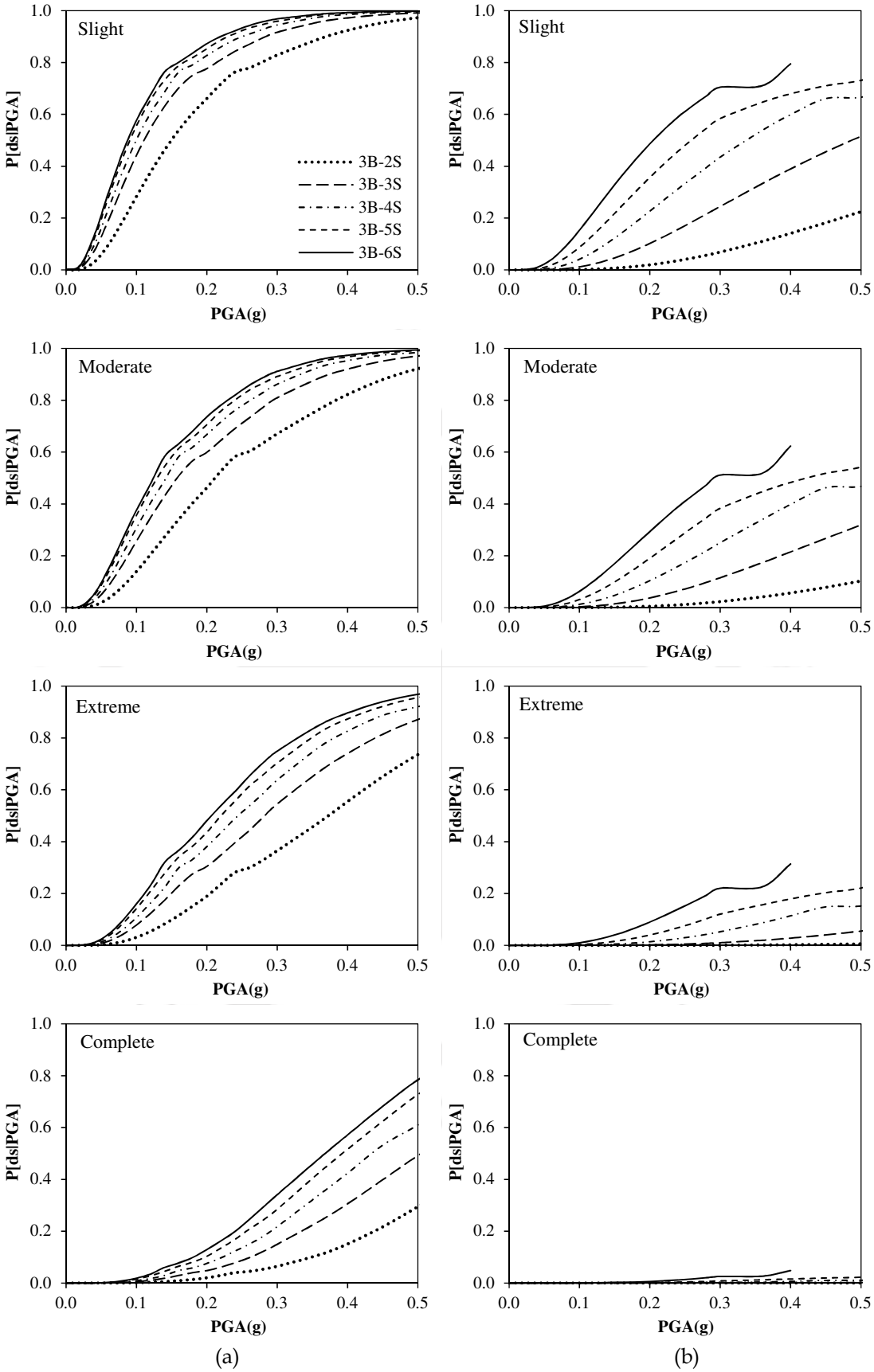

Figure 7.13 Comparison of fragility curves for 3B-RC frame with varying number of stories (2S to 6S) for (a) OGS and (b) FI frames with respect to PGA.

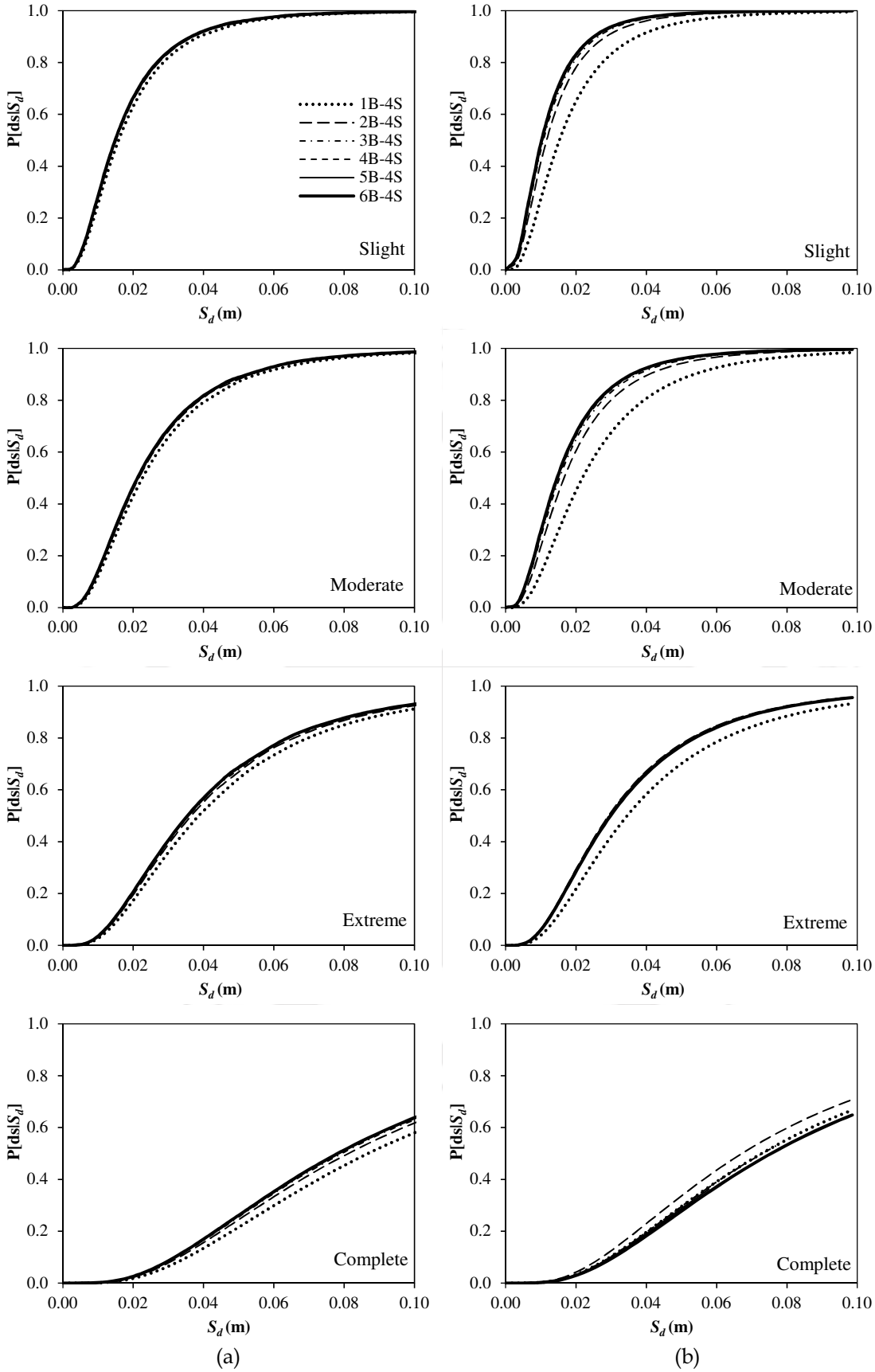

Figure 7.14 Comparison of fragility curves for 4S-RC frame with varying number of bays (1B to 6B) for (a) OGS and (b) FI frames with respect to spectral displacement (S_d).

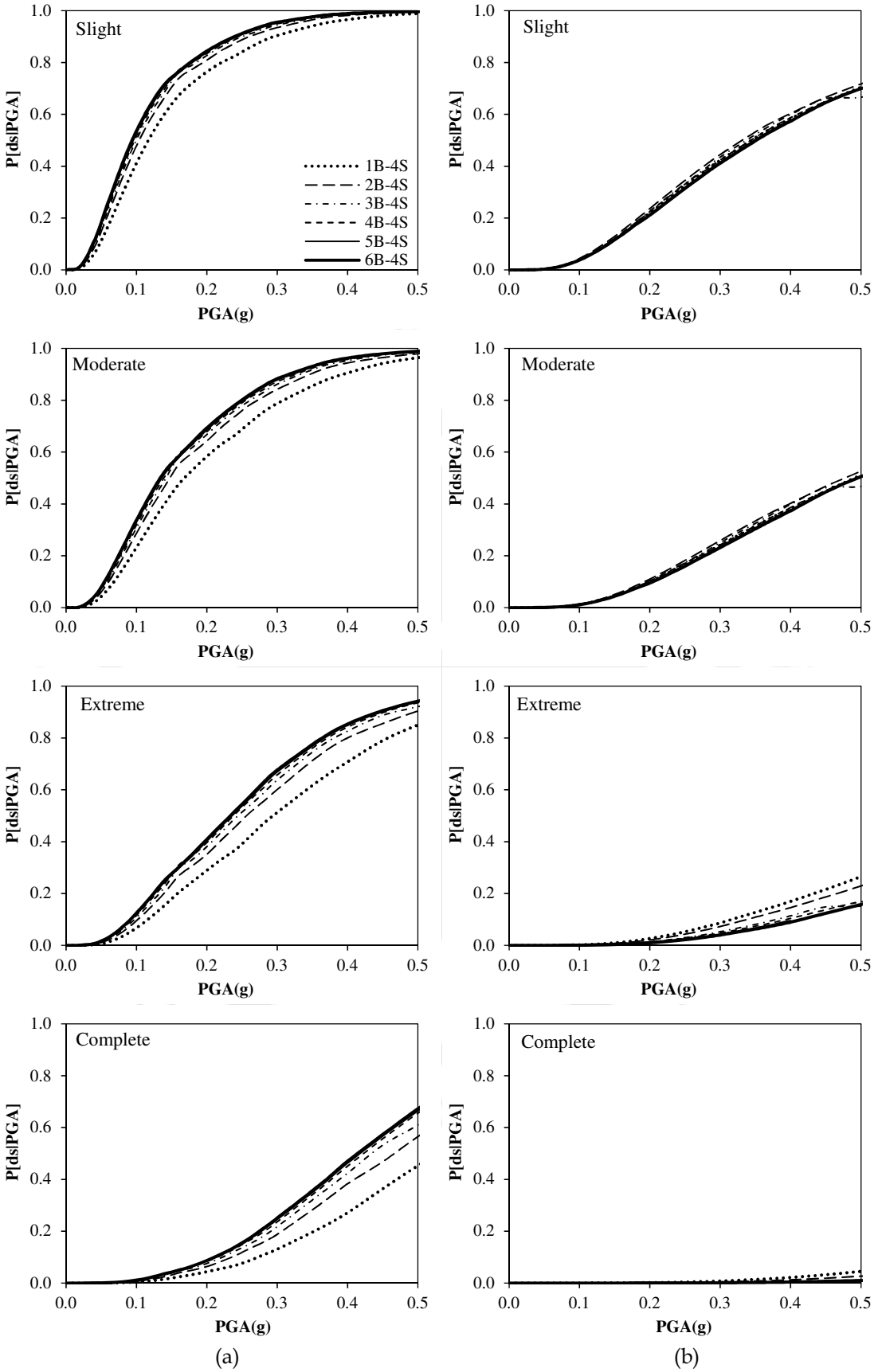

Figure 7.15 Comparison of fragility curves for 4S-RC frame with varying number of bays (1B to 6B) for (a) OGS and (b) FI frames with respect to PGA.

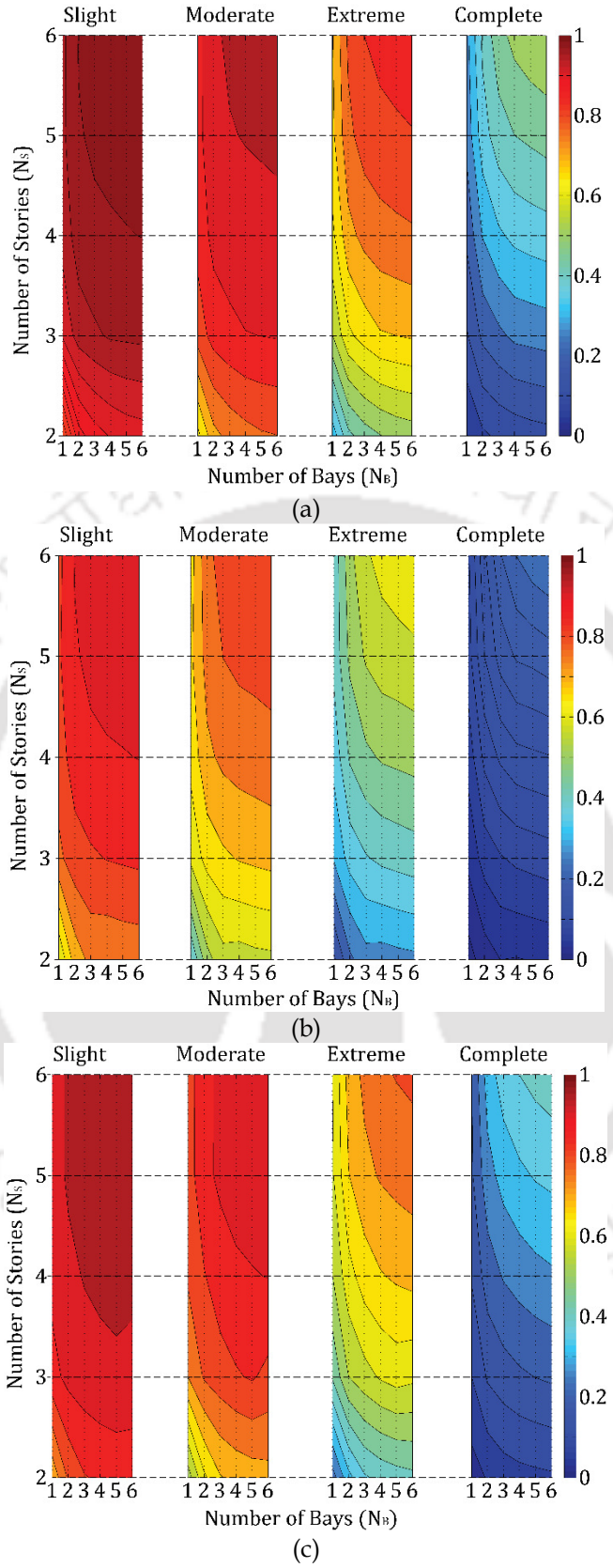

Figure 7.16 Contour plot for seismic fragility showing influence of change in N_B and N_S for OGS frames with (a) 0% *Op* for PGA of 0.36g (b) 0% *Op* for PGA of 0.24g, and (c) 50% *Op* for PGA of 0.36g. The vertical color bar shows the probability of exceedance of a damage state.

Seismic fragility is obtained for the mean (or base) models of all the three frames using results of both nonlinear static and dynamic analysis as shown in Fig 7.17 and Fig. 7.18. Nonlinear static analysis is found to slightly underestimate the seismic fragility when observed with respect to PGA for all the damage states. However, with respect to displacement at top level, the seismic fragility obtained using nonlinear static analysis overestimates the fragility. When fragility is assessed with respect to PGA, nonlinear dynamic analysis methods seem to provide realistic results as the seismic fragility for OGS frames is found to be highest for all the damage states and for all values of PGA, except for the complete damage state for higher values of PGA (> 1.2g). The relative fragility curves for the three frames obtained using static and dynamic methods remain more or less similar when plotted with respect to top level displacement. Though the seismic fragility of FI frames plotted with respect to top level displacement is found to be highest due to reasons already discussed, the OGS frames are found to be more fragile than the BF for all damage states and at all PGAs.

7.5.5 Influence of EDPs

The effectiveness of using relevant engineering demand parameters (EDPs) in seismic performance assessment of building typologies is already discussed in detail in Chapter 4. It was observed from the results of nonlinear time-history analyses that the global engineering demand parameters may not always suffice for the realistic damage, and hence, seismic fragility estimation of vertically irregular (OGS) building frames. Thus, in this section the effect of different engineering demand parameters on the seismic fragility estimates of RC frames with and without masonry infill walls is investigated for each of the seven ground motion records as shown in Table 3.5 individually by scaling the PGA from 0.1g to 1.0g. The peak interstorey drift (θ_d) is considered as the engineering demand parameter and the threshold values are taken from HAZUS (2013) for different damage states considered as shown in Table 7.1. The interstorey drift thresholds (Table 7.1) are suitably converted to displacement thresholds to estimate the seismic fragility in terms of displacement. The value of total uncertainty in seismic fragility estimation (β_T) for all the damage states is considered to be 0.7. The discrete seismic fragilities observed for the considered regular and irregular building frames by the use of different EDPs obtained from nonlinear dynamic analysis of the frames are illustrated in the continuing sections.

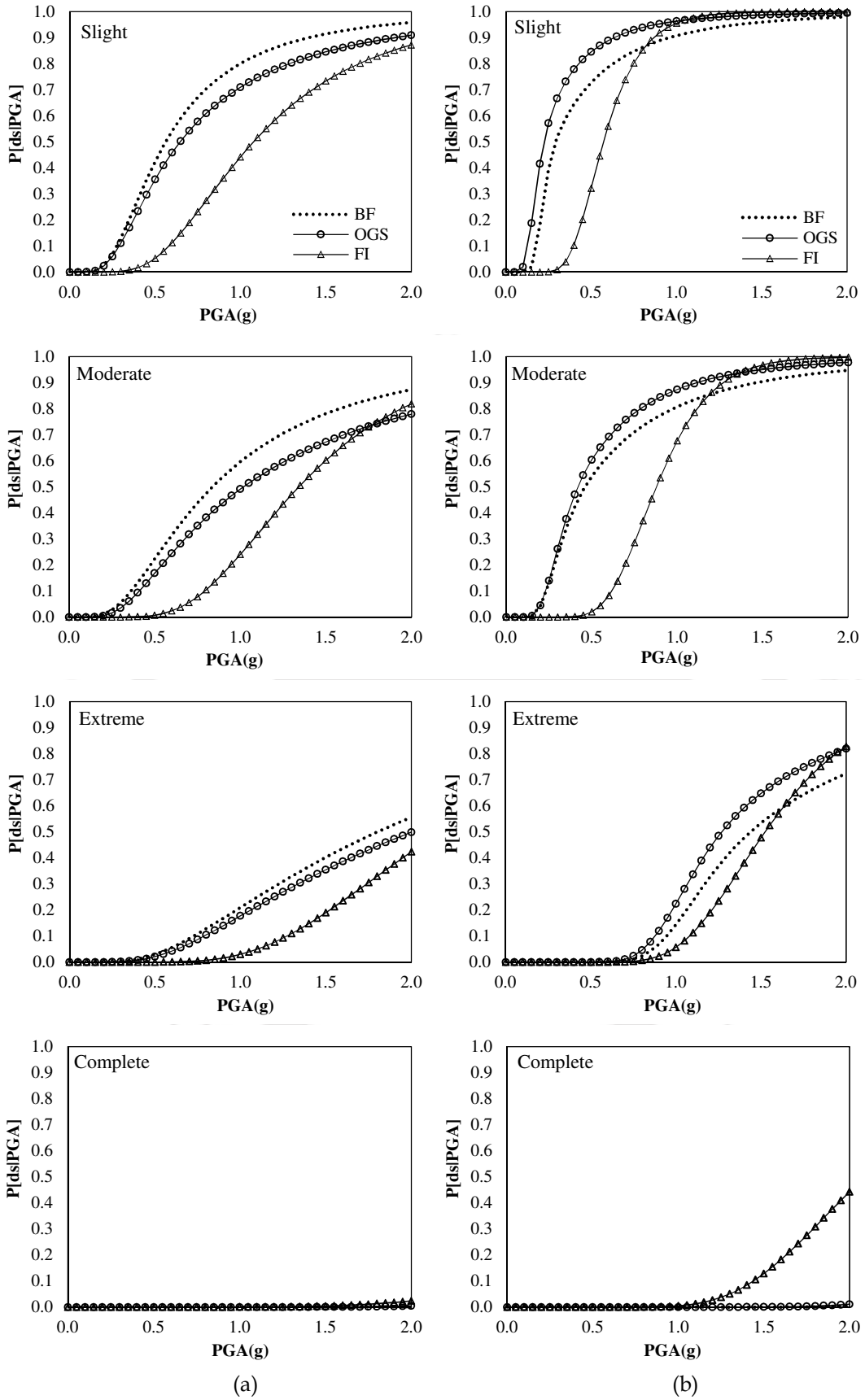

Figure 7.17 Seismic fragility curves obtained using (a) nonlinear static analysis, and (b) nonlinear dynamic analysis with respect to PGA.

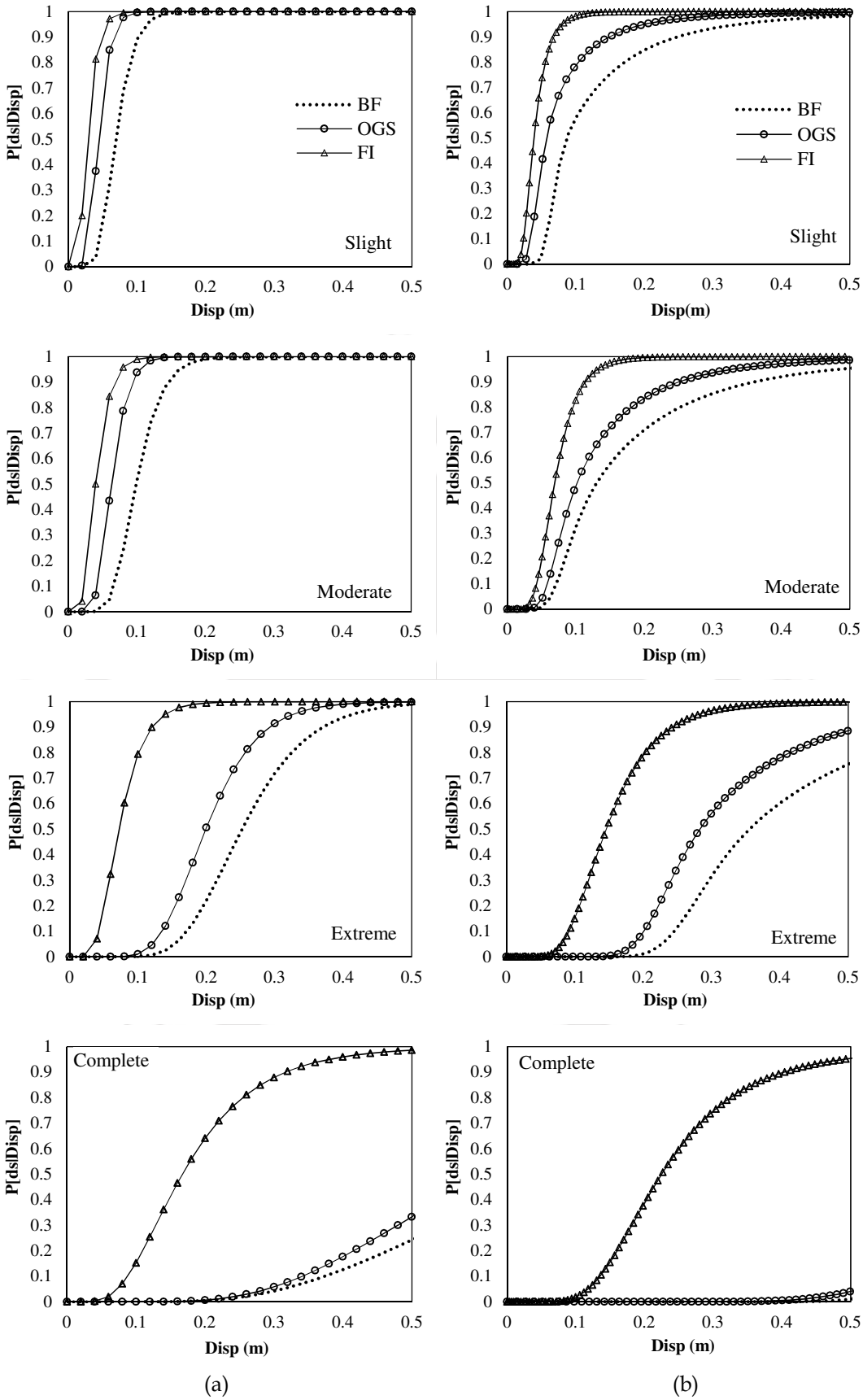

Figure 7.18 Seismic fragility curves obtained using (a) nonlinear static analysis, and (b) nonlinear dynamic analysis with respect to TL displacement.

7.5.5.1 Peak Top Level Displacement as EDP

Peak top level (TL) or roof displacement is the most common EDP considered in the literature for fragility assessment of buildings. Fig. 7.19 shows the seismic fragility (in terms of the probability of exceedance of a particular damage state) for BF, OGS and FI frames for three PGA levels (0.5g, 0.7g, and 1.0g) evaluated considering peak roof or top level displacement as EDP obtained from the nonlinear time-history analyses. Discrete seismic fragilities are obtained for each of the ground motions at four distinguished damage states (S, M, E, and C). Fig. 7.19(a) shows the comparison of discrete fragilities for OGS frames with those obtained for BFs for the three PGA levels. Similarly, Fig. 7.19(b) shows the variation in discrete fragilities obtained for OGS frames with FI frames.

It follows from Fig. 7.19(a) that for any PGA level (0.5g, 0.7g, 1.0g), BFs are comparatively less fragile than the OGS frames for slight damage state. Whereas, for higher damage states (M, E, and C), the fragility of the two frames (BF and OGS) does not show a uniform pattern, i.e., for some of the ground motions OGS frames show higher fragility, while BFs show higher fragility for the other ground motions. Similarly, Fig. 7.19(b) shows that for 0.5g PGA, the FI frames are less fragile than OGS frames for any damage state. But with increasing PGA (0.7g and 1.0g), the fragility of FI and OGS frames also do not follow a uniform trend primarily because of failure of the masonry infill walls in the ground storey converting the FI frames into OGS frames. Similar trend of fragility variation was observed for other PGA values as well (0.1g to 1.0g).

Thus, when the TL displacement is considered as an EDP, no definite fragility pattern can be established as observed from the comparison of OGS frames with either BFs or FI frames. Experience from past earthquakes certainly hints towards higher seismic fragility of OGS frames because of their poor performance compared to BFs or FI frames. However, the fragility estimation with TL displacement as an EDP gives a wrong essence of the physical behavior or failure pattern of irregular OGS frames under the effect of seismic input. Some cases show early failure of the BF or FI frames compared to OGS frames, for a given PGA. Whereas, in some other cases, OGS frames fail early compared to the regular frames (either bare or FI frames). In many cases, OGS frames are seen to be less fragile and hence less vulnerable as compared to either BF or FI frames. Such results are contradictory to the past experiences from earthquake, where the OGS buildings are

found to have failed even during minor shaking. Thus, this choice of EDP needs to be revised and modified for irregular frames, such as, OGS frames for fragility estimation.

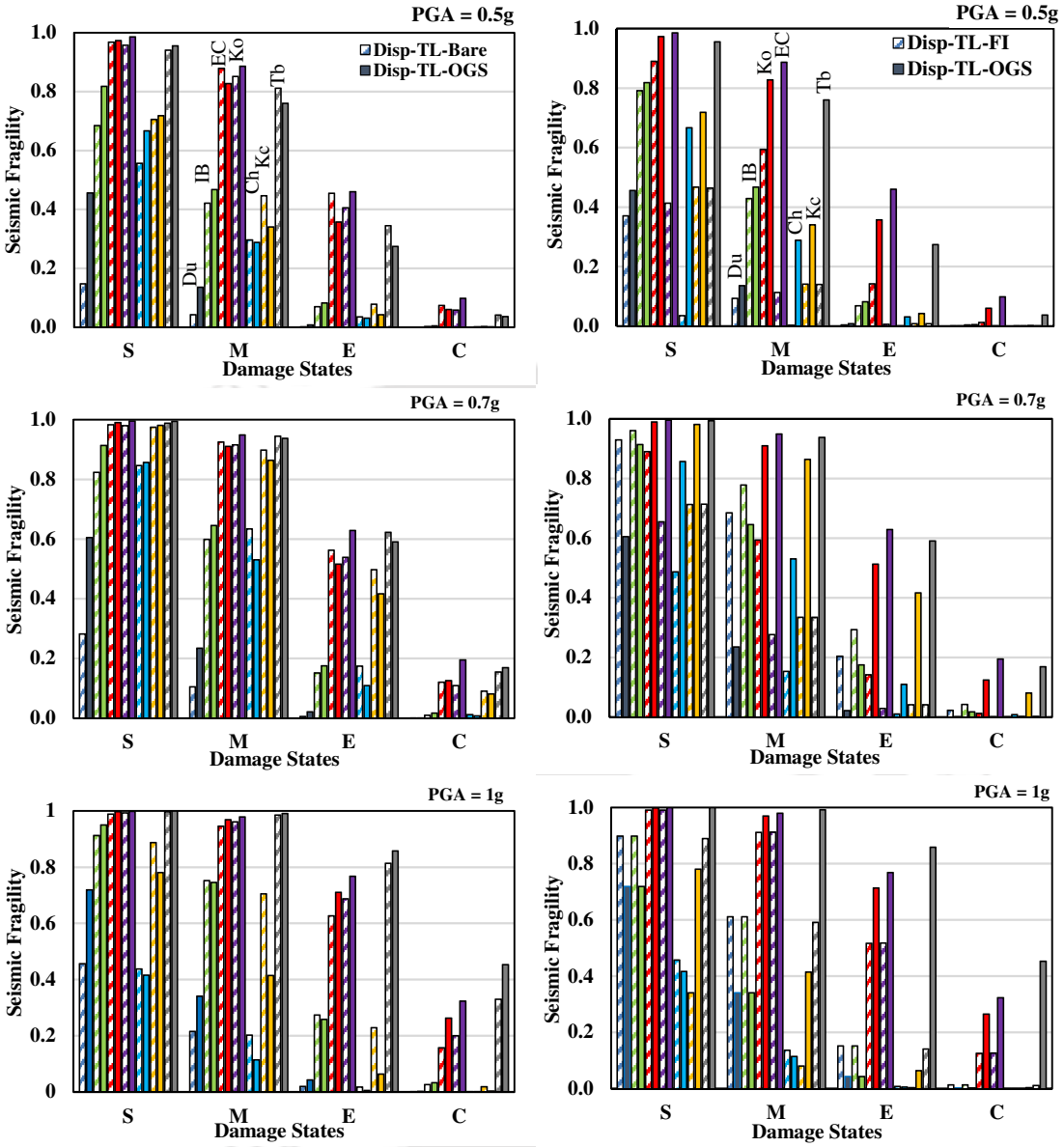

Figure 7.19 Comparison of seismic fragility obtained for three PGA levels considering top level (TL) displacement as EDP: (a) BFs vs OGS frames (b) FI vs OGS frames.

7.5.5.2 Storey Displacement as EDP

An alternative EDP used in the past for seismic fragility assessment is storey-wise lateral displacement corresponding to the peak top level displacement. Seismic fragility with respect to displacement at all the floors corresponding to peak displacement at roof or top level is obtained by considering linear distribution of the threshold displacements along the building height. The average interstorey drift (Δ_{ds}) threshold is multiplied by

the respective height of each floor from the base of the building to obtain the displacement threshold as per HAZUS (2013).

Fig. 7.20(a) and Fig.7.20(b) show comparative discrete fragility for BFs vs OGS frames and FI frames vs OGS frames, respectively, developed considering storey displacement corresponding to peak displacement at roof or top level of the building frames as the EDP. The displacement at the other floors are obtained at the time instant when the displacement at top level is maximum. The figures represent seismic fragility values obtained for El Centro ground motion for different PGA values at all damage states. On observing from top to bottom storey of each building frame, the highest seismic fragility in OGS frames is found to be at the ground storey level. In the other frames (BF and FI), however, the seismic fragility at the ground storey level is not necessarily maximum. Further, the seismic fragility of OGS frames is higher than that of the BF as well as FI frames at all the stories for all the other ground motions at any PGA value.

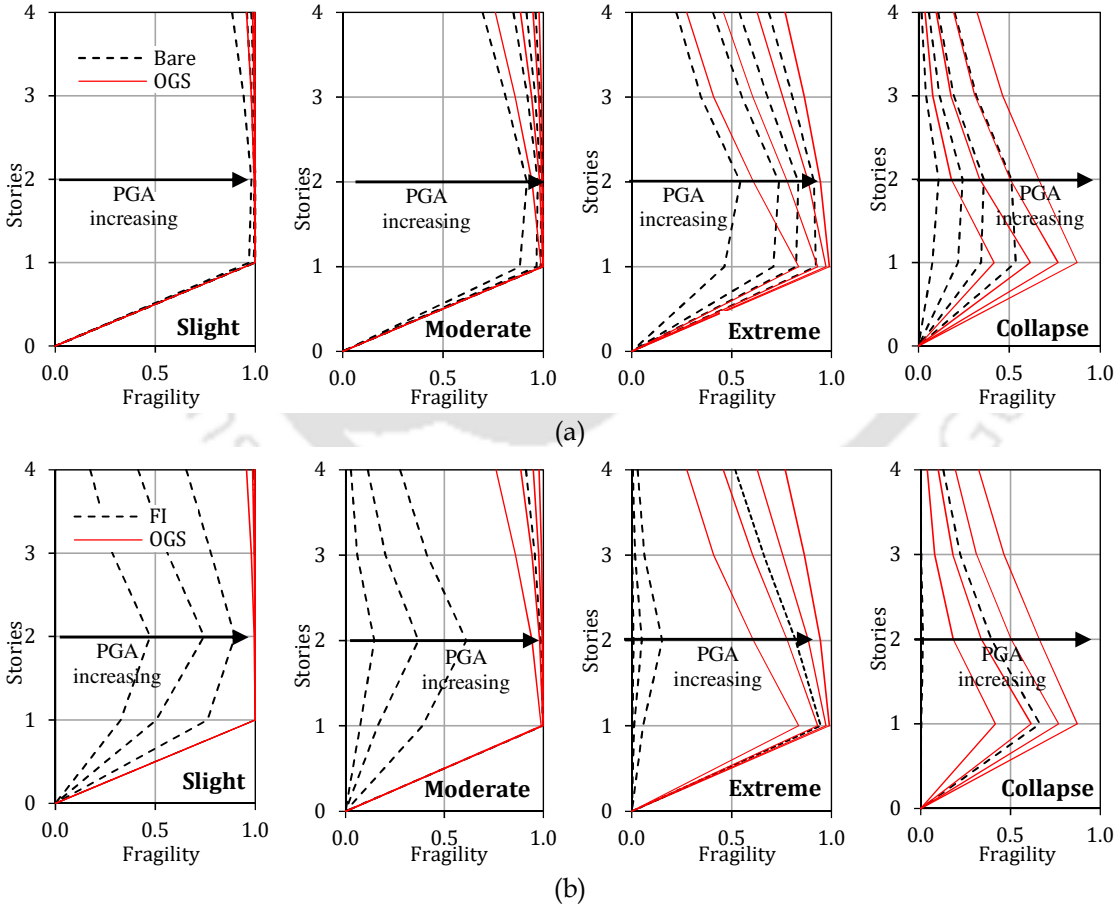

Figure 7.20 Storey-wise fragility profile considering displacement demand at each floor level obtained from time-history analysis for El Centro motion scaled for different PGA values (0.3g, 0.5g, 0.7g, 1g): (a) BF vs OGS frame, (b) FI frame vs OGS frame.

The OGS frames are most fragile at the ground storey as observed during past several earthquakes. The open ground storey being relatively flexible undergoes highest lateral deformation compared to upper stories, and hence damage is concentrated only at the columns of ground storey without any damage to the upper story columns. This type of damage distribution along the height is, however, not reflected in the fragility estimated using the storey displacement at each floor level corresponding to peak TL displacement as an EDP. It is clear from Fig. 7.20(a) that though the fragility of the upper stories of OGS frames is lesser than that of the adjacent lower stories in each frame, the upper storey columns are also fragile and undergo significant damage. Therefore, although this is a common choice for EDP to estimate fragility for regular frames, it does not give the true essence of the fragility for the irregular frames. Similarly, the fragilities of BFs and FI frames are quite high at the second floor level, which also does not reflect the realistic damage observed in such frames during past earthquakes.

7.5.5.3 Interstorey drift (ISD) at Each Floor Level as EDP

Interstorey drift at different floor levels is also considered as EDP in seismic fragility assessment instead of considering storey-wise lateral displacement corresponding to the peak top-level displacement as EDP. Seismic fragility with respect to peak ISD at each storey is obtained by considering the drift thresholds for each damage state as suggested in HAZUS (2013). In such assessment, the seismic fragility of OGS frames is found to be almost nil in the upper stories, whereas, it is maximum at the ground storey level (Fig. 7.21(a)). This resembles the observed damage in OGS buildings in the past, since the OGS buildings fail due to failure of the ground storey columns. In contrast, the fragility of bare frames (Fig. 7.21(b)) is distributed throughout the height of the building, obviously with highest fragility at the ground storey level. The OGS columns are found to be more vulnerable than the ground storey columns of the bare frame, which is expected. Hence, this form of representation of EDP can give us a better estimation and understanding of the seismic fragility in terms of damage incurred in irregular frames, such as an OGS frame. Fragility obtained with respect to ISD as EDP clearly differentiates the failure pattern of the regular and irregular frames. Fig. 7.21(c) shows the discrete fragilities obtained for FI frames for the four damage states at different PGA levels. The FI frame shows higher fragility at the upper floors at each damage state for lower PGA (up to about 0.7g), after which, the ground storey becomes more fragile as seen at a PGA of 1g due to the failure of ground storey infills. For lower intensities of ground motion

(i.e., from 0.1g to 0.7g PGA), it is observed that the FI frame shows fragility pattern similar to the BF, but the magnitude of fragility in FI frame is much less. This suggests that for lower intensity ground motions, the ground storey infills resist most of the lateral load without early failure, and therefore, the FI frames behave like a regular frame, and undergo damage uniformly throughout the height of the building.

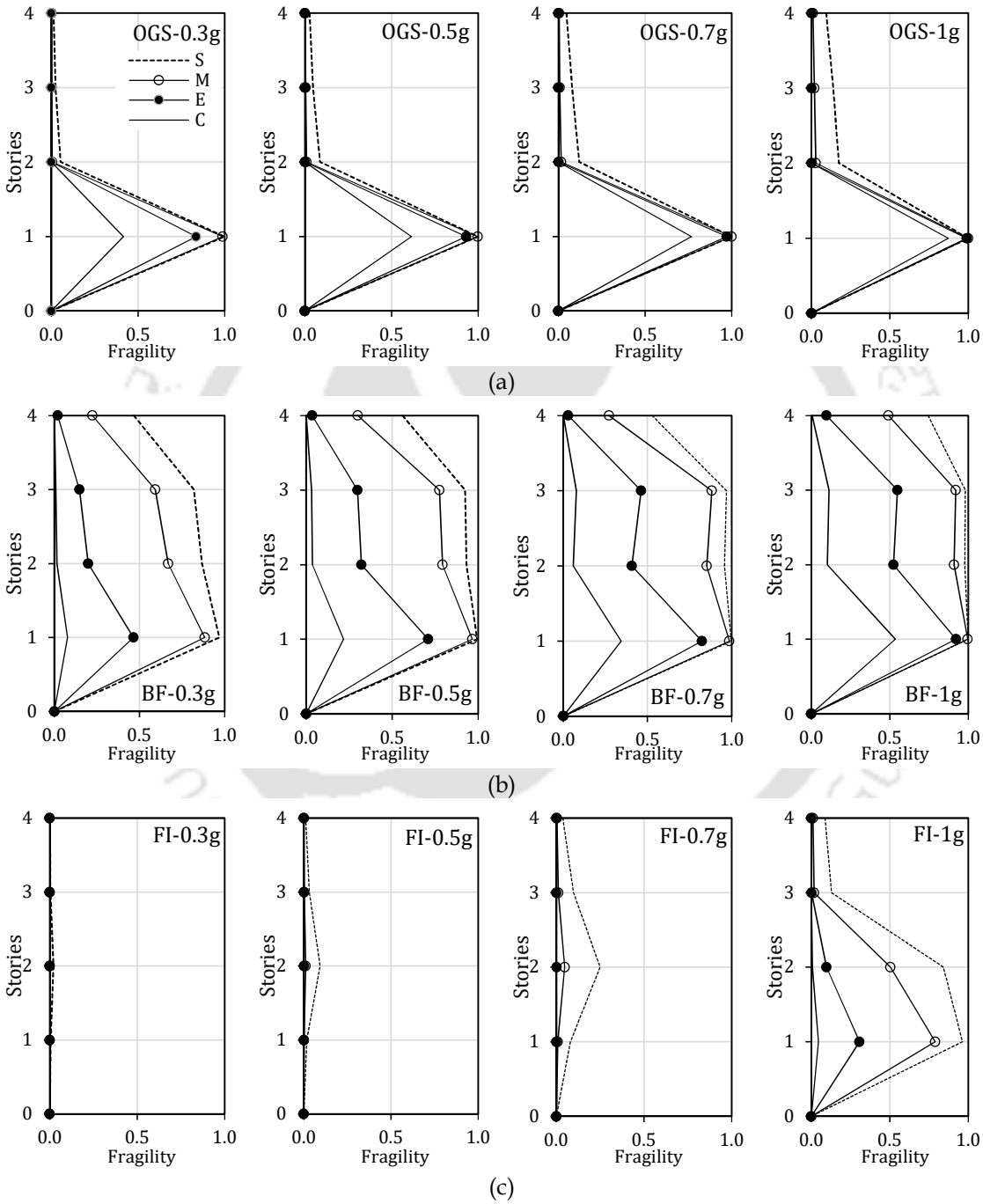

Figure 7.21 Storey-wise fragility profile of the frames considering ISD demand at each floor level obtained from time-history analysis for El Centro motion scaled for different PGA (0.3g, 0.5g, 0.7g, 1g): (a) OGS frames, (b) Bare frames, and (c) FI frames.

As soon as the ground storey infills fail with increasing intensity of ground motion, the ground storey becomes relatively flexible and a soft storey is created in the FI frames at the ground storey, and hence it starts behaving like an OGS frame. Fig. 7.22 further supports these observations, where it can be clearly seen that the seismic fragility of the top storey columns of the OGS frames, obtained using peak ISD at top storey as EDP, is almost nil compared to those of either BFs (Fig. 7.22(a)) or FI frames (Fig. 7.22(b)). Fig. 7.22 is plotted for all ground motions with PGA of only 0.5g, 0.7g, and 1.0g, however, the results are equally applicable to all PGA levels considered in the study.

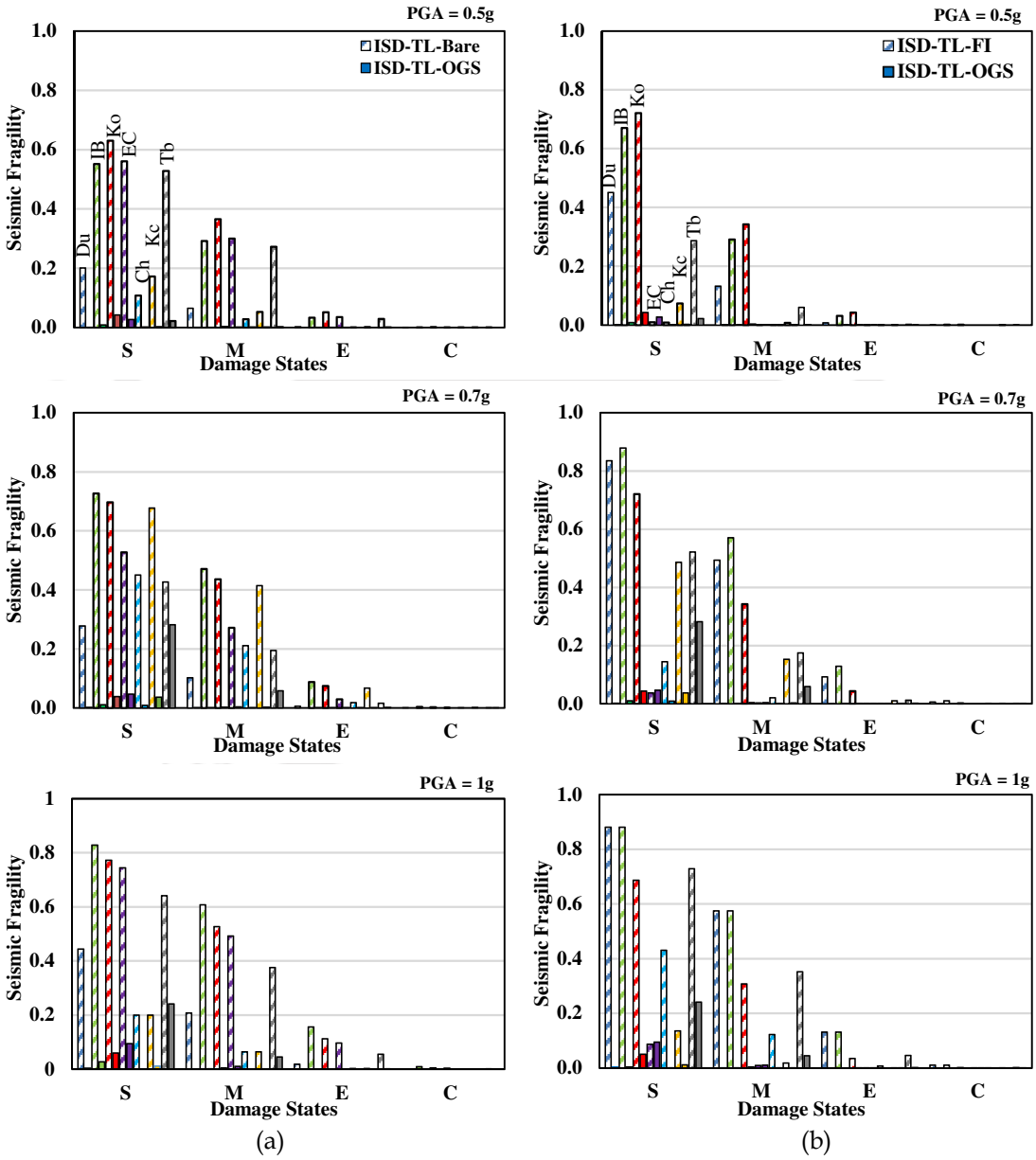

Figure 7.22 Seismic fragility of columns of the top storey obtained for three PGA levels considering top level (TL) ISD as EDP: (a) BFs vs OGS frames (b) FI vs OGS frames.

7.5.5.4 Interstorey Drift at Ground Storey Level as EDP

In the previous sections, it is observed that estimation of realistic fragility requires consideration of relevant component level EDPs, for example, ISD at different floor levels, instead of a global EDP like top level displacement. This is even truer for irregular buildings in which lateral deformation is not distributed along the height. Therefore, in order to get more insight on importance of a component level EDP on seismic vulnerability assessment, another EDP (GL-ISD) is considered in this section. Fig. 7.23 shows the component level fragility obtained for the ground storey columns computed considering the peak ISD demand at GL as EDP for all the ground motions with PGA scaled at 0.5g, 0.7g, and 1.0g. Clearly, seismic fragility of the frames increases with increasing PGA. From the comparison of the discrete fragility values of the frames for different ground motions, the ground storey columns of OGS frames are found to be consistently more fragile than those of either BF (Fig. 7.23(a)) or FI frame (Fig. 7.23(b)) at all damage states. Similar results are obtained for other PGA values as well. Also, it is to be noted that the fragility values considering GL-ISD as EDP are much higher than the fragility obtained using any other EDP. Undoubtedly, using the GL-ISD as EDP provides the realistic seismic fragility of OGS frames.

Summing up, it can be stated that the choice of EDP for fragility estimation should depend on buildings' physical behavior. Seismic fragility of regular RC moment frames, such as the bare frames, can be estimated easily considering top level displacement as the EDP, since in such buildings the displacement at the top or roof is critical and it decreases uniformly as we go down to the bottom stories. Whereas, consideration of EDP for RC moment frames with masonry infill walls depends on the existence of the irregularity (a soft or flexible storey) in the building frame. For the typical case of OGS frame as an example of an irregular frame, it is reported in several earthquakes that the ground storey columns are more vulnerable than the upper storey columns. OGS buildings sustain localized damage mainly at the level where the irregularity lies, i.e., at the ground storey columns, with negligible or no damage in the upper floors. Fragility description at component level helps in locating the members that can be actually damaged during an earthquake and need repairing or retrofitting. Instead of considering global roof or top level displacement, when local demand parameters, such as, ISD at each storey are considered, the localized fragility of the members in consideration can be realistically estimated at a component level.

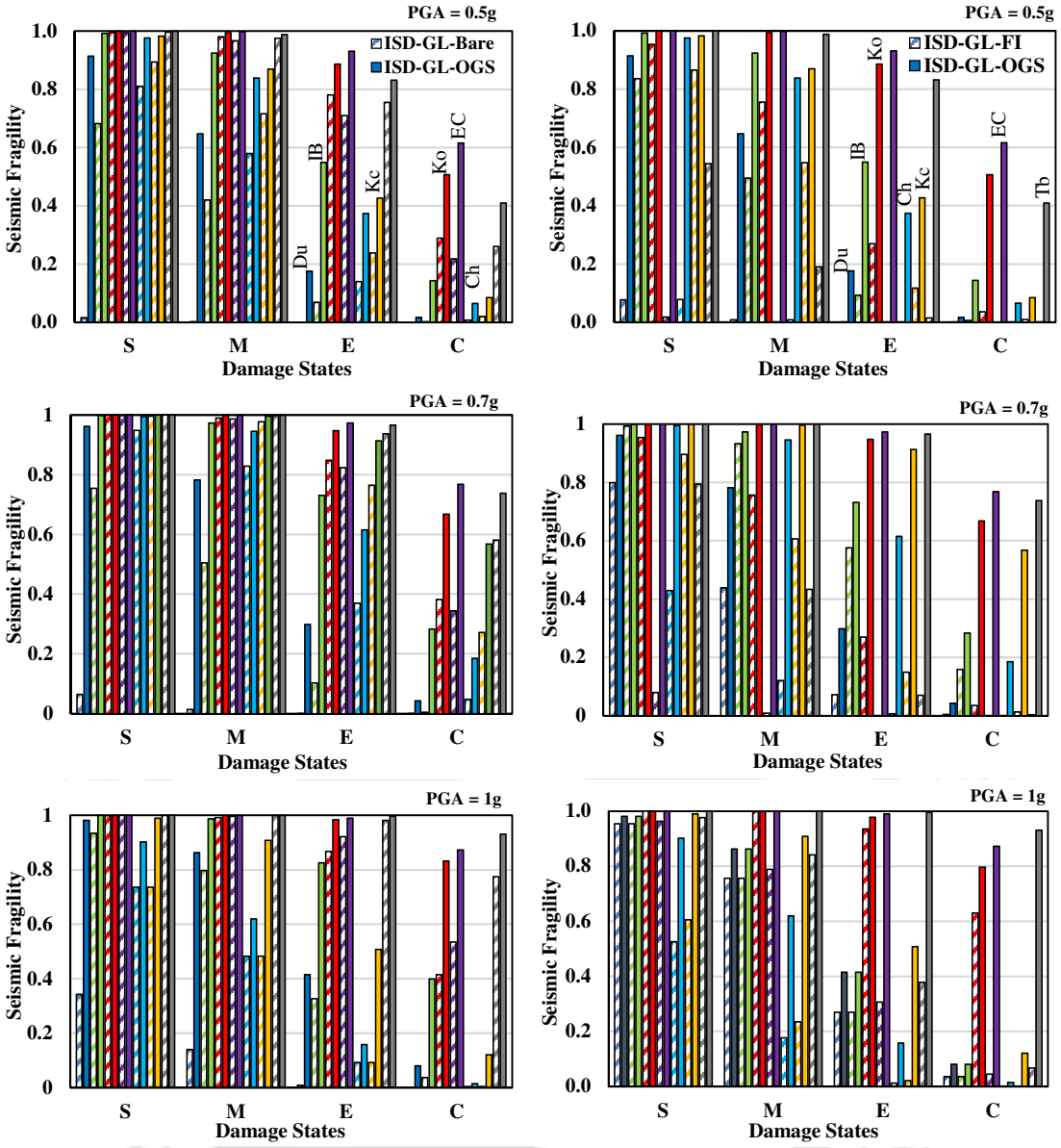

Figure 7.23 Seismic fragility of ground storey columns for three PGA levels considering ground level ISD as EDP: (a) BFs vs OGS frames (b) FI frames vs OGS frames.

Thus, the influence of several structural parameters on seismic fragility of RC building frame typologies emanates from Section 7.5. Broadly, the opening size in infills majorly affects the seismic fragility of fully infilled frames for any combination of number of bay and storey. Furthermore, the impact of change in number of stories is more compared to the change in number of bays on seismic fragility. It is also worthwhile to mention that one should judiciously make use of EDPs based on the requirement. Taking into consideration, the various aspects of seismic fragility estimation, a new way of

representing seismic fragility is presented in the next section that can also potentially assist as a design aid.

7.6 Seismic Fragility Flow Plot (FFP)

7.6.0 General

Damage is a progressive and irreversible process, and discrete quantification of damage (such as those given by Barbat et al. 2008) with the help of strength or displacement parameters brings uncertainty into the picture. In order to represent the damage and associated fragility in a continuous manner, the concept of Fragility Flow Plot (FFP) is introduced (Fig. 7.24), where the damage is represented in a continuous form without any discretization. FFP is a bivariate plot of seismic fragility (shown as radial lines) with respect to displacement threshold ($\overline{S_d}$) and displacement demand (S_d). FFPs relate several parameters (natural period of vibration, number of stories, number of bays, displacement demand, displacement capacity of the building, probability of exceeding a building function limit state) that can be used for rapid quantification of fragility of structures for a given level of uncertainty and seismic hazard. FFP provides more information than that provided by the parameterized fragility discussed in the past (e.g., Mackie and Stojadinovic 2006, Ghosh et al. 2014, Lallemant et al. 2015). In addition to providing a direct relation between seismic capacity and seismic displacement demand for a given uncertainty and probability of exceeding a building's limit state, FFPs combine results of parameterized performance assessment for a given earthquake intensity.

7.6.1 Application of FFP

FFP is useful in multiple ways: for instance, if the displacement threshold is known for a given seismic demand on any structure, the user can graphically quantify probability of exceedance of the displacement threshold value. Thus, FFPs give a continuous flow of probability of exceedance for any damage threshold and for a given spectral displacement demand. Moreover, for a given seismic fragility of some damage level, if the seismic displacement demand is known (Y-axis), then the threshold or the limiting value of displacement capacity that should be available in the structure can be determined from the X-axis. The structure can then be designed for that limiting displacement capacity to avoid damage due to a seismic event that imposes a demand S_d

on the structure. In this way, one can possibly include seismic fragility check in building design procedures.

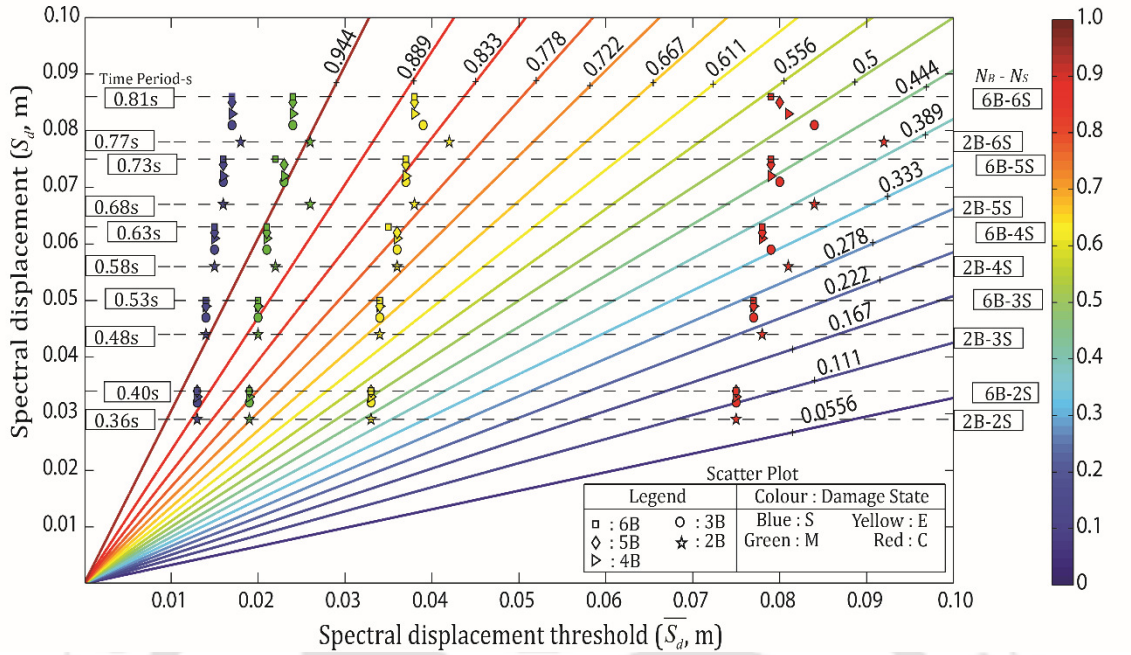

Figure 7.24 Fragility Flow Plot for OGS frame with 0% *Op* for a range of 2B-2S to 6B-6S frames for PGA of 0.36g and $\beta_T = 0.7$.

A few past studies (e.g., Mackie and Stojadinovic 2006, Ghosh et al. 2014, Lallemant et al. 2015) suggested probabilistic seismic demand models in the form of ln(EDP) = a+b×ln(IM), where EDP is any engineering demand parameter, IM is the intensity measure parameter, and a and b are constants to be determined from regression analysis. This model was then related to damage parameters in order to develop damage fragility curves. Unlike FFPs, such models cannot combine all the above mentioned parameters, and therefore, cannot give an overall picture of the seismic fragility of buildings considering a range of parameters. Moreover, results of such linear fits cannot be extrapolated beyond the range of data available, and paucity of experimental or analytical data increases the uncertainty associated with the damage models. Though use of the FFPs is also subject to some limitations and assumptions discussed later, FFPs can be useful for rapid and large-scale fragility estimation of buildings.

Fig. 7.24 shows the proposed FFP for OGS frames without opening (0% *Op*) including a scatter plot of displacement demand and capacity for different damage states (S, M, E, and C) for a PGA of 0.36g and a total uncertainty of 0.7. Here, the radial lines give the conditional probability of exceedance for a given threshold. The plot covers

buildings from low height (2S) to mid-height (6S) having a natural period in the range of 0.36s to 0.81s, thus, including a wide range of buildings constructed over hard soil type as per the Indian seismic code (BIS 2016a). Similar curves can be plotted for different values of *Op*, β_T, and PGA. The dotted horizontal lines delineate the natural time period obtained from modal analysis of the frames analyzed for different combination of N_B and N_S. The color bar represents the value of conditional probability of exceedance of a given damage threshold based on Eq. (7.1). The blue, green, yellow, and red color markers in the scatter represent PPs obtained from nonlinear static analysis of the frames for the four damage states S, M, E, and C, respectively. Each set of scatter plots (for individual damage states) consists of five points showing variation in fragility for frames with different N_B (2B to 6B) keeping N_S constant. Further, such set of scatter plots are shown for five different N_S (2S to 6S).

A wide gap in displacement threshold values is observed in between extreme damage state and complete damage state because of consideration of discrete damage states from literature (Barbat et al. 2008). For instance, the observed d_y and d_u values from the analysis of 3B-4S OGS frame with 0% *Op* are 21 mm and 79 mm, respectively, using which the displacement threshold values for S, M, E, and C are estimated as 15 mm, 21 mm, 36 mm, and 79 mm, respectively (Barbat et al. 2008). These threshold limits are marked as circles (for 3B-4S) in different color fills for the four damage states in the FFP developed for the frame (Fig. 7.24). The relative difference between the displacement threshold values between S-M, M-E, and E-C damage states are 6 mm, 14 mm, and 43 mm, respectively. Clearly, there is a gap of a wide range of displacement thresholds between E and C having no description of damage level, and hence seismic damage as well as fragility cannot be determined for any displacement threshold value between E and C using conventional damage states and fragility curves. FFP provides an advantage of determining the seismic demand as well as fragility for any intermittent displacement threshold values.

For the 3B-4S OGS frame, the spectral displacement demand (58 mm) and the seismic fragility in terms of probability of exceedance for different damage state thresholds (nearly 100% for S, 92% for M, 75% for E, and 34% for C) can be picked out easily using the FFP. It is also interesting to note a slight variation in fragility with changing N_B, keeping N_S constant (as shown by each group of scatter plot). This variation is more pronounced for higher N_S (> 4S). The variation in fragility is, however, quite

noticeable when the N_S is varied keeping N_B constant. Such comparison of bivariate data with other parameters, such as, natural period, N_B, and N_S, is possible only in the FFP. Fig. 7.24 can also be used as a design tool for integrating the seismic fragility with the seismic design process. It is possible to estimate the range of S_d and $\overline{S_d}$ from fragility flow plots for given values of N_B, N_S, and fragility level. Inversely, for an assumed displacement threshold (e.g., design lateral drift in seismic codes) required in a frame to be designed, the number of maximum bays and stories can be estimated from FFP for considered seismic fragility.

Fig. 7.25(a) shows another fragility flow plot for the four damage states in 3 bay – 4 storey OGS frame with central opening size varying from 0% to 90% for a PGA of 0.36g and with total uncertainty β_T of 0.7. The two horizontal dotted lines in the plot represent the outer bounds of the scatter, i.e., for 0% and 90% *Op* for different damage states. As already discussed while developing the conventional fragility curves, seismic fragility decreases uniformly, though marginally, from 0% to 90% *Op* for each damage state. A large gap is again observed between the E and C damage states covering wide displacement threshold values of about 0.045 m to 0.08 m. Seismic fragility for such missing displacement threshold range can be estimated easily using the proposed FFP. While the conventional fragility curves (for e.g., Fig. 7.10 and Fig. 7.11) give information on variation in S_d only, a clear variation in fragility is observed in FFP both with respect to S_d and $\overline{S_d}$ with the change in *Op*. For example, for a 3B-4S OGS frame the variation in fragility for a uniform increase in *Op* from 0% to 90% for the four damage states can be easily obtained using FFP as: 97% to 91% for S, 92% to 79% for M, 76% to 57% for E, and 34% to 19% for C.

Fig. 7.25(b) and Fig. 7.25(c) show the conventional fragility curves for the Extreme damage state in OGS frames with different *Op* considering PGA and S_d as the IM, respectively. Say, a region or zone has a design PGA of 0.36g, then from Fig. 7.25(b) the corresponding seismic fragility for frames with 0%, 50%, and 90% *Op* are obtained approximately as 0.75, 0.65, and 0.55, respectively. This, however, does not give information on S_d, for which Fig. 7.25(c) is additionally required to be used considering the seismic fragility values already obtained. For a given structure and hazard level, complete information on seismic fragility and S_d for different *Op*, N_B, and N_S can be easily obtained for any displacement threshold using FFP.

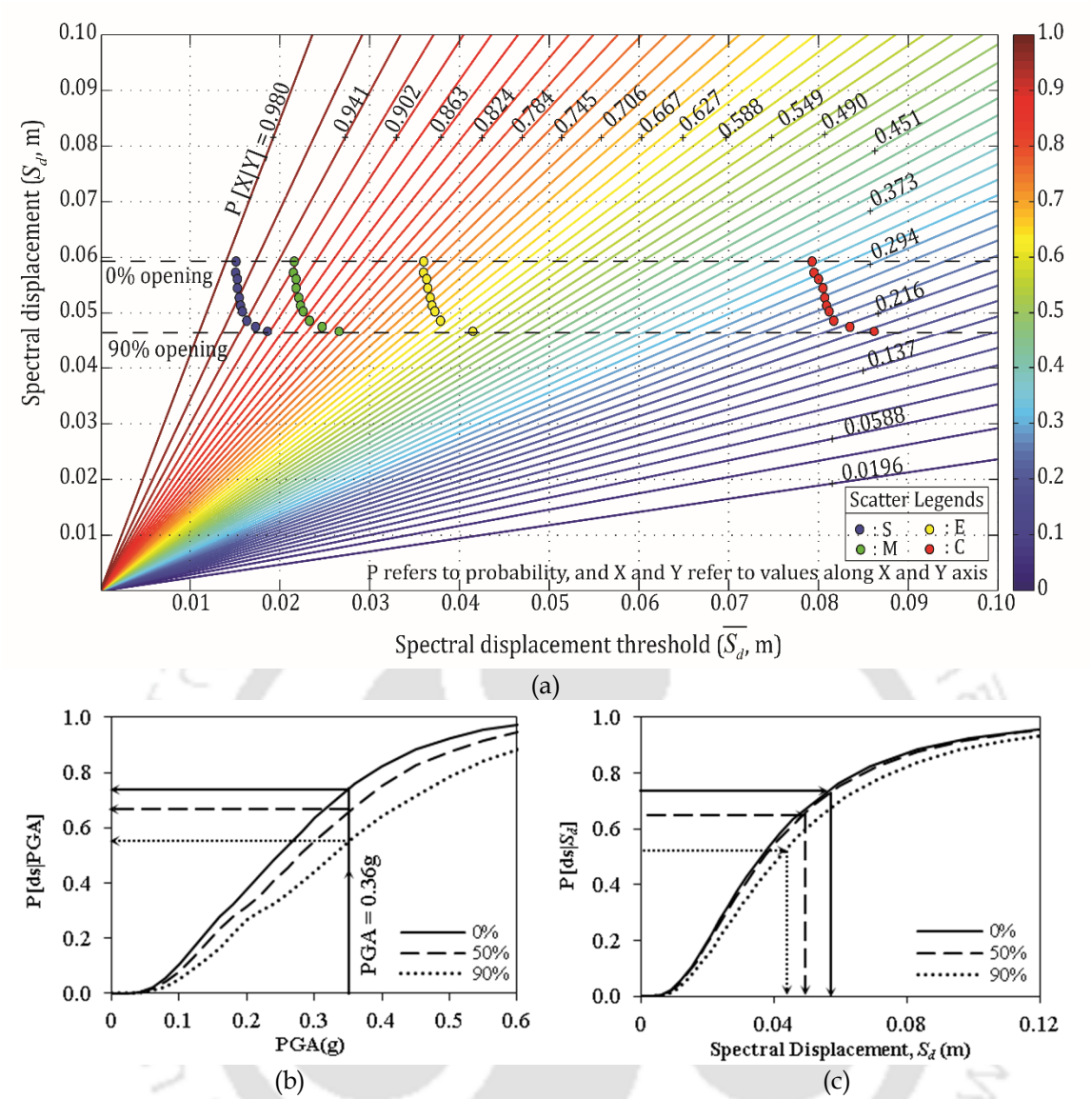

Figure 7.25 Fragility flow plot and conventional fragility curves for 3B-4S OGS frames with varying *Op* for PGA of 0.36g and β_T of 0.7: (a) fragility flow plot, (b) fragility curves with PGA as IM, and (c) fragility curves with S_d as IM.

7.7 Summary and Conclusion

The present chapter addresses a number of issues related to seismic fragility of the three reinforced concrete (RC) frame typologies with particular emphasis on masonry infilled RC frames. The key idea behind the study is to explore the influence of several structural and analytical parameters, such as central opening size, number of bays and number of stories, analysis type, etc. Emphasis is also given on the judicious use of engineering demand parameters (EDPs) and their relative importance on the estimation of seismic fragility of masonry infilled RC frames. Results of both nonlinear static analyses and nonlinear dynamic analyses have been utilized for the estimation of peak

seismic demand on the frames. Necessary assumptions are made regarding different damage states based on past literature. The principal parameters in seismic fragility assessment, i.e., the damage state threshold or the performance limits and the total uncertainty in the engineering demand parameters are appropriately taken care of in the analyses. The salient contributions derived from the seismic fragility analyses of the frames are summarized below:

1. Seismic fragility analyses of all the reinforced concrete frames reveal that variation in the fragility due to uncertainty in the material, geometric, and loading parameters (i.e., epistemic uncertainty) is significant only for higher damage states. On the other hand, ground motion variability (i.e., aleatoric uncertainty) affects the fragility assessment significantly at any damage state.

2. It is shown with the help of fragility curves that various code documented building typologies, such as those in HAZUS, for masonry infilled RC frames are not sufficient to consider the effect of vertical irregularities on fragility assessment.

3. Comparative fragility analyses of the RC frames show two different types of fragility curves that can be used. PGA-based fragility curves that rely more on the characteristics of the ground motion, and displacement-based fragility curves that rely more on building characteristics. Independent observations can be made in the structural response using the two types of curves. For instance, the FI frames appear to have the lowest fragility when perceived with respect to PGA. On the other hand, OGS frames are found to be most vulnerable if fragility curves are plotted with respect to displacement demand.

4. The issue of providing openings in the infill walls of OGS frames to reduce their seismic vulnerability is critically reviewed. It becomes clear that increasing the opening size in infills of OGS frames does not reduce their seismic fragility. On the other hand, providing openings (greater than 50%) is favorable for the FI frames, since their seismic fragility reduces significantly and becomes identical to that of the BF when sufficiently large openings are provided.

5. Seismic fragility is mostly affected by the addition of number of stories than adding number of bays in any type of masonry infilled RC frames. The effect is, however dependent on the parameter (displacement demand or peak ground acceleration) with respect to which seismic fragility of the frames is observed.

6. Seismic fragility analyses using the EDP values obtained from nonlinear static as well as nonlinear dynamic analysis are compared to understand if fragility can be assessed using simplified static analysis results. The static analysis slightly underestimates the fragility when observed with respect to PGA, however, the seismic fragility is overestimated with respect to TL displacement. With respect to PGA, the dynamic analysis seems to provide realistic results as the seismic fragility for OGS frames is found to be highest.

7. Consideration of roof or top level (TL) displacement as EDP (conventional method) does not suffice the contemporary need for seismic analysis and fragility assessment of irregular frames (open ground storey frames). Further, it is also observed that using the conventional EDP (roof displacement or lateral drift at top level) is quite simple and effective for fragility assessment of regular frames.

8. Finally, a new concept of fragility flow plot (FFP) is presented here for a rapid assessment of the seismic fragility of structures based on the conventional assumption of lognormal cumulative distribution function for seismic fragility. FFP is independent of discrete damage states and allows for considering several building parameters together. The assistance of fragility flow plot in seismic fragility based design of structures, given a level of uncertainty, seems to be promising.

❄ ❄ ❄

Chapter 8

SUMMARY AND CONCLUSION

8.0 Overview

A study on the seismic performance and fragility assessment of reinforced concrete buildings infilled with masonry wall panels has been carried out in the present thesis. The study distinctly focusses on open ground storey (OGS) building frames, which are considered as one of the most vulnerable building typologies. Seismic capacity and performance of the RC building frames is determined based on state-of-the-art methods comprising of nonlinear static and nonlinear dynamic methods. Large variation in central opening sizes in masonry infill panels, and in number of bays and number of stories are considered for low-rise and mid-rise RC building frames. Seismic demand is considered in the form of seven real ground motions and their frequency envelop dependent synthetic samples scaled for large number of PGA values. In addition, response spectra of the different ground motions along with code specified response spectra are considered. Results of nonlinear analyses are statistically interpreted in order to analyze the sensitivity and uncertainty related to various engineering demand parameters, and finally to estimate the seismic fragility of the frames. A summary of the conclusions drawn as a result of the work carried out in the present thesis, limitations and recommendations for further research are presented in this chapter.

8.1 Summary

The present study on masonry infilled RC frames is summarized into following parts: (i) Seismic performance assessment, (ii) Effective engineering demand parameter, (iii) Sensitivity of the EDPs to random input variables, (iv) Treatment of uncertainty in

the estimation of EDPs, and (v) Seismic fragility assessment. Observations made in each of the part are briefly reviewed in the following sections.

8.1.1 Seismic Performance Assessment

Performance assessment of the masonry infilled RC frames (OGS and FI) and bare frames (BF) is undertaken by carrying out substantial number of nonlinear static and dynamic analyses. Masonry infilled RC frames with open ground storey are recognized as seismically highly vulnerable due to the soft storey effect. It is a common perception that the soft storey effect is reduced due to the presence of openings in the upper storey infills. This aspect has been investigated in the present study by varying opening sizes in infill panels of OGS and FI frames. Further, in order to cover different sizes of existing low-rise and mid-rise building typologies, the number of bays and stories are also varied. Nonlinear static analysis followed by capacity spectrum approach is applied to obtain the structural demand parameters. Effort is also put in developing a multi-variable linear regression model for rapid seismic performance assessment of RC buildings. Nonlinear dynamic analyses considering seven ground motions and their frequency envelop dependent samples scaled for large number of PGAs are carried out to obtain the peak structural responses from which the IM-EDP relation is established. Based on the comparative assessment, results of nonlinear static and dynamic analysis are related with simple amplification factors.

8.1.2 Engineering Demand Parameters

Choosing relevant and effective engineering demand parameters form an essential part of performance based seismic design of structures and estimation of seismic fragility. Global demand parameters, such as peak roof displacement or maximum drift over the height of the building, are commonly used to estimate seismic fragility. However, in case of buildings with vertical irregularities (e.g., OGS buildings), the global demand parameters may not suffice since the maximum demand in such building is mostly concentrated at the level of irregularity. Nonlinear dynamic analyses of RC frames subjected to a number of ground motions, each scaled for different PGAs, are carried out to estimate the component level drift demands and global drift demands. The effectiveness of component level EDP in predicting the actual damage scenarios in such buildings observed during past earthquakes in comparison to the damage predicted by the global EDP is discussed. The focus of the study is to establish an effective EDP for

irregular building frames. Both global and component level EDPs are verified for the frames. The demand parameters are appreciably dependent on several random input parameters, such as compressive strength of concrete and column dimensions. It is therefore, essential to understand the sensitivity and uncertainty related to these EDPs, which are discussed next.

8.1.3 Sensitivity Analysis of EDPs

The probabilistic modelling framework for performance assessment requires specifying the uncertainties in key input parameters in terms of probability distributions, sampling the distribution of the specified parameters in an iterative fashion, and propagating the effects of uncertainties through the model. The basic purpose of sensitivity analysis is to identify and statistically predict the influence of uncertainty in the input parameters on the response of the considered model. In the present thesis, random samples of the uncertain parameters are used as input parameters in nonlinear dynamic analyses of the RC frames. The sensitivity of the EDPs is discussed using different statistical and graphical methods, such as displacement sensitivity radar charts, response sensitivity bar diagrams, tornado diagrams, Sobol' indices, Lasso regression, and weighted pie charts. The sensitivity of the seismic response of BF, OGS frames, and FI frames is evaluated for different input parameters and compared to shortlist the parameters on which the seismic response of these frames mostly depends. Further, the influence of highly uncertain input variables on uncertainty of seismic response of the frames is evaluated and discussed in the next section.

8.1.4 Treatment of Uncertainty in Fragility

Uncertainty in response of buildings originates from two basic sources – seismic demand (Aleatoric uncertainty) and capacity (Epistemic uncertainty). The influence of these uncertainties on the damage state dependent fragility estimates of the RC frames are investigated. The variation in nonlinear material properties, sectional properties, and loading are taken into consideration for evaluating the epistemic uncertainty. Aleatoric uncertainty stems from the ground motion record-to-record and sample-to-sample variability. The approach used is based on nonlinear dynamic analyses of the representative building frames. Random samples of uncertain input variables are generated based on Latin Hypercube Sampling to estimate the epistemic uncertainty. Several real and synthetic ground motions are considered for determining the aleatoric

uncertainty and its influence on the frame response. RC building categories and associated uncertainties specified in the literature are evaluated for sufficiency to predict damage and failure pattern in the frames. Estimates for both the uncertainties in the frame responses are provided in terms of PGA and median drift thresholds for different damage states. Seismic fragility assessment of the frames for the derived uncertainty values and those available in literature is discussed in the next section.

8.1.5 Seismic Fragility Analysis

Seismic fragility analysis is the key component in seismic vulnerability and risk assessment. In the present thesis, analytical assessment of seismic fragility for the three configurations of the building frames is carried out. Results of both nonlinear static and dynamic analyses have been utilized in the assessment process. Assumptions are made regarding different damage states for which the analyses are carried out based on the past literature. The primary motivation is to explore the influence of several structural and analytical parameters, such as central opening size in masonry walls, number of bays and stories, analysis type, engineering demand parameters and their relative importance, on the estimation of seismic fragility. Comparative fragility assessment is carried out using PGA-based fragility curves that rely more on the characteristics of the ground motion, and displacement-based fragility curves that rely more on building characteristics. A new concept of fragility flow plots (FFP) is developed for rapid fragility assessment of RC frames. FFPs are independent of any discrete damage states, and therefore, provide an advantage of determining the seismic demand as well as fragility for any intermittent displacement threshold values between those defined by the damage states.

8.2 Conclusion

A brief summary of the work carried out in the present thesis is discussed in the previous sections. Results obtained in each of the sections are used in the succeeding section for achieving the objectives set in the study. Major conclusions drawn from the study are summarized below:

- The OGS frames have the highest interstorey drift demand at the ground storey level irrespective of the intensity of ground motion showing that the ground storey columns are highly vulnerable.

- Effect of central opening in masonry infill walls on the lateral load capacity of the OGS frames is negligible, and therefore, presence of openings does not reduce their seismic fragility. On the other hand, the seismic performance and fragility of FI frames is significantly affected by the opening size in infill walls. This observation draws attention towards the importance of providing masonry infill walls in the ground storey of building frames in safely resisting the lateral loads and reducing the seismic vulnerability.

- A change in number of bays or stories influences the global mass and stiffness of the buildings. In case of OGS frames the mass effect is prominent, whereas, the stiffness effect is more pronounced in case of FI frames. Seismic fragility is mostly affected by the addition in number of stories in all the frame configurations.

- The two-level seismic demand model developed by multiple linear regression of several parameters (N_B, N_S, O_p, PGA, T_N) gives good estimate of building frame responses, and can be conveniently used for rapid assessment of seismic displacement demand.

- Dynamic amplification factors (DAF) are developed to relate the peak static response of the frames with the peak dynamic response. Estimation of dynamic response from static response using DAF can reduce the modeling complicacy and computation cost.

- For regular RC frames (e.g., BF), global EDPs can be conveniently used to predict the seismic damage and seismic fragility. However, in case of vertically irregular frames (OGS frames), or even in FI frames that can become irregular after the failure of ground storey infills, a component level EDP is required to be used to predict the realistic damage and seismic fragility.

- Seismic response of BF and OGS frames is most sensitive to the uncertainty in compressive strength of concrete and width of column. The parameters related to infill do not affect the response of the frames in which either the infills are provided in vertically irregular fashion (OGS frames), or not

provided at all (BF). In case of FI frames, uncertainty in width of the diagonal strut and the masonry prism strength plays a vital role in response sensitivity.

- The degree of uncertainty in input parameters does not solely decide their contribution in response sensitivity. For example, ultimate strain at failure in masonry, having relatively higher uncertainty, do not significantly affect the response sensitivity.

- Contribution of aleatoric uncertainty arising from the ground motion variability is indispensable in the estimation of total uncertainty and seismic fragility. The epistemic uncertainties, arising from the uncertainty in material, geometric, and loading parameters, have significant contribution in estimation of total uncertainty at higher seismic intensities only. Similarly, role of epistemic uncertainty is significant in fragility estimation only at higher damage states.

- Unlike BF and FI frames, the uncertainty in seismic response of OGS frames is similar for both global and component level EDPs.

- At high values of uncertainty (greater than 0.7), the seismic fragility obtained assuming the lognormal cumulative distribution function does not alter much with varying uncertainties.

- Uncertainty and seismic fragility analyses show that various documented building typologies, such as those in HAZUS, for masonry infilled RC frames are not sufficient to consider the effect of vertical irregularities, arising due to irregular placement of infills in the frames, on seismic response.

- Comparative fragility analyses show that two types of fragility curves can be used to make independent observations in the structural behavior: PGA-based fragility curves that rely more on the characteristics of the ground motion, and displacement-based fragility curves that depend more on building characteristics.

- A new concept of fragility flow plot (FFP) is presented that is independent of discrete damage states and allows for consideration of several parameters together for a detailed and comparative fragility assessment. FFPs can prove to be very useful in fragility-based seismic design of structures.

8.3 Limitations of the Study

The results presented in the thesis are subjected to following limitations, though the conclusions derived based on the results remain unaffected.

- The study is applicable to low and mid-rise RC frames with maximum six bays and six stories with and without masonry infill walls.
- Columns are assumed to be fixed at their bases without accounting for soil structure interaction.
- Results are not applicable to buildings with dominating torsional mode response since buildings vibrating primarily in translational mode shapes are considered in the analysis.
- The frames are considered to be of structural behavioral type "C" as per ATC 40; this type represents poor hysteretic behavior with a substantial reduction of loop area (severely pinched).
- Shear-flexure interaction is not considered in the RC members of the frames.

8.4 Recommendations for Future Research

The study can be further extended by eliminating some of the above mentioned limitations as well as by studying the following details:

- Influence of change in location of openings in the masonry infill walls on seismic fragility can be studied.
- The present study can be extended to OGS buildings with basement and shear walls.

- Seismic vulnerability and risk assessment can be carried out by integrating seismic hazard, fragility, repair cost, and population density models.
- Application of fragility flow plots can be further studied in development of fragility based seismic design of structures.

❋ ❋ ❋

REFERENCES

Alembagheri, M., and Seyedkazemi, M. (2015). "Seismic performance sensitivity and uncertainty analysis of gravity dams." *Earthquake Engineering and Structural Dynamics*, Vol. 44(1), pp. 41-58.

Al-Nimry, H., Resheidat, M., and Qeran, S. (2015). "Rapid assessment for seismic vulnerability of low and medium rise infilled RC frame buildings." *Earthquake Engineering and Engineering Vibration*, Vol. 14(2), pp. 275-293.

ASCE (2013). "Seismic evaluation and retrofit of existing buildings." ASCE/SEI 41-13, Reston, VA.

Aslani, H., Cabrera, C., and Rahnama, M. (2012). "Analysis of the sources of uncertainty for portfolio-level earthquake loss estimation." *Earthquake Engineering and Structural Dynamics*, Vol. 41(11), pp. 1549-1568.

Asteris, P.G., Chronopoulos, M.P., Chrysostomou, C.Z., Varum, H., Plevris, V., Kyriakides, N., and Silva, V. (2014). "Seismic vulnerability assessment of historical masonry structural systems". *Engineering Structures*, 62-63, pp: 118–134.

ATC 13 (1985). "Earthquake Damage Evaluation Data for California, Report ATC 13", *Applied Technology Council*, Redwood City, CA.

ATC 40 (1996). "Seismic Evaluation and Retrofit of Concrete Buildings." *Applied Technology Council*, Volumes 1 and 2, Redwood City, CA, USA.

ATC 58 (2004). ATC 58 project task report: Engineering demand parameters for structural framing systems. Prepared for the Applied Technology Council by the ATC 58 Structural Performance Products Team. USA.

Bai, J. W., Gardoni, P., and Hueste, M. B. D. (2011). "Story-specific demand models and seismic fragility estimates for multi-story buildings." *Structural Safety*, Vol. 33(1), pp. 96-107.

Baker, J. W. (2015) "Efficient analytical fragility function fitting using dynamic structural analysis." *Earthquake Spectra*, EERI, Vol. 31(1), pp. 579-599.

Baker, J. W., and Cornell, C. A. (2008). "Uncertainty propagation in probabilistic seismic loss estimation." *Structural Safety*, Vol. 30(3), pp. 236-252.

Barbat, A.H., Pujades, L.G., and Lantada, N. (2008). "Seismic damage evaluation in urban areas using the capacity spectrum method: Application to Barcelona". *Soil Dynamics and Earthquake Engineering*, Vol. 28(10), pp. 851–865.

Basha, S.H., and Kaushik, H.B. (2015). "Evaluation of Non-linear Material Properties of Fly Ash Brick Masonry under Compression and Shear", *Journal of Materials in Civil Engineering*, ASCE, Vol. 27(8): 04014227.

BIS (2016a). "IS 1893 (Part 1): 2002, Criteria for Earthquake Resistant Design of Structures: Part 1 General Provisions and Buildings." 5th Revision, *Bureau of Indian Standards*, New Delhi, India.

BIS (2016b). "IS 13920, Ductile Detailing of Reinforced Concrete Structures Subjected to Seismic Forces–Code of Practice." *Bureau of Indian Standards*, New Delhi, India.

BIS (2000). "IS 456, Indian standard code of practice for plain and reinforced concrete", 4th Revision, *Bureau of Indian Standards*, New Delhi, India.

Borzi, B., Pinho, R., and Crowley, H. (2008). "Simplified pushover-based vulnerability analysis for large-scale assessment of RC buildings". *Engineering Structures*, Vol. 30, Issue 3, pp: 804–820.

Brzev, S., Scawthorn, C., Charleson, A.W., Allen, L., Greene, M., Jaiswal, K., and Silva, V. (2013), "GEM Building Taxonomy (Version 2.0), *GEM Foundation*, Pavia, Italy, doi: 10.13117/GEM.EXP-MOD.TR2013.02.

Calvi, G.M., Pinho, R., Magenes, G., Bommer, J.J., and Crowley, H. (2006). "Development of Seismic Vulnerability Assessment Methodologies Over The Past 30 Years". *ISET Journal of Earthquake Technology*, Vol. 43(472), pp. 75–104.

Cardona, O. D., and Yamin, L. E. (1997). "Seismic microzonation and estimation of earthquake loss scenarios: integrated risk mitigation project of Bogotá, Colombia". *Earthquake Spectra*, EERI, Vol. 13(4), pp. 795-814.

Cavaleri, L., and Di Trapani, F. (2014). "Cyclic response of masonry infilled RC frames: Experimental results and simplified modeling." *Soil Dynamics and Earthquake Engineering*, Vol. 65, pp. 224-242.

Celarec, D., and Dolšek, M. (2013). "The impact of modelling uncertainties on the seismic performance assessment of reinforced concrete frame buildings." *Engineering Structures*, Vol. 52, pp. 340-354.

Celarec, D., Ricci, P., and Dolšek, M. (2012). "The sensitivity of seismic response parameters to the uncertain modelling variables of masonry-infilled reinforced concrete frames." *Engineering Structures*, Vol. 35, pp. 165-177.

Celik, O. C., and Ellingwood, B. R. (2010). "Seismic fragilities for non-ductile reinforced concrete frames–Role of aleatoric and epistemic uncertainties." *Structural Safety*, Vol. 32(1), pp. 1-12.

Chintanapakdee, C. and Chopra, A.K. (2004). "Seismic response of vertically irregular frames: response history and modal pushover analyses." *Journal of Structural Engineering*, ASCE, Vol. 130 (8), pp. 1177-1185.

Chopra, A. K., and Goel, R. K. (1999a). "Capacity-demand-diagram methods based on inelastic design spectrum". *Earthquake Spectra*, EERI, Vol. 15(4), pp. 637-656.

Chopra, A. K. and Goel, R. K., (1999b). "A report on Capacity-Demand-Diagram Methods for Estimating Seismic Deformation of Inelastic Structures: SDF Systems". *Pacific Earthquake Engineering Research Center*, University of California, Berkeley.

Chopra, A. K., and Goel, R. K. (2000) "Evaluation of NSP to estimate seismic deformation: SDF systems." *Journal of Structural Engineering*, ASCE, Vol. 126(4), pp. 482-490.

Choudhury, T., and Kaushik, H.B. (2018b) "Component Level Fragility Estimation for Vertically Irregular Reinforced Concrete Frames." *Journal of Earthquake Engineering*, Taylor & Francis, In Press. DOI: 10.1080/13632469.2018.1453413.

Choudhury, T., and Kaushik, H.B. (2018c) "Seismic response sensitivity to uncertain variables in RC frames with infill walls" under review in *Journal of Structural Engineering*, ASCE.

Choudhury, T., and Kaushik, H.B. (2018a) "Seismic Fragility of Open Ground Storey RC Frames with Wall Openings for Vulnerability Assessment." *Engineering Structures*, Vol 155, Elsevier, pp. 345-357. DOI: 10.1016/j.engstruct.2017.11.023.

Cornell, C. A, Jalayer, F., Hamburger, R. O., and Foutch, D. A. (2002) "Probabilistic basis for 2000 SAC federal emergency management agency steel moment frame guidelines." *Journal of Structural Engineering*, ASCE, Vol. 128(4), pp. 526-533.

Crozet, V., Politopoulos, I., Yang, M., Martinez, J. M., and Erlicher, S. (2017) "Sensitivity analysis of pounding between adjacent structures." *Earthquake Engineering and Structural Dynamics*, pp. 1-17, DOI: 10.1002/eqe.2949.

CSI (2015). "Structural Analysis Program (SAP2000) – Advanced, static and dynamic finite element analysis of structures," *Computers and Structures Inc.*, Berkeley, USA.

D' Ayala, D., Meslem, A., Vamvatsikos, D., Porter, K., Rossetto, T., and Silva, V. (2015). "Guidelines for analytical vulnerability assessment of low/mid-rise buildings, Vulnerability Global Component Project. DOI: 10.13117/GEM.VULN-MOD.TR2014.12

Davis P.R., Padhy, T.K., Menon, D., and Prasad, A.M. (2010). "Seismic fragility of open ground story buildings in India." *Proceedings of 9th U.S. National and 10th Canadian Conference on Earthquake Engineering*, Toronto, Ontario, Canada.

Dolce, M., Kappos, A. J., Masi, A., Penelis, G., and Vona, M. (2006) "Vulnerability assessment and earthquake damage scenarios of the building stock of Potenza (Southern Italy) using Italian and Greek methodologies." *Engineering Structures*, Vol. 28(3), pp. 357-371.

Dolšek, M, and Fajfar, P. (2001) "Soft storey effects in uniformly infilled reinforced concrete frames." *Journal of Earthquake Engineering*, Vol. 5 (1), pp. 1-12.

Dolšek, M. (2009). "Incremental dynamic analysis with consideration of modeling uncertainties." *Earthquake Engineering and Structural Dynamics*, Vol. 38(6), pp. 805-825.

Dolšek, M., and Fajfar, P. (2005). "Simplified non-linear seismic analysis of infilled reinforced concrete frames." *Earthquake Engineering and Structural Dynamics*, Vol. 34(1), pp. 49-66.

Dutta, S.C., Mukhopadhyay, P.S., Saha, R., and Nayak, S. (2015). "2011 Sikkim earthquake at Eastern Himalayas: Lessons learnt from performance of structures." *Soil Dynamics and Earthquake Engineering*, Vol. 75, pp. 121-129.

Dymiotis, C., Kappos, A. J., and Chryssanthopoulos, M. K. (1999). "Seismic reliability of RC frames with uncertain drift and member capacity." *Journal of Structural Engineering*, ASCE, Vol. 125(9), pp. 1038-1047.

Dymiotis, C., Kappos, A. J., and Chryssanthopoulos, M. K. (2001). "Seismic reliability of masonry-infilled RC frames." *Journal of Structural Engineering*, ASCE, 127(3), pp. 296-305.

Eldin, M. N., and Kim, J. (2016). "Sensitivity analysis on seismic life-cycle cost of a fixed-steel offshore platform structure." *Ocean Engineering*, Vol. 121, pp. 323-340.

Eleftheriadou, A.K. and Karabinis, A.I. (2011). "Development of damage probability matrices based on Greek earthquake damage data". *Earthquake Engineering and Engineering Vibration*, Vol. 10(1), pp. 129–141.

Ellingwood, B. R., Celik, O. C., & Kinali, K. (2007). "Fragility assessment of building structural systems in Mid-America." *Earthquake Engineering & Structural Dynamics*, 36(13), pp. 1935-1952.

Fajfar P. (2000). "A Nonlinear Analysis Method for Performance Based Seismic Design". *Earthquake Spectra*, EERI, Vol. 16(3), pp. 573–592.

Fajfar, P, and Gašperšič, P. (1996). "The N2 method for the seismic damage analysis of RC buildings." *Earthquake Engineering and Structural Dynamics*, Vol. 25(1), pp. 31-46.

Fajfar, P., and Dolšek, M. (2012). "A practice-oriented estimation of the failure probability of building structures." *Earthquake Engineering and Structural Dynamics*, Vol. 41(3), pp. 531-547.

FEMA 273 (1997). "NEHRP Guidelines For The Seismic Rehabilitation Of Buildings." *Federal Emergency Management Agency*, Washington, D.C.

FEMA 350 (2000). "SAC Joint Venture and Guidelines Development Committee, Recommended seismic design criteria for new steel moment-frame buildings." *Federal Emergency Management Agency*.

FEMA 356 (2000). "Prestandard and commentary for the seismic rehabilitation of buildings". Federal Emergency Management Agency, *Building Seismic Safety Council (US), and Applied Technology Council*, Washington, D.C.

FEMA 440. (2005). "Improvement of nonlinear static seismic analysis procedures." *Applied Technology Council* (ATC). Report No. FEMA-440, Washington, D.C.

FEMA P-154 (2015) "Rapid visual screening of buildings for potential seismic hazards: a handbook." *Federal Emergency Management Agency* Report.

FEMA P-58. (2012). "Next-Generation methodology for seismic performance assessment of buildings." *Prepared by the Applied Technology Council (ATC) for the Federal Emergency Management Agency (FEMA)*, Report No. FEMA P-58, Washington, D.C.

FEMA P-695. (2009). "Quantification of Building Seismic Performance Factors." *Prepared by Applied Technology Council (ATC) for the Federal Emergency Management Agency (FEMA)*, Washington, D.C.

FEMA 154 (2002). "Rapid Visual Screening of Buildings for Potential Seismic Hazards: A Handbook". FEMA-154, *Federal Emergency Management Agency*. Washington, D.C.

Freddi, F., Padgett, J. E., and Dall'Asta, A. (2017). "Probabilistic seismic demand modeling of local level response parameters of an RC frame." *Bulletin of Earthquake Engineering*, Vol. 15(1), pp. 1-23.

Freeman, S. A. (1998). "The Capacity Spectrum Method as a Tool for Seismic Design". *Proceedings of the 11th European Conference on Earthquake Engineering*, pp. 6–11.

Ghosh, J., Rokneddin, K., Padgett, J. E., and Dueñas-Osorio, L. (2014). "Seismic reliability assessment of aging Highway Bridge networks with field instrumentation data and correlated failures: methodology." *Earthquake Spectra*, EERI, Vol. 30(2), pp. 795-817.

Gokkaya, B. U., Baker, J. W., and Deierlein, G. G. (2016). "Quantifying the impacts of modeling uncertainties on the seismic drift demands and collapse risk of buildings with implications on seismic design checks." *Earthquake Engineering and Structural Dynamics*, Vol. 45(10), pp. 1661-1683.

Grünthal (1998) "European Macroseismic Scale 1998". EMS 98, *European Seismological Commission*. Luxembourg, Joseph Beffort, Helfent-Bertrange.

Gueguen, P. (2013). "Seismic vulnerability of structures". *ISTE Ltd. and John Wiley & Sons*, Inc, New Jersey.

Hahn, G. T., Bhargava, V., and Chen, Q. (1990). "The cyclic stress-strain properties, hysteresis loop shape, and kinematic hardening of two high-strength bearing steels." *Metallurgical Transactions*, Vol. 21(2), pp. 653-665.

Haldar, P and Singh, Y. (2009). "Seismic performance and vulnerability of Indian code designed RC frame buildings." ISET Journal of Earthquake Technology, Vol. 46(1), pp. 29-45.

HAZUS (2013). "Multi-hazard loss estimation methodology: Earthquake model, Technical Manual, Department of Homeland Security, Developed by *Federal Emergency Management Agency (FEMA)*, Washington, DC. (https://www.fema.gov/media-library/assets/documents/24609 accessed on 05 February 2018).

Ibarra, L., and Krawinkler, H. (2011). "Variance of collapse capacity of SDOF systems under earthquake excitations." *Earthquake Engineering and Structural Dynamics*, Vol. 40(12), pp. 1299-1314.

Jain, S. K., Mitra, K., Kumar, M., and Shah, M. (2010). "A proposed rapid visual screening procedure for seismic evaluation of RC-frame buildings in India." *Earthquake Spectra*, EERI, Vol. *26*(3), pp. 709-729.

Jaiswal, K., Wald, D., and Porter, K. (2010). "A Global Building Inventory for Earthquake Loss Estimation and Risk Management". *Earthquake Spectra*, EERI, Vol. 26(3), pp. 731–748.

Jalayer, F., and Cornell, C. A. (2003). "A technical framework for probability-based demand and capacity factor design (DCFD) seismic formats." Report No. 08 to the PEER Center, Department of Civil and Environmental Engineering, Stanford University, Stanford, CA 2003.

Jalayer, F., De Risi, R., Manfredi, G. (2015). "Bayesian Cloud Analysis: efficient structural fragility assessment using linear regression." *Bulletin of Earthquake Engineering*, Vol. 13(4), pp. 1183-1203.

Jalayer, F., Cornell, C. A. (2009). "Alternative non-linear demand estimation methods for probability-based seismic assessments." *Earthquake Engineering and Structural Dynamics*, Vol. 38(8), pp. 951-972.

Jalayer, F., Elefante, L., Iervolino, I., and Manfredi, G. (2011). "Knowledge-based performance assessment of existing RC buildings." *Journal of Earthquake Engineering*, Vol. 15(3), pp. 362–389.

Jalayer, F., Franchin, P., Pinto, P. E. (2007). "A scalar decision variable for seismic reliability analysis of RC frames." *Earthquake Engineering and Structural Dynamics*, Vol. 36(13, pp. 2050–2079.

Jalayer, F. (2003). "Direct probabilistic seismic analysis: Implementing non-linear dynamic assessments." Doctoral dissertation, Stanford University, Stanford, California, USA.

James, G., Witten, D., Hastie, T., and Tibshirani, R. (2013). "An introduction to statistical learning." Vol. 112, New York: Springer.

Kappos, A. J., Panagopoulos, G., Panagiotopoulos, C., and Penelis, G. (2006). "A hybrid method for the vulnerability assessment of R/C and URM buildings". *Bulletin of Earthquake Engineering*, Vol. 4(4), pp. 391-413.

Kaushik, H. B., and Choudhury, T. (2015). "Vulnerability analysis of buildings for seismic risk assessment: A review." The Bridge and Structural Engineer, The Journal of Indian National Group (ING) of International Association for Bridge and Structural Engineering (IABSE), Vol. 45(1), pp. 63-76.

Kaushik, H. B., and Dasgupta, K. (2013), "Assessment of Seismic Vulnerability of Structures in Sikkim, India, based on Damage Observation during Two Recent Earthquakes", *Journal of Performance of Constructed Facilities*, ASCE, Vol. 27(6), pp. 697-720.

Kaushik, H. B., and Jain, S. K. (2007), "Impact of great December 26, 2004 Sumatra earthquake and tsunami on structures in Port Blair", *Journal of Performance of Constructed Facilities*, ASCE, Vol. 21(2), pp. 128-142.

Kaushik, H. B., Dasgupta, K., Sahoo, D. R., and Kharel, G. (2006), "Performance of structures during the Sikkim earthquake of 14 February 2006", *Current Science*, Vol. 91(4), Indian Academy of Sciences, Bangalore, India, pp. 449-455.

Kaushik, H. B., Rai, D. C., and Jain, S. K. (2007), "Stress-strain characteristics of clay brick masonry under uniaxial compression", *Journal of Materials in Civil Engineering*, ASCE, Vol. 19(9), pp. 728-739.

Kaushik, H. B., Rai, D. C., and Jain, S. K. (2009). "Effectiveness of some strengthening options for masonry-infilled RC frames with open first storey." *Journal of Structural Engineering*, ASCE, Vol. 135(8), pp. 925-937.

Kazantzi, A. K., and Vamvatsikos, D. (2015). "Intensity measure selection for vulnerability studies of building classes." *Earthquake Engineering and Structural Dynamics*, Vol. 44(15), pp. 2677-2694.

Kennedy, R. P., Cornell, C. A., Campbell, R. D., Kaplan, S., and Perla, H. F. "Probabilistic seismic safety study of an existing nuclear power plant." *Nuclear Engineering and Design,* Vol. 59(2), pp. 315-338.

Kim, J., and Han, S. (2013). "Sensitivity analysis for seismic response of reinforced concrete staggered wall structures." *Magazine of Concrete Research*, ICE, Vol. 65(22), pp. 1348-1359.

Kim, J., Park, J. H., and Lee, T. H. (2011). "Sensitivity analysis of steel buildings subjected to column loss." *Engineering Structures*, Vol. 33(2), pp. 421-432.

Kiureghian, A. D., and Ditlevsen, O. (2009). "Aleatory or epistemic? Does it matter?" *Structural Safety*, Vol. 31(2), pp. 105-112.

Koliopoulos, P. K., Margaris, B. N., and Klimis, N. S. (1998). "Duration and energy characteristics of Greek strong motion records." *Journal of Earthquake Engineering*, Vol. 2(3), pp. 391-417.

Kosič, M., Fajfar, P., and Dolšek, M. (2014). "Approximate seismic risk assessment of building structures with explicit consideration of uncertainties." *Earthquake Engineering and Structural Dynamics*, Vol. 43(10), pp. 1483-1502.

Kwon, O. S., and Elnashai, A. (2006). "The effect of material and ground motion uncertainty on the seismic vulnerability curves of RC structure". *Engineering Structures*, Vol. 28(2), pp. 289-303.

Lagomarsino, S. and Giovinazzi, S. (2006). "Macroseismic and mechanical models for the vulnerability and damage assessment of current buildings". *Bulletin of Earthquake Engineering*, Vol 4(4), pp. 415–443.

Lallemant, D., Kiremidjian, A., and Burton, A. (2015) "Statistical procedures for developing earthquake damage fragility curves", *Earthquake Engineering and Structural Dynamics*, Vol. 44(9), pp. 1373–1389.

Lee, T. H., and Mosalam, K. M. (2005). "Seismic demand sensitivity of reinforced concrete shear-wall building using FOSM method." *Earthquake Engineering and Structural Dynamics*, Vol. 34(14), pp. 1719-1736.

Liel, A. B., Haselton, C. B., Deierlein, G. G., and Baker, J. W. (2009). "Incorporating modeling uncertainties in the assessment of seismic collapse risk of buildings." *Structural Safety*, Elsevier, Vol. 31(2), pp. 197-211.

Liu, X. X., Wu, Z. Y., and Liang, F. (2016). "Multidimensional performance limit state for probabilistic seismic demand analysis." *Bulletin of Earthquake Engineering*, Vol. 14(12), pp. 3389-3408.

Mackie, K. R., and Stojadinović, B. (2006). "Post-earthquake functionality of highway overpass bridges." *Earthquake Engineering and Structural Dynamics*, Vol. 35(1), pp. 77-93.

Mander, J. B., Priestley, M. J., and Park, R. (1988). "Theoretical stress-strain model for confined concrete." *Journal of Structural Engineering,* ASCE, Vol. 114(8), pp. 1804-1826.

Mazza, F., and Vulcano, A. (2010). "Nonlinear dynamic response of RC framed structures subjected to near-fault ground motions." *Bulletin of Earthquake Engineering*, Vol. 8(6), pp. 1331-1350.

McKay, M. D., Beckman, R. J., and Conover, W. J. (1979). "Comparison of three methods for selecting values of input variables in the analysis of output from a computer code." *Technometrics*, Vol. *21*(2), pp. 239-245.

Medvedev, S. V., and Sponheuer, W. (1969). "Scale of seismic intensity." *Proceedings of 4th World Conference of Earthquake Engineering*, Santiago, Chile, pp. 143-153.

Mehanny, S. S. F., and Ayoub, A. S. (2008). "Variability in inelastic displacement demands: Uncertainty in system parameters versus randomness in ground records." *Engineering Structures*, Vol. 30(4), pp. 1002-1013.

Moghaddam, H.A., and Dowling, P.J. (1987). "ESEE Research Report No. 87-2, The state of the art in infilled frames." Imperial College of Science and Technology. Civil Engineering Department, London.

Mondal, G., and Tesfamariam, S. (2014). "Effects of vertical irregularity and thickness of unreinforced masonry infill on the robustness of RC framed buildings." *Earthquake Engineering Structural Dynamics*, Vol. 43 (2), pp. 205–223.

Murty, C. V. R., Rai, D. C., Jain, S. K., Kaushik, H. B., Mondal, G., and Dash, S. R. (2006), "Performance of structures in the Andaman and Nicobar Islands (India) during the December 2004 Great Sumatra earthquake and Indian Ocean tsunami", *Earthquake Spectra*, EERI, Vol. 22(S3), USA, Special Issue, pp. S321-S354.

NICEE Workshop (2014). Seismic safety agenda in north-eastern region of India, *Proceedings of the workshop organized by National Information Centre of Earthquake Engineering (NICEE) and Indian Institute of Technology (IIT) Guwahati* on 22 March 2014 at IIT Guwahati.

Nithin, V. L., Das, S., and Kaushik, H. B., (2017), "Wavelet-based simulation of scenario-specific nonstationary accelerograms and their GMPE compatibility", *Soil Dynamics and Earthquake Engineering*, Vol. 99, pp. 56-67

O' Reilly, G. J., and Sullivan, T. J. (2017). "Quantification of modelling uncertainty in existing Italian RC frames." *Earthquake Engineering and Structural Dynamics*. DOI: 10.1002/eqe.3005

Olsson, A., Sandberg, G., and Dahlblom, O. (2003). "On Latin hypercube sampling for structural reliability analysis." *Structural Safety*, Vol. 25(1), pp. 47-68.

Özhendekci, N., and Özhendekci, D. (2012). "Rapid seismic vulnerability assessment of low-to mid-rise reinforced concrete buildings using Bingöl's regional data." *Earthquake Spectra*, EERI, Vol. 28(3), pp. 1165-1187.

Padgett, J. E., and DesRoches, R. (2007). 'Sensitivity of seismic response and fragility to parameter uncertainty.' *Journal of Structural Engineering*, ASCE, Vol. 133(12), pp. 1710-1718.

Padgett, J. E., Nielson, B. G. and DesRoches, R. (2008). "Selection of optimal intensity measures in probabilistic seismic demand models of highway bridge portfolios." *Earthquake Engineering and Structural Dynamics*, Vol. 37(5), pp. 711-725.

Park, Y. J., and Ang, A. H. S. (1985) "Mechanistic seismic damage model for reinforced concrete." *Journal of Structural Engineering*, Vol. 111(4), pp. 722-739.

Paulay, T., and Priestley, M. J. N. (1992). "Seismic Design of Concrete and Masonry Structures." *John Wiley and Sons*. New York.

Porter, K. A., Beck, J. L., and Shaikhutdinov, R. V. (2002). "Investigation of sensitivity of building loss estimates to major uncertain variables for the Van Nuys testbed." *PEER Report 2002/03*.

Porter, K. A., Beck, J. L., and Shaikhutdinov, R. V. (2002). "Sensitivity of building loss estimates to major uncertain variables." *Earthquake Spectra*, EERI, Vol. 18(4), pp. 719-743.

Porter, K. (2016) "A beginner's guide to fragility, vulnerability, and risk." *Encyclopedia of Earthquake Engineering*.

Rai, D. C., Singhal, V., and Kaushik, H. B., (2017), "M6.7 January 4, 2016 Imphal Earthquake: Dismal Performance of Publicly-Funded Buildings", *Current Science*, Vol. 113(12), Indian Academy of Sciences, Bangalore, India, pp. 2341-2350. DOI: 10.18520/cs/v113/i12/2341-2350.

Ramamoorthy, S. K., Gardoni, P., and Bracci, J. M. (2006). Probabilistic demand models and fragility curves for reinforced concrete frames. *Journal of Structural Engineering*, ASCE, Vol. 132(10), pp. 1563-1572.

Ranganathan, R. (1999). "*Structural reliability analysis and design*." Jaico Publishing House, Mumbai, India.

Rossetto T., Ioannou, I., and Grant, D. N. (2013). "Existing Empirical Fragility and Vulnerability Relationships: Compendium and Guide for Selection". *GEM Technical Report* 2013-X, GEM Foundation, Pavia, Italy.

Rossetto, T. and Elnashai, A. (2003). "Derivation of vulnerability functions for European-type RC structures based on observational data." *Engineering Structures*, Vol. 25(10), pp. 1241-1263.

Rota, M., Penna, A., and Magenes, G. (2010). "A methodology for deriving analytical fragility curves for masonry buildings based on stochastic nonlinear analyses." *Engineering Structures*, Vol. 32(5), pp. 1312-1323.

Ruiz-García, J., and Miranda, E. (2006). "Evaluation of residual drift demands in regular multi-storey frames for performance-based seismic assessment." *Earthquake Engineering and Structural Dynamics*, Vol. 35(13), pp. 1609-1629.

Ruiz-García, J., and Miranda, E. (2010). "Probabilistic estimation of residual drift demands for seismic assessment of multi-story framed buildings." *Engineering Structures*, Vol. 32(1), pp. 11-20.

Seo, J. (2013). "Statistical determination of significant curved I-girder bridge seismic response parameters." *Earthquake Engineering and Engineering Vibration*, Vol. 12(2), pp. 251-260.

Seo, J. and Linzell, D.G. (2013). "Nonlinear seismic response and parametric examination of horizontally curved steel bridges using 3D computational models." *Journal of Bridge Engineering*, Vol. 18(3), pp. 220-231.

Shah, H. C. (1984). "Glossary of terms for probabilistic seismic-risk and hazard analysis." *Earthquake Spectra*, EERI, Vol. 1(1), pp. 33-40.

Silva, V., Crowley, H., Varum, H., Pinho, R., and Sousa, R. (2014). "Evaluation of analytical methodologies used to derive vulnerability functions." Earthquake Engineering and Structural Dynamics, Vol. 43(2), pp. 181-204.

Singhal, A. and Kiremidjian, A. S., (1996). "Method For Probabilistic Evaluation Of Seismic Structural Damage". *Journal of Structural Engineering*, ASCE, Vol. 122 (12), pp. 1459–1467.

Sinha, R., and Goyal, A. (2004) "A national policy for seismic vulnerability assessment of buildings and procedure for rapid visual screening of buildings for potential seismic vulnerability." Report to Disaster Management Division, Ministry of Home Affairs, Government of India, Hindistan.

Sobol', I. M. (1993). "Sensitivity estimates for nonlinear mathematical models." *Mathematical Modelling and Computational Experiments*, Vol. 1(4), pp. 407-414.

Soleimani, F., Vidakovic, B., DesRoches, R. and Padgett, J. (2017). "Identification of the significant uncertain parameters in the seismic response of irregular bridges." *Engineering Structures*, Vol. 141, pp. 356-372.

Sucuoğlu, H., Yazgan, U., and Yaklut, A. (2007) "A screening procedure for seismic risk assessment in urban building stocks." *Earthquake Spectra*, EERI, Vol. 23(2), pp. 441-458.

Surendran, S. (2012). "Lateral Load Behavior of Masonry Infilled RC Frames with Central Opening." Master's Dissertation, Indian Institute of Technology Guwahati, India.

Surendran, S., and Kaushik, H. B. (2012), "Masonry infill RC frames with openings: Review of in-plane lateral load behaviour and modeling approaches", *The Open Construction and Building Technology Journal*, Bentham Science Publishers, Vol. 6, pp. 126-154.

Takeda, T., Sozen, M. A., and Neilsen, N. N. (1970). "Reinforced concrete response to simulated earthquakes." *Journal of the Structural Division*, Vol. 96(12), pp. 2557-2573.

Tibshirani, R. (1996). "Regression shrinkage and selection via the lasso." *Journal of the Royal Statistical Society,* Series B (Methodological), pp. 267-288.

Uva, G., Raffaele, D., Porco, F., and Fiore, A. (2012). "On the role of equivalent strut models in the seismic assessment of infilled RC buildings." *Engineering Structures*, Vol. 42, pp. 83-94.

Vamvatsikos, D. and Fragiadakis, M. (2010). "Incremental dynamic analysis for estimating seismic performance sensitivity and uncertainty." *Earthquake Engineering and Structural Dynamics*, Vol. 39(2), pp. 141-163.

Vamvatsikos, D., and Cornell, C. A. (2002). "Incremental dynamic analysis." *Earthquake Engineering and Structural Dynamics*, Vol. 31(3), pp. 491-514.

Whitman, R. V., Reed, J. W., and Tien, H. S. (1973). "Earthquake Damage Probability Matrices". *Proceedings of 5th World Conference on Earthquake Engineering*, Vol. 2, pp. 2531–2540, Rome.

Wilson, E. L. (1996). "Three-dimensional static and dynamic analysis of structures." *Computers and Structures*, Inc., Berkeley, CA.

Yuen, Y. P. and Kuang, J. S. (2015) "Nonlinear seismic responses and lateral force transfer mechanisms of RC frames with different infill configurations." *Engineering Structures*, Vol. 91, pp. 125–40.

Yun, S. Y., Hamburger, R. O., Cornell, C. A., and Foutch, D. A. "Seismic performance evaluation for steel moment frames." *Journal of Structural Engineering*, ASCE, Vol. 128(4), pp. 534-545.

Zona, A., Ragni, L., and Dall'Asta, A. (2012). "Sensitivity-based study of the influence of brace over-strength distributions on the seismic response of steel frames with BRBs." *Engineering Structures*, Vol. 37, pp. 179-192.

❋ ❋ ❋

APPENDIX A

Details of the case study building at Sankhu in Nepal

As a case study, an internal frame of a 4-storey school building (Fig. A.1) at Sankhu in Nepal is considered for performance assessment based on nonlinear analysis. In order to account for the doors and windows in the masonry infill walls, an average central opening size of 45% is considered in determining the width of equivalent diagonal struts. Basic structural materials considered are those as detailed in Chapter 3 for concrete, reinforcing steel and masonry. Fig. A.1(a) and A.1(b) show the elevation of the school building at site with different damaged members (marked in red) and plan dimensions, respectively. The observed column and beam sections, as shown in Figures A.1(c) and A.1(d), reveal that the sections were not designed and detailed adequately to withstand earthquake forces. The building was marked as *unsafe for use without structural intervention* by experts.

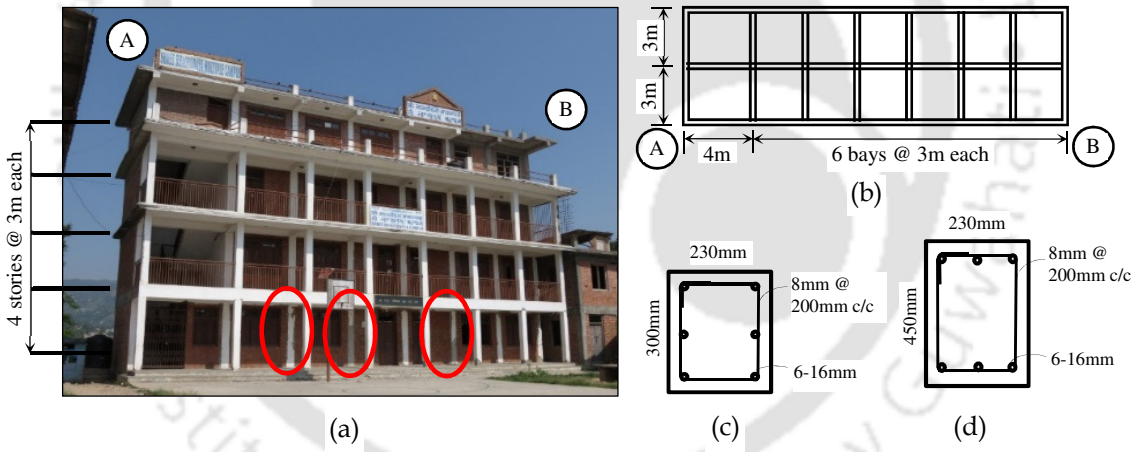

Figure A.1 4-storey school building at Sankhu in Nepal after April 25, 2015 Nepal earthquake (a) Front elevation showing damage in columns (b) Plan dimensions; Observed sectional detail of (c) columns and (d) beams. [Source: *Earthquake Engineering Research Institute*]

❋ ❋ ❋

LIST OF PUBLICATIONS

Refereed Journals

1. Choudhury, T., and Kaushik, H. B., (2018), "Seismic Response Sensitivity to Uncertain Variables in RC Frames with Infill Walls" *Journal of Structural Engineering*, ASCE, Vol 144 (10): 04018184, DOI: 10.1061/(ASCE)ST.1943-541X.0002190 .
2. Choudhury, T., and Kaushik, H. B., (under review), "Treatment of Uncertainties in Seismic Fragility of RC Buildings with Infill Walls" *Journal of Structural Engineering*, ASCE.
3. Choudhury, T., and Kaushik, H. B., (2018), "Seismic Fragility of Open Ground Storey RC Frames with Wall Openings for Vulnerability Assessment", *Engineering Structures*, Vol 155, 15 January 2018, Elsevier, pp. 345-357.
4. Choudhury, T., and Kaushik, H. B., (2018), "Component Level Fragility Estimation for Vertically Irregular Reinforced Concrete Frames", *Journal of Earthquake Engineering*, Taylor & Francis, In Press. DOI: 10.1080/13632469.2018.1453413.
5. Kaushik, H.B. and Choudhury, T., (2015), "Vulnerability Analysis of Buildings for Seismic Risk Assessment: A Review", The Bridge and Structural Engineer, *The Journal of the Indian National Group (ING) of International Association for Bridge and Structural Engineering* (IABSE), 45(1), March 2015, pp. 63-76.

Conferences

6. Choudhury, T., and Kaushik, H.B. (2019), "Purview of Nonlinear Static and Dynamic Analysis Procedures on Seismic Fragility Estimation of RC Buildings with Masonry Infills", *National Conference on Advances in Structural Technologies*, Department of Civil Engineering, National Institute of Technology (NIT) Silchar, INDIA – 788010.
7. Choudhury, T., and Kaushik, H.B. (2018), "Sensitivity of Seismic Response of Vertically Irregular Masonry Infilled RC Frames to Critical Uncertain Parameters", *16th Symposium on Earthquake Engineering*, 20-22 December 2018, Paper No. 281, IIT Roorkee, India.
8. Choudhury, T., and Kaushik, H.B. (2018), "Seismic Fragility Flow Plots for Risk Assessment of Reinforced Concrete Buildings with Open Ground Storey", CESDOC 2018, *2nd International Conference on Sustainability*, 18-19 December, Guwahati, Assam.
9. Choudhury, T., and Kaushik, H.B. (2017), "A Simplified Method for Seismic Vulnerability Assessment of RC Buildings with Open Ground Storey", Proceedings of the *16th World Conference on Earthquake Engineering*, 9-13 January 2017, Paper No. 1684, Santiago, Chile.
10. Choudhury, T., and Kaushik, H.B. (2016), "Seismic Fragility of Reinforced Concrete Frames with Vertical Irregularities", Proceedings of *Structural*

Engineering Convention (SEC-2016), 21-23 December 2016, Paper ID 469, CSIR-SERC, Chennai, India.

11. Choudhury, T., and Kaushik, H.B. (2015), "Seismic Fragility of Masonry Infilled Reinforced Concrete Frames with Open Ground Story", Proceedings of *12th International Conference on Vibration Problems* (ICOVP), December 14-17, 2015, Paper No. O0202, Indian Institute of Technology Guwahati, India.

Book Chapters

12. Choudhury, T., and Kaushik, H.B. (2018), Seismic Fragility of Reinforced Concrete Frames with Vertical Irregularities in *Recent Advances in Structural Engineering*, Volume – 2, ISBN: 978-981-13-0364-7, Ramanjaneyulu, K. and Rao, A. R. M. (Editors), Springer.

❋ ❋ ❋